

Complexing ability and activity of N-containing bisphosphonates in bone cancer treatment

by

José Soares Castelo Branco

Submitted in partial fulfilment of the requirements for the degree of

Master of Science

in the Faculty of Natural and Agricultural Science

University of Pretoria

Pretoria

Supervisor: Professor Ignacy Cukrowski

May, 2007

Declaration

I declare that this dissertation is my own work. It is being submitted for the partial fulfillment of the degree of **Master of Science** in the faculty of Natural and Agricultural Science at the University of Pretoria. It has not been submitted before for any degree or examination in any other University.

J.S. Castelo Branco

_____ day of _____ 2007.

Abstract

The nitrogen-containing bisphosphonates (N-BPs), 4-amino-1-hydroxy-1,1-butyldenebisphosphonic acid, or Alendronate, (ALN) and 6-amino-1-hydroxy-1,1-hexylidenebisphosphonic acid, or Neridronate (NED), were studied with metal ions Mg(II), Ca(II), Cd(II) and Pb(II) at ionic strength 0.15 M at 25 °C in NaCl. The complexes of ALN and NED with Mg(II) and Ca(II) were studied by glass electrode potentiometry (GEP), and with Cd(II) and Pb(II) by sampled direct current polarography (DCP) and normal pulse polarography (NPP) at fixed total ligand to total metal concentration ratios and varied pH values.

Virtual potential was used in the modelling of the metal ligand-system derived from DCP and NPP. Protonation constants and complex formation constants for ligands ALN and NED with metal ions are reported. The structures of metal-complexes proposed were compared to the reported crystal structures of the metal-complexes of the ligands ALN and NED.

The linear free energy relationships (LFER) that include stability constants $\log K_{ML}$ for Mg(II), Ca(II) and Cd(II) with ligands ALN and NED were used to estimate $\log K_{ML}$ values for Sm(III) and Ho(III) with ALN and NED. The stability constants estimated here might be regarded as not reliable due to the few points available for that purpose.

Dedication

To my parents

Acknowledgments

I would like to express my appreciation to my supervisor, Prof. I. Cukrowski, for the insightful assistance during the development of ideas in this thesis, comments on the text, understanding and for teaching me how to be a researcher.

For financial support, I thank the World Bank–Sponsor of Capacity Building Programme at the “Universidade Pedagógica” of Mozambique.

I am grateful to the Electrochemistry Research Group especially Tumaini and Philemon for their advice and support in this work.

I acknowledge my family members, especially my spouse Aissa, for supporting and encouraging me to pursue this degree. My friends for their moral support throughout the study period.

Table of Contents

Declaration	ii
Abstract	iii
Dedication	iv
Acknowledgements	v
List of Figures	ix
List of Tables	xviii
List of Symbols and Abbreviations	xx

Chapter 1 Introduction

1.1	Bone Cancer: Remodelling and Metastasis	2
1.2	Radiopharmaceuticals in Bone Cancer	4
1.3	Bisphosphonate Ligands in Bone Cancer	5
1.4	Linear Free Energy Relationship	7
1.5	Previous Studies of Bisphosphonate Ligands	9
1.6	Research Aims	10
1.7	References	11

Chapter 2 Theory and Data Treatment

2.1	Potentiometry	14
	2.1.1 General Principles	14
	2.1.2 Equilibrium Studies of Metal-Ligand Systems	16
	2.1.3 The Analysis of Data	18
2.2	Polarography	21
	2.2.1 General Principles	21
	2.2.2 Selected Voltammetric Techniques	23
	2.2.3 Equilibrium Studies of Metal-Ligand Systems	25
2.3	Virtual Potentiometry	30
2.4	References	33

Chapter 3 Experimental Methodology

3.1	Reagents	35
3.2	Preparation of Solutions	36
3.3	Glass Electrode Potentiometry	36
3.3.1	Instrumentation	36
3.3.2	Standardisation of Solutions	37
3.3.3	Glass Electrode Calibration	38
3.3.4	Protonation Equilibria Study by GEP	39
3.3.5	Determination of Stability Constants by GEP	40
3.4	Polarography	41
3.4.1	Instrumentation	41
3.4.2	Ligands Adsorption Studies	42
3.4.3	Determination of Stability Constants by Polarography	42
3.5	References	45

Chapter 4 Results and Discussion

4.1	Equilibria by Glass Electrode Potentiometry	46
4.1.1	Protonation of Alendronate	47
4.1.2	Protonation of Neridronate	50
4.1.3	Mg(II)–Alendronate System	53
4.1.4	Ca(II)–Alendronate System	58
4.1.5	Mg(II)–Neridronate System	61
4.1.6	Ca(II)–Neridronate System	64
4.2	Equilibria by Polarography	67
4.2.1	Ligands Adsorption Study	67
4.2.2	Fitting of Polarographic Curves	70
4.2.3	Cd(II)-Alendronate System	71
4.2.4	Pb(II)-Alendronate System	85
4.2.5	Cd(II)-Neridronate System	95
4.2.6	Pb(II)-Neridronate System	108
4.3	Linear Free Energy Relationships for Alendronate and Neridronate	112

4.4	Comparison of Formation Constants for Ligands ALN, NED and others Ligands with Metal Ions	116
4.5	References	122

Chapter 5 Conclusions

5.1	Conclusions and Future work	125
5.2	References	128
	Appendices	129

List of Figures

- Figure 1.1** Linear free energy relationships for $\log K_1$ (ionic strength = 0, $t = 25$ °C) for Fe^{3+} and UO_2^{2+} vs. ligand pK_a for unidentate ligands with negatively charged oxygen donors [32].
- Figure 1.2** Relationships between $\log K_1$ for fluoride complexes of metal ions vs. Z^2/r , where Z is the cationic charge on the metal ion, and r the ionic radius. Formation constant data at ionic strength = 0, $t = 25$ °C [32].
- Figure 1.3** Relationship between $\log K_1$ for chelating ligands containing negative oxygen donors, and $\log K_1$ for the formation of the hydroxide complex, for a variety of metal ions. The ligands shown are catechol (•), 5-nitrosalicylic acid (O), Kojate (♦), and malonate (). Formation constants data at ionic strength = 0, and 25 °C [32].
- Figure 2.1** An example of a polarogram showing limiting diffusion current, background current and the position of the half-wave potential from DC polarography.
- Figure 3.1** An example of a calibration curve obtained by a GEP experiment for metal-ligand system. Linear fit (—); experimental points (o). In this example, $E^o = 409.58$ mV and the response slope 60.828 mV.
- Figure 4.1** Experimental (circles) and theoretical (solid line) protonation curves for ALN at ionic strength 0.15 M in NaCl and 25 °C, $[\text{L}_T] = 1.0000 \times 10^{-2}$ M.
- Figure 4.2** Experimental (circles) and theoretical (solid line) protonation curves for NED at ionic strength 0.15 M in NaCl and 25 °C, $[\text{L}_T] = 9.979 \times 10^{-3}$ M.
- Figure 4.3** Experimental (circles) and theoretical (solid line) potentiometric complex formation curves for Mg(II)–ALN system $\text{L}_T : \text{M}_T$ ratio 2 obtained for the model $\text{Mg}(\text{H}_2\text{L})$, $\text{Mg}_2(\text{HL})$, $\text{Mg}(\text{HL})$, MgL , $\text{MgL}(\text{OH})$ and $\text{MgL}_2(\text{OH})_2$ at 25 °C and ionic strength 0.15 M in NaCl.

- Figure 4.4** Species distribution diagrams for Mg(II)–ALN system $L_T : M_T$ ratio 2 obtained for the model $M(H_2L)$, $M_2(HL)$, $M(HL)$, ML , $ML(OH)$ and $ML_2(OH)_2$ at 25 °C and ionic strength 0.15 M in NaCl. $[M_T]= 9.9847 \times 10^{-4}$ M.
- Figure 4.5** Experimental (points) and theoretical (solid line) potentiometric complex formation curves for Ca(II)–ALN (\circ) and Mg(II)–ALN systems (\bullet) $L_T : M_T$ ratio 2 obtained for the models $Ca(H_2L)$, $Ca_2(HL)$, $Ca(HL)$, CaL , $CaL(OH)$ and $CaL(OH)_2$ and $Mg(H_2L)$, $Mg_2(HL)$, $Mg(HL)$, MgL , $MgL(OH)$ and $MgL_2(OH)_2$ at 25 °C and ionic strength 0.15 M in NaCl.
- Figure 4.6** Species distribution diagrams for Ca(II)–ALN system $L_T : M_T$ ratio 2 obtained for the model $M(H_2L)$, $M_2(HL)$, $M(HL)$, ML , $ML(OH)$ and $ML(OH)_2$ at 25 °C and ionic strength 0.15 M in NaCl. $[M_T]= 9.9985 \times 10^{-4}$ M.
- Figure 4.7** Species distribution diagrams for Ca(II)–ALN system $L_T : M_T$ ratio 2 obtained for the model $M_2(HL)$, $M_2(HL)$, $M(HL)$, M_2L , ML , $ML(OH)$ and $ML(OH)_2$ at 25 °C and ionic strength 0.15 M in NaCl. $[M_T]= 9.9985 \times 10^{-4}$ M.
- Figure 4.8** Experimental (points) and theoretical (solid line) potentiometric complex formation curves for Mg(II)–NED (\circ) and Mg(II)–ALN (\bullet) systems $L_T : M_T$ ratio 2 obtained for the model $Mg(H_2L)$, $Mg_2(HL)$, $Mg(HL)$, MgL , $MgL(OH)$ and $MgL_2(OH)_2$ at 25 °C and ionic strength 0.15 M in NaCl.
- Figure 4.9** Species distribution diagrams for Mg(II)–NED system $L_T : M_T$ ratio 2 obtained for the model $M(H_2L)$, $M_2(HL)$, $M(HL)$, ML , $ML(OH)$ and $ML_2(OH)_2$ at 25 °C and ionic strength 0.15 M in NaCl. $[M_T]= 9.9848 \times 10^{-4}$ M.
- Figure 4.10** Experimental (points) and theoretical (solid line) potentiometric complex formation curves for Ca(II)–NED (\circ) and Ca(II)–ALN systems (\bullet) $L_T : M_T$ ratio 2 obtained for the models $Ca(H_2L)$, $Ca_2(HL)$, $Ca(HL)$ and CaL (\circ) and $Ca(H_2L)$, $Ca_2(HL)$, $Ca(HL)$, CaL , $CaL(OH)$ and $CaL(OH)_2$ (\bullet) at 25 °C and ionic strength 0.15 M in NaCl.

- Figure 4.11** Species distribution diagrams for Ca(II)–NED system $L_T : M_T$ ratio 2 obtained for the model $M(H_2L)$, $M_2(HL)$, M_2L and ML at 25 °C and ionic strength 0.15 M in NaCl. $[M_T] = 3.9540 \times 10^{-4}$ M.
- Figure 4.12** Species distribution diagrams for Ca(II)–NED system $L_T : M_T$ ratio 2 obtained for the model $M(H_2L)$, $M_2(HL)$, $M(HL)$ and ML at 25 °C and ionic strength 0.15 M in NaCl. $[M_T] = 3.9540 \times 10^{-4}$ M.
- Figure 4.13** An example of AC voltamogram of 0.03 M n-pentanol in 0.1 M KNO_3 . HMDE (Hanging Mercury Dropping Electrode) used as working electrode.
- Figure 4.14** AC voltamogram for 0.01 M ALN and NED in 0.15 M NaCl at different pH. (A) pH: **a** = 7.15 (background), **b** = 6.13, **c** = 9.60 and **d** = 10.52; (B) pH: **a** = 7.01 (background), **b** = 6.41, **c** = 9.41 and **d** = 10.84. HMDE used as working electrode.
- Figure 4.15** Example of the fitted polarogram for Cd(II)–ALN system studied by sampled DCP at $L_T : M_T = 266.6$, ionic strength 0.15 M (NaCl), 25 °C, initial $[M_T] = 1.4978 \times 10^{-5}$ M. The circles represent experimental points; thin solid line represents theoretically fitted curve using the curve-fitting method based on the Ružić equation (Equation 4.8); the thick solid line represents computed curves corresponding to fully reversible reduction processes using the I_d and $E_{1/2}^r$ values obtained from curve-fitting based on the Ružić equation; dashed line represent background current.
- Figure 4.16** Variation in limiting diffusion current for Cd(II)–ALN system studied by sampled DC polarography at $L_T : M_T = 266.6$, ionic strength 0.15 M (NaCl), 25 °C, initial $[M_T] = 1.4978 \times 10^{-5}$ M. The triangles indicate the normalized limiting diffusion current, diamonds indicate the observed diffusion current and the circles indicate the expected current.

- Figure 4.17** Analysis of variation in $E_{1/2}^r(\text{virt})$ as a function of pH for Cd(II)–ALN system studied by sampled DC polarography at $L_T : M_T = 266.6$, ionic strength 0.15 M (NaCl), 25 °C, initial $[M_T] = 1.4978 \times 10^{-5}$ M. $E_{1/2}^r(\text{virt})$ is reversible half-wave potential obtained using the Ružić curve-fitting method (Equation 4.8).
- Figure 4.18** Analysis of variation in $E_{1/2}^r(\text{virt})$ as a function of $\log [H_2L]$ for Cd(II)–ALN system studied by sampled DC polarography at $L_T : M_T = 266.6$, ionic strength 0.15 M (NaCl), 25 °C, initial $[M_T] = 1.4978 \times 10^{-5}$ M.
- Figure 4.19** Analysis of variation in $E_{1/2}^r(\text{virt})$ as a function of $\log [HL]$ for Cd(II)–ALN system studied by sampled DC polarography at $L_T : M_T = 266.6$, ionic strength 0.15 M (NaCl), 25 °C, initial $[M_T] = 1.4978 \times 10^{-5}$ M.
- Figure 4.20** Analysis of variation in $E_{1/2}^r(\text{virt})$ as a function of $\log [L]$ for Cd(II)–ALN system studied by sampled DC polarography at $L_T : M_T = 266.6$, ionic strength 0.15 M (NaCl), 25 °C, initial $[M_T] = 1.4978 \times 10^{-5}$ M.
- Figure 4.21** Experimental and calculated complex formation curves obtained using reversible half-wave potentials for Cd(II)–ALN system studied by sampled DC polarography at $L_T : M_T = 266.6$, ionic strength 0.15 M (NaCl), 25 °C, initial $[M_T] = 1.4978 \times 10^{-5}$ M. The circles represent the ECFC and solid line represents the CCFC for the optimized M–L model contained $M_2(HL)$, $M(HL)$ and ML .
- Figure 4.22** Species distribution as a function of pH for the model $M_2(HL)$, M_2L , and ML for Cd(II)–ALN system studied by sampled DC polarography at $L_T : M_T = 266.6$, ionic strength 0.15 M (NaCl), 25 °C, initial $[M_T] = 1.4978 \times 10^{-5}$ M.
- Figure 4.23** Species distribution as a function of pH for the model $M_2(HL)$, $M(HL)$, and ML for Cd(II)–ALN system studied by sampled DC polarography at $L_T : M_T = 266.6$, ionic strength 0.15 M (NaCl), 25 °C, initial $[M_T] = 1.4978 \times 10^{-5}$ M.

- Figure 4.24** Species distribution as a function of pH for the all species predicted $M(H_2L)$, $M(HL)$, and ML for $Cd(II)$ –ALN system studied by sampled DC polarography at $L_T : M_T = 266.6$, ionic strength 0.15 M (NaCl), 25 °C, initial $[M_T] = 1.4978 \times 10^{-5}$ M.
- Figure 4.25** Species distribution as a function of pH for the all species predicted $M(H_2L)$, $M_2(HL)$, $M(HL)$, M_2L , and ML for $Cd(II)$ –ALN system studied by sampled DC polarography at $L_T : M_T = 266.6$, ionic strength 0.15 M (NaCl), 25 °C, initial $[M_T] = 1.4978 \times 10^{-5}$ M.
- Figure 4.26** Behaviour of some of NP–waves recorded for $Pb(II)$ –ALN system studied by NP polarography at $L_T : M_T = 160$, ionic strength 0.15 M (NaCl), 25 °C, initial $[M_T] = 4.9751 \times 10^{-5}$ M.
- Figure 4.27** Variation in limiting diffusion current for $Pb(II)$ –ALN system studied by NP polarography at $L_T : M_T = 160$, ionic strength 0.15 M (NaCl), 25 °C, initial $[M_T] = 4.9751 \times 10^{-5}$ M. The triangles indicate the normalized limiting diffusion current, diamonds indicate the observed diffusion current and the circles indicate the expected current.
- Figure 4.28** Analysis of variation in $E^r_{1/2}(virt)$ as a function of pH for $Pb(II)$ –ALN system studied by NP polarography at $L_T : M_T = 160$, ionic strength 0.15 M (NaCl), 25 °C, initial $[M_T] = 4.9751 \times 10^{-5}$ M.
- Figure 4.29** Analysis of variation in $E^r_{1/2}(virt)$ as a function of $\log [H_2L]$ for $Pb(II)$ –ALN system studied by NP polarography at $L_T : M_T = 160$, ionic strength 0.15 M (NaCl), 25 °C, initial $[M_T] = 4.9751 \times 10^{-5}$ M.
- Figure 4.30** Analysis of variation in $E^r_{1/2}(virt)$ as a function of $\log [HL]$, respectively, for $Pb(II)$ –ALN system studied by NP polarography at $L_T : M_T = 160$, ionic strength 0.15 M (NaCl), 25 °C, initial $[M_T] = 4.9751 \times 10^{-5}$ M.
- Figure 4.31** Analysis of variation in $E^r_{1/2}(virt)$ as a function of $\log [L]$ for $Pb(II)$ –ALN system studied by NP polarography at $L_T : M_T = 160$, ionic strength 0.15 M (NaCl), 25 °C, initial $[M_T] = 4.9751 \times 10^{-5}$ M.

- Figure 4.32** Experimental and calculated complex formation curves obtained using reversible half-wave potentials for Pb(II)–ALN system studied by NP polarography at $L_T : M_T = 160$, ionic strength 0.15 M (NaCl), 25 °C, initial $[M_T] = 4.9751 \times 10^{-5}$ M. The circles represents the ECFC and solid line represents the CCFC for the optimized M–L model contained $M_2(HL)$, $M(HL)$.
- Figures 4.33** Species distribution as a function of pH for the model $M_2(HL)$, $M(HL)$, for Pb(II)–ALN system studied by sampled NP polarography at $L_T : M_T = 160$, ionic strength 0.15 M (NaCl), 25 °C, initial $[M_T] = 4.9751 \times 10^{-5}$ M.
- Figures 4.34** Species distribution as a function of pH for the model $M_2(HL)$, $M(HL)$, for Pb(II)–ALN system studied by sampled NP polarography at $L_T : M_T = 160$, ionic strength 0.15 M (NaCl), 25 °C, initial $[M_T] = 4.9751 \times 10^{-5}$ M.
- Figure 4.35** Example of fitting from NP polarographic study of Cd(II)–NED system at $L_T : M_T = 266.7$, 25 °C, $[M_T] = 2.9910 \times 10^{-5}$ M. Circles are experimental points representing the recorded current at a particular applied potential; solid lines represent theoretically fitted curves; thick solid line represent computed curves corresponding to fully reversible reduction processes using the I_d and $E_{1/2}^r$ values obtained from curve-fitting based on the Ružić equation; dashed line represent background current.
- Figure 4.36** Variation in limiting diffusion current for Cd(II)–NED system studied by NP polarography at $L_T : M_T = 266.6$, ionic strength 0.15 M (NaCl), 25 °C, initial $[M_T] = 2.9910 \times 10^{-5}$ M. The triangles indicate the normalized limiting diffusion current, diamonds indicate the observed diffusion current and the circles indicate the expected current.
- Figure 4.37** Analysis of variation in $E_{1/2}^r(\text{virt})$ as a function of pH for Cd(II)–NED system studied by NP polarography at $L_T : M_T = 266.6$, , ionic strength 0.15 M (NaCl), 25 °C, initial $[M_T] = 2.9910 \times 10^{-5}$ M.

- Figure 4.38** Analysis of variation in $E_{1/2}^r(\text{virt})$ as a function of $\log [\text{H}_3\text{L}]$ for Cd(II)–NED system studied by NP polarography at $L_T : M_T = 266.6$, ionic strength 0.15 M (NaCl), 25 °C, initial $[\text{M}_T] = 2.9910 \times 10^{-5}$ M.
- Figure 4.39** Analysis of variation in $E_{1/2}^r(\text{virt})$ as a function of $\log [\text{H}_2\text{L}]$ for Cd(II)–NED system studied by NP polarography at $L_T : M_T = 266.6$, ionic strength 0.15 M (NaCl), 25 °C, initial $[\text{M}_T] = 2.9910 \times 10^{-5}$ M.
- Figure 4.40** Analysis of variation in $E_{1/2}^r(\text{virt})$ as a function of $\log [\text{HL}]$ for Cd(II)–NED system studied by NP polarography at $L_T : M_T = 266.6$, ionic strength 0.15 M (NaCl), 25 °C, initial $[\text{M}_T] = 2.9910 \times 10^{-5}$ M.
- Figure 4.41** Analysis of variation in $E_{1/2}^r(\text{virt})$ as a function of $\log [\text{L}]$ for Cd(II)–NED system studied by NP polarography at $L_T : M_T = 266.6$, ionic strength 0.15 M (NaCl), 25 °C, initial $[\text{M}_T] = 2.9910 \times 10^{-5}$ M.
- Figure 4.42** Experimental and calculated complex formation curves obtained using reversible half-wave potentials for Cd(II)–NED system studied by NP polarography at $L_T : M_T = 266.6$, ionic strength 0.15 M (NaCl), 25 °C, initial $[\text{M}_T] = 2.9910 \times 10^{-5}$ M. The circles represents the ECFC and solid line represents the CCFC for the optimized M–L model contained $\text{M}(\text{H}_3\text{L})$, $\text{M}(\text{H}_2\text{L})$, $\text{M}(\text{HL})$, and ML .
- Figure 4.43** Species distribution as a function of pH for the model $\text{M}(\text{H}_3\text{L})$, $\text{M}(\text{H}_2\text{L})$, $\text{M}(\text{HL})$, and ML for Cd(II)–NED system studied by sampled NP polarography at $L_T : M_T = 266.6$, , ionic strength 0.15 M (NaCl), 25 °C, initial $[\text{M}_T] = 2.9910 \times 10^{-5}$ M.
- Figure 4.44** Species distribution as a function of pH for the model $\text{M}(\text{H}_3\text{L})$, $\text{M}(\text{H}_2\text{L})$, M_2L and ML for Cd(II)–NED system studied by sampled NP polarography at $L_T : M_T = 266.6$, ionic strength 0.15 M (NaCl), 25 °C, initial $[\text{M}_T] = 2.9910 \times 10^{-5}$ M.
- Figure 4.45** Species distribution as a function of pH for the model $\text{M}(\text{H}_3\text{L})$, $\text{M}(\text{H}_2\text{L})$, $\text{M}_2(\text{HL})$, M_2L and ML for Cd(II)–NED system studied by sampled NP polarography at $L_T : M_T = 266.6$, ionic strength 0.15 M (NaCl), 25 °C, initial $[\text{M}_T] = 2.9910 \times 10^{-5}$ M.

- Figure 4.46** Species distribution as a function of pH for the model $M(H_3L)$, $M(H_2L)$, $M_2(HL)$, $M(HL)$, and ML for $Cd(II)$ –NED system studied by sampled NP polarography at $L_T : M_T = 266.6$, ionic strength 0.15 M (NaCl), 25 °C, initial $[M_T] = 2.9910 \times 10^{-5}$ M.
- Figure 4.47** Species distribution as a function of pH for the model $M(H_3L)$, $M(H_2L)$, $M_2(HL)$, $M(HL)$, M_2L and ML for $Cd(II)$ –NED system studied by sampled NP polarography at $L_T : M_T = 266.6$, ionic strength 0.15 M (NaCl), 25 °C, initial $[M_T] = 2.9910 \times 10^{-5}$ M.
- Figure 4.48** Behaviour of some of NP–waves recorded for $Pb(II)$ –NED system studied by NP polarography at $L_T : M_T = 50$, ionic strength 0.15 M (NaCl), 25 °C initial $[M_T] = 7.9365 \times 10^{-5}$ M.
- Figure 4.49** Variation in limiting diffusion current for $Pb(II)$ –NED system studied by NP polarography at $L_T : M_T = 50$, ionic strength 0.15 M (NaCl), 25 °C initial $[M_T] = 7.9365 \times 10^{-5}$ M. The triangles indicate the normalized limiting diffusion current, diamonds indicate the observed diffusion current and the circles indicate the expected current.
- Figure 4.50** Experimental and calculated complex formation curves obtained using reversible half–wave potentials for $Pb(II)$ –NED system studied by NP polarography at $L_T : M_T = 50$, ionic strength 0.15 M (NaCl), 25 °C initial $[M_T] = 7.9365 \times 10^{-5}$ M. The circles represents the ECFC and solid line represents the CCFC for the optimized M–L model contained $M(HL)$, $M_2(HL)$.
- Figure 4.51** Species distribution as a function of pH for the model $M_2(HL)$, $M(HL)$, for $Pb(II)$ –NED system studied by sampled NP polarography at $L_T : M_T = 50$, ionic strength 0.15 M (NaCl), 25 °C initial $[M_T] = 7.9365 \times 10^{-5}$ M.
- Figure 4.52** Linear free energy relationship of formation constants for metal-ion complexation by ALN and hydroxide.
- Figure 4.53** Linear free energy relationship of formation constants for metal-ion complexation by NED and hydroxide.

- Figure 4.54** Linear free energy relationship between $\log K_{M(OH)}$ and $\log K_{ML}$ for indicated metal ions (all divalent) and the ligand ALN.
- Figure 4.55** Linear free energy relationship between $\log K_{M(OH)}$ and $\log K_{ML}$ for indicated metal ions (all divalent) and the ligand NED.
- Figure 4.56** Crystallographic structure of Catena-(bis(μ_2 -4-Ammonium-1-hydroxybuta-1,1-diylbis(phosphonato)))-calcium(II) [33].
- Figure 4.57** Crystallographic structure of Bis(μ_2 -6-amino-1-hydroxyhexylidene-1,1-bisphosphonate)-diaqua-bis(4-amino-1-hydroxyhexylidene-1,1-bisphosphonate)-di-cadmium dehydrate [15].
- Figure 4.58** Proposed structures for ALN and NED complexation of divalent metal-ions.
- Figure 4.59** Crystallographic structure of Catena-(4-Amino-1-hydroxybutylidene-1,1-bisphosphonite-cadmium monohydrate [34].
- Figure 4.60** Proposed structures for ALN and NED complexation of divalent metal-ions.

List of Tables

Table 3.1	Composition of the solutions for ligand titration studied by GEP.
Table 3.2	Specifications of the metal-ligand solutions $L_T : M_T$ ratio 2 studied by GEP.
Table 3.3	Specification of the metal-ligand solutions studied by sampled DC (A) and NP polarography (B).
Table 4.1	Protonation constants (as $\log K$) for ALN at 25 °C and ionic strength of 0.15 M in NaCl obtained by GEP.
Table 4.2	Reported protonation constants for alendronate.
Table 4.3	Protonation constants (as $\log K$) for NED at 25 °C and ionic strength of 0.15 M in NaCl obtained by GEP.
Table 4.4	Reported protonation constants for neridronate.
Table 4.5	(A) Dissociation constant for water and overall stability constants for Mg(II) complexes with OH ⁻ . (B) Overall stability constants for Mg(II)–ALN $L_T : M_T$ ratio 2 found in this work by GEP at ionic strength 0.15 M in NaCl and 25 °C. The proposed final model is indicated in bold.
Table 4.6	Comparison of M–L model for Mg(II)-HEDP[19], Mg(II)-APD [14] and Mg(II)-ALN.
Table 4.7	(A) Dissociation constant for water and overall stability constant for Ca(II) complexes with OH ⁻ . (B) Overall stability constants for Ca(II)–ALN $L_T : M_T$ ratio 2 found in this work by GEP at ionic strength 0.15 M in NaCl and 25 °C. The proposed final model is indicated in bold.
Table 4.8	(A) Dissociation constant for water and overall stability constants for Mg(II) complexes with OH ⁻ . (B) Overall stability constants for Mg(II)–NED $L_T : M_T$ ratio 2 found in this work by GEP at ionic strength 0.15 M in NaCl and 25 °C. The proposed final model is indicated in bold.

- Table 4.9** (A) Dissociation constant for water and overall stability constant for Ca(II) complexes with OH⁻. (B) Overall stability constants for Ca(II)–NED L_T : M_T ratio 2 found in this work by GEP at ionic strength 0.15 M in NaCl and 25 °C. The proposed final model is indicated in bold.
- Table 4.10** (A) Dissociation constant for water and overall stability constants for Cd(II) complexes with OH⁻. (B) Overall stability constants for Cd(II)–ALN found in this work by sampled DCP at ionic strength 0.15 M in NaCl and 25 °C, L_T : M_T ratio 266.6, [Cd_T] = 1.4978 × 10⁻⁵ M. The proposed final model is indicated in bold.
- Table 4.11** (A) Dissociation constant for water and overall stability constants for Pb(II) complexes with OH⁻. (B) Overall stability constants for Pb(II)–ALN found in this work by NPP at ionic strength 0.15 M in NaCl and 25 °C, L_T : M_T ratio 160, [M_T] = 4.9751 × 10⁻⁵ M. The proposed final model is indicated in bold.
- Table 4.12** Overall stability constants for Cd(II)–NED system determined at 25 C and μ = 0.15 M by NPP for L_T : M_T ratio 266.7, [M_T] = 2.9910 × 10⁻⁵ M. The proposed final model is indicated in bold.
- Table 4.13** Overall stability constants for Pb(II)–NED system determined at 25 C and μ = 0.15 M by NPP for L_T : M_T ratio 50, [M_T] = 7.9365 × 10⁻⁵M. The proposed final model is indicated in bold.
- Table 4.14** Data for log K_{ML} for the ligands ALN and NED and log K_{M(OH)} for several metal ions.
- Table 4.15** Data for log K_{ML} for the ligands MDP and HEDP, log K_{ML'} for the ligands ALN and NED and log K_{M(OH)} for several metal ions. (Where L' = HL).
- Table 4.16** Comparison of protonation constants (log K) for MDP, HEDP, APD, ALN and NED.
- Table 4.17** Comparison of formation constants (log β) for MDP, HEDP, APD, ALN and NED.

List of Symbols and Abbreviations

ECCLES	Evaluation of Constituent Concentrations for Large Equilibrium Studies
BPs	Bisphosphonates
MDP	Methylene-diphosphonic acid
APD	(3-aminohydroxypropylidene)-1-1-disphosphonate
Cl2	(Dichloromethylene)bis-phosphonate also known as Clodronate
HEDP	1-hydroxy-ethylene-diphosphonic acid also known as Etidronate
EDTMP	Ethylenediamine-tetramethylenephosphonate
ALN	4-amino-1-hydroxy-1,1-butylidenebisphosphonic acid
NED	6-amino-1-hydroxy-1,1-hexylidenebisphosphonic acid
ATP	Adenosine triphosphate
LFER	Linear Free Energy Relationship
NMR	Nuclear Magnetic Resonance
SHE	Standard Hydrogen Electrode
O / R	Oxidant / Reductant
<i>E</i>	Potential

E°	Standard thermodynamic potential
R	Gas constant ($8.31 \text{ J}\cdot\text{mol}^{-1}\cdot\text{K}^{-1}$)
T	Absolute temperature / K
F	Faraday constant
$E^{\circ'}$	Formal potential
E_j	Liquid junction potential
ISE	Ion-selective electrode
ESTA	Equilibrium Simulation for Titration Analysis
T_i	Total analytical concentration of the reactant i
c_i	Concentration of the free reactant i
q_{ij}	Stoichiometric coefficient of the species j for the reactant i
β_j	Overall stability constant of the species j
C_j	Concentration of the species j
U	Objective function
w_i	Weights of each observation i
ZBAR	Formation function

QBAR	Deprotonation function; the average number of protons released as a result of complexation per metal ion
NBAR	The average number of protons per ligand in the absence of metal ion
GEP	Glass electrode potentiometry
ZBAR(H)	The average number of protons bound per ligand
ZBAR(M)	The average number of ligand bound per metal ion
H _T or [H _T]	Total concentrations of proton
L _T or [L _T]	Total concentrations of ligand
DME	Dropping mercury electrode
DCP	Direct current polarography (Sampled direct current polarography)
D	Diffusion coefficient
n	Number of electrons
m	Mass flow rate of Hg
t	Drop lifetime
c	Analyte concentration
E _{1/2}	Half-wave potential
NPP	Normal pulse polarography

dc	Direct current
E_{dc}	dc component of potential
E_{ac}	ac component of potential
I_d	Limiting diffusion current
E_c	Potential of the complexed metal ion
[L] or L	Free ligand concentration
$E(M)$	Potential (e.g. $E_{1/2}(M)$) in the absence of metal complexes
$E(comp)$	Potential (e.g. $E_{1/2}(comp)$) in the presence of metal complexes
$I(M)$	Limiting diffusion current in the absence of metal complexes
$I(comp)$	Limiting diffusion current in the presence of metal complexes
$\beta_{M_p L_q OH_r}$	Overall stability constant
β_n^H	Overall protonation constant
[M]	Free metal ion concentration
[H]	Free proton concentration
K_n^H	Stepwise protonation constants
$\Delta E_{1/2}$	Shift in the half-wave potential
ECFC	Experimental complex-formation curve

CCFC	Computed complex-formation curve
$E_{1/2}(\text{virt})$	Virtual half-wave potential
GE	Glass electrode
MME	Multi-mode mercury electrode
WE	Working electrode
AE	Auxiliary electrode
RE	Reference electrode
HMDE	Hanging mercury drop electrode
ACV	Alternating current voltammetry
i_{ac}	Capacitive current
pH	Negative logarithm of proton concentration
$\text{p}K_{\text{w}}$	Negative logarithm of the water dissociation constant
$\text{p}K_{\text{a}}$	Negative logarithm of the acid dissociation constant
$K_1 \dots K_n$	Stepwise stability or formation constants
pA	negative logarithm of the free deprotonated ligand concentration
SDD	Species distribution diagram
ACP	Alternating current polarography

I_{red}	Reduction current
I_{b}	Background current
I_{obs}	Observed total current
E_{appl}	Stepwise applied potential
α	Cathodic transfer coefficient
$E_{1/2}^{\text{r}}$	Reversible half-wave potential
$E_{1/2}^{\text{irr}}$	Irreversible half-wave potential
$E_{1/2}^{\text{r}}(\text{virt})$	Virtual reversible half-wave potential

CHAPTER 1

Introduction

Cancer occurs more frequently in humans and is showing ever-increasing impact on the human race. The considerable morbidity and frequency in cancer patients with bone metastases represent a major health and financial problem for any country [1]. Tumour metastasis¹ to the bone is the third most common metastatic site in all cancers but is the second most common site of disease spread in breast and prostate cancer [2].

Malignant bone disease causes the majority of cancer-associated chronic pain, which often requires palliative radiotherapy [3]. Bone-seeking radio-pharmaceuticals play a significant role in the treatment of pain caused by osteoblastic disease. The radio-pharmaceuticals are beta or electron-emitters with a chemical affinity for sites of new bone formation by one of several mechanisms [4]. Other radio-pharmaceuticals which emit gamma rays are used as bone imaging agents [5]. Bisphosphonates (BPs) are widely used in nuclear medicine as ligands for radio-metals in bone-seeking diagnostic and therapeutic agents [6].

Presently extensive animal tests are required in order to describe *in vivo* behaviour of potential radiopharmaceuticals and to verify their degree of success. In most cases failures are not reported and consequently the reasons for unsuccessful results are not well understood. There is a growing opposition from the public towards this approach and, in particular, the large number of animal tests that are performed. It is therefore clear that an alternative approach towards the study and development of radiopharmaceuticals is necessary.

The approach taken in the development of bone-seeking agents relies upon the successful complexation of a radioactive metal by a suitable ligand. Thermodynamic

¹ Spread of cancer from one part of the body to another. Tumors formed from cells that have spread are called “secondary tumors” and contain cells that are like those in the original (primary) tumor.

and kinetic data describes the complexation equilibria and the stabilities of the metal complexes allowing for modelling of the behaviour of the modality. Much of the research carried out to date focused on constructing blood plasma speciation models, using programs such as ECCLES (Evaluation of Constituent Concentrations for Large Equilibrium Studies) [7], for various metal-ligand compounds. Radiopharmaceuticals containing both ^{166}Ho and ^{117}Sn (and also ^{153}Sm for comparison) were studied [8]. ECCLES was used in these studies to gain insight into certain aspects of the *in vivo* behaviour of proposed radiopharmaceuticals in advance, thus, minimising the amount of animal testing [9].

For better understanding of ligand design for radiopharmaceuticals, and construction of blood plasma speciation models using computer blood plasma models for various metal-ligand compounds, the stability constants with different metal ions with ligands are required. Stability constants of certain metal ions, such as Sm(III) and Ho(III) can be estimated from linear free energy correlation, thus, stability constants of a number of metal ions with the ligand are needed for this propose [9].

1.1 Bone Cancer: Remodelling and Metastasis

The skeleton is a complex organ that is composed mainly of two types of specialized connective tissue, namely, cartilage and bone. The skeleton serves three basic functions; *viz* mechanical, protective, and metabolic. It provides support and site for muscle attachment. It protects bone marrow from injury. It serves as a reservoir of calcium and phosphate ions in the body [10].

Bone is a very active tissue. In the developing skeleton, these activities are primarily concerned with bone growth and bone remodelling – the process by which a bone achieves its characteristic size and shape. In the adult skeleton, the processes of growth and modelling are reserved for the repair of gross fractures and microfractures. Normal metabolic activities of the adult skeleton involve predominantly remodelling. Bone remodelling is a life-long and continuous process of destruction and renewal that is intimately related to calcium and phosphate homeostasis. The balance of the two processes, bone formation and resorption, maintains the skeletal integrity [10, 11]. If the balance shifts to the bone resorption, the reduction of bone mass occurs (called

osteoporosis²) [12], and the increase of bone mass (called Paget's disease³) [13,] occurs when the balance shift to the bone formation.

Three types of bone cells that profoundly influence the development and turnover of the skeleton exist within and on the surface of the matrix of mineralised and unmineralized bone. These cells (osteoclasts, osteoblasts, and osteocytes) participate directly in mineral homeostasis [10].

Osteoclasts are primarily responsible for initiating the process of bone remodelling by creating an acidic environment in which a number of secreted enzymes are able to solubilize hydroxyapatite crystals.

The cells responsible for bone formation are osteoblasts. Osteoblasts have two functions with respect to bone formation. They synthesize the collagen matrix of new bone, and they also play a pivotal role in the mineralization or calcification of the newly formed matrix.

Osteocytes are the most numerous of the three bone cell types. They are former osteoblasts that have been become embedded in the bone matrix. It now seems likely that these cells, through their extensive interconnections, are important in maintaining bone integrity. They may additionally play a role in the process of bone remodelling.

Metastases of malignant tumours, particularly breast [14] and prostate cancer [15], occurs preferentially in the skeleton. It is known that bone metastases can also occur by other cancer types such as thyroid, lung, and kidney. Most metastatic lesions in humans are found in the red bone marrow areas [16].

The mechanism of spread of malignant tumours to the bone is not fully understood. In general, malignant tumour formed or resulting from interaction between bone cells and bone matrix probably secretes growth factors that stimulate bone remodelling. Normal bone remodelling combines two processes: (i) bone resorption and (ii) bone formation,

² A condition characterized by a decrease in bone mass and deterioration in the bone microarchitecture, resulting in increased bone fragility and fracture risk.

³ A condition characterized by an increased bone density secondary to the production of bony lesions and deformities.

carried out by osteoclasts and osteoblasts, respectively. The normal bone balance is maintained by synchronized action of bone resorption, and bone formation. Once the bone is colonized by cancer cells, the balance between two processes is no longer maintained. This results in the change in bone resorption (lytic tumours), bone formation (blastic tumours), or both (mixed tumours) at the site of metastasis due of cytokines and growth factors released by metastatic cells [16].

The most frequent form of cancer metastases that are particularly common in breast cancer patients is lytic bone metastases, which develops faster, and present major clinical problem due to increased propensity for fractures associated with pain and disability. The blastic type characterised by bone formation is most common in prostate cancer and has a lesser impact on bone health relative to lytic tumours [16].

Patients with bone cancer present several complications such as pathological fracture, severe pain, cranial nerve palsies, spinal cord compression, bone marrow suppression, and hypercalcaemia. Pain is the major symptom caused by a variety factors that alter quality of life of the patients [17]. Treatment modalities includes: surgery, external beam radiotherapy, endocrine treatments, chemotherapy, bisphosphonates (BPs), and radioisotopes [18]. The latter is currently an area of considerable interest and involves the use of radiopharmaceuticals.

It is well known that BPs have ability to reduce bone resorption and inhibit osteoclast function [19]. The presence of amino group in aliphatic carbon chain increase antiresorptive activity of BPs [12, 20].

1.2 Radiopharmaceuticals in Bone Cancer

Radiopharmaceuticals have been defined as drugs containing a radioactive substance that is used in the diagnosis and treatment of cancer and pain (palliative) management of bone metastases [21].

Bone scintigraphy with technetium-99m, as method for diagnosis of bone metastases, has been used in medicine. Technetium-99m has a half-life of six hours, emits gamma rays and low energy electrons. The gamma rays are easily detected by a gamma camera

[22]. The use of BPs as bone scanning agents to detect metastases is due to its strong binding to bone mineral, and its ability to link to a gamma-emitting technetium isotope [23]. Methylene-diphosphonic acid (MDP) [24] and (3-aminohydroxypropylidene)-1-1-disphosphonate (APD) [25] are some of BPs that are used as bone scanning agents and they can be labelled with technetium-99m. The mechanism of uptake of bone-seeking radiopharmaceuticals is not completely understood. It is thought that the uptake occurs by chemisorption of the phosphonate group onto the calcium of hydroxyapatite in bone [26].

The treatment of bone metastases is usually palliative; there are no specific modalities available yet for curing malignant cells. It is important in the design of a radiopharmaceutical, to consider optimal dose of radiation for relief of pain with low bone marrow toxicity [4].

Iodine-131, phosphorus-32, strontium-89, samarium-153, holmium-166 and rhenium-186 are some beta-emitting radioisotopes usually used for pain relief. They differ in terms of efficacy, duration of pain relief, ability to repeat treatments, toxicity, and expense [16]. Goeckeler *et al* [27] reported good skeletal localization of ^{153}Sm -EDTMP which is ideal for radionuclide therapy.

The radionuclide used as radiopharmaceutical with a specific ligand, must be deposited to hydroxyapatite by dissociation from its respective ligand. The rate and extent of this reaction depend on the kinetic and thermodynamic stability of the complexes in general [28].

1.3 Bisphosphonate Ligands in Bone Cancer

Bisphosphonate compounds (BPs) have been identified as suitable ligands for the complexation of radioactive metal isotopes, and are a major class of drugs for treatment of bone diseases. They are analogues of pyrophosphate (P-O-P) with a carbon instead of an oxygen atom (P-C-P), which gives them, more chemical stability and possibility of many structural variations [19, 29]. Some compounds exhibit short side chains, such as clodronate (Cl2) and etidronate (HEDP); others have aliphatic chains of different lengths bearing terminal amino groups (pamidronate (APD), alendronate (ALN) and

neridronate (NED)). The latter BPs are several orders of magnitude more potent at inhibiting bone resorption *in vivo* than the simple bisphosphonates [16]. Among the last BPs with cyclic side chains, zoledronate with a nitrogen atom in an imidazole ring is the most potent bisphosphonate described so far to inhibit bone resorption [30].

A comparative study of three BPs ligands, pamidronate $-(\text{CH}_2)_2\text{NH}_2$, alendronate $-(\text{CH}_2)_3\text{NH}_2$, and neridronate $(\text{CH}_2)_5\text{NH}_2$, varying only in the length of their aliphatic chain attached to the bridging carbon, suggested that interactions involving these chains affect the ability of the BPs to act as anti-resorption agents. [30].

BPs have been reported to inhibit bone resorption by cellular effects [29]. The exact molecular mechanism by which BPs inhibit bone resorption are becoming clearer. BPs such as clodronate (Cl2) and etidronate (HEDP) can be metabolically incorporated into nonhydrolysable analogue of adenosine triphosphate (ATP) that may inhibit ATP-dependent intracellular enzymes. The more potent N-BPs (such as APD, ALN) interfere with other metabolic reactions, for example, can inhibit enzymes of the mevalonate pathway, and may affect cellular activity and cell survival by interfering with protein prenylation and therefore the signalling functions of key regulatory proteins. The inhibition of protein prenylation and the disruption of the function of these key regulatory proteins explains the loss of osteoclast activity and induction of apoptosis. BPs also prevent bone mineral (hydroxyapatite) dissolution and therefore have been considered as ligands to complex radioactive metals for new bone therapeutic radiopharmaceuticals [29, 31].

BPs have the potential to exercise anti-tumour effects *in vivo* in bone metastases as the local concentration is increased due to resorption of BP-loaded bone. This high local concentration of BPs is thought to cause the tumour reduction in bone. [30].

1.4 Linear Free Energy Relationship

The linear free energy relationship (LFER) was firstly used in organic chemistry with correlations involving rates and proton basicity of many organic aromatic bases. Other relationships can be derived between free energies or rates of complex formation of sets of complexes and properties of the metal ions, ligands, or complexes [32].

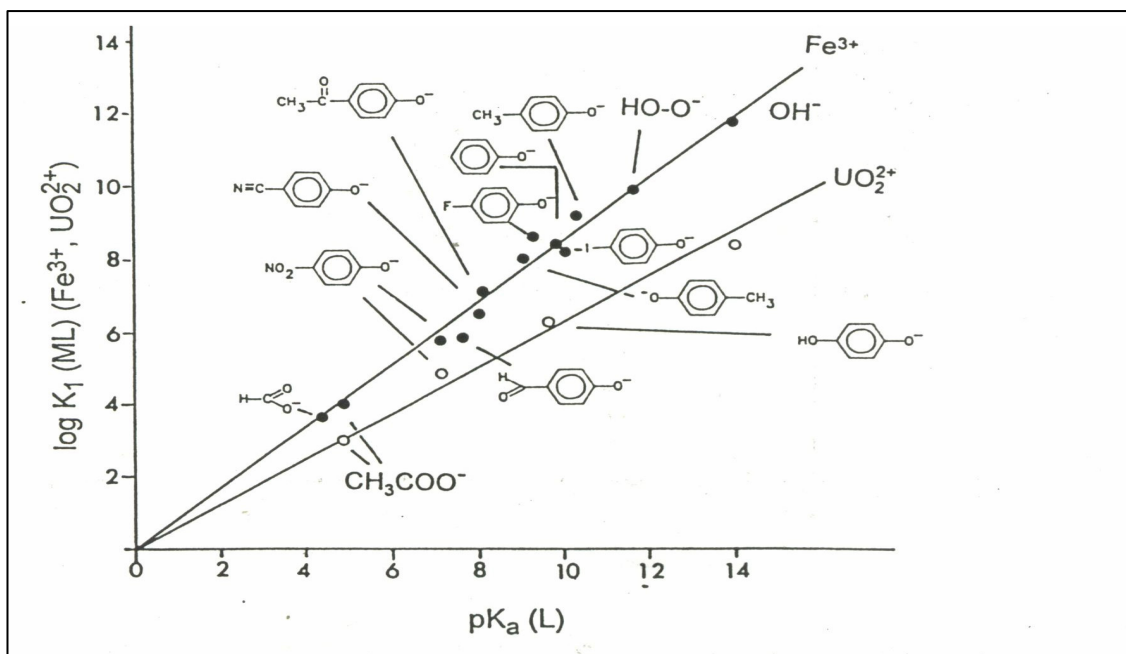


Figure 1.1 Linear free energy relationships for $\log K_1$ (ionic strength = 0, $t = 25^\circ\text{C}$) for Fe^{3+} and UO_2^{2+} vs. ligand $\text{p}K_a$ for unidentate ligands with negatively charged oxygen donors [32].

Extra-thermodynamic relationships were also used in the derivation of such regularities. The LFER can be used to predict unknown formation or rate constants that for various reasons are impossible to study directly. The first observation of LFER was correlation between protonation constant of the ligand and $\log K_{\text{ML}}$ for the metal ions [33] as shown in Figure 1.1.

A linear correlation was observed on the graph $\log K_{\text{ML}}$ for Fe^{3+} and UO_2^{2+} vs. protonation constants of the ligands for a series of unidentate RO^- type ligands (phenols and carboxylic acids). The linearity of the relationship demonstrates that factors that increase or decrease the $\text{p}K_a$ of the ligand by increasing or decreasing the electron density on the oxygen donor atoms, affects the $\log K_1(\text{ML})$ values in a parallel manner, see Figure 1.1 [34].

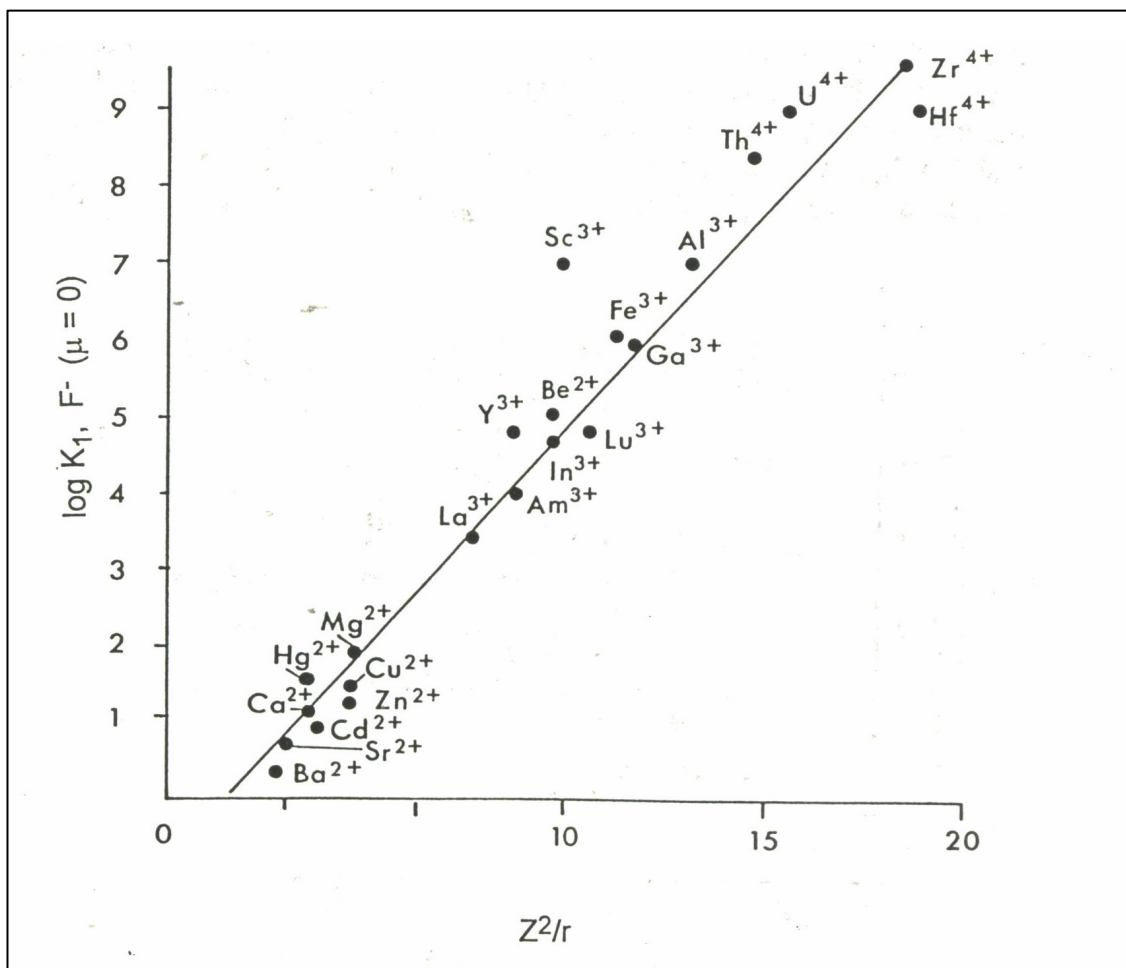


Figure 1.2 Relationships between $\log K_1$ for fluoride complexes of metal ions vs. Z^2/r , where Z is the cationic charge on the metal ion, and r the ionic radius. Formation constant data at ionic strength = 0, $t = 25\text{ }^\circ\text{C}$ [32].

The LFER of $\log K_1$ values against non-thermodynamic properties of the metal ions or ligands may be also drawn. A correlation of $\log K_1$ (F^-) for a variety of metal ions against Z^2/r (Z = cationic charge, r = ionic radius) for the metal ions is shown in Figure 1.2. This plot indicates that the M-F bonds are largely electrostatic [34].

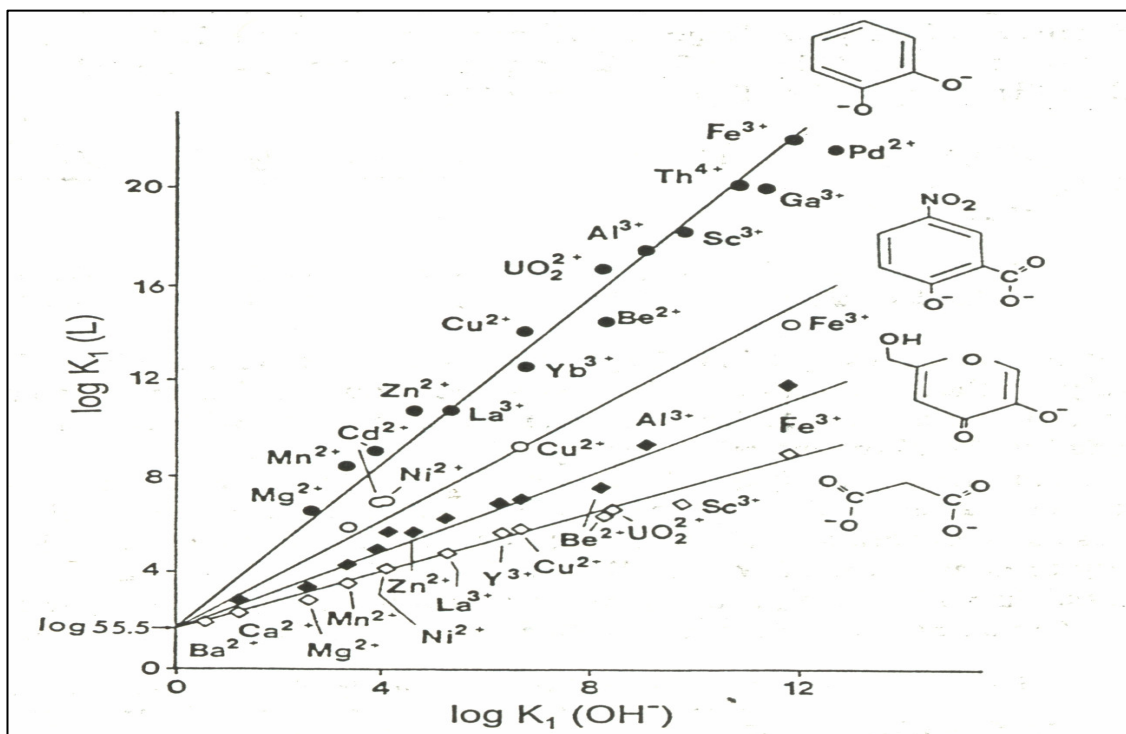


Figure 1.3 Relationship between $\log K_1$ for chelating ligands containing negative oxygen donors, and $\log K_1$ for the formation of the hydroxide complex, for a variety of metal ions. The ligands shown are catechol (●), 5-nitrosalicylic acid (○), Kojate (◆), and malonate (◇). Formation constants data at ionic strength = 0, and 25 °C [32].

Hancock and Martell [32] found that LFER exist between $\log K_1(ML)$ for the ligands containing RO^- donors and $\log K(MOH)$. The affinity of the metal ion for the chelate with negatively charged oxygen donors is a simple function of $\log K(MOH)$, as shown in Figure 1.3 [32].

1.5 Previous Studies of Bisphosphonate Ligands

Methylene diphosphonic acid (MDP), 1-hydroxy-ethylene-diphosphonic acid (HEDP) and 1-hydroxy-3-amino-propylidene-diphosphonic acid (APD) with metal ions such as Mg(II), Ca(II), Sr(II), Zn(II) [35], Ni(II) [36] and Cd(II) [9] among others, have been studied by GEP and polarographic techniques. Zeevaart *et al* [8] introduced LFER in order to estimate the first formation constants of Sm(III) and Ho(III) involving these ligands.

Few studies have been performed with BPs ligands, ALN and NED with metal ions. Hägele *et al.*[37] determined protonation constants of HEDP, APD and ALN using

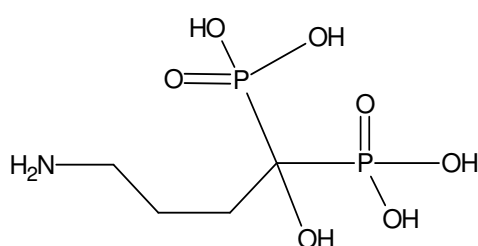
NMR technique. The protonation constants of ALN and NED, and stability constants of Ca(II), Co(II), and Cu(II) with ALN were determined by Katkov *et al.* [38] using thermodynamic methods without need for numerical and graphical differentiation.

1.6 Research Aims

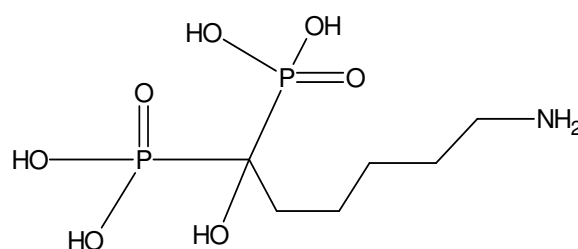
The aims of this study are as follows:

- (i) Developing methodologies for elucidation of reliable metal–ligand speciation models allowing for the accurate determination of concentration equilibrium constants for metal ion complexation equilibria with N-containing bisphosphonate ligands that are potentially useful as complexing agents in radiopharmaceuticals
- (ii) Consider the influence of the length of aliphatic chain of the N-containing bisphosphonate ligands on complex formation, reaction and stability constants.
- (iii) Estimate stability constants of $^{153}\text{Sm(III)}$ and $^{166}\text{Ho(III)}$ using Linear Free Energy Relationship (LFER).

The structures of the ligands studied in this work are shown below:



Alendronate



Neridonate

1.7 References

- [1] J.C. Dumon, F. Journé, N. Kheddoumi, L. Lagneaux and J.J. Body, *European Urology*, Vol. 45, Issue 4, **2004**, p. 521.
- [2] E.C. Li, PharmD, L.E. Davis, and PharmD, *Clinical Therapeutics*, Vol. 25, No. 11, **2003** p. 2669.
- [3] F. Saad and C.C. Schulman, *European Urology, Review*, 45, **2004**, p. 26.
- [4] E.B. Silberstein, *Semin Nucl Med* , Vol. 35, **2005**, p. 152.
- [5] K.T. Cheng, S.M. Shaw, T.C. Pinkerton, D.J. Hoch and D.C.V. Sickle, *Int. J. Nucl. Med. Biol.*, Vol. 12, No. 3, **1985** p. 197.
- [6] S.S. Jurisson, D. Berning and W. Jia, *Chem Rev.*, Vol. 93, **1993** p.1137.
- [7] P.M. May, D.R. Williams and P.W. Linder, *J. Chem. Soc. Dalton Trans.*,**1977**, p. 588
- [8] J.R. Zeevaart, Metal Ion Speciation in Blood Plasma as a Tool in Predicting the In vivo Behaviour of Potential Bone-seeking Radiopharmaceuticals, Ph.D. Thesis, Delft University Press, The Netherlands, **2001**.
- [9] I. Cukrowski, J.R. Zeevaart and N.V. Jarvis, *Anal. Chim. Acta*, Vol. 379, **1999**, p. 217.
- [10] E. Shane and J.P. Bilezikian, in: O.L.M. Bijvoet, H.A. Fleish, R.E. Canfield and R.G.G. Russel (Eds), *Bisphosphonates on Bones*, Elsevier, Amsterdam, **1995**, p. 3.
- [11] M.W. Lark and I.E. James, *Current Opinion in Pharmacology*, Vol. 2, **2002**, p. 330.
- [12] G.Y. Boivin, P.M. Chavassieux, A.C. Santora, J. Yates and P.J. Meunier, *Bone*, Vol. 27, No. 5, **2000**, p. 687.
- [13] P. Filipponi, S. Cristallini, G. Policani, C. Casciari and F. Gregorio, *Bone*, Vol. 23, No. 6, **1998**, p. 543.
- [14] A.T.M. van Holten–Verzantvoort, in: O.L.M. Bijvoet, H.A. Fleish, R.E. Canfield and R.G.G. Russel (Eds), *Bisphosphonates on Bones*, Elsevier, Amsterdam, **1995**, p. 365.
- [15] J. Pinski and T.B. Dorff, *European Journal of Cancer*, Vol. 41, Issue 6, **2005**, p. 932.
- [16] C.M. Bagi, *Advanced Drug Delivery Reviews*, Vol. 57, **2005**, p. 995.

- [17] R.D. Rubens, in: O.L.M. Bijvoet, H.A. Fleish, R.E. Canfield and R.G.G. Russel (Eds), *Bisphosphonates on Bones*, Elsevier, Amsterdam, **1995**, p. 337.
- [18] R.E. Coleman, in: O.L.M. Bijvoet, H. A. Fleish, R.E. Canfield and R.G.G. Russel Eds), *Bisphosphonates on Bones*, Elsevier, Amsterdam, **1995**, p. 349.
- [19] D. Heymann, B. Ory, F. Gouin, J.R. Green and F. Rédini, *TRENDS in Molecular Medicine Review*, Vol. 10, No.7, **2004**, p. 337.
- [20] V. Braga, D. Gatti, F. Colapietro, E. Battaglia, D. Righetti, R. Prizzi, M. Rossini and S. Adami, *Bone*, Vol. 33, **2003**, p. 342.
- [21] <http://www.radiochemistry.org/nuclearmedicine/radiopharma-define>.
- [22] <http://www.radiochemistry.org/nuclearmedicine/diagnostics/index>.
- [23] G.H. Nancollas, R. Tanga, R.J. Phipps, Z. Henneman, S. Gulde, W. Wu, A. Mangood, R.G.G. Russell and F.H. Ebetino, *Bone*, Vol. 38, Issue 5, **2006**, p. 617.
- [24] R. Chisin, D. Gazit, M. Ulmansky, A. Laron, H. Atlan and J. Sela, *Nucl. Med. Biol.* Vol. 15, No. 4, **1988**, p.469.
- [25] O.J. Degrossi, P. Olivri, H. Garcia del Rio, R. Labriola, D. Artagavery and E.B. Degrossi, *J Nucl Med*, Vol. 26, No. 10, **1985**, p. 1135.
- [26] P.J. Ryan and I. Fogelman, in: O.L.M. Bijvoet, H.A. Fleish, R.E. Canfield and R.G.G. Russel (Eds), *Bisphosphonates on Bones*, Elsevier, Amsterdam, **1995**, p. 87.
- [27] W.F. Goeckeler, D.E. Troutner, W.A. Volkert, B. Edwards, J. Simon and D. Wilson, *Nucl. Med. Biol.*, Vol. 13, No. 4, **1986**, p. 479.
- [28] W.A. Volkert and T.J. Hoffman, *Chem. Rev.*, Vol. 99, **1999**, p. 2269.
- [29] R.G.G. Russel and M.J. Rogers, *Bone*, Vol. 25, No. 1, **1999**, p. 97.
- [30] M. Neves, L. Gano, N. Pereira, M.C. Costa, M.R. Costa, M. Chandia, M. Rosado and R. Fausto, *Nuclear Medicine and Biology*, Vol. 29, **2002**, p. 329.
- [31] M.J. Rogers, *Calcif Tissue Int*, Vol. 75, **2004**, p. 451.
- [32] A.E. Martell and R.D. Hancock, *Metal Complexes in Aqueous Solutions*, New York: Plenum Press, **1996**.
- [33] E. Larson *Z. Phys. Chem.*, A. Vol. 32, **1934**, p. 169.
- [34] L.P. Hammett, *Physical Organic Chemistry*, New York: McGraw-Hill, **1940**.
- [35] J.R. Zeevaart, N.V. Jarvis, W.K. A. Louw, G.E. Jackson, I. Cukrowski and C.J. Mouton, *J. Inorg. Biochem.*, Vol. 73, **1999**, p. 265.

- [36] I. Cukrowski, D.M. Mongano and J.R. Zeevaart, *J. Inorg. Biochem*, Vol. 99, **2005**, p. 2308.
- [37] G. Hägele, Z. Szakács, J. Ollig, S. Hermens and C. Pfaff, *Hetroatom Chemistry*, Vol. 11, No. 7, **2000**, p. 562.
- [38] A.P. Katkov, T.A. Matkovskaya, T.M. Balashova, A.S. Monakhov and G.R. Allakhverdov, *Zhumal Fizicheskoi Khimii*, Vol. 63, No. 6, **1989**, p. 1459.

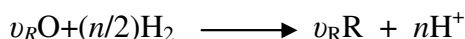
C H A P T E R 2

Theory and Data Treatment

2.1 Potentiometry

2.1.1 General Principles

The main use of potentiometry is to measure the concentration (strictly activity) of a target analyte. For this purpose, consider a simple redox reaction:



where, v_i ($i = O$ or R) represents the stoichiometric coefficients. Since the activities of H^+ and H_2 in the SHE are unities, the *Nernst equation*, describing the potential of the O / R couple as a function of the activities of O and R is

$$E = E^o - \frac{RT}{nF} \ln \frac{a_R^{v_R}}{a_O^{v_O}} \quad (2.1)$$

or in terms of concentrations:

$$E = E^o - \frac{RT}{nF} \ln \frac{\gamma_R^{v_R}}{\gamma_O^{v_O}} - \frac{RT}{nF} \ln \frac{[R]^{v_R}}{[O]^{v_O}} \quad (2.2)$$

were γ_i ($i = O$ or R) denotes the activity coefficients. Under conditions in which the activities are effectively constant (for example in systems with large excess of supporting electrolyte), we may introduce the formal potential, $E^{o'}$, of the O / R couple as follows:

$$E^{o'} = E^o - \frac{RT}{nF} \ln \frac{\gamma_R^{v_R}}{\gamma_O^{v_O}} \quad (2.3)$$

allowing us to simplify the Nernst relation:

$$E = E^{o'} - \frac{RT}{nF} \ln \frac{[R]^{v_R}}{[O]^{v_O}} \quad (2.4)$$

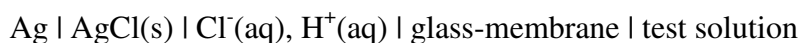
It is convenient to express Equation. 2.4 on a \log_{10} scale so that

$$E = E^{o'} - \frac{2.303RT}{nF} \log_{10} \frac{[R]^{v_R}}{[O]^{v_O}} \quad (2.5)$$

When evaluating the prelogarithmic term, it follows that the potential of the cell changes by $\pm 59/n$ mV (at 298 K) for a decade change in concentration of either the O or R species (for $v_O = v_R = 1$), which is the basis of analytical potentiometry.

To record the potential of such a system, one would typically use an inert metal, such as Pt, as the indicator electrode. There are many other examples of potentiometric electrodes, including a metal in contact with a solution containing the corresponding metal ions, as in the case of the Ag | Ag⁺ electrode.

The glass electrode is by far the most common potentiometric electrode for measuring the pH of aqueous, partially aqueous, and some nonaqueous systems. It is a type of membrane electrode with general form:



The electrode response in aqueous solution at 25 °C can be given as:

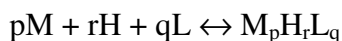
$$E = E' - E_{j2} + \frac{2.303RT}{nF} \log a(\text{H}^+) \quad (2.6)$$

where E' incorporates the difference in reference-electrode potentials, and E_{j2} is the liquid junction potential. The factor $2.303RT/nF$ is the slope of ion-selective electrode (ISE) and is determined by calibration of the ISE. When electrode response is rapid, the stable potentials are generally achieved fast. The potential across the glass-barrier membrane is measured with reference electrodes in each phase. The functioning of the glass electrode is complicated [1-2].

2.1.2 Equilibrium Studies of Metal-Ligand Systems

Potentiometric method for determining stability constants was used by Arrhenius, Ostwald and Nernst, who provided the basis for the introduction of electrodes responding reversibly and selectively to only one species present in solution. Approximately 80 % of the stability constants reported in the literature were determined by potentiometry [3].

In the determination of the thermodynamic stability constants, attention must be given to the choice of standard states, units and activity coefficients. The thermodynamic stability constant, for the system shown below is defined by Equation 2.7.



$$\beta_{M_pH_rL_q}^{th} = \frac{\{M_pH_rL_q\}}{\{M\}^p\{H\}^r\{L\}^q} \quad (2.7)$$

where $\beta_{M_pH_rL_q}^{th}$ is the thermodynamic overall stability constant marked by the superscript *th* for the formation of complexed species $M_pH_rL_q$. Negative subscripts for hydrogen ion refer to complex formation reactions in which a hydrogen ion is eliminated. In Equation 2.7, the brackets { } denote activity [3]. In this chapter charge will be omitted for simplicity.

The determination of activities of complex ionic species under real conditions and at infinite dilution is very difficult. To avoid this difficulty, stability constants have been

determined in the presence of relatively large concentration of inert electrolytes; hence the activity coefficients can be taken as constant [4]. Thus, equilibrium concentrations for overall formation constants replaces the activity constants and are calculated from the experimental measurements as shown in Equation 2.8

$$\beta_{M_pH_rL_q} = \frac{[M_pH_rL_q]}{[M]^p[H]^r[L]^q} \quad (2.8)$$

The concentrations of the species involved in Equation 2.8 can be substituted directly into the mass-balance equations used in solving the equations for the equilibrium constant or stability constant of the metal ion complexes.

In the application of the potentiometric method, the problem is to determine the nature of all the species present in the solution from the measured pH, using a pH-electrode, for example, a glass electrode-reference electrode system. Below pH 2 and above pH 12, hydrogen ion and hydroxide ions begin to be responsible for appreciable fractions of the conductance, so that liquid junction potentials change as the pH is lowered and raised below and above these limits. Accurate measurements of hydrogen ion concentration (or activity) with a glass electrode-reference electrode system are restricted therefore to the pH range 2–12 [3].

A precondition for the appropriate application of potentiometric equilibrium measurements is the suitable calibration of the electrode system. For calibration of the glass electrode, a strong acid-base titration is first performed in the presence of a background electrolyte [5].

The titration method is employed in the course of potentiometric measurements because is a rapid method for the study of systems in which the equilibrium state is attained within at most a few minutes [5]. The essence of the potentiometric experiment involving a glass electrode is the monitoring of the change in the free proton concentration throughout the experiment. During potentiometric titrations the free proton concentration varies due to neutralization of mineral acid, deprotonation of a ligand, and the formation of metal-containing complexes. The change in hydrogen ion

concentration is monitored by the direct readings of the potential of a calibrated glass electrode. It is important that the change in hydrogen ion concentration in potentiometry comes predominantly from the formation of metal complexes to provide enough information about their formation [6-7].

For determination of all parameters of chemical model simultaneously, the use of computer methods is preferred. Various models are tested until the best one is obtained. Good experimental data of as high precision as possible, with no systematic and low random errors is the necessity.

2.1.3 The Analysis of Data

The potentiometric titration data was analysed by ESTA (Equilibrium Simulation for Titration Analysis), a library of computer programs described by P.M. May *et al.* [8-9]. These programs provide an investigative tool in the determination of formation constants. The programs are used to calculate equilibrium distributions of chemical species, to analyse and manipulate potentiometric titration data.

The mass-balance equations for a system of NR reactants and N species can be written in general way:

$$T_i = c_i + \sum_j q_{ij} \beta_j \prod_k c_k q_{kj} = c_i + \sum_j q_{ij} C_j \quad (2.9)$$

where T_i and c_i are the total analytical and free concentration of the reactant i , q_{ij} is the stoichiometric coefficient of the species j for the reactant i , β_j is the stability constant of the species j , and C_j refers to the concentration of the species j . The experimentally known quantities in a potentiometric titration are: (i) the initial analytical concentrations of the reactants in the solution; (ii) the added volumes of the titrant solution of known concentration; and (iii) the free concentration of one (or more) reactants in the solution, which implies previous calibration of the potentiometric cell.

There are NR mass-balance equations at each potentiometric point. For NP titration points, there will be $NR \times NP$ mass-balance equations. As one or more free

concentrations (NE) are measured potentiometrically, and N stability constants should be estimated, there is a total of $(NR - NE) \times NP + N$ parameters to be evaluated. Usually not all the stability constants of one system should be evaluated with the same data, and often the simpler equilibria are studied previously.

There are three kinds of quantities or parameters in the mass balance equations, namely, (i) those which are common to all the titration points (stability constants); (ii) those which are only common to each titration (initial concentration of the reactants, initial volume, electrode-calibration parameters, titrant concentration) from which the analytical concentrations at each titration point will be calculated, and those particular to each titration point (unknown free concentrations).

In order to estimate the unknown parameters (e.g., the stability constants), the least-squares method is used. In this procedure, the simultaneous optimization of the unknown parameters, x_1, x_2, \dots, x_N is achieved through minimization of the error square sum:

$$U = \sum_i w_i (f_{oi} - f_i(x_1, x_2, \dots, x_N))^2 = \sum_i w_i (f_{oi} - f_{ci})^2 \quad (2.10)$$

where f_{oi} are the observed quantities and $f_i(x_1, x_2, \dots, x_N) = f_{ci}$ are the corresponding calculated values, by means of a functional relationship which is assumed to be known; w_i are the weights of each observation i . In general, f_{ci} is considered to be a non-linear function of the parameters to be estimated [10].

A Gauss-Newton and Levenberg-Marquardt method is the most frequent approach used for minimizing objective function (U), and this has also been adopted in ESTA as the main means of optimization [9].

ESTA accommodates chemical systems of up to 10 components forming up to 99 complexes. Titrations involving up to three electrodes and three burettes are permitted. The programs can take into account variations in ionic strength and the associated changes in activity coefficients. They also permit corrections of titration data affected

by liquid-junction potentials and imperfect ion-selectivity of electrodes. The ESTA library contains program modules, many of which perform more than one kind of calculation (specified as different “task”). In this dissertation ESTA1 and ESTA2 modules will be described as they have been used in this work [9].

ESTA 1: the simulation module

By setting up and solving the mass-balance equations, ESTA1 can determine, on a point-by-point basis, single values for almost any titration parameter. The calculations fall into two categories: (i) species-distribution calculations and (ii) potentiometric titration calculations. The latter include determination of *emf* values, formation constants estimates, total analytical concentrations, initial vessel concentrations, and initial burette concentrations. Formation function values (task *ZBAR*), deprotonation function values (task *QBAR*) and protonation values (task *NBAR*) are commonly generated by this program [9]. In this project the *ZBAR* task was used for modelling of GEP data.

The protonation formation function $ZBAR(H)$ [11] is the average number of protons bound per ligand at a certain pH value and is defined as

$$ZBAR(H) = \frac{[H_T] - [H^+] + [OH^-]}{[L_T]} \quad (2.11)$$

where $[H_T]$ and $[L_T]$ are total concentrations of protons and ligand.

The metal formation function $ZBAR(M)$ [11] is the number of ligands bound per metal ion defined as

$$ZBAR(M) = \frac{L_T - A \left(1 + \sum_{n=1}^N \beta_{n01} [H^+]^n \right)}{M_T} \quad (2.12)$$

where

$$A = \frac{H_T - [H^+] + [OH^-]}{\sum_{n=1}^N \beta_{n01} [H^+]^n} \quad (2.13)$$

The identity of the species that constitute a model can be obtained plotting $ZBAR(H)$ against pH or $ZBAR(M)$ against pL. The nature of dominant species can often be deduced from the shapes of these curves, which provide a useful means of comparing observed and calculated data. Such information can be useful in choosing species as well as providing initial estimates of their formation constants.

ESTA2: the optimisation module

ESTA2A and ESTA2B are two optimisation programs differing in the way the weights are calculated [12]. They are used when it is desired to determine, for one or more parameters, the “best” values, based on a least-squares procedure applied to a whole system of titrations. The following parameters can thus be refined: formation constants, vessel and burette concentrations, electrode intercept, electrode slope, and initial vessel volume. It is possible to group together, over any combination of titrations, local parameters of the same type and with the same value so that they are refined together as a single parameter [9].

2.2 Polarography

2.2.1 General Principles

Polarography, using a dropping mercury electrode (DME) as the working electrode, is the oldest form of voltametry discovered by J. Heyrovský. For his achievements, he was recognised with the Nobel Prize in chemistry in 1959 [13].

The essence of the polarographic technique is the production of a polarogram as a function of applied potential as electroactive species are reduced or oxidized at the working electrode [3]. A three-electrode system is used in conventional direct current (DC) polarography, a *working electrode* (a narrow capillary through which mercury is constantly flowing), a *reference electrode* and an *auxiliary electrode*. The potential is applied between the working and the reference electrode, and the current flow is

measured between the working and auxiliary electrode. The working electrode provides the surface for electron transfer to occur for the system under investigation [13-14].

Before any potential is applied it is necessary to flush the working solution with inert gas, such as nitrogen, in order to remove dissolved oxygen, which causes interference. Immediately, after start of the negative-going potential sweep, small current passes, the so-called *residual current*. This is essentially a charging or capacitive current arising from the charging of the mercury double layer at each drop and is non-faradaic.

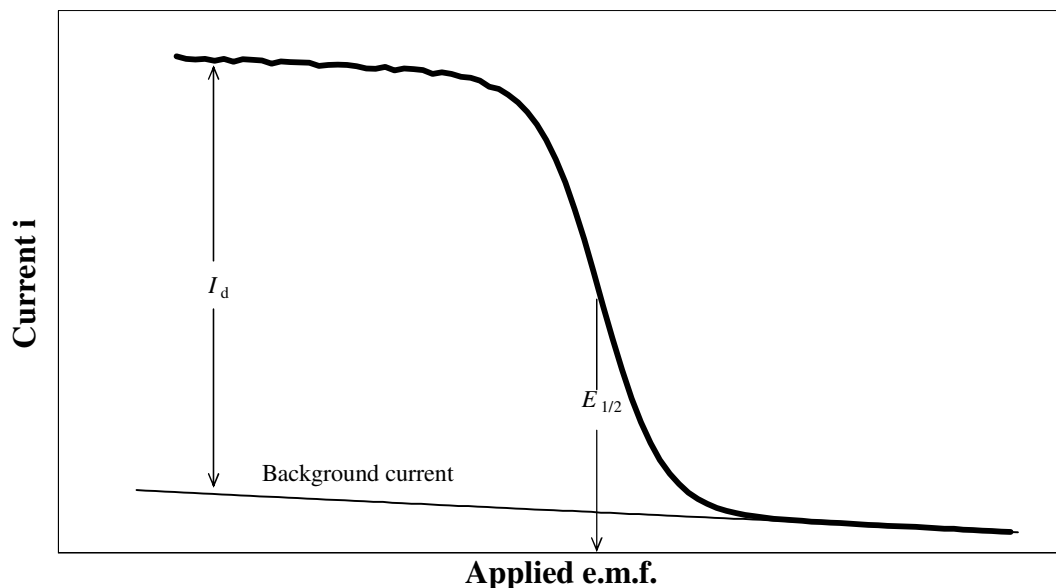


Figure 2.1 An example of a polarogram showing limiting diffusion current, background current and the position of the half-wave potential from DC polarography.

Once the deposition potential of metal is reached by residual current, the current rises rapidly, reaching a limit value (the plateau on the sigmoid) called *limiting current*, whose value is independent of applied potential – see Figure 2.1.

The limiting current is (i) diffusion-controlled and is called the *limiting diffusion current* (i_d) [15] since diffusion is the principal contribution to the flux of electroactive material (ii) is related to analyte concentration by the Ilkovič equation:

$$I_d = 708nD^{1/2} m^{2/3} t^{1/6} c \quad (2.14)$$

where D is the diffusion coefficient of the analyte in the medium (cm^2/s), n is the number of electrons transferred per mole of analyte, m is the mass flow rate of Hg through the capillary (mg/sec), and t is the drop lifetime in seconds, and c is analyte concentration in $\text{mol}/\text{cm}^{-3}$ [16].

Another important parameter is the half-wave potential, ($E_{1/2}$). This is the potential at half the limiting diffusion current value; $E_{1/2}$ is independent of the concentration of electroactive species. Its value is approximately equal to the standard thermodynamic potential, E° , and in general, the $E_{1/2}$ value is a characteristic of the compound undergoing reduction or oxidation. Therefore, it is a parameter that can be used for qualitative characterization of substances [13].

Often, the shapes of polarograms are distorted by current maxima. They interfere with the accurate evaluation of diffusion currents and half-wave potentials. The cause or causes of maxima are not fully understood but can be normally eliminated by the addition of a small quantity of surfactant, such as gelatine, to the solution [17].

Polarography can have definite advantages, and sometimes can provide answers that are inaccessible by other means. Complexes at low pH [7] and low total metal concentration can be studied by polarography. The ability of polarography to work at very low total metal ion concentrations means (i) that precipitation of solid hydroxides will thermodynamically occur at much higher pH values, and (ii) making it advantageous also in situations of low complex solubility. Mercury, as an electrode material, allows one to study systems in potential range from -2.0 to $+0.3$ V vs. SCE, above which mercury dissolves. Another advantage of the electrode is that as each drop forms and falls from the electrode the surface of the mercury is continually kept clean [3, 15].

2.2.2 Selected Voltammetric Techniques

In conventional direct current (DC) polarography, the current is monitored as a function of potential at the mercury drop electrode. Mercury drop formation and its growth during the DC polarographic scan cause the current to increase and produces a large fluctuation in current with time. In addition, the charging of the electrical double layer

(capacitive current) at the drop generally masks the faradaic current when the concentration of electroactive species is in the 10^{-6} to 10^{-5} M region. Thus, the limit of detection is also in this range. However, even in the 10^{-5} to 10^{-4} M concentration range, the magnitude of the charging current is significant. Alternatively, any method automatically compensating for or subtracting the charging current and minimizing fluctuations may be advantageous [3, 13].

(i) Sampled Direct Current Polarography

In sampled DC polarography the potential is varied in a series of steps; the drop time is enforced at a fixed value by dislodging each drop mechanically just after the current is recorded. The measurement from the experiment is a trace of the sampled currents vs. potential, which is equivalent to time; the current flow at the electrode is the same as that observed in conventional DC polarography with a controlled drop time. The difference is that the recording system is fed only by signals proportional to the sampled currents. The improvements in this method yield detection limits near 10^{-6} M, perhaps slightly lower than those of conventional polarographic currents and reduce the large current fluctuation associated with changing drop size. All conclusions about the shapes of waves and all diagnostics developed for conventional measurements of maximum currents also apply to the fast technique [18].

(ii) Normal Pulse Polarography

In normal pulse polarography (NPP), the potential is pulsed (40-60 ms) at the end of the drop life and the current is sampled at the end of the pulse. Potential pulses of gradually increasing amplitude are applied to an electrode, starting from an initial potential where no faradaic current flows. When the mercury drop is dislodged from the capillary by a drop knocker at accurately timed intervals, the potential is returned to the initial value. If the area of the electrode is changing, e.g., in case of a dropping mercury electrode (DME), the pulses are always applied at a fixed time in the life of the drop. The polarogram is obtained by plotting the measured current against each step potential. As a result, the current is not followed during mercury drop growth, and normal pulse polarogram has the typical shape of a sigmoid. The advantage of NPP is in an improved faradaic-to-charging current ratio, [16, 18] and hence lower the detection limit.

(iii) Alternating Current Polarography

The faradaic impedance method is frequently used for the evaluation of the heterogeneous charge-transfer parameters and for studies of double-layer structure. A variation in the faradaic impedance method is called *ac voltammetry* (or, with a DME, *ac polarography*). In these experiments, a three-electrode cell is used in the conventional manner, and the potential program imposed on the working electrode is a *dc* mean value, E_{dc} , which is scanned slowly with time, plus a sinusoidal component, E_{ac} , of 5 to 20 mV peak-to-peak amplitude. The measured responses are the magnitude of the *ac* component of the current at the frequency of E_{ac} and its phase angle with respect to E_{dc} .

In the fundamental mode, one employs phase-sensitive detection to measure the current component in phase with the excitation signal E_{ac} . In contrast, the charging current is ideally 90° out of phase with E_{ac} , since it passes through a purely capacitive element. It therefore has no projection in phase with E_{ac} . Thus, we expect the current in phase to be purely faradaic, whereas the current at 90° (*the quadrature current*) contains a second faradaic component plus the nonfaradaic contribution. By taking the current in phase as the analytical signal, we discriminate effectively against the capacitive interference [18].

2.2.3 Equilibrium Studies of Metal-Ligand Systems

Polarography has been in some ways infamous compared to glass electrode potentiometry as far as the study of solution equilibria is concerned. Reluctance to use polarography relates to the greater ease of interpretation of the results from glass electrode potentiometry, particularly with the advent of computer programs that greatly facilitate analysis of the potentiometric data [3].

Polarography constitutes a powerful and versatile technique for the study of complexes in solution. For many metal-ligand systems it is possible to determine the degree of formation, distribution and stability constants of all species present [19]. As all other voltametric techniques, it is a dynamic and in principle nonequilibrium analytical technique; it does not allow a direct measurement of any free ion concentration. Polarographic measurements, however, result in a signal whose position and intensity depends on the solution composition [7].

Two important different observations in polarographic reduction wave can be seen when metal ions in solution undergo complexation. Firstly, the half-wave potential is shifted, almost invariably in the more negative direction of applied potential. Secondly, the diffusion current usually becomes smaller. The determination of stabilities of metal complexes by polarography involves the determination of shifts in half-wave potential of metal ions in the presence of ligands, relative to the half wave potential for the solution in the absence of ligand. The shift in half-wave potential is towards the more negative direction of applied potential [4, 19].

Several important contributions were made over last 60 years in the studies and development of methods of determination of stability constants. Lingane [20] was the first, he derived an equation (Equation 2.15, at 25 °C) describing a shift in half-wave potential as a function of the excess of a ligand at fixed pH, allowing an evaluation of a stability constant for a single labile metal complex present in a solution when a fully dynamic labile complex and reversible electrochemical processes were observed

$$E = E_M - E_c = \frac{0.0592}{n} \log_{10} \beta_{ML_j} + \frac{0.0592}{n} \log_{10} [L]^j \quad (2.15)$$

where E_M stands the half-wave potential of the free metal ion and E_c is the half-wave potential of the complexed metal ion, $[L]$ is the free ligand concentration, j is the number of ligands in a complex ML_j .

A significant progress was made by DeFord and Hume [21-22]. They modified the Lingane equation [20] to the form that allowed evaluation of stability constants of several complexes formed in consecutive fashion with exactly the same conditions as it was described by Lingane, e.g., titration of a metal ion solution by ligand at fixed pH with strict requirement of full reversibility of electrochemical signal recorded on a dynamic (labile) metal-ligand system. Schaap and McMasters [23] extended the DeFord and Hume methodology to systems involving two competing ligands. All the above methodologies showed very limited field of applications as they were based on a simple data interpretation without involving mass-balance equations.

The most successful methodology for the polarographic study of non-labile complexes was achieved by Schwarzenbach *et al.* [24-25]. It is based on the competition of two metal ions for the equivalent amount of a ligand at fixed pH.

Among many theories and methodologies described in a book by Crow [19] there is not a single contribution that involves mass-balance equations and a typical GEP analytical procedure, e.g., acid-base titration. The analytical procedures employed as well as exclusion of mass-balance equations lead to significantly restricted applications related mainly to the formation of ML_q complexes investigated by a ligand titration at a fixed pH value [7].

New methodology and theory of speciation by polarography was recently developed by Cukrowski [26, 27]. He derived an equation (Equation.2.16) based on mass-balance equations for the study fully labile (dynamic) [28-29], inert (nonlabile) [26, 30] or mixed [31] metal ligand systems on the polarographic time scale at fixed $L_T : M_T$ ratio and varied pH (acid-base titration). Cukrowski's equation [26-27] can be successfully employed in the modelling and refinement operations. A concept of complex formation curves [27-28] (experimental and theoretical) has been used in modelling and refinement operations that involve simultaneous solution of mass-balance equations for $[M_T]$ and $[L_T]$ which also allows a successful use of polarography in the study of polynuclear species [32].

$$(E(M) - E(comp))_{x(i)} - \frac{RT}{nF} \ln \left(\frac{I(comp)}{I(M)} \right)_{x(i)} = \frac{RT}{nF} \ln \left(\frac{[M_T]}{[M]} \right)_{x(i)} \quad (2.16)$$

In Equation 2.16 $E(M)$ and $E(comp)$ stand for the potential (e.g. $E_{1/2}$) in the absence and presence of metal complexes, respectively; $I(M)$ and $I(comp)$ stand for current (limiting diffusion) in the absence and presence of metal complexes, respectively; $x(i)$ stands for pH(i) or $[L_T](i)$ for the i th polarogram recorded during acid-base (at fixed $L_T : M_T$ ratio) or ligand titration (at fixed pH), respectively, of a metal-ligand system under investigation; R, T, F and n have their usual meaning.

Refinement of Stability Constants

Equation 2.16 constitutes the foundation of modelling and refinement operation performed on data coming from voltammetric experiments. The right-hand side of Equation 2.16 can be used as a theoretically computed complex formation curve that has to reproduce the experimental complex formation curve, *i.e.*, the left-hand side of Equation 2.16. It is important to note that the left-hand side in Equation 2.16 can only be calculated when $E(M)$ is available from the experiment. The plot of the left-hand side of Equation 2.16 vs either pH or log [L] generates the experimental complex-formation curve (ECFC) – Equation 2.17.

$$(E(M) - E(C))_{x(i)} - \frac{RT}{nF} \ln \left(\frac{I(C)}{I(M)} \right)_{x(i)} = f(pH \text{ or } pL) \quad (2.17)$$

The ECFC is used as the experimental objective function that has to be reproduced by a theoretical function, the computed complex-formation curve (CCFC) – Equation 2.18.

$$\frac{RT}{nF} \ln \left(\frac{[M_T]}{[M]} \right)_{x(i)} = f(pH \text{ or } pL) \quad (2.18)$$

The refinement of stability constants is achieved by the computation of the free metal ion concentration [M] from mass-balance equations written for the assumed model. The computed [M] is then used by the right-hand side of Equation 2.16. During the iterative operation, the values of refined stability constants are varied. The refinement operation is completed when the CCFC fits best the experimental objective function, *i.e.*, the ECFC.

An experiment involving the determination of a model and stability constants is conducted in such a way that the experimental values of the total metal ion $[M_T]$ and ligand $[L_T]$ concentrations are known at any stage of the experiment. The experimental values of $[M_T]$ and $[L_T]$ can also be computed from the mass-balance equations, *i.e.*, Equations 2.19 and 2.20

$$[M_T] = [M] + \sum_{p=1} \sum_{q=1} \sum_{r=0} p \beta_{M_p L_q OH_r} [M]^p [L]^q [OH]^r + \sum_{x=1} \sum_{y=1} x \beta_{M_x OH_y} [M]^x [OH]^y \quad (2.19)$$

$$[L_T] = [L] + \sum_{p=1} \sum_{q=1} \sum_{r=0} q \beta_{M_p L_q OH_r} [M]^p [L]^q [OH]^r + [L] \sum_{n=1} \beta_n^H [H]^n \quad (2.20)$$

where $\beta_{M_p L_q OH_r}$ and β_n^H stands for the overall stability and protonation constant, respectively, and [M], [L], [H], and [OH] are the free metal ion, free ligand, proton, and hydroxide concentration, respectively. In case of the formation of complexes involving the protonated form of a ligand, e.g., MLH, the term $[M]^p [L]^q [OH]^r$ would be replaced by $[M]^p [L]^q [H]^r$. In this chapter charges are omitted for simplicity.

Let us assume the following arbitrary M-L-OH model that involves MLH, and ML with the hydrolyses species M(OH), M(OH)₂, M(OH)₃, M(OH)₄, M₂(OH), and M₄(OH)₄. For the metal-ligand system assumed, Equations 2.19 and 2.20 would be replaced by Equations 2.21 and 2.22 where K_n^H stands for the stepwise protonation constants of the ligand H₂L. The stepwise protonation constants of the ligand and hydrolyses constants for the metal are kept fixed during the refinement operations [7].

$$\begin{aligned} [M_T] = [M] + & \beta_{M(HL)} [M][L][H] + \beta_{ML} [M][L] + \beta_{M(OH)} [M][OH] + \beta_{M(OH)_2} [M][OH]^2 \\ & + \beta_{M(OH)_3} [M][OH]^3 + \beta_{M(OH)_4} [M][OH]^4 + 2\beta_{M_2(OH)} [M]^2 [OH] \\ & + 4\beta_{M_4(OH)_4} [M]^4 [OH]^4 \end{aligned} \quad (2.21)$$

$$\begin{aligned} [L_T] = [L] + & K_1^H [H][L] + K_1^H K_2^H [H]^2 [L] + \beta_{M(HL)} [M][L][H] \\ & + \beta_{ML} [M][L] \end{aligned} \quad (2.22)$$

The refinement procedure starts with initial guesses for the values of stability constants $\beta_{M(HL)}$ and β_{ML} . The initial guesses for stability constants can easily be calculated by performing a single point calculation at a particular pH value where the free ligand concentration [L] is obtained from a simplified form of Equation 2.22 solved with an assumption that all the ligand is involved only in the protonation reactions; [H] is

obtained from a direct pH measurement. Equations 2.21 and 2.22 must hold at any stage of the experimental procedure (here after each addition of the standardized NaOH solution) and represent the calculated the total metal ion and ligand concentrations at each pH(i) value. Hence we know analytical concentrations of M_T and L_T throughout the experiment, we can write

$$\{[M_T](exp)\}_{pH(i)} = \{[M_T](calc)\}_{pH(i)} \quad (2.23)$$

$$\{[L_T](exp)\}_{pH(i)} = \{[L_T](calc)\}_{pH(i)} \quad (2.24)$$

where, *exp* and *calc* stands for experimental and calculated values. Equations 2.23 and 2.24 are solved at each pH(i) value simultaneously (with particular values of refined stability constants) for the free metal ion and free ligand concentrations. The free metal ion concentration obtained at each pH(i) value is then used by the right-hand side of Equation 2.16. The value generated by the right-hand side of Equation 2.16 is compared with the left-hand side of Equation 2.16. This is followed by a change in the refined values of stability constants in such a way that the computed free metal ion concentration from Equations 2.21 and 2.22 will reproduce the objective function ECFC best for all experimental points collected.

The refinement operations employed in the evaluation of polarographic data do not include mass-balance equation for the total proton concentration $[H_T]$. This is the fundamental difference between the voltammetric and potentiometric theories and mathematical procedures employed. The free proton or hydroxide concentrations ($[H]$ and $[OH]$) are obtained directly from the pH measurements by the calibrated glass electrode and K_w for water [7, 33].

2.3 Virtual Potentiometry

Polarography is a dynamic electrochemical technique that involves many complex processes occurring at the electrode-solution interface, among them thermodynamics, kinetics and transport. In the study of metal complexes by polarography the experimental recorded change in the observed signal, e.g., $\Delta E_{1/2}$ is used rather than

theoretically predicted position of a signal along the potential scale because often it is impossible to predict theoretically the observed polarograms.

From Equation 2.16, it is seen that all recorded curves, e.g., $E(comp)$ are compared with a single experimental value of $E(M)$. The shift in the half-wave potential is used and not the observed values ($E_{1/2}$) at each $pH(i)$. This means, the refined stability constants must change with the change in the experimental value of $E(M)$ even though the metal-ligand model together with the overall fit of CCFC in ECFC and the standard deviations in stability constants will remain the same. This implies that $E(M)$ value must be determined with as highest accuracy as possible [7, 33-34]. However, the experimental value of $E(M)$ is not always accurate [29], or it might be unavailable [6, 33].

In Equation 2.16 the term $I(comp)/I(M)$ represents the normalised change in the intensity of the recorded polarographic signal. The change in the recorded current (I_d) can be due to the change in the diffusion coefficients of different labile metal complexes formed [19] as well as the formation of polarographically inactive metal complexes [6, 26, 30-33]. Cukrowski has interpreted the term $\{(RT/nF)\ln(I(comp)/I(M))\}_{pH(i)}$ as a fraction of a potential (experimentally not observed) by which the recorded polarographic signal should have shifted more provided that there was no change in the value of intensity of the recorded polarographic wave. With this supposition holding, the expected (or corrected) position of the polarographic signal can be written as

$$\left(E(comp) + \frac{RT}{nF} \ln \left(\frac{I(comp)}{I(M)} \right) \right)_{X(i)} = E(virt)_{X(i)} \quad (2.25)$$

and it can be calculated at any $pH(i)$ from available experimental data. There is a well defined relationship between $E_{1/2}$ and the standard redox potential if the system under investigation can be regarded as thermodynamically fully reversible. The concept of virtual potential ($E(virt)$) was interpreted as a thermodynamic potential of a virtual sensor or probe obtained from dynamic, non-equilibrium polarographic data. This virtual potentiometric sensor must be sensitive to the change in the free metal ion concentration when metal complexes are formed and is metal ion non-specific and yet should be able to work for any metal ion that is polarographically active and reversibly reduced. With reversible reduction as prerequisite, the virtual sensor must have a linear

response with the Nernstian slope in unlimited concentration range of the free metal ion concentration.

The concept of virtual potentiometric sensor implies that it should be possible to employ potentiometric software, such as ESTA [8-9] in the refinement of stability constants using, in principle, data coming from a dynamic electrochemical technique.

From the above it follows that virtual potential $E(\text{virt})$ rather than the $E(\text{comp})$, obtained directly from the experiment, should be used in modelling of a M-L-OH system when analysis of slopes, such as E vs pH , E vs log [HL], or E vs log [L], is employed.

2.4 References

- [1] Bard–Stratman, Encyclopedia of Electrochemistry–Instrumentation and Electroanalytical Chemistry, Volume 3, Edited by Pat Unwin, **2003**.
- [2] J.A. Plambeck, Electroanalytical Chemistry: Basic Principles and Applications, New York: John Wiley & Sons, **1982**
- [3] A.E. Martell and R.D. Hancock, Metal Complexes in Aqueous Solutions, New York: Plenum Press, **1996**.
- [4] G.H. Nancollas and M.B. Tomson, *Pure and Applied Chemistry*, Vol. 54, **1982**, p. 2676.
- [5] M.T. Beck and I. Nagypal, Chemistry of Complex Equilibria, New York: John Wiley & Sons, **1990**.
- [6] I. Cukrowski and J.M. Zhang, *Chem. Anal.* Vol. 50, **2005**, p. 3.
- [7] I. Cukrowski, J.M. Zhang and A. Van Aswegen, *Helv. Chim. Acta*, Vol. 87, **2004**, p. 2135.
- [8] P.M. May, K. Murray and D.R. Williams, *Talanta*, Vol. 32, No. 6, **1985**, p. 483.
- [9] P.M. May, K. Murray and D.R. Williams, *Talanta*, Vol. 35, No. 11, **1988**, p. 825.
- [10] E. Casassas, R. Tauler and M. Filella, *Analytica Chimica Acta*, Vol. 191, **1986**, p. 399.
- [11] F. Marsicano, C. Monberg, B.S. Martincigh, K. Murray, P.M. May and D.R. Williams, *J. Coord. Chem.* Vol. 16, **1988**, p. 321.
- [12] P.M. May and K. Murray, *Talanta*, Vol. 35, No. 12, **1988**, p. 927.
- [13] A.M. Bond, Modern Polarographic Methods in Analytical Chemistry, New York: Marcell Dekker, **1980**.
- [14] <http://faculty.kutztown.edu/betts/html/Electrochemistry.htm>.
- [15] C.H. Hamann, A. Hamnett and W. Vielstich, Electrochemistry, New York: Wiley–VCH, **1998**.
- [16] <http://www.chemistry.adelaide.edu.au/external/soc-rel/content/polarogr.htm>.
- [17] D.A. Skoog and D.M. West, Fundamentals of Analytical Chemistry, Second Edition, New York, **1969**.
- [18] A.J. Bard and L.R. Faulkner, Electrochemical Methods: Fundamentals and Applications, Second Edition. New York: John Wiley & Sons, **2001**.

- [19] D.R. Crow, *Polarography of Metal Complexes*, New York: Academic Press, **1969**.
- [20] J.J. Lingane, *Chem. Rev.* Vol. 29, **1941**, p. 1.
- [21] D.D. DeFord and D.N. Hume, *Journal of American Chemical Society*, Vol. 73, **1951**, p. 5321.
- [22] D.N. Hume, D.D DeFord and G.C.B. Cave, *Journal of American Chemical Society*, Vol. 73, **1951**, p. 5323.
- [23] W.B. Schaap and D.L. McMasters, *Journal of American Chemical Society*, Vol. 83, **1961**, p. 4699.
- [24] G. Schwarzenbach and H. Ackermann, *Helvetica Chimica Acta*, Vol. 35, **1952**, p. 485.
- [25] G. Schwarzenbach, R. Gut and G. Anderegg, *Helvetica Chimica Acta*, Vol. 37, **1954**, p. 937.
- [26] I. Cukrowski, R.D. Hancock and R.C. Luckay, *Analytica Chimica Acta*, Vol. 319, **1996**, p. 39.
- [27] I. Cukrowski, *Analytica Chimica Acta*, Vol. 336, **1996**, p. 23.
- [28] I. Cukrowski and M. Adsetts, *J. Electroanal. Chem.* Vol. 429, **1997**, p.129.
- [29] I. Cukrowski and S.A. Loader, *Electroanalysis*. Vol. 10, **1998**, p. 877.
- [30] I. Cukrowski, *Electroanalysis*, Vol. 11, **1999**, p. 606.
- [31] I. Cukrowski, *J. Electroanal. Chem.*, Vol. 460, **1999**, p. 197.
- [32] I. Cukrowski, J.R. Zeevaart and N.V. Jarvis, *Anal. Chim. Acta*, Vol. 379, **1999**, p. 217.
- [33] I. Cukrowski and J.M. Zhang, *Electroanalysis*, Vol. 16, No. 8, **2004**, p. 612.
- [34] I. Cukrowski, D.M. Mongano and J.R. Zeevaart, *J. Inorg. Biochem.*, Vol. 99, **2005**, p. 2308.

CHAPTER 3

Experimental Methodology

3.1 Reagents

Alendronate monosodium trihydrate ($C_4H_{12}NNaO_7P_2 \cdot 3H_2O$) (4.39 g, 70%), as white crystals, m.p. 270–274 °C, F. W. 325.117, 1H NMR (D_2O): δ 2.97 (2H, *t*), 1.93 (4H, *t*), ^{13}C NMR (D_2O): δ 39.97, 30.56, 22.10 (d), elemental analysis, % calculated: C 14.78, H 5.58, N 4.31, found: C 14.70, H 5.63, N 4.11, and Neridronate monosodium monohydrate ($C_6H_{16}NNaO_7P_2 \cdot 0.5H_2O$) (3.99 g, 42%), as a white solid, m.p. 263–266 °C, F. W. 308.134, 1H NMR (D_2O): δ 3.05 (2H, *t*, $J_{C-Pn} = 7.6$ Hz), 1.90–2.05 (2H, *m*), 1.61–1.79 (4H, *m*), 1.44 (2H, *m*), ^{13}C NMR (D_2O): δ 74.92 (*t*, $J_{C-Pn} = 132$ Hz), 40.06, 36.00, 26.81, 26.66, 26.36 ((*t*, $J_{C-Pn} = 6.8$ Hz), elemental analysis, % calculated: C 23.39, H 5.56, N 4.55; found: C 22.90 H 5.65 N 4.39 were synthesized and purified in Portuguese National Institute of Engineering, Technology and Innovation, INETI, Portugal. The elemental analyses were also done by Institute for Soil, Climate and Water, Agriculture Research Council in Pretoria, and the results found were close to that reported by INETI. Elemental analysis for Alendronate, % found: C 14.91 H 5.86 N 4.37 and for Neridronate found: C 23.25 H 5.89 N 4.65. Cadmium Nitrate tetrahydrate ($Cd(NO_3)_2 \cdot 4H_2O$, F.W. 308.47, 98% pure) and Lead Nitrate ($Pb(NO_3)_2$, F.W. 331.20, 99% pure) were obtained from Sigma Aldrich (Germany). Calcium Chloride dehydrate ($CaCl_2 \cdot 2H_2O$, F.W. 147.02, 99.5% pure) was obtained from BDH (England). Magnesium Chloride hexahydrate ($MgCl_2 \cdot 6H_2O$, F.W. 203.31, 99% pure) was obtained from Merck (Darmstadt, Germany). Sodium Chloride ($NaCl$, F.W. 58.44, 99.5% pure) was obtained from ACE (South Africa). Sodium Hydroxide ($NaOH$, F.W. 40, 98% pure), Hydrochloric Acid (HCl , F.W. 36.46, 32% pure) and Potassium Hydrogen Phthalate (KHP, F.W. 204.23, 99.5%) were obtained from Saarchem (Muldersdrift, South Africa). The metal salts were of analytical grade and were used without further purification. KHP was heated at 110 °C, cooled and stored in a dessicator. De-ionized

water was obtained by passing distilled water through a Milli-Q-water purification system (Millipore, Bedford, MA, USA).

3.2 Preparation of Solutions

1. The titrant solution (of about 0.05 M NaOH) was prepared by weighing out the required amount of solid NaOH and dissolving it in de-ionised water in a 2000 ml volumetric flask. An appropriate amount of NaCl was added to adjust the ionic strength to 0.15 M. The solution was standardised weekly by use of KHP.
2. The stock solution (of approximately 0.05 M HCl) was prepared by diluting in de-ionised water an appropriate volume of 32% HCl in a 1000 ml volumetric flask. An appropriate amount of NaCl was added to adjust the ionic strength to 0.15 M. The solution was standardised against the standardised solution of 0.05 M NaOH (adjusted ionic strength 0.15 M).
3. The metal ion stock solutions (of about 0.01 M) of Mg(II), Ca(II), Cd(II) and Pb(II) were prepared by weighing out the required amount of the appropriate salt and dissolving it in de-ionised water in a 50 ml volumetric flask. An appropriate amount of NaCl was added to adjust the ionic strength to 0.15 M.
4. The ligand stock solutions (of about 0.01 M) were prepared by weighing out the required amount of a ligand and dissolving it in a solution of 0.15 M NaCl. All the ligands received were in the form of a salt. They dissolved completely in 5 minutes and were used as received without any pre-treatment.
5. A standard solution of 0.15 M NaCl was prepared by weighing out the appropriate amount of NaCl(s) and dissolving it in de-ionised water. The solution of 0.15 M NaCl was used as the background electrolyte in all experiments performed at ionic strength 0.15 M and 25 °C.

3.3 Glass Electrode Potentiometry

3.3.1 Instrumentation

All experiments were performed in a jacketed glass vessel equipped with a magnetic stirrer (Methrom) and thermostatted at 25.0 ± 0.1 °C by water circulating from a constant temperature bath. The pH measurements were made using combination glass electrode with built-in temperature probe (Ag/AgCl/3M KCl; Pt 1000) model

6.0258.010 (Metrohm) connected to a 713 pH meter (Metrohm). The potential and pH of solutions were measured to within ± 0.1 mV (± 0.001 pH unit).

Potentiometric titrations of ligands and standardization of solutions were performed using a computer controlled automatic titration instrumental set-up model 809 Titrando equipped with digital burette model 800 Dosino, a magnetic stirrer model 801 (all from Metrohm). Two titration modes were used: (i) Dynamic, for standardization of solutions and (i) monotonic, for combination glass electrode calibration and ligand-titration.

Potentiometric titrations of metal-ligand systems were performed using a dedicated LabVIEW-controlled instrumental set-up [1]. The 765 Dosimat was used as digital burette, a magnetic stirrer model 728 and 713 pH meter (all from Metrohm) were used.

All solutions were adjusted to the same ionic strength of 0.15 M by the addition of appropriate amount of NaCl. High purity nitrogen was used for de-aeration of the sample solutions, i.e., to remove the dissolved oxygen from the solutions.

3.3.2 Standardisation of Solutions

Stock solutions of 0.05 M NaOH and 0.05 M HCl (all adjusted to ionic strength 0.15 M with NaCl) were standardised in the following way as described below.

Standardisation of NaOH

Small amount of KHP was weighted out and dissolved in the titration cell using 0.15 M NaCl solution and titrated by a solution of NaOH placed in the burette of the autotitrando. The concentration of NaOH solution was determined at the end point of titration by Equation 3.1

$$[\text{NaOH}] = \frac{m_{\text{KHP}} \cdot 1000}{M_{\text{KHP}} \cdot V_{\text{NaOH}}} \quad (3.1)$$

where m_{KHP} is the mass of KHP, M_{KHP} stands for the molecular mass of KHP and V_{NaOH} represents the total volume of added NaOH at the end point.

The concentration of the standardised NaOH solution was found by taking the average of concentrations obtained from three different titrations.

Standardisation of HCl

An appropriate volume of HCl solution was placed in the titration cell and titrated with a standardised solution of 0.05 M NaOH (adjusted to ionic strength 0.15 M with NaCl). The concentration of HCl solution was determined using Equation 3.2.

$$[\text{HCl}] = V_{\text{NaOH}} \cdot C_{\text{NaOH}} / V_{\text{HCl}} \quad (3.2)$$

where V_{NaOH} stands for the total volume of NaOH added at the end point, C_{NaOH} is the concentration of standardised solution of NaOH, and V_{HCl} represents the volume of HCl placed in the titration cell.

The concentration of the standardised HCl solution was found by taking the average of concentrations obtained from three different titrations.

3.3.3 Glass Electrode Calibration

In the determination of protonation and stability constants, using potentiometry or polarography, the values of E° and a response slope of the GE are needed. In metal-ligand studies at constant ionic strength, GE calibration (as a hydrogen ion concentration probe, $\text{pH} = -\log [\text{H}^+]$) should be performed by titration of a strong acid with a strong base under the same experimental conditions [2, 3] as employed in the equilibrium studies.

The GE calibration was performed automatically with the use of the dedicated LabVIEW-controlled instrumental set-up [1] or model 809 Titrando (Metrohm) using monotonic mode of titration. In calibration titrations, 10.0 ml of a standardized solution of 0.05 M HCl (adjusted to ionic strength 0.15 M with NaCl) was mixed with 15.0 ml of 0.15 M NaCl (as background electrolyte) and a standardised solution of 0.15 M NaOH (adjusted to ionic strength 0.15 M with NaCl) was used as a titrant.

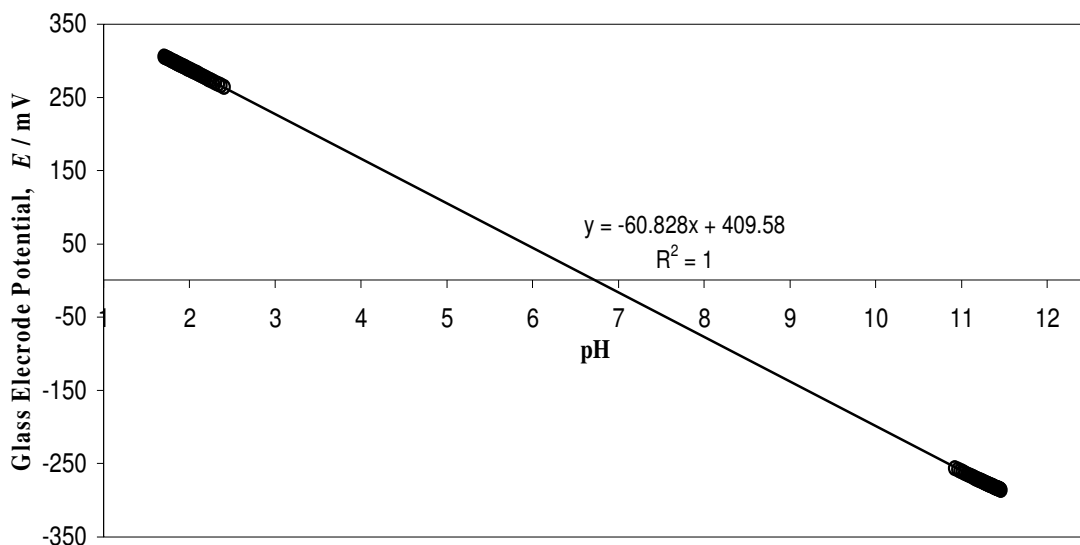


Figure 3.1 An example of a calibration curve obtained by a GEP experiment for metal-ligand system. Linear fit (—); experimental points (o). In this example, $E^{\circ} = 409.58$ mV and the response slope 60.828 mV.

The titrant volume increment was 0.2 ml. Readings in the potential of combination GE were collected in the pH range 1.5–11.5. Experimental points were fitted with a straight line to establish the value of E° and a response slope of the GE, as seen in the Figure 3.1 above. The combination GE was calibrated before and after each experiment, and the average value of E° and a response slope from both titrations was used in the data analysis.

3.3.4 Protonation Equilibria Study by GEP

Protonation constants of the ligands, ALN and NED were determined by GEP. Two titrations were performed for each ligand. The following procedure was followed:

1. Initially, the cell was rinsed with de-ionised water and further cleaned with 0.5 M HNO_3 , followed by rinsing with de-ionised water.
2. The combination GE was calibrated prior the ligand involving experiments using strong acid and strong base titration (see section 3.3.3) in order to obtain E° and the response slope.

- Appropriate volume of 0.15 M NaCl was added to the cell followed by an accurately weighed amount of the ligands. The ligands dissolved completely, given concentration of about 0.008–0.01 M. The pH of the solution was adjusted to 1.5–2.0 with standardised acid.
- The ligand solutions were titrated with a standardized solution of 0.05 M NaOH (adjusted to ionic strength 0.15 M with NaCl) in pH range 1.5–12.0. High purity nitrogen was continuously purged into the cell to remove dissolved oxygen. In the ligand-titration experiments, the volume increment of 0.1 ml, the signal drift of 0.5 mV / min, the minimum waiting time of 10 s, and the maximum waiting time of 480 s were applied;
- After each experiment, the combination GE was calibrated again. The average of E^0 and slope from the two titrations was used in the refinement operations.

Different compositions of sample solutions employed in ligand titrations are shown in Table 3.1.

Table 3.1 Composition of the solutions for ligand acid-base titrations studied by GEP

Ligand	Titration	V_{Back} (ml)	m_L (g)	V_{HCl}^1 (ml)	[L] (M)
ALN	1	14.00	6.50×10^{-2}	6.00	1.00×10^{-2}
	2	14.00	5.20×10^{-2}	6.00	8.00×10^{-3}
NED	1	15.00	6.16×10^{-2}	5.00	1.00×10^{-2}
	2	14.00	4.93×10^{-2}	6.00	8.00×10^{-3}

¹ For ALN titration 1 and 2 [HCl]= 0.1455 M and for NED titration 1 and 2 [HCl]= 0.0484 M.

3.3.5 Determination of Stability Constants by GEP

The metal–ligand systems Mg(II)–ALN, Mg(II)–NED, Ca(II)–ALN, and Ca(II)–NED at $L_T : M_T$ ratio 2 were studied by GEP. The following procedure was employed:

- The cell was initially rinsed and the combination GE was calibrated as described in section 3.3.4.
- Appropriate volume of background electrolyte (0.15 M NaCl) was added to the cell. To achieve the required $L_T : M_T$ in the cell, appropriate volumes of about

0.01 M metal ion solutions (adjusted to ionic strength 0.15 M with NaCl) and 0.01 M ligand solution (in 0.15 M NaCl) were transferred to the cell.

3. The metal-ligand solutions were titrated with a standardized solution of 0.05 M NaOH (adjusted to ionic strength 0.15 M with NaCl) within pH range 4.5–10.7. High purity nitrogen was continuously purged into the cell to remove dissolved oxygen. The ligand volume increment of 0.01 ml, sampling rate of pH meter of 2 s, the equilibration time of 180 s and the maximum waiting time of 300 s were applied.
4. After the experiment, the combination GE was calibrated again.

All the titrations were checked for the possible formation of a precipitate. In the Ca(II) – NED system, the precipitate was observed at pH of about 6 for the $L_T : M_T$ ratio 2. In order to avoid early precipitation, the $[Ca(II)]$ and $[L_T]$ were decreased given the same $L_T : M_T$ ratio allowing the study in the pH range from 4.5–9.5.

Table 3.2 Specifications of the metal-ligand solutions at $L_T : M_T$ ratio 2 studied by GEP.

Ligand	Cation	V_{Back} (ml)	V_M (ml)	V_L (ml)	$[M_T]$ (M)	$[L_T]$ (M)
ALN	Mg(II)	14.00	2.00	4.00	9.9847×10^{-4}	2.0000×10^{-3}
	Ca(II)	14.00	2.00	4.00	9.9850×10^{-4}	2.0000×10^{-3}
NED	Mg(II)	14.00	2.00	4.00	9.9848×10^{-4}	2.0000×10^{-3}
	Ca(II)	17.60	0.80	1.60	3.9540×10^{-4}	8.0000×10^{-4}

3.4 Polarography

3.4.1 Instrumentation

All experiments were performed in a jacketed glass vessel equipped with a magnetic stirrer model 728 (Metrohm) and thermostatted at 25.0 ± 0.1 °C by water circulating from a constant temperature bath. The titrant additions were performed with the use a digital burette 765 Dosimat (Metrohm). The pH measurements were made using combination glass electrode with built-in temperature probe (Ag/AgCl/3M KCl; Pt 1000) model 6.0258.010.(Metrohm) connected to a 713 pH meter (Metrohm). The potential and pH of solutions were measured to within ± 0.1 mV (± 0.001 pH unit).

Polarographic measurements were performed using three electrodes. A multi-mode mercury electrode (MME) (Metrohm, model 6.1246.020) was used as the working electrode (WE) employed in the dropping mercury electrode (DME) mode, a platinum rod electrode was used as the auxiliary electrode (AE), and Ag/AgCl (3 M KCl) electrode was used as the reference electrode (RE) (Metrohm, model 6.0728.000). The reference electrode was connected to the solution by means of a glass salt bridge (Metrohm, model 6.1245.000).

Normal pulse polarograms were obtained with the use of 757 VA computrace (Metrohm) and sampled DC polarograms were obtained with the use of dedicated LabVIEW-controlled instrumental set-up [1]. The CV-27 Voltammograph (*Bioanalytical Systems*, Indiana, USA) was used as potentiostat. All voltammetric measurements were performed using the valve block of 663 VA stand (Metrohm) incorporated in the instrumental set-up.

3.4.2 Ligand Adsorption Studies

The adsorption studies of ALN and NED on a hanging mercury drop electrode (HMDE) were performed by use of alternating current voltammetry (ACV) generated from 757 VA computrace (Metrohm). Adsorption of n-pentanol was studied as an example.

The following parameters were selected: amplitude of sinusoidal current of 20 mV, a frequency of 50 Hz, the modulation time of 0.040 s, the capacitive current (i_{ac}) was measured at a phase angle of 90° , voltage step time of 0.500 s, voltage step of 0.010 V, equilibration time of 10 s and initial purge time of 800 s. A volume of 25.0 ml solutions of 0.01 M of ALN or NED in 0.15 M NaCl were used in this study performed at three different pH values: 4.27, 6.13 and 10.52. The potential range scanned in the experiments was from -0.2 to -1.5 V vs. Ag/AgCl (3 M KCl).

3.4.3 Determination of Stability Constants by Polarography

Metal–ligand systems Cd(II)–ALN, Cd(II)–NED, Pb(II)–ALN, and Pb(II)–NED, were studied by sampled DC polarography and NPP at fixed $L_T : M_T$ ratios and varied pH. The following procedure was employed:

1. The cell was initially rinsed with de-ionised water and further cleaned with 0.5 M HNO₃ followed by thorough rinsing with de-ionised water.
2. The combination GE was calibrated prior the ligand involving experiments using strong acid and strong base titration (seen section 3.3.3) in order to obtain E° and the response slope.
3. A required volume of background electrolyte (0.15 M NaCl) was added to the cell followed by few corns of gelatine to suppress polarographic maxima. High purity nitrogen was purged for 30 minutes to remove dissolved oxygen.
4. A polarogram was recorded in a sample solution containing only background electrolyte to check the purity of the solution. For studies of Cd(II) and Pb(II) by sampled DC polarography, the range of applied potential was -0.20 to -1.60 V, drop time of 2.0 s and step potential was 4 mV, integration time of 300 ms for Cd(II) and 80 ms for Pb(II). The large value of integration time for Cd(II) was applied to enhance the signal. The parameters used in NPP were: (i) for Cd(II): equilibration time of 30 s, start potential of -0.350 V, end potential of -0.850 V, voltage step of 0.004 V, voltage step time of 1.00 s, sweep rate : 0.004 V/s, base potential -0.300 V, pulse time 0.080 s; (ii) for Pb(II): equilibration time of 30 s, start potential of -0.150 V, end potential of -0.600 V, voltage step of 0.004 V, voltage step time of 1.00 s, sweep rate : 0.004 V/s, base potential -0.130 V, pulse time 0.08 s.
5. The required volume of the metal ion stock solution (Cd(NO₃)₂, or Pb(NO₃)₂) was added to the cell by an appropriate micro-syringe (Hamilton, Bonaduz, Switzerland) to give required the total metal ion concentration (M_T). Three consecutive polarograms were recorded for determination of $E_{1/2}(M)$ and $I_d(M)$ for Cd(II) and Pb(II) in absence of the ligand.
6. An appropriate amount of the ligand (ALN or NED) was weighed out and then, introduced into the cell to give the required $L_T : M_T$ ratio. High purity nitrogen was purged again for about 30 minutes. The volume increment was set 0.005 ml and the dedicated LabVIEW-based virtual instrument [1] was employed to perform an automated acid-base titration in pH range 4.5–10.7 using a solution of 0.05 M NaOH. A set of polarograms, 50 to 70 was recorded on the solution after the pH increments of 0.04–0.05 pH units.
7. After the experiment, the combination GE was calibrated again.

All the titrations were checked for the possible formation of a precipitate. In the Cd(II)–ALN and Cd–NED systems, the precipitates were observed at pH 6 and $L_T : M_T$ ratio 50. In order to avoid early precipitation, the [Cd(II)] was decreased to give a $L_T : M_T$ ratio of 266.6, allowing thus, to study in pH range from 4.5–9. Specifications of metal–ligand solutions are shown in Table 3.3.

Table 3.3 Specification of the metal–ligand solutions studied by sampled DC (A) and NP polarography (B).

(A)

Ligand	Cation	Ratio	V_{Back} (ml)	V_M (μ l)	m_L (g)	$[M_T]$ (M)	$[L_T]$ (M)
ALN	Cd(II)	266.6	25.00	37.5	3.2500×10^{-2}	1.4978×10^{-5}	3.9936×10^{-3}
	Pb(II)	50.0	25.00	200	3.2500×10^{-2}	7.9365×10^{-5}	3.9678×10^{-3}
NED	Cd(II)	266.6	25.00	37.5	3.0800×10^{-2}	1.4978×10^{-5}	3.9936×10^{-3}
	Pb(II)	50.0	25.00	200	3.0800×10^{-2}	7.9365×10^{-5}	3.9678×10^{-3}

(B)

Ligand	Cation	Ratio	V_{Back} (ml)	V_M (μ l)	m_L (g)	$[M_T]$ (M)	$[L_T]$ (M)
ALN	Cd(II)	-	-	-	-	-	-
	Pb(II)	160.0	25.00	125	6.5000×10^{-2}	4.9751×10^{-5}	7.9573×10^{-3}
NED	Cd(II)	266.6	25.00	75	6.1600×10^{-2}	2.9910×10^{-5}	7.9726×10^{-3}
	Pb(II)	50.0	25.00	200	3.0800×10^{-2}	7.9365×10^{-5}	3.9678×10^{-3}

3.5 References

- [1] I. Cukrowski, P. Magampa and T.S. Mkwizu, *Helv. Chim. Acta*, Vol. 89 **2006**, p. 2934.
- [2] R.G. Bates, *The Determination of pH*, 2nd ed, Wiley, New York, **1973**.
- [3] H..M. Irving, M.G. Miles and L.D. Pettit, *Anal. Chim. Acta.*, Vol. 38, **1967**, p. 475.

CHAPTER 4

Result and Discussion

4.1 Equilibria by Glass Electrode Potentiometry

The protonation constants for ligands ALN and NED as well as stability constants for the systems: Mg(II)–ALN, Ca(II)–ALN, Mg(II)–NED and Ca(II)–NED (all at $L_T : M_T$ ratio 2) were determined by GEP and the ESTA program [1, 2] was employed in modelling and refinement of GEP data.

In general the overall stability constants for the systems mentioned above are defined by the Equation 4.1 (charges are omitted for simplification).



$$\beta_{M_pH_rL_q} = \frac{[M_pH_rL_q]}{[M]^p[H]^r[L]^q} \quad (4.1)$$

where L stands for ALN or NED ligand and M stands for metal ion.

The value of pK_w at 25 °C and ionic strength 0.15 M, in NaCl, has never been reported. In order to estimate its value the experimental data related to the determination of protonation constants of the ALN were used. Thus, the pK_w value was refined simultaneously together with protonation constants of ALN. Two values of pK_w resulted, 13.68 and 13.70, but from results obtained (data not shown) value 13.68 gave slightly better estimates and better statistical data.

During the refinement of the stability constants the value for $pK_w = 13.68$ and, hydrolyses constants of metal ions [3, 4] were used as fixed parameters, as well as the

protonation constants of ALN and NED that were determined in this work. All experiments were performed at 25.0 ± 0.1 °C and ionic strength of 0.15 M NaCl. Values of the protonation function, $ZBAR(H)$, [5] and of the complex formation function, $ZBAR(M)$, [5] were calculated for each datum point.

4.1.1 Protonation of Alendronate

Alendronate (ALN) is N-containing bisphosphonate, in which each of the phosphonate groups (PO_3H_2) is capable of accepting two protons and the aliphatic nitrogen atom one proton (see structure in section 1.6). The fully protonated form of ligand contains five dissociable protons, $[H_5L]$. Depending on the pH of the solution, successive deprotonation of the ligand occurred at phosphonate groups (PO_3H_2) and at amino group.

Initially, the pH of the solution was adjusted to pH about 1.5 with standardized acid and two titrations were performed. The program ESTA [1, 2] was used to calculate the protonation constants in the range of pH 1.5–11.7. The refined values of protonation constants are shown in Table 4.1.

The protonation function $ZBAR(H)$ was generated after each refinement operation using the refined protonation constant values. The best fit was not achieved with all data points collected, the calculated (solid line) and experimental curves (circles) diverged considerably at high pH (see Figure A.1-Appendix A). Some points were removed, step by step, from the data at high pH and the refinement was repeated until good fit between the calculated function (solid line) and the experimental data (circles), with low Hamilton R-factor and standard deviations for protonation constants was obtained – see Figure 4.1. Experimental parameters, such as initial acid, ligand and base concentrations were also refined (see Table A.1-Appendix A) to check for possible systematic errors. The percentage change in concentration parameters was calculated for each titration. The ESTA program often showed correlation between parameters when protonation constants were refined without or simultaneously with acid, ligand or base concentrations in titrations 1, 2 and combined refinement.

Table 4.1 Protonation constants (as log K) for ALN at 25 °C and ionic strength of 0.15 M in NaCl obtained by GEP.

Experimental Data ²	Equilibrium ¹					R-factor and n°points	Refined initial parameter
	H + L = HL	H + HL = H ₂ L	H + H ₂ L = H ₃ L	H + H ₃ L = H ₄ L	H + H ₄ L = H ₅ L		
Titration 1	10.79 ±0.01	10.562 ±0.009	6.16 ±0.01	2.11 ±0.02	1.32 ±0.04	0.00940 (334)	Nothing ³
	10.98 ±0.01	10.491 ±0.009	6.16 ±0.01	2.11 ±0.01	1.32 ±0.03	0.00624 (281)	Nothing ⁴
	11.033 ± 0.004	10.417 ± 0.003	6.128 ±0.003	2.116 ± 0.004	1.331 ± 0.008	0.00189 (281)	Ligand ⁴
Titration 2	10.74 ±0.02	10.56 ±0.01	6.15 ±0.01	2.07 ±0.02	1.18 ±0.06	0.01082 (320)	Nothing ³
	10.99 ±0.01	10.451 ±0.008	6.153 ±0.009	2.07 ±0.01	1.18 ±0.03	0.00497 (262)	Nothing ⁴
	11.030 ± 0.005	10.400 ± 0.004	6.128 ±0.004	2.073 ± 0.006	1.193 ± 0.01	0.00215 (262)	Ligand ⁴
Combined Refinement	11.032 ± 0.004	10.410 ± 0.003	6.128 ±0.003	2.099 ± 0.004	1.278± 0.009	0.00246 (543)	Ligand ⁴
	11.033 ± 0.002	10.410 ± 0.001	6.128 (fixed)	2.100 ± 0.003	1.278 ± 0.008	0.00246 (543)	Ligand³

¹Charges on species are omitted for simplicity. ²Ligand refined: Titration 1: 0.010000 M ⇒ 0.009875 M, % change = - 1.27 %; Titration 2: 0.008000 M ⇒ 0.007912 M, % change = -1.10 %; Combined refinement: Titration 1: 0.010000 M ⇒ 0.009871 M, % change -1.30 %; Titration 2: 0.008000 M ⇒ 0.007915 M, % change -1.25%. ; ³No correlation seen. ⁴Correlation seen between pK_{a(2)} and pK_{a(3)}.

When looking at Table 4.1, titration 1, one can see that no correlations were seen when 334 experimental data points were used in the refinement operations. However, the fit between the calculated function and the experimental data was not good at high pH. Therefore, more points were removed from the data at high pH and the refinement was repeated and good fit was obtained with 281 experimental data points but with correlation seen between pK_{a(2)} and pK_{a(3)}. It is important to note that the pK_{a(3)} value obtained was the same as obtained initially. When either acid, ligand, or base concentration was refined simultaneously with protonation constants, ESTA showed correlation between pK_{a(2)} and pK_{a(3)}. The pK_{a(3)} had the same refined value of 6.128 when ligand concentration was refined in titrations 1, 2 and combined refinement of both titrations. In the following refinement operation the pK_{a(3)} value was fixed at 6.128 and the ligand concentration was refined together with protonation constants in the combined refinement; no correlation was observed.

Five protonation constants were found for ALN from both titrations. The differences in the 4th and 5th protonation constants from both titrations might be linked to the pH-

related uncertainty in highly acidic medium. For the determination of stability constants, the second and third protonation constants are most important since the pH range of the experiments concerned was between 4.5 and 10.7. This is because species formed in the vicinity of blood plasma pH were at highest importance and main interest in this work. It is seen in Table 4.1 that $pK_{a(1)}$, $pK_{a(2)}$, as well as $pK_{a(3)}$ were almost identical for both titrations.

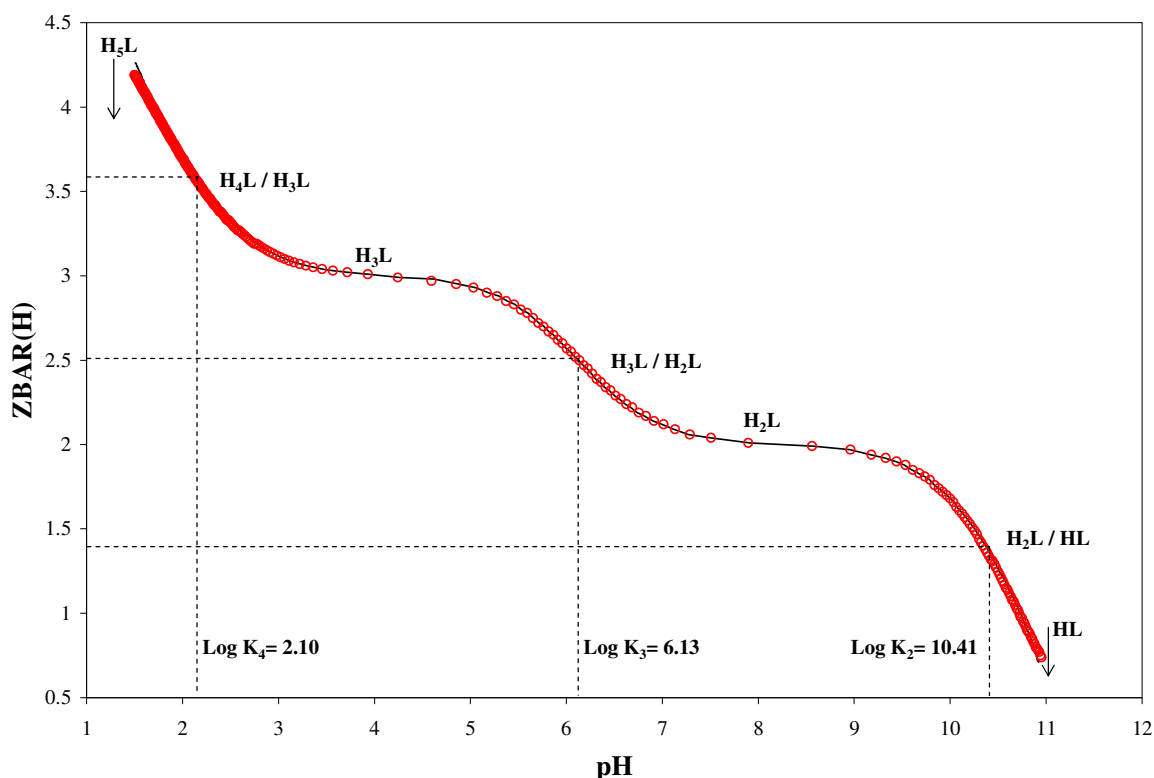


Figure 4.1 Experimental (circles) and theoretical (solid line) protonation curves for ALN at ionic strength 0.15 M in NaCl and 25 °C, $[L_T] = 1.0000 \times 10^{-2}$ M.

The final protonation constant values seen in bold in Table 4.1 were taken from optimization procedure involving simultaneous refinement of initial ligand concentration; note low Hamilton R-factor and standard deviations obtained. The protonation constants calculated from combined refinement were used in calculation of formation constants of metal complexes with ALN.

The protonation constants values found in this work are generally slightly lower than reported by Hägele *et al.* [6]. Relatively large discrepancy in the 1st, 3rd and 4th protonation constants is observed when our results are compared with data reported by Katkov *et al.* [7].

Table 4.2 Reported protonation constants for alendronate.

Log K_n	This work	Katkov ¹ <i>et al.</i> [7]	Hägele ² <i>et al.</i> [6]
log K_1	11.03	(11.6)	11.82
log K_2	10.41	10.5	10.96
log K_3	6.13	8.73	6.39
log K_4	2.10	2.72	2.22
log K_5	1.28	-	1.33

¹ $\mu=0.1$ M (0.1 M KCl), 25 °C; ² $\mu=0.1$ M (0.1 M NaCl), 25 °C

Zeevaart [8] reported a wide variation of protonation constants in his studies with HEDP and MDP compared with results reported by other authors (Dietsche *et al* [9], Nash *et al* [10], results compiled by Martell and Smith [3], Van Der Linde *et al* [11] and Grabenstetter *et al* [12]). Zeevaart explained these facts by the use of different media and ionic strengths. The same argument could be used to explain differences between data generated here and reported in the literature. However, the $pK_{a(3)}$ value of 8.73 reported by Katkov *et al* appears to be a suspect.

4.1.2 Protonation of Neridronate

Neridronate is N-containing bisphosphonate, with six carbons in the aliphatic chain (see structure in section 1.6). The fully protonated ligand contains as ALN, five dissociable protons. Successive deprotonation occurs initially at phosphonate groups (PO_3H_2) and at amino group at high pH.

Since the fifth protonation constant (at very low pH) was of no interest and importance in this work, the pH of the solution was adjusted to about 2 with standardized acid. This resulted in smaller acid addition and hence should have smaller impact on accuracy of protonation constants determined here. The protonation constants obtained in this work are shown in Table 4.3.

Table 4.3 Protonation constants (as log K) for NED at 25 °C and ionic strength of 0.15 M in NaCl obtained by GEP.

Experimental Data ²	Equilibrium ¹				R-factor and n°points	Refined initial parameter
	H + L = HL	H + HL = H ₂ L	H + H ₂ L = H ₃ L	H + H ₃ L = H ₄ L		
Titration 1	10.65 ±0.03	10.99 ±0.01	6.57 ±0.01	2.42 ±0.02	0.02241 (354)	Nothing ²
	10.71 ±0.03	10.96 ±0.02	6.57 ±0.02	2.42 ±0.02	0.02507 (302)	Nothing ¹
	10.938 ± 0.007	10.698 ± 0.005	6.490 ± 0.005	2.447 ± 0.005	0.00600 (302)	Ligand ¹
Titration 2	10.72 ±0.04	10.80 ±0.02	6.57 ±0.02	2.46 ±0.03	0.02275 (164)	Nothing ²
	10.89 ±0.06	10.73 ±0.04	6.57 ±0.04	2.46 ±0.04	0.02598 (127)	Nothing ¹
	11.09 ±0.03	10.49 ±0.02	6.48 ±0.02	2.49 ±0.02	0.01300 (127)	Ligand ¹
Combined Refinement	10.98 ± 0.01	10.639 ± 0.007	6.489 ± 0.008	2.457 ± 0.009	0.01049 (429)	Ligand ¹
	10.982 ± 0.008	10.639 ± 0.003	6.489 (fixed)	2.456 ± 0.005	0.01049 (429)	Ligand²

¹Charges on species are omitted for simplicity. ²Ligand refined: Titration 1: 0.009979 M \Rightarrow 0.009631 M, % change = - 3.49 %; Titration 2: 0.008000 M \Rightarrow 0.007689 M, % change = -3.89 %; Combined refinement: Titration1: 0.009979 M \Rightarrow 0.009604 M, % change -3.76 %; Titration 2: 0.008000 M \Rightarrow 0.007761 M, % change -2.99%. ³No correlation seen. ⁴Correlation seen between pK_{a(2)} and pK_{a(3)}.

The $ZBAR(H)$ functions seen in Figure 4.2 were generated using the refined protonation constants from combined refinement – see Table 4.3. The best fit together with low Hamilton R-factor and standard deviations in protonation constants were obtained when some points at high pH were deleted (see an example in Figure A.1-Appendix A.). As expected (due to experimental conditions employed) only four protonation constants were found. Excellent agreement is seen for pK_{a(3)} and pK_{a(4)} obtained from both titrations, but small spread in optimised pK_{a(1)} and pK_{a(2)} observed can be related to the pH uncertainty in basic medium. Experimental parameters, such as initial acid, initial ligand and base concentrations were also refined (see Table A.2- Appendix A) and the final protonation constant values were obtained using the same refinement strategies as for ALN. The final protonation constants calculated from combined refinement seen in bold in Table 4.3 were used in calculation of formation constants of metal complexes with NED.

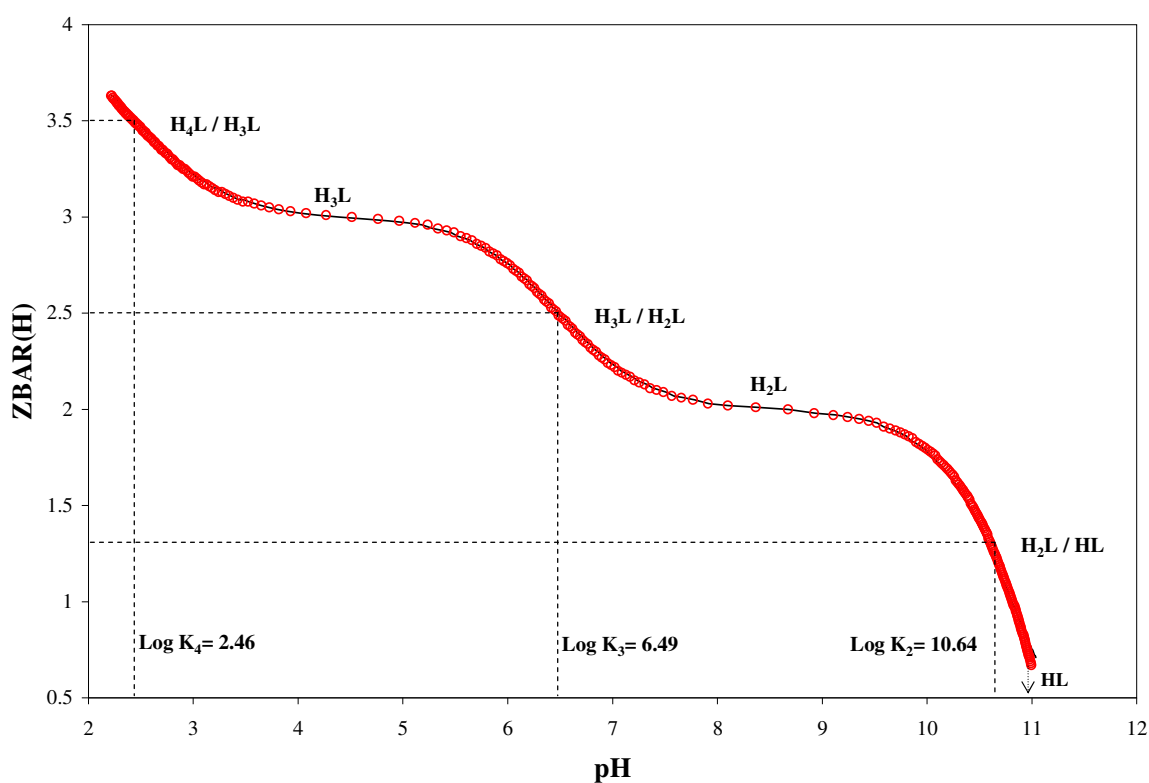


Figure 4.2 Experimental (circles) and theoretical (solid line) protonation curves for NED at ionic strength 0.15 M in NaCl and 25 ° C, $[L_T] = 9.979 \times 10^{-3}$ M.

The only literature data related to protonation constants of NED was that by Katkov *et al* [7]—see Table 4.4. The protonation constants values found in this work are generally higher and quite different than those reported by Katkov *et al*. This could not be explained only by the differences in ionic strength and medium used. Since we trust our results, the data reported by Katkov could be seen as questionable.

Table 4.4 Reported protonation constants for neridronate.

$\log K_n$	This work	Katkov¹ <i>et al.</i> [7]
$\log K_1$	10.98	(10.9)
$\log K_2$	10.64	8.63
$\log K_3$	6.49	5.49
$\log K_4$	2.46	2.90

¹ $\mu = 0.1$ M (0.1 M KCl), 25 °C

4.1.3 Mg(II) – Alendronate System

All details regarding the experimental conditions were given in Chapter 3, section 3.4.2. No precipitation was observed in the whole pH range of the experiment (between 4.5–10.5). All data points collected in this pH range were used in the refinement operation in order to obtain most reliable model of the system under investigation. ESTA accepted several models and generated comparable statistical outputs. This is not surprising as bisphosphonates can form many different complexes with metal ions using different binding sides [13, 14]. Different modes of bond formation can be appreciated from the analysis of available crystallographic structures [15, 16]. Inability of arriving to a final metal–ligand model based only on GEP data was also reported recently [17, 18] in the study of complexation abilities of Good buffers. Clearly, another analytical technique would possibly help in arriving to most likely final metal-ligand model. Unfortunately, Mg(II) cannot be determined by polarography because it is polarographically inactive (hydrogen evolution proceeds the reduction of magnesium ion).

The analysis of refinement data seen in Table A.1-2 Appendix A indicates that simultaneous refinement of base, acid, or ligand (i) did not change refined pK_a values significantly with variation observed on the second decimal place, (ii) increase in base concentration resulted that might be considered as unreliable output, (iii) only very small decrease (between 1–2 %) is observed in acid concentration that did not have a significant impact on the refinement operation, (iv) a very small decrease in the initial ligand concentration, consistent for both titration, was obtained and this is justifiable as no purification took place of ligands synthesised in Portugal; however, the refined ligand concentration did not have a significant influence on refined protonation constants.

From the above, it would appear that the analytical procedures followed in this work were of high quality and there was no real need to simultaneously refine additional parameters. It is well-known fact that the smaller number of simultaneously refined parameters the more reliable outputs is expected. Hence it has been decided to refine stability constants only and as can be seen from Table 4.5 (B), R-factor and standard deviations obtained are supporting this approach.

Table 4.5 (A) Dissociation constant for water and overall stability constants for Mg(II) complexes with OH⁻. (B) Overall stability constants for Mg(II)–ALN L_T : M_T ratio 2 found in this work by GEP at ionic strength 0.15 M in NaCl and 25 °C. The proposed final model is indicated in bold.

(A)

Equilibrium	Log β	Equilibrium	Log β
H ⁺ + OH ⁻ = H ₂ O	13.68	Mg ²⁺ + OH ⁻ = Mg(OH) ⁺	1.87
		4Mg ²⁺ + 4OH ⁻ = Mg ₄ (OH) ₄ ⁴⁺	16.10
		Mg ²⁺ + 2OH ⁻ = Mg(OH) ₂ (s)	-9.20

(B)

Complex	Model 1	Model 2	Model 3	Model 4
M ₂ (H ₂ L)	27.48 ± 0.03	27.27 ± 0.04	NI	NI
M(H ₂ L)	23.40 ± 0.18	24.02 ± 0.03	24.314 ± 0.008	24.27 ± 0.01
M ₂ (HL)	21.03 ± 0.01	20.62 ± 0.02	20.42 ± 0.02	20.86 ± 0.02
M(HL)	NI	17.114 ± 0.005	17.134 ± 0.005	NI
M ₂ L	13.07 ± 0.01	R	R	13.10 ± 0.01
ML	8.041 ± 0.007	7.913 ± 0.007	7.895 ± 0.008	8.028 ± 0.009
ML(OH)	11.873 ± 0.009	11.919 ± 0.007	11.934 ± 0.008	11.89 ± 0.01
ML(OH) ₂	R	R	R	NI
ML ₂ (OH) ₂	19.681 ± 0.01	19.668 ± 0.008	19.667 ± 0.009	19.68 ± 0.01
R-Factor	0.00928	0.00734	0.00834	0.01096

NI- Not included; R- Rejected

The results from selected models, which present reasonable fit, are illustrated in Table 4.5 (B). The refinement operation for the present system started by including M₂(H₂L), M₂(HL), M(LH), ML, ML(OH), ML(OH)₂ and ML₂(OH)₂ in the M/L/OH model but ESTA not converged. It was decided to remove from or include in the model some species, such as ML₂(OH)₂, ML(OH)₂, or M₂(H₂L). After these procedures, ESTA converged to either model 1 or, for instance model 3, with slight differences in R factors; see Table 4.5 (B).

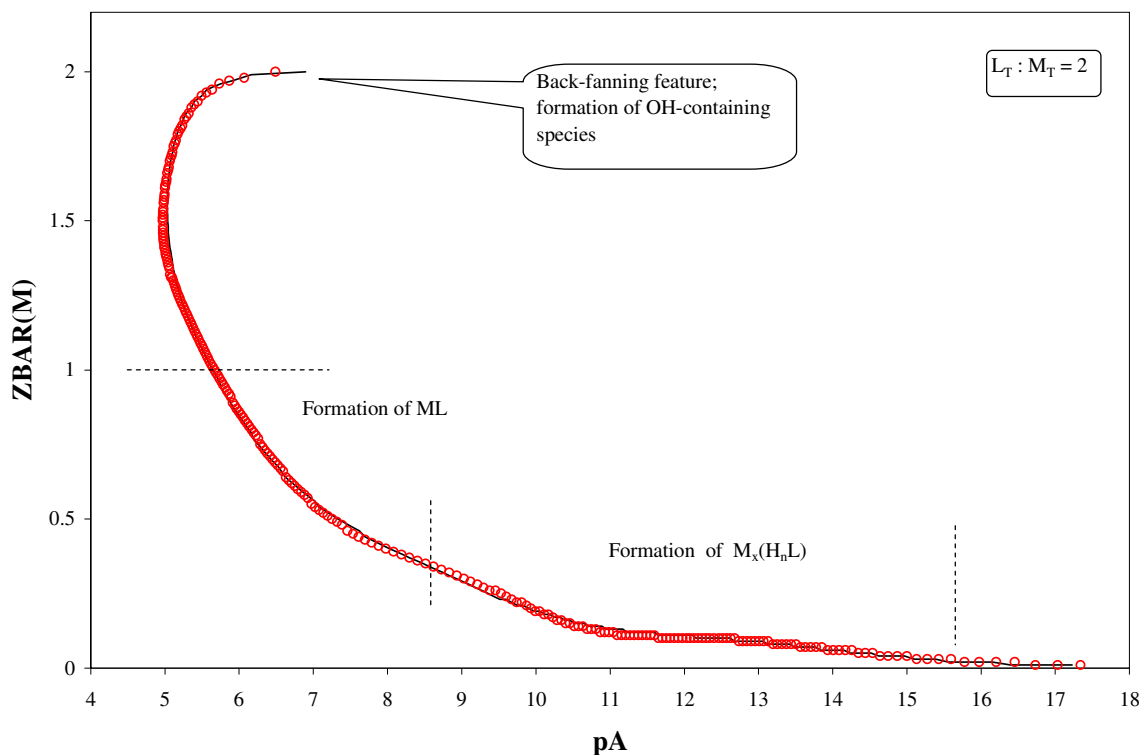


Figure 4.3 Experimental (circles) and theoretical (solid line) potentiometric complex formation curves for Mg(II)–ALN system $L_T : M_T$ ratio 2 obtained for the model $Mg(H_2L)$, $Mg_2(HL)$, $Mg(HL)$, MgL , $MgL(OH)$ and $MgL_2(OH)_2$ at 25 °C and ionic strength 0.15 M in NaCl.

Model 3 was selected for further analysis and the complex formation function, ZBAR(M), for this model was analysed – see Figure 4.3. The analysis of the ZBAR(M) function indicates the formation of ML since ZBAR(M) function, close to the value of 1.0, is growing steadily. A typical feature (backfanning), indicates the formation of OH-containing species, in this case, $ML(OH)$ and possibly $ML_2(OH)_2$. At the beginning a very small increase in the ZBAR(M) function is observed; this is typical in the presence of protonated species in the solution. There is a wide range in pA (between 17 and 8) where ZBAR(M) is above zero value but not increase in value significantly. This suggests that protonated species are predominant metal containing species in a wide pH range.

A species distribution diagram as a function of pH is a powerful tool in the assessment of the concentrations of the species suggested. Figure 4.4, shows the species distribution diagram for the model 3. It is seen that all suggested complexes are major species that reach over 20 % at the total metal concentration, hence none of them can be

seen as a suspect (species that formed only up to 1–5 % of a total metal ion concentration can usually be rejected).

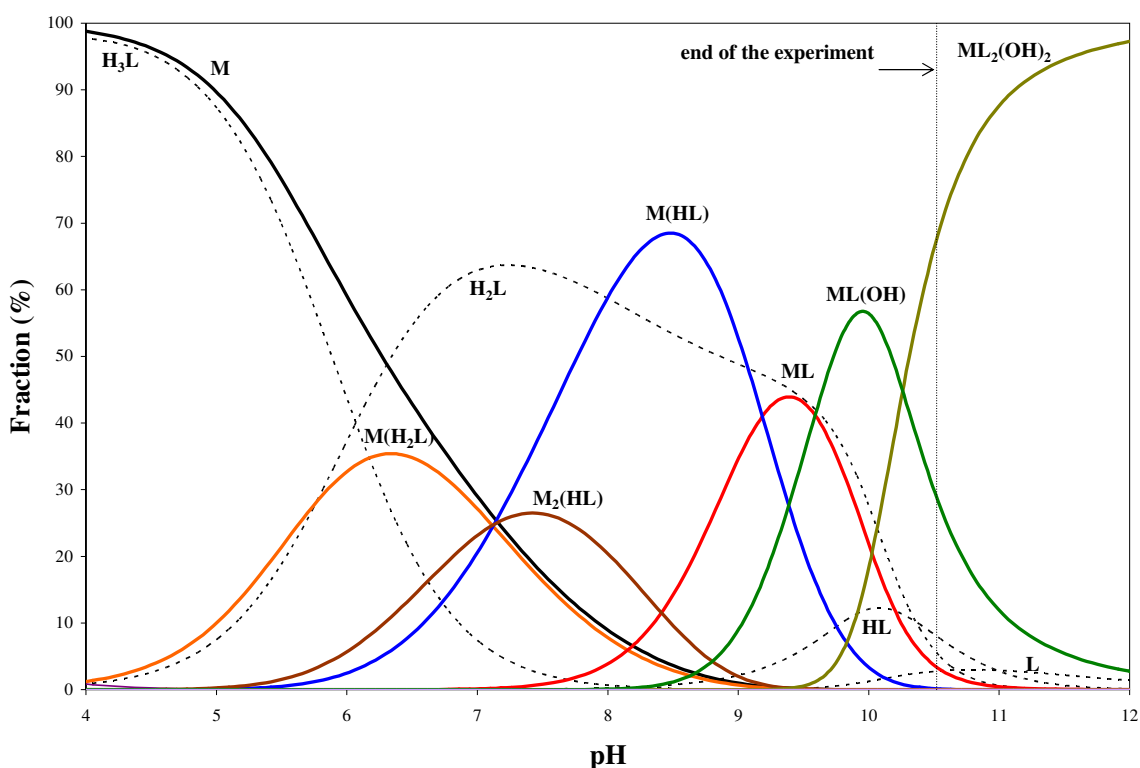


Figure 4.4 Species distribution diagrams for Mg(II)–ALN system $L_T : M_T$ ratio 2 obtained for the model $M(H_2L)$, $M_2(HL)$, $M(HL)$, ML , $ML(OH)$ and $ML_2(OH)_2$ at 25 °C and ionic strength 0.15 M in NaCl. $[M_T] = 9.9847 \times 10^{-4}$ M.

From the blood plasma point of view, it appears that aliphatic nitrogen is not involved in complex formation to any significant degree. At pH of about 7.2, about 25 % of metal is involved in three different protonated species, only about 3 % is in ML (here N-donor atom is involved in the complex formation) and about 25 % of free magnesium is still present. Interestingly, at biological pH of blood, there are four metal species (M , $M(H_2L)$, $M_2(HL)$ and $M(HL)$) at comparable concentrations.

Since N-atom is not involved in complexation when $M(H_2L)$, $M_2(HL)$ and $M(HL)$ are considered, one could assume that the mode of complexation of ALN should be similar, if not identical, as that for HEDP. If, for the sake of this discussion $ALN=L$ is redefined as $L'=HL$ (with the proton attached to nitrogen not involved in complexation) then the above these complexes might be written as $M(HL')$, $M_2(L')$, and ML' . All of these

complexes ($M(HL)$, M_2L , and ML , where $L = HEDP$) were reported for HEDP with several metal ions [19].

For purposes of comparison, Table 4.6 contains M-L models obtained for Mg(II)-APD, Mg(II)-ALN and Mg(II)-HEDP.

Table 4.6 Comparison of M–L model for Mg(II)-HEDP[19], Mg(II)-APD [14] and Mg(II)-ALN¹

Mg-APD	Mg-ALN	Mg-HEDP
M(HL)	M(HL)	ML
M(H ₂ L)	M(H ₂ L)	M(HL)
M ₂ (HL)	M ₂ (HL)	M ₂ L

¹This work

From the Table 4.6, the M–L models of APD and ALN are the same, but differ from HEDP only in numbers of protons involved in the species because in HEDP N-atom is absent. If N-atom is not involved in complexation of ALN and APD, as was assumed above, then the ligands APD and ALN should form bonds through the diphosphate oxygen atoms. If the ligands APD and ALN are redefined as above, then the mode of complexation of APD and ALN at pH below 8.0 is similar to that of HEDP.

From Figure 4.4 is seen that $M(HL)$ and $ML_2(OH)_2$ are predominant metal containing species. It would be advantageous if one could generate crystal structures of at least these two complexes to confirm the proposed model (not attempted in this work). Growing crystals might be quite difficult (if not impossible) task because (i) $M(HL)$ is accompanied by other four complexes that might co-crystallise with $M(HL)$, and (ii) at very high pH (and high M_T necessary to grow crystals) a precipitation of $M(OH)_2$ might most likely be a problem.

This analysis suggests that $M(H_2L)$, $M_2(HL)$, $M(LH)$, ML , $ML(OH)$ and $ML_2(OH)_2$ might constitute the most likely model for the system Mg(II)-ALN at $L_T : M_T$ ratio 2.

4.1.4 Ca(II)–Alendronate System

The refined formation constants for different models are presented in Table 4.7 (B). The refinement operations resulted in different models with statistical parameter, R-factor, being very much the same. Plots of ZBAR(M) vs. pA for Ca(II) (model 2 in Table 4.7) and Mg(II) (model 3 in Table 4.5) are shown in Figure 4.5 as curves (○) and (•), respectively.

Table 4.7 (A) Dissociation constant for water and overall stability constant for Ca(II) complexes with OH⁻. (B) Overall stability constants for Ca(II)–ALN L_T : M_T ratio 2 found in this work by GEP at ionic strength 0.15 M in NaCl and 25 °C. The proposed final model is indicated in bold.

(A)

Equilibrium	Log β	Equilibrium	Log β
H ⁺ + OH ⁻ = H ₂ O	13.68	Ca ²⁺ + OH ⁻ = Ca(OH) ⁺	1.30
		Ca ²⁺ + 2OH ⁻ = Ca(OH) ₂ (s)	-5.29

(B)

Complex	Model 1	Model 2	Model 3	Model 4	Model 5
M ₂ (H ₂ L)	NI	R	NI	26.46 ± 0.03	26.34 ± 0.04
M(H ₂ L)	22.87 ± 0.10	23.38 ± 0.03	23.30 ± 0.03	NI	R
M ₂ (HL)	20.596±0.008	20.430±0.007	20.471±0.009	20.458±0.008	20.620±0.007
M(HL)	NI	16.427±0.005	16.325 ± 0.02	16.402±0.005	NI
M ₂ L	11.890 ± 0.01	NI	11.15 ± 0.08	NI	11.900±0.008
ML	7.277 ± 0.006	7.243 ± 0.005	7.250 ± 0.005	7.250 ± 0.005	7.286 ± 0.006
ML(OH)	9.74 ± 0.09	9.61 ± 0.09	9.68 ± 0.08	9.32 ± 0.18	9.72 ± 0.09
ML(OH) ₂	13.93 ± 0.01	13.950±0.008	13.944±0.007	13.956±0.008	13.942±0.009
R-Factor	0.00742	0.00607	0.00584	0.00622	0.00680

NI- Not included; R- Rejected

The complex formation curve of Ca(II) is observed at smaller values of pA but with similarities in the shape of the curve of Mg(II). For Ca(II)–ALN system a “back-fanning” feature, typical for systems in which complex hydrolysis takes place is clear. The ZBAR(M) function clearly provided evidence for the formation of ML and at the beginning of the curve much smaller pA range (between 14 and 12) when compared with Mg(II) is seen that indicates much less Ca(H₂L) than Mg(H₂L) is formed. On the other hand, there is no plateau at 0.5 for both ZBAR(M) functions; this plateau would be expected when M₂L were formed. However, species M₂L was accepted by ESTA

refinement (Table 4.7 (B)). The SDD (Figure 4.7) shows that species M_2L coexists with $M(HL)$ at the same pH but is formed to a smaller extent than $M(HL)$.

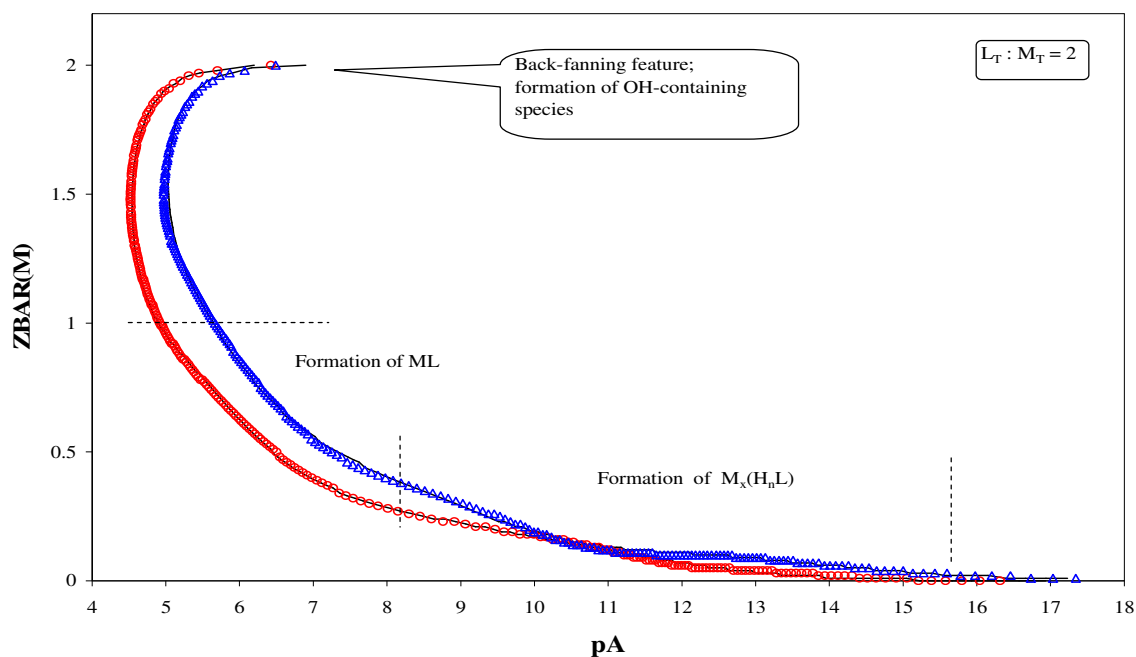


Figure 4.5 Experimental (points) and theoretical (solid line) potentiometric complex formation curves for Ca(II)–ALN (\circ) and Mg(II)–ALN systems (\bullet) $L_T : M_T$ ratio 2 obtained for the models $Ca(H_2L)$, $Ca_2(HL)$, $Ca(HL)$, CaL , $CaL(OH)$ and $CaL(OH)_2$ and $Mg(H_2L)$, $Mg_2(HL)$, $Mg(HL)$, MgL , $MgL(OH)$ and $MgL_2(OH)_2$ at 25 °C and ionic strength 0.15 M in NaCl.

From above analysis it follows that all metal species suggested in model 3 might be present in solution and hence model 2 and/or 3 can be suggested as the likely models for this system.

Three calcium complexes $M(H_2L)$, $M(HL)$ and ML and their stability constants, as $\log \beta$, 27.46, 17.6, and 6.1, respectively, at ionic strength 0.1 M in KCl and 25 °C were reported by Katkov *et al.*[7]. The larger differences in the stability constants of the species ML and $M(HL)$ between this work and those reported by Katkov *et al.*[7] is due to the different protonation constants used by Katkov.

Since hydrolysis constant of Ca(II) is smaller, less OH-containing species for Ca(II) is expected at $pH \approx 10.5$ (where experiment was completed) when compared with Mg(II); this is indeed seen in Figure 4.6, $Ca_2(HL)$ and $Ca(HL)$ are as seen for Mg(II). However,

Ca(H₂L) is a suspect as it is predicted at quite low fraction (%), but this kind of a complex was also selected for Mg(II)–ALN model.

From the Figure 4.6:

- Ca(II) forms weaker complexes with ALN than Mg(II), for instance at pH 7 about 35% of Ca(II) is not involved in complexation reactions with ALN, whereas only about 25% of Mg(II) remains free at this pH.
- M₂(HL) equivalent to Ca₂(HEDP) is a major species at blood plasma pH.
- M₂(HL) is by far most important major species in blood plasma, quite different when compared with Mg(II)-ALN.
- Less hydrolysed species is formed (correlates well with MOH values for Ca(II) and Mg(II)).
- Only protonated Ca(II)-complexes are present in blood plasma, hence NH₂-R is not involved in complexation. From this follows that higher activity of N-containing BPs in bone cancer is not directly related to complexation because the NH₂-R functional group is not involved in complex formation reaction with the central metal ion at blood plasma pH.

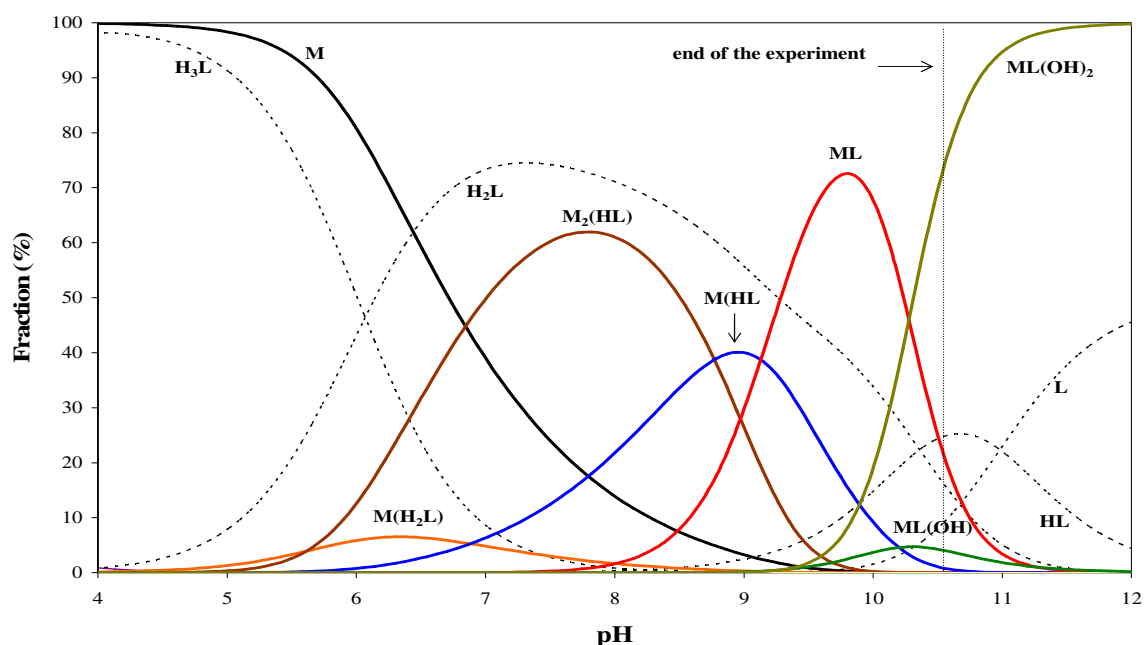


Figure 4.6 Species distribution diagrams for Ca(II)–ALN system $L_T : M_T$ ratio 2 obtained for the model M(H₂L), M₂(HL), M(HL), ML, ML(OH) and ML(OH)₂ at 25 °C and ionic strength 0.15 M in NaCl. $[M_T] = 9.9985 \times 10^{-4}$ M.

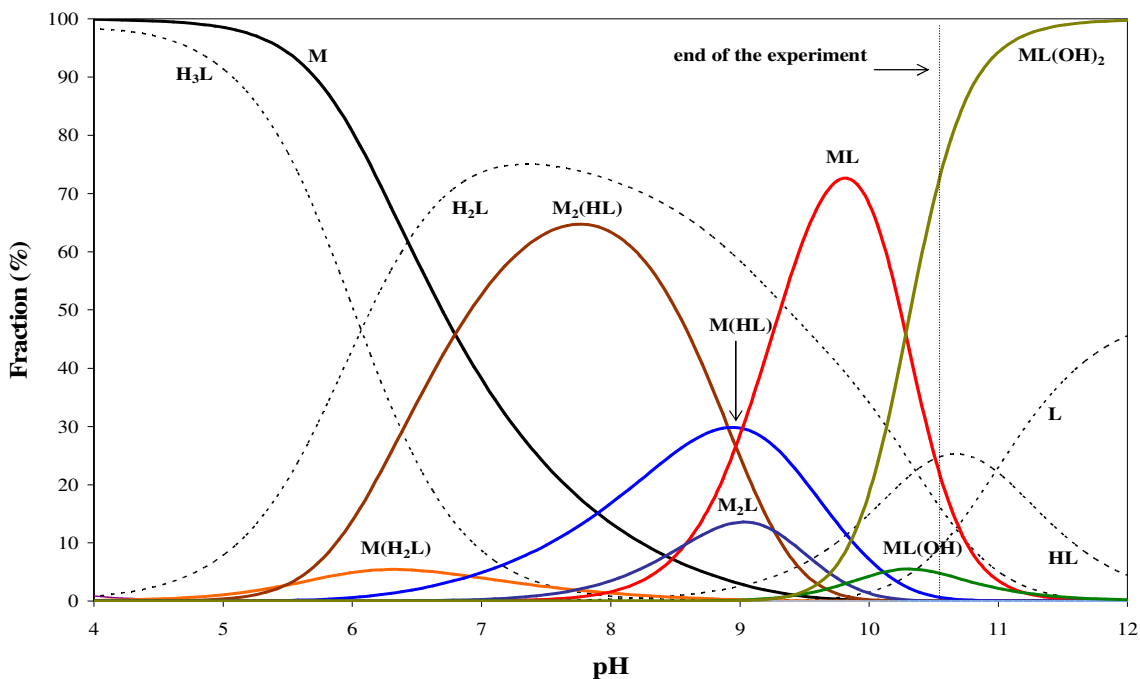


Figure 4.7 Species distribution diagrams for Ca(II)–ALN system $L_T : M_T$ ratio 2 obtained for the model $M_2(HL)$, $M_2(HL)$, $M(HL)$, M_2L , ML , $ML(OH)$ and $ML(OH)_2$ at 25 °C and ionic strength 0.15 M in NaCl. $[M_T] = 9.9985 \times 10^{-4}$ M.

4.1.5 Mg(II)–Neridronate System

Neridronate is structurally similar to alendronate and pamidronate. The 2nd, 3rd, and 4th protonation constants of ALN and NED are very much the same. In addition, N-atom is not involved in complexation up to pH about 7 hence similar protonated species would be expected.

Table 4.8 (B) shows results obtained from various refinement operations. Different models were tried involving $M(H_2L)$, $M_2(HL)$, $M(HL)$, M_2L , ML , $ML(OH)$, $ML_2(OH)$ and $ML_2(OH)_2$. The model 2 was chosen for further analysis.

Table 4.8 (A) Dissociation constant for water and overall stability constants for Mg(II) complexes with OH⁻. (B) Overall stability constants for Mg(II)–NED L_T : M_T ratio 2 found in this work by GEP at ionic strength 0.15 M in NaCl and 25 ° C. The proposed final model is indicated in bold.

(A)

Equilibrium	Log β	Equilibrium	Log β
H ⁺ + OH ⁻ = H ₂ O	13.68	Mg ²⁺ + OH ⁻ = Mg(OH) ⁺	1.87
		4Mg ²⁺ + 4OH ⁻ = Mg ₄ (OH) ₄ ⁴⁺	16.10
		Mg ²⁺ + 2OH ⁻ = Mg(OH) ₂ (s)	-9.20

(B)

Complexes	Model 1	Model 2	Model 3	Model 4
M(H₂L)	24.69 ± 0.01	24.703 ± 0.005	24.66 ± 0.01	24.670 ± 0.005
M₂(HL)	20.71 ± 0.02	20.60 ± 0.01	20.93 ± 0.02	20.902 ± 0.008
M(HL)	16.82 ± 0.01	16.890 ± 0.006	R	NI
M₂L	NI	NI	12.45 ± 0.02	12.526 ± 0.008
ML	7.86 ± 0.01	7.770 ± 0.006	7.920 ± 0.009	7.852 ± 0.004
ML(OH)	10.63 ± 0.07	11.294 ± 0.007	10.22 ± 0.15	11.241 ± 0.007
ML(OH)₂	14.62 ± 0.01	R	14.64 ± 0.01	R
ML₂(OH)₂	NI	18.323 ± 0.009	NI	18.349 ± 0.007
R-Factor	0.01265	0.00659	0.01186	0.00576

NI- Not included; R- Rejected

The ZBAR(M) function curves using model 2 of Mg(II)–NED (○) and model 3 of Mg(II)–ALN (•) are seen in Figure 4.8. The curves have similar shapes, which might indicate the presence of the same kind of species. In pA values between 18 and 11, the ZBAR(M) function value for both curves are almost the same and are above of zero, this suggests the presence of protonated species.

Below pA 11, the complex formation curve of Mg(II)–NED is observed at smaller values of pA than that of Mg(II)–ALN. At ZBAR(M) value of 0.5 there is no plateau that provides evidence for the formation of M₂L for both curves. For both systems, ZBAR(M) provided evidence for the formation of ML and OH-containing species.

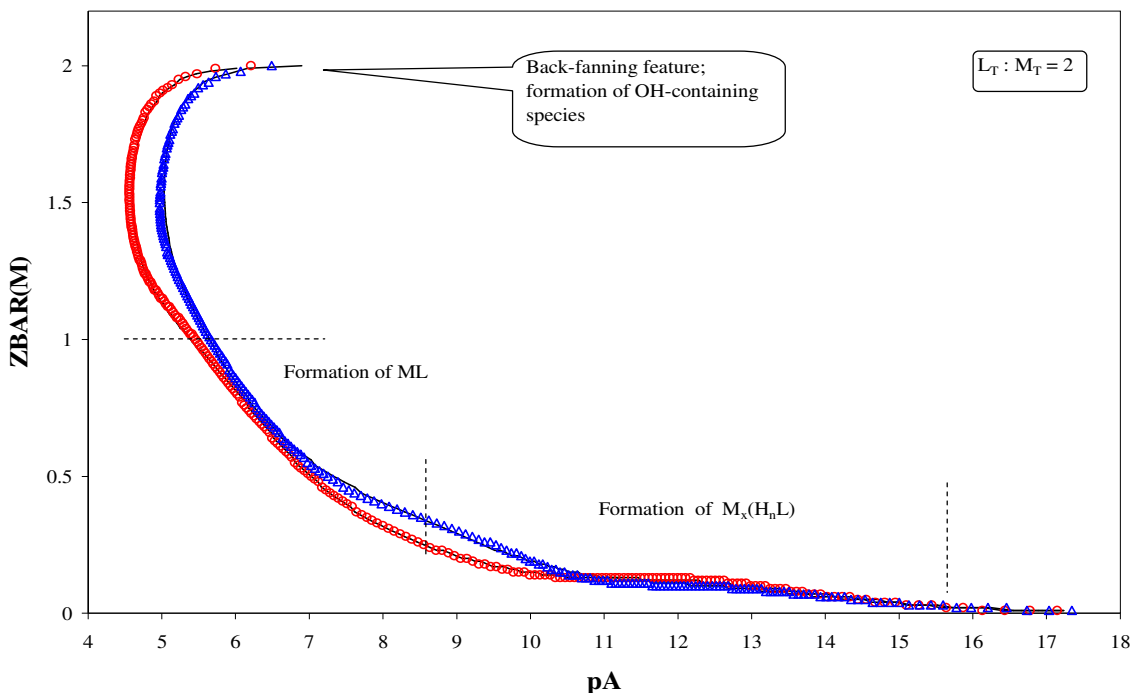


Figure 4.8 Experimental (points) and theoretical (solid line) potentiometric complex formation curves for Mg(II)–NED (○) and Mg(II)–ALN (•) systems $L_T : M_T$ ratio 2 obtained for the model $Mg(H_2L)$, $Mg_2(HL)$, $Mg(HL)$, MgL , $MgL(OH)$ and $MgL_2(OH)_2$ at 25 °C and ionic strength 0.15 M in NaCl.

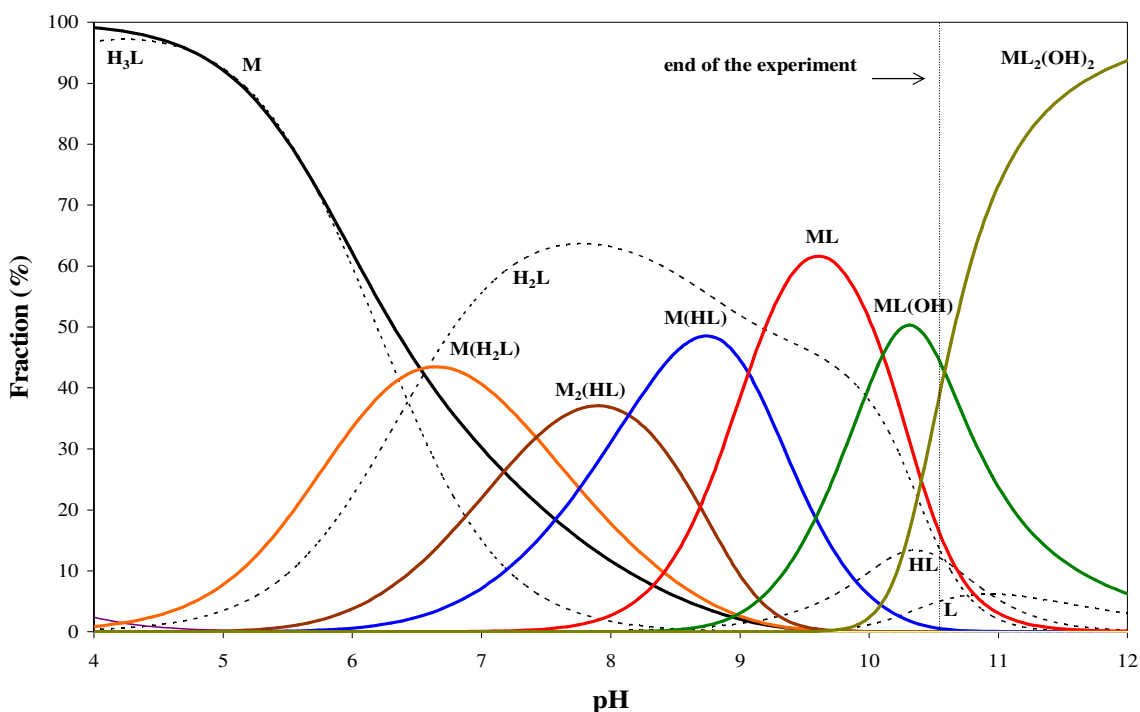


Figure 4.9 Species distribution diagrams for Mg(II)–NED system $L_T : M_T$ ratio 2 obtained for the model $M(H_2L)$, $M_2(HL)$, $M(HL)$, ML , $ML(OH)$ and $ML_2(OH)_2$ at 25 °C and ionic strength 0.15 M in NaCl. $[M_T] = 9.9848 \times 10^{-4}$ M.

The species distribution diagram plotted for the model $M(H_2L)$, $M_2(HL)$, $M(HL)$, ML , $ML(OH)$ and $ML_2(OH)_2$ shows all complexes as major species-see Figure 4.9. About 30 % of $M(H_2L)$, $M_2(HL)$, and about 20 % of $M(HL)$ and free $Mg(II)$ could be present in the blood plasma; a similar composition when compared with $Mg(II)$ –ALN. ML complex starts to form at pH about 7.5, which means its contribution at blood plasma pH of 7.4 will be insignificant.

4.1.6 Ca(II)–Neridronate System

Four models were refined with reasonable R-factor and are present in Table 4.9 (B). Models 3 and 4 have lower R-factor and could be proposed as representative for the system.

Table 4.9 (A) Dissociation constant for water and overall stability constant for Ca(II) complexes with OH⁻. (B) Overall stability constants for Ca(II)–NED $L_T : M_T$ ratio 2 found in this work by GEP at ionic strength 0.15 M in NaCl and 25 °C. The proposed final model is indicated in bold.

(A)

Equilibrium	Log β	Equilibrium	Log β
$H^+ + OH^- = H_2O$	13.68	$Ca^{2+} + OH^- = Ca(OH)^+$	1.30
		$Ca^{2+} + 2OH^- = Ca(OH)_2(s)$	-5.29

(B)

Complexes	Model 1	Model 2	Model 3	Model 4
$M(H_2L)$	NI	24.26 ± 0.03	24.23 ± 0.03	24.25 ± 0.03
$M_2(HL)$	20.20 ± 0.06	NI	20.29 ± 0.03	19.68 ± 0.08
$M(HL)$	NI	16.44 ± 0.01	NI	16.42 ± 0.01
M_2L	11.38 ± 0.04	NI	11.57 ± 0.02	R
ML	6.91 ± 0.03	6.81 ± 0.01	6.97 ± 0.02	6.89 ± 0.02
R-Factor	0.02469	0.01487	0.01192	0.01172

NI- Not included; R- Rejected.

In Figure 4.10 two curves of ZBAR(M) functions are presented Ca(II)–NED (○) and Ca(II)–ALN (•) systems. The curve of the Ca(II)–NED starts at pA of about 16 and grows coincidentally with the one of the Ca(II)–ALN until pA of about 12. The same shifts observed for the both curves between pA 14 and 12 should be due to the formation of the same types of protonated species. Between pA about 9 and 11.5 some

points were removed from the curve of the Ca(II)–NED due to the formation of precipitate of one of the protonated species in the solution, which starts to dissolve from pA about 9. Above pA of 8, the curve of the Ca(II)–NED follows the one of the Ca(II)–ALN.

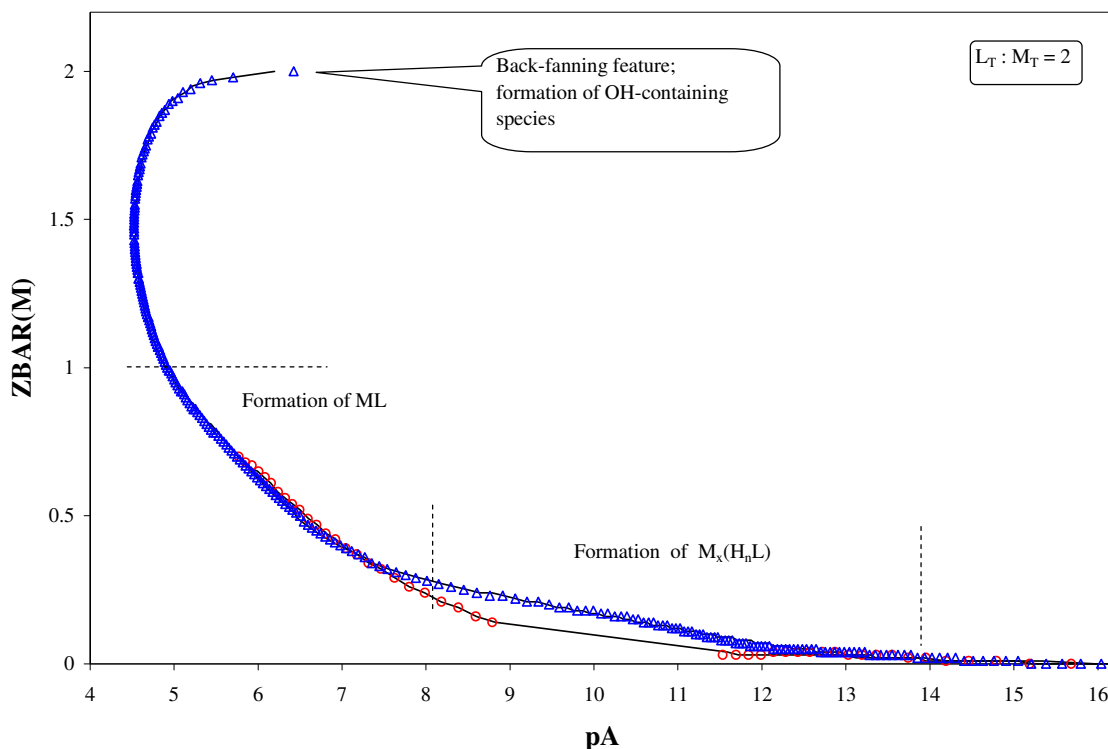


Figure 4.10 Experimental (points) and theoretical (solid line) potentiometric complex formation curves for Ca(II)–NED (\circ) and Ca(II)–ALN systems (\bullet) $L_T : M_T$ ratio 2 obtained for the models $\text{Ca}(\text{H}_2\text{L})$, $\text{Ca}_2(\text{HL})$, $\text{Ca}(\text{HL})$ and CaL (\circ) and $\text{Ca}(\text{H}_2\text{L})$, $\text{Ca}_2(\text{HL})$, $\text{Ca}(\text{HL})$, CaL , $\text{CaL}(\text{OH})$ and $\text{CaL}(\text{OH})_2$ (\bullet) at 25 °C and ionic strength 0.15 M in NaCl.

The species distribution diagram of the model 3 is presented in Figure 4.11. From this figure is seen that species $\text{M}_2(\text{HL})$ and M_2L are predominant in solution. The species $\text{M}_2(\text{HL})$ constitutes about 40 % of the solution composition and species M_2L about 50 % while $\text{M}(\text{H}_2\text{L})$ contributes about 15 % and ML 40 %. At pH 9.5 ML is not form in its totality in solution due the formation of precipitate. The SDD of the model 4 in Figure 4.12 shows that the species $\text{M}(\text{HL})$ is the major in solution and is formed exactly in the same pH range as M_2L and constitutes about 50 % of solution composition. The species $\text{M}(\text{H}_2\text{L})$ and $\text{M}_2(\text{HL})$ constitute about 15 % each of solution composition and $\text{M}_2(\text{HL})$ forms in the same pH range of the species $\text{M}(\text{HL})$.

From the Figures 4.11–12, about 60 % of Ca(II) is free at blood plasma pH and the rest is in the form of protonated species.

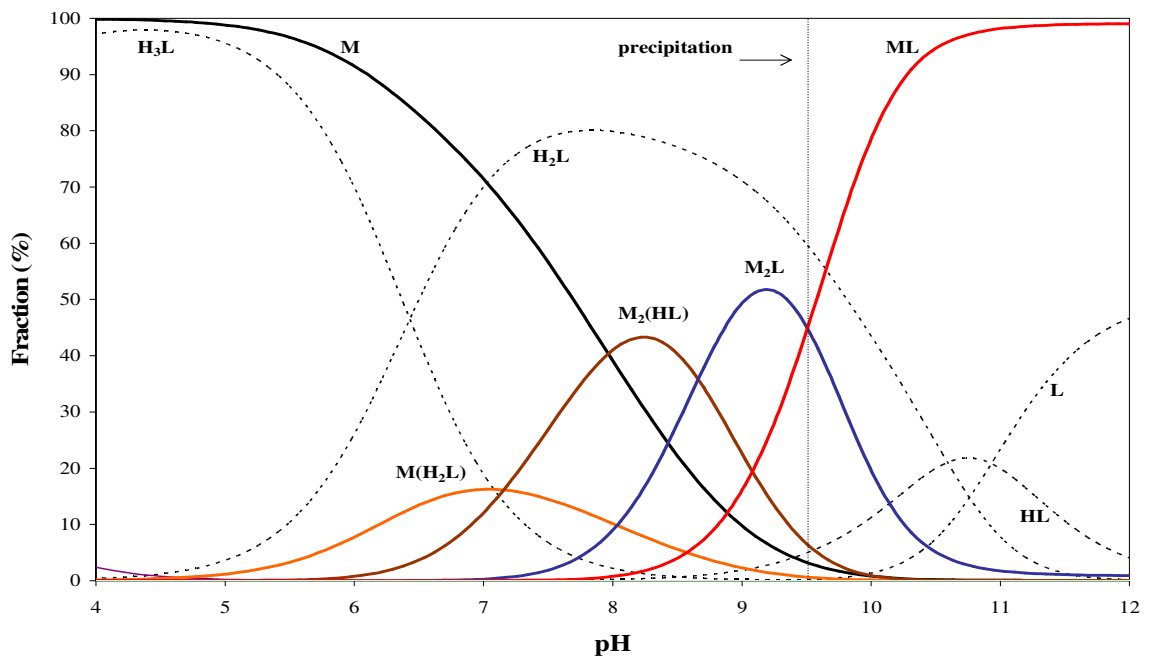


Figure 4.11 Species distribution diagrams for Ca(II)–NED system $L_T : M_T$ ratio 2 obtained for the model $M(H_2L)$, $M_2(HL)$, M_2L and ML at 25 °C and ionic strength 0.15 M in NaCl. $[M_T] = 3.9540 \times 10^{-4}$ M.

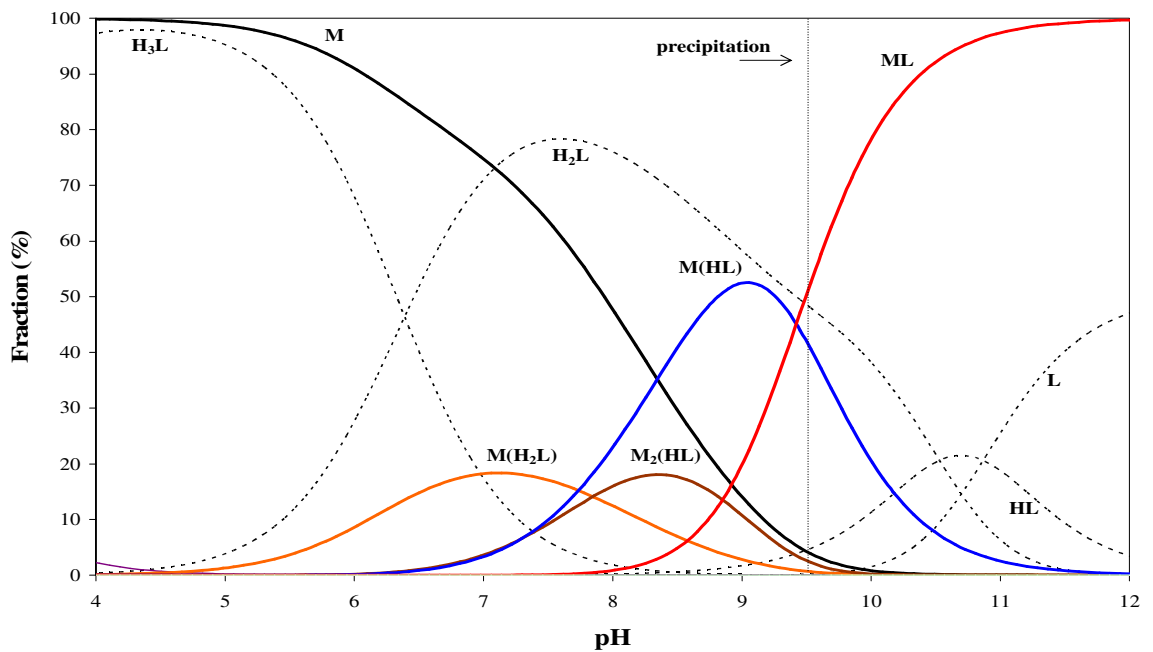


Figure 4.12 Species distribution diagrams for Ca(II)–NED system $L_T : M_T$ ratio 2 obtained for the model $M(H_2L)$, $M_2(HL)$, $M(HL)$ and ML at 25 °C and ionic strength 0.15 M in NaCl. $[M_T] = 3.9540 \times 10^{-4}$ M.

4.2 Equilibria by Polarography

When metal-ligand systems are studied by GEP, the speed with which the system reaches equilibrium can be estimated from the potential readings. This however, does not explain which species is responsible for slow kinetics in the complex formation reactions [20].

Polarography constitutes a powerful and versatile technique for the study of complexes in solution. For many metal-ligand systems it is possible to determine the degree of formation, distribution and stability constants of all species present. Studies of the stability constants of metal complexes polarographically involve the determination of shifts in half-wave potentials and limiting currents of metal ions in the presence of complexing ligands [21–25].

4.2.1 Ligands Adsorption Study

Adsorption process can be defined as the accumulation at the interface of a substance present in the bulk of the solution, in such a way that the surface concentration is in excess of the bulk concentration [17]. Because metal stability constants calculated by polarographic techniques can only be determined in the absence of adsorption of the ligand, ACP at phase angle of 90° was used to test ALN and NED adsorption at the mercury electrode. This phase angle was chosen because the current is then capacitive in nature and proportional to the double layer capacity [18].

Figure 4.13 shows a typical example of an AC voltamogram of n-pentanol in potassium nitrate. From this figure the adsorption process can be seen and interpreted by the appearance of an adsorption peak at more positive potential and a desorption peak at much more negative potential.

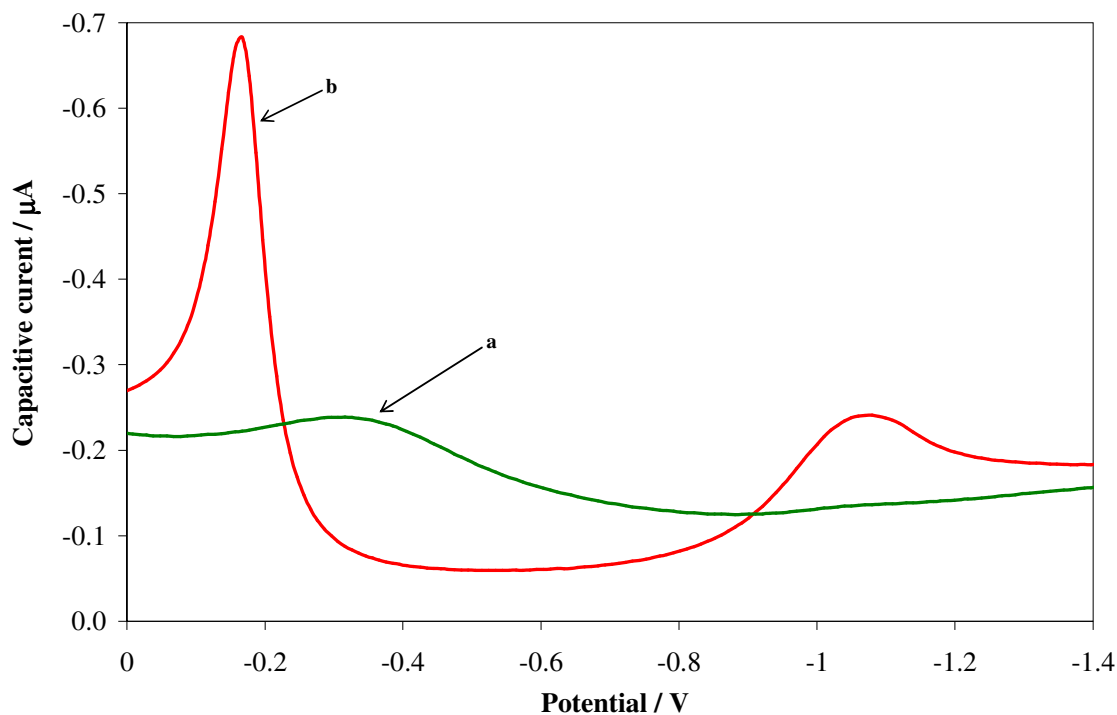


Figure 4.13 An example of AC voltamogram of 0.03 M n-pentanol in 0.1 M KNO₃. HMDE (Hanging Mercury Dropping Electrode) used as working electrode.

In this work, the adsorption studies were carried out at three pH values to check the extent of adsorption of the different ligand forms. A solution 0.15 M NaCl was used as a background electrolyte. To evaluate whether ALN or NED adsorb at the mercury electrode, curves of alternating current versus applied potential ($i_{ac} = f(E)$) were recorded between -0.20 and -1.5 V – see Figure 4.14.

For ALN at pH 6.13 and 9.60, and NED at pH 9.41 a slight departure from the curve without ligand (0.15 M NaCl, curve **a**) was observed in the potential range between -0.2 and -0.6 V (curves **b**, **c**). For NED, at pH 6.41, $i_{ac} = f(E)$ curve (curve **b**) was superimposed with the curve without ligand (0.15 M curve **a**) in the whole potential range showing that no adsorption occurred. The behaviour of the background electrolyte alone is similar to the one containing the ligands at different pH for both ligands.

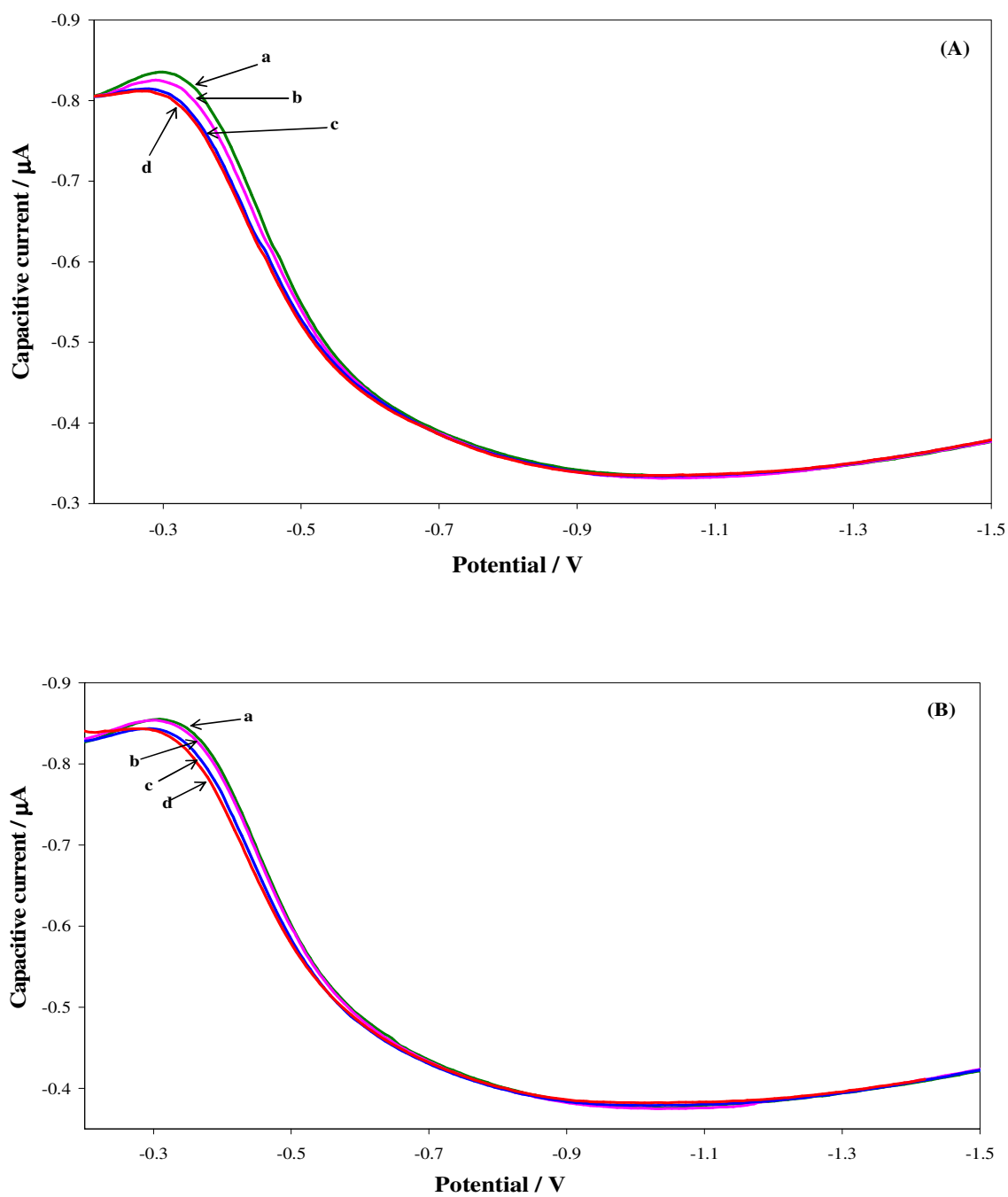


Figure 4.14 AC voltamogram for 0.01 M ALN (A) and NED (B) in 0.15 M NaCl at different pH. (A) pH: **a** = 7.15 (background), **b** = 6.13, **c** = 9.60 and **d** = 10.52; (B) pH: **a** = 7.01 (background), **b** = 6.41, **c** = 9.41 and **d** = 10.84. HMDE used as working electrode.

4.2.2 Fitting of Polarographic Curves

An appropriate method for accurate estimating the values of I_d and $E_{1/2}$ from polarograms is needed for modelling and for determination of stability constants.

Cukrowski [26–27] proposed a simple curve fitting method for analysis of DC or NP polarograms.

$$I_{red} = \frac{I_d}{\exp \frac{\delta n F}{RT} (E_{appl} - E_{1/2}) + 1} \quad (4.2)$$

The sampled DC or NP waves are the sum of the reduction and background current at any applied potential. For fitting experimental polarograms, the reduction current, I_{red} and the background current I_b are given by Equation 4.3:

$$I_{obs} = \frac{I_d}{\exp \frac{\delta n F}{RT} (E_{appl} - E_{1/2}) + 1} + I_b \quad (4.3)$$

were, I_{obs} stands for the observed total current, n stands for a number of electrons, E_{appl} is the stepwise applied potential at which the total current was recorded, I_d is the limiting diffusion current, and δ is a coefficient describing how steep the polarographic wave is and is used for evaluating electrochemical reversibility of DC or NP curves, and I_b is background current that can be:

(i) Linear function

$$I_b = a + bE_{appl} \quad (4.4)$$

(ii) Polynomial function

$$I_b = a + bE_{appl} + cE_{appl}^2 \quad (4.5)$$

$$I_b = a + bE_{appl} + cE_{appl}^2 + dE_{appl}^3 \quad (4.6)$$

(iii) Exponential function

$$I_b = a + bE_{appl} + c \exp(-dE_{appl}) \quad (4.7)$$

Based on the δ value, it is possible to decide which method or function is the most appropriate to estimate I_d and $E_{1/2}$. For fully reversible systems (δ equals to 1) or close to reversible systems (δ values above 0.9), Cukrowski's curve-fitting method (Equation 4.2) is useful. For quasi-reversible systems (δ between 0.5–0.9), we can use Equation 4.8 [28] that was derived from Ružić method [29]:

$$I_{obs} = \frac{I_d}{\exp \frac{\alpha n F}{RT} (E_{appl} - E_{1/2}^{irr}) + \exp \frac{n F}{RT} (E_{appl} - E_{1/2}^r) + I} + I_b \quad (4.8)$$

were I_{obs} stands for the observed total current, n stands for number of electrons, E_{appl} is the stepwise applied potential at which the total current was recorded, α is the cathodic transfer coefficient, $E_{1/2}^r$ is the reversible half-wave potential, $E_{1/2}^{irr}$ is the 'irreversible' half-wave potential corresponding to the irreversible part of the DC or NP wave and I_b is a function describing the background current (Equations 4.4–4.7).

Initially, Cukrowski curve-fitting procedure was used in this project for fitting and checking the degree of electrochemical reversibility of systems in order to choose the appropriate method to extract the parameters I_d and $E_{1/2}$ for use in the modelling and determination of stability constants [28].

The DC or NP waves of metal-ligand systems studied here showed significant departure from reversibility; δ varied with pH in the range 0.88–0.50 showing characteristics of quasi-reversible system. In this case Ružić-based curve-fitting method [28] was useful for estimating reversible half-wave potentials and limiting currents.

4.2.3 Cd(II)–Alendronate–System

Data fitting

The polarographic study of Cd(II)–ALN, $L_T : M_T$ ratio 266.6, was performed by sampled DC polarography. The polarograms were recorded in the pH range 4.88 to 8.87. Above pH 8.87 the polarographic wave disappeared; no precipitation was observed in the pH range in which the data was collected.

The polarographic data were fitted as obtained from the experiment; the limiting diffusion current, half-wave potential and the parameters of background (values of a , b ,) were allowed to vary as described in Equations 4.2–4.8. In the cases where the background current of the curves was not varied in linear manner, the polynomial function was used to account for the background current in the recorded polarograms.

Three consecutive polarograms were recorded for Cd(II) in absence of the ligand at pH 5.47. These polarograms were fitted using Equations 4.2–4.3 to check the degree of electrochemical reversibility given by the parameter delta (δ). The parameter δ varied between 0.91 and 0.96 which indicated reversible reduction process. Afterwards, a ligand solution was added to the sample solution and polarograms were recorded in the presence of the ligand. The parameter δ varied between 0.52 and 0.86 which indicated quasi-reversible reduction process. To account for the departure from the electrochemical reversibility Ružić-based equation (Equation 4.8) was used for fitting of polarograms as well as Equation 4.6 to account for background current. Example of the fitted polarogram for this system is shown in Figure 4.15.

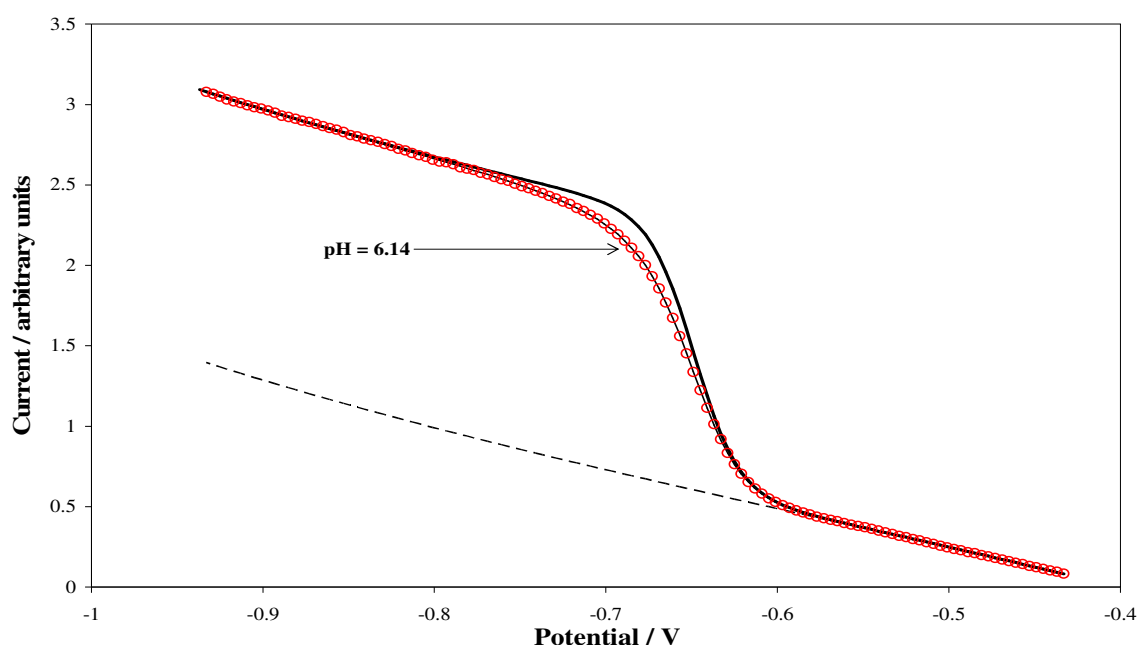


Figure 4.15 Example of the fitted polarogram for Cd(II)–ALN system studied by sampled DCP at $L_T : M_T = 266.6$, ionic strength 0.15 M (NaCl), 25 °C, initial $[M_T] = 1.4978 \times 10^{-5}$ M. The circles represent experimental points; thin solid line represents theoretically fitted curve using the curve-fitting method based on the Ružić equation (Equation 4.8); the thick solid line represents computed curves corresponding to fully reversible reduction processes using the I_d and $E_{1/2}^F$ values obtained from curve-fitting based on the Ružić equation; dashed line represent background current.

Modelling of experimental data

i) Variation in limiting diffusion current vs pH

From Figure 4.16, between pH 4.88 and 6.06, there is small change in normalized limiting diffusion current (seen as triangles), which might be interpreted as the formation of labile metal species, such as protonated species $M(H_nL)$. Above pH 6.06 there is a large decrease in I_d which indicates formation of inert complex. Between pH 6.56 and 7.32 there is a broad range where the diffusion current is almost constant that might be attribute the formation or presence of another labile complex in solution. Above pH value of about 7.51, the I_d continues to decrease until the wave disappears above pH 8.87. The expected current (seen in Figure 4.16 as circles) didn't change much indicating no significant dilution of sample solution throughout the whole experiment.

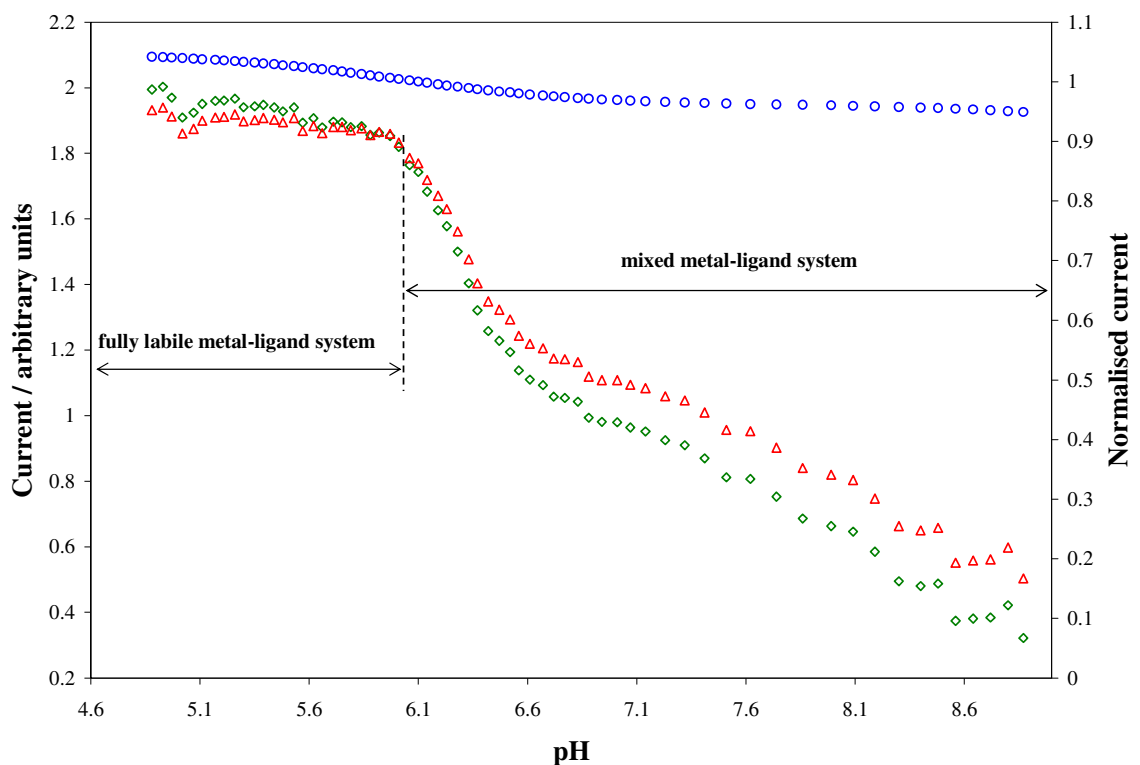


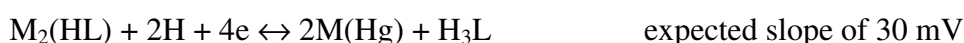
Figure 4.16 Variation in limiting diffusion current for Cd(II)–ALN system studied by sampled DC polarography at $L_T : M_T = 266.6$, ionic strength 0.15 M (NaCl), 25 °C, initial $[M_T] = 1.4978 \times 10^{-5}$ M. The triangles indicate the normalized limiting diffusion current, diamonds indicate the observed diffusion current and the circles indicate the expected current.

It has been demonstrated [30] that the concept of virtual potential must be applied when decrease in the intensity of recorded signal is significant when polarographically inert and electrochemically inactive metal-containing species are formed in solution. From the Figure 4.16, large decrease in I_d was observed hence the use of the concept of virtual potential is important in predicting the kind of species forming in the solution.

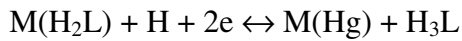
ii) *Variation in virtual half-wave potential, $E'_{1/2}$ vs pH*

The use of slope analysis has been demonstrated useful in prediction of labile metal species [13, 23]. A Nernstian slope of $m(RT/nF)$ is expected when labile protonated complexes metal are formed (where m and n stand for the number of protons and electrons, respectively, involved in the electrochemical reaction). The change in the slope is caused by the change in the predominant form of the ligand in the solution and as a result different number of protons is involved in the electrochemical process at the dropping mercury electrode (DME) [25]. When a polynuclear species is involved in the complex formation reaction with two metal ions such as M_2L , the commonly used Nernstian type of slope written above has to be modified to the following form $\{m(RT/nF)\}/p$, where p stands for the number of metal ions involved in the electrochemical process [13].

In Figure 4.17, a plot of $E'_{1/2}(virt)$ vs pH for this system is shown. In the pH range between 4.88 and about 6.06, where the major form of the ligand is H_3L , the observed slope confirms the supposition made from the analysis of I_d vs. pH , whereby protonated metal complexes $M(H_nL)$ are formed in this pH range. If the metal complex formed in this pH range was $M(H_3L)$, the expected shift would be closed to null in which no proton is involved, but this is not the case. As it can be seen in Figure 4.17, a slope of about 25 mV per pH unit is observed. This might suggest the presence of metal species $M_2(HL)$ and/or $M(H_2L)$, whose theoretical slope is 30 mV per pH unit when the complex is fully formed in the solution. These metal species require the involvement of one proton per metal ion, according to the following electrochemical reactions (charges are omitted for simplicity):



and/or



expected slope of 30 mV

Between pH 4.88–6.06 there is already a lot of H_2L in solution. Slope of 30 mV per pH unit is expected when only H_3L is present. This might explain why the observed slope is below 30 mV.

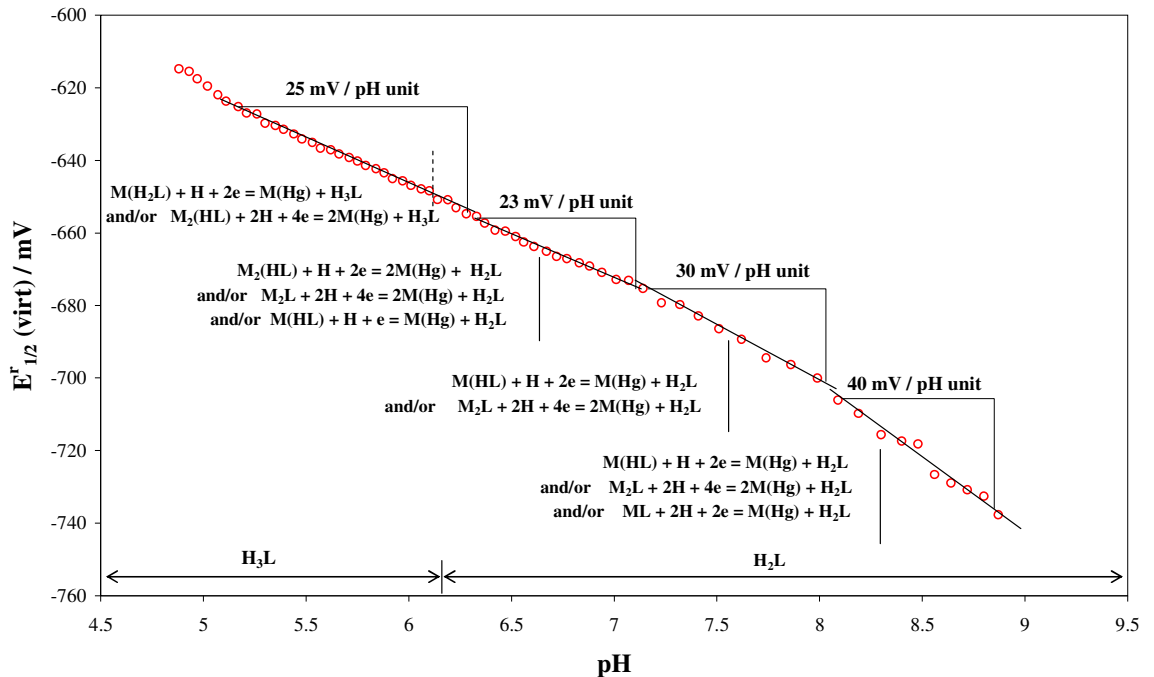
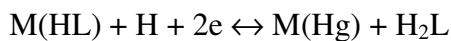


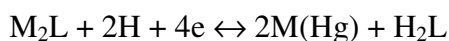
Figure 4.17 Analysis of variation in $E_{1/2}^r$ (virt) as a function of pH for Cd(II)–ALN system studied by sampled DC polarography at $L_T : M_T = 266.6$, ionic strength 0.15 M (NaCl), 25 °C, initial $[M_T] = 1.4978 \times 10^{-5}$ M. $E_{1/2}^r$ (virt) is reversible half-wave potential obtained using the Ružić curve-fitting method (Equation 4.8).

In the pH range between 6.33 and 7.07 the slope of about 23 mV per pH unit is observed. The major form of the ligand in this pH range is H_2L . This slope might be a result of the following two electrochemical processes:



expected slope of 30 mV

and/or



expected slope of 30 mV

The reduction of both species requires one proton per metal ion hence the expected slope is 30 mV per pH unit. However, the observed slope is smaller and corresponds to an average value between 15 and 30 mV per pH unit, which means that there is a

mixture of complexes in solution. One of the metal species could be $M_2(HL)$ with the following electrochemical reaction:



As pH increases further, from 7.01 to about 8.09, a slope of 30 mV per pH unit is observed. This indicates the involvement of one proton in the electrochemical reaction. The metal complexes that result from the slope 30 mV per unit in this pH range could be $M(HL)$ and/or M_2L . The possible electrochemical reactions are:



and/or



Another slope of 40 mV per pH unit is observed at the pH values above 8.09. The predominant form of ligand is still H_2L . The possible complex existing is ML according to the following reactions:



The expected slope should be 60 mV per pH unit when this complex is fully formed in solution. However, the observed slope is smaller, and corresponds to an average between 30 and 60 mV per pH unit, which means that a mixture of complexes has to be present. The possible complexes should be $M(HL)$ and/or M_2L both with the slope 30 mV per pH unit as indicated above.

At this stage, it is possible to suggest the most likely model for this systems: $M(H_2L)$, $M_2(HL)$, $M(HL)$, M_2L (as labile complexes) and ML (as non-labile complex).

iii) Variation in half-wave potential, $E_{1/2}^r$ vs. $\log [H_nL]$

The new method of modelling was developed for analysing of the slopes of the species $M_p(H_nL)$ [31]. Thus, complexes like $M(H_2L)$ can be predicted using this type of analysis.

The plot of $E_{1/2}^r(virt)$ vs $\log [H_2L]$ (shown in Figure 4.18) was plotted to predicte $M_p(H_2L)$ type of species in solution. The slope of about 32 mV per $\log [H_2L]$ is observed in Figure 4.18. A theoretical slope of about 30 mV per $\log [H_2L]$ unit is expected for $M(H_2L)$. This indicates the presence of the species $M(H_2L)$ in solution according to the following electrochemical process:

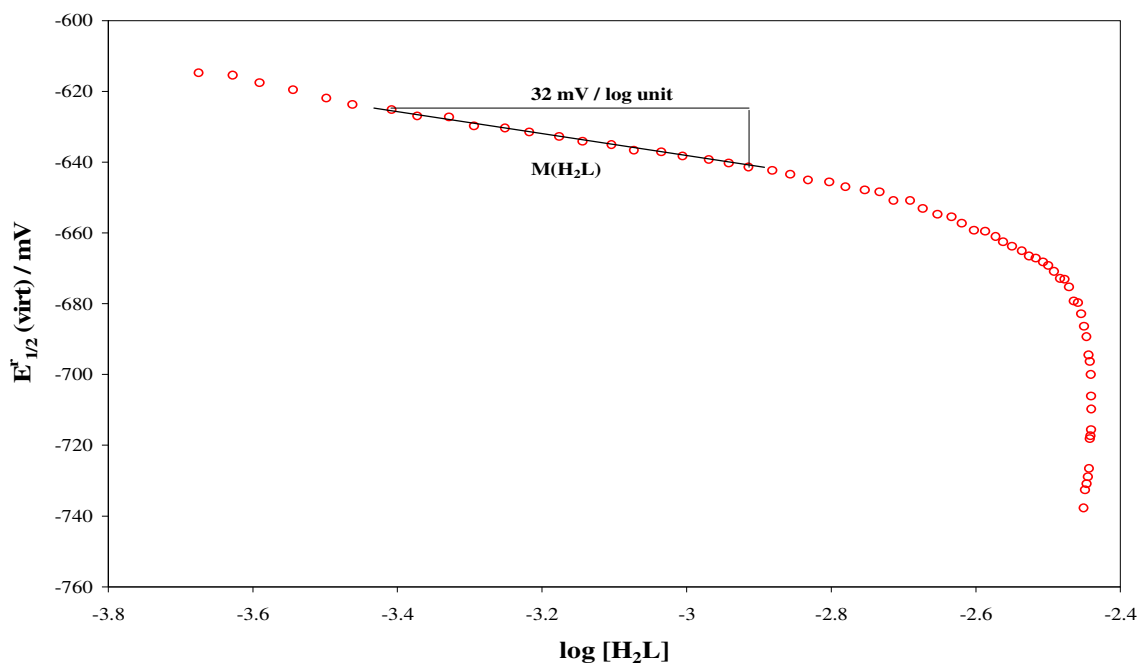
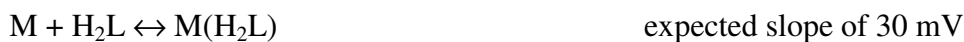


Figure 4.18 Analysis of variation in $E_{1/2}^r(virt)$ as a function of $\log [H_2L]$ for Cd(II)–ALN system studied by sampled DC polarography at $L_T : M_T = 266.6$, ionic strength 0.15 M (NaCl), 25 °C, initial $[M_T] = 1.4978 \times 10^{-5}$ M.

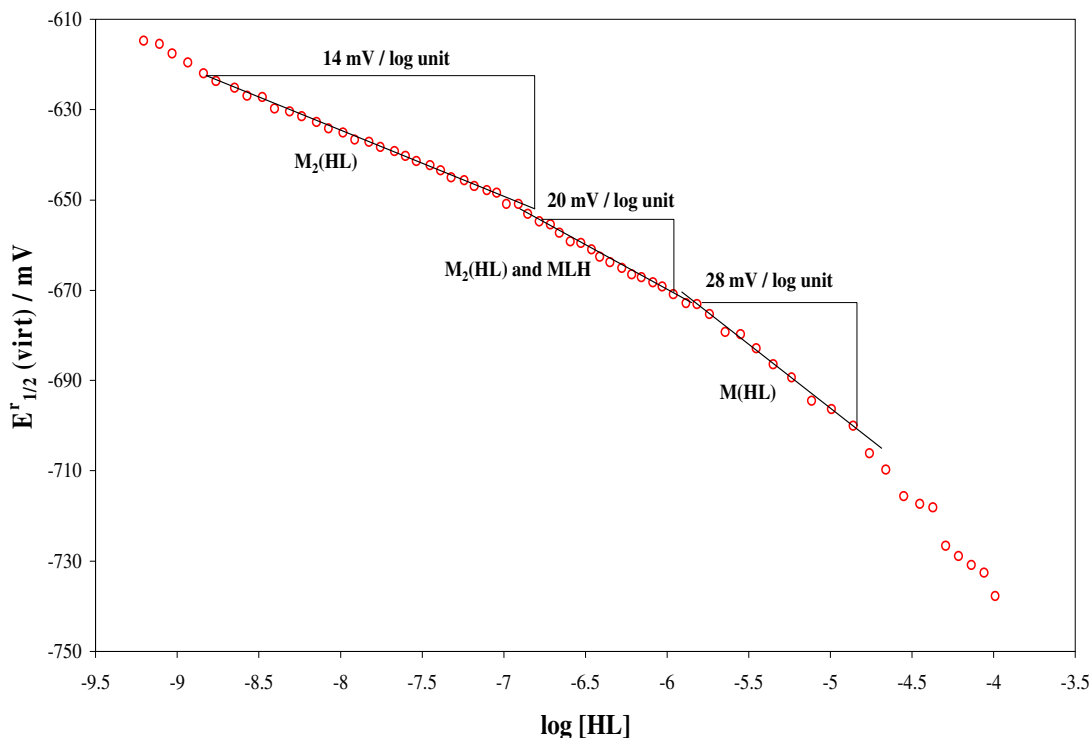


Figure 4.19 Analysis of variation in $E_{1/2}^r(\text{virt})$ as a function of $\log [\text{HL}]$ for Cd(II)–ALN system studied by sampled DC polarography at $L_T : M_T = 266.6$, ionic strength 0.15 M (NaCl), 25 °C, initial $[M_T] = 1.4978 \times 10^{-5}$ M.

The same metal complex, $M(\text{H}_2\text{L})$ was predicted to be formed in solution in the same pH range as shown in Figure 4.17. Thus the metal complex $M(\text{H}_2\text{L})$ is supported to be formed in solution by Figure 4.18.

On the other hand in Figure 4.19, a slope of about 14 mV per $\log [\text{HL}]$ can be seen which suggests the formation of the species $M_2(\text{HL})$ according to the complex formation reaction:



A slope about 20 mV per $\log [\text{HL}]$ is also seen in Figure 4.19. This clearly shows a mixture of species with average slope between 15 and 30 mV per $\log [\text{HL}]$. They could be $M_2(\text{HL})$ and $M(\text{HL})$ whose resultant theoretical slope should be about 22.5 mV per $\log [\text{HL}]$ when they are formed in equal amounts in solution according to the complex formation reactions:



and/or



A slope of about 27 mV per log [HL] is observed as well. This slope indicates the presence of the species M(HL) according to the reaction:



The same metal complex, M(HL) was predicted to be formed in solution in the same pH range as shown in Figure 4.17 and hence it's formation in solution is supported here.

iv) Variation in half-wave potential, $E'_{1/2}$ vs. log [L]

The formation of the species of the type M_pL_q can be confirmed from the analysis of a shift in the $E_{1/2}$ potential when plotted vs. log [L]. The Nernstian slope of $\{(mRT/nF)\}/p$, [13, 23] can be applied and in this case m stands for the number of ligands involved in the complex formation reaction.

In Figure 4.20, the slope of about 15 mV per log unit was observed in the same pH range as seen in Figure 4.17, which indicates the presence of M_2L . The reaction involved is:



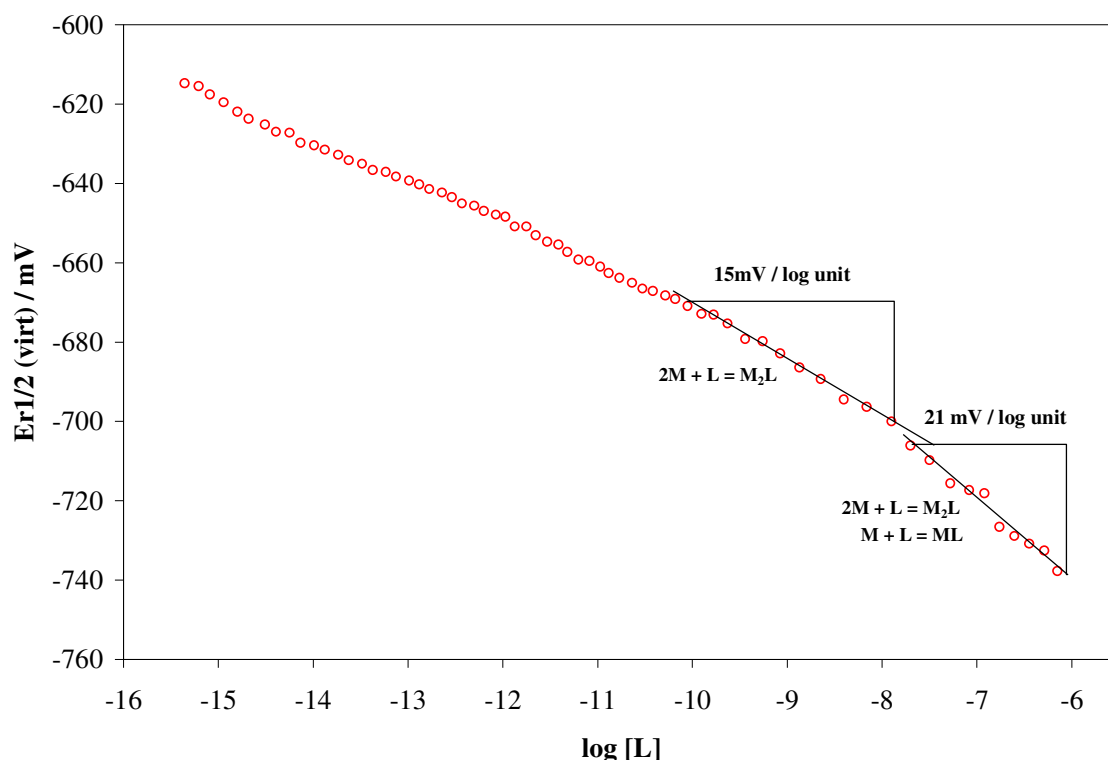


Figure 4.20 Analysis of variation in $E_{1/2}^{\text{virt}}$ as a function of $\log [L]$ for Cd(II)–ALN system studied by sampled DC polarography at $L_T : M_T = 266.6$, ionic strength 0.15 M (NaCl), 25 °C, initial $[M_T] = 1.4978 \times 10^{-5}$ M.

A slope of about 21 mV per $\log [L]$ unit is also seen, which in principle could be ML whose expected slope is 30 mV per $\log [L]$ but the smaller slope obtained indicates a mixture of complex with slope between 15 and 30 mV per $\log [L]$ unit. This means M_2L should be the complex present with ML in this pH range that can give the resultant slope of about 21 mV.

The species M_2L and ML are formed in the same pH range as seen in Figure 4.19. This observation supports the existence of the species M_2L and ML in solution. On the other hand, formation of M_2L is predicted in the same position (seen in Figure 4.19) where $M(HL)$ is also predicted.

From the above analyses of data (relationships seen in Figures 4.17–4.20) it is difficult to arrive to a single metal-ligand model. One can suggest two most likely models from the above modelling procedures: $M(H_2L)$, $M(HL)$ and ML or $M_2(HL)$, M_2L and ML plus all known $Cd_x(OH)_y$ species.

v) Optimization of a metal–ligand model and refinement of stability constants

The optimisation of the model and the refinement of the stability constants from the polarographic data were performed using the experimental (ECFC) and calculated complex formation curves (CCFC) generated using the dedicated software 3D Complex Formation Curves (3D–CFC) [32] developed for refinement of polarographic data – see Figure 4.21.

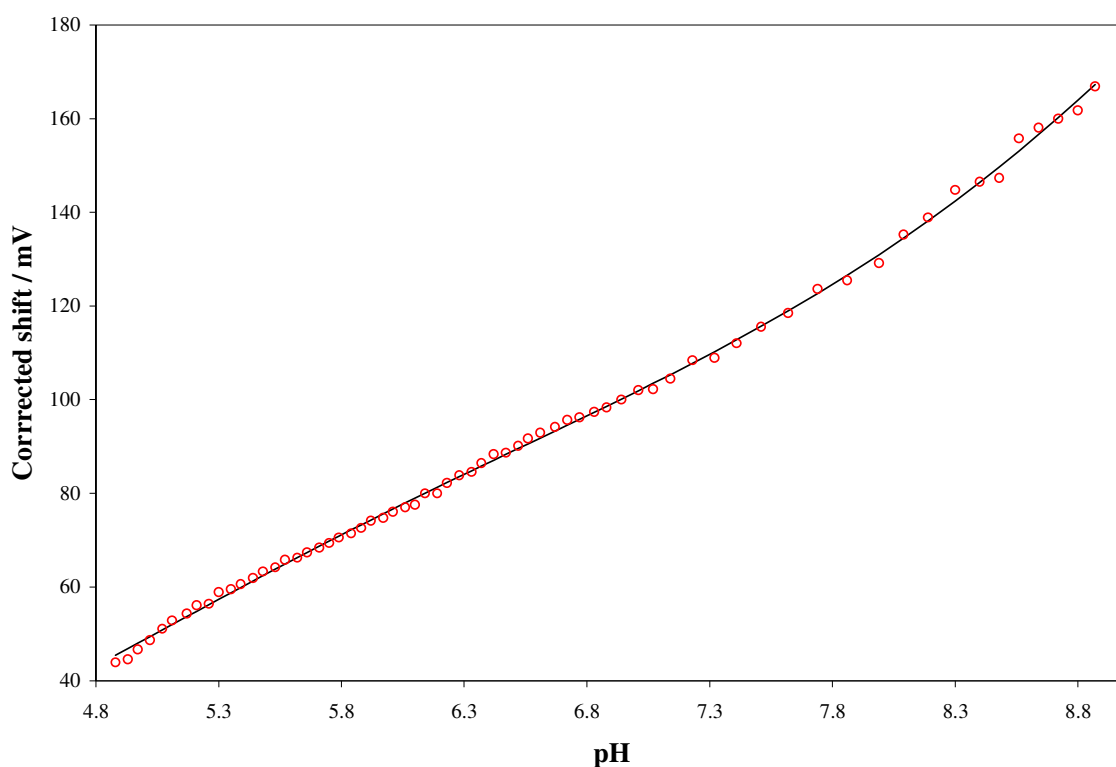


Figure 4.21 Experimental and calculated complex formation curves obtained using reversible half-wave potentials for Cd(II)–ALN system studied by sampled DC polarography at $L_T : M_T = 266.6$, ionic strength 0.15 M (NaCl), 25 °C, initial $[M_T] = 1.4978 \times 10^{-5}$ M. The circles represents the ECFC and solid line represents the CCFC for the optimized M–L model contained $M_2(HL)$, $M(HL)$ and ML .

The strategy used in the refinement process is presented in Table 4.10 (B):

Table 4.10 (A) Dissociation constant for water and overall stability constants for Cd(II) complexes with OH. (B) Overall stability constants for Cd(II)–ALN found in this work by sampled DCP at ionic strength 0.15 M in NaCl and 25 ° C, $L_T : M_T$ ratio 266.6, $[Cd_T] = 1.4978 \times 10^{-5}$ M. The proposed final model is indicated in bold.

(A)

Equilibrium	log β	Equilibrium	log β
$H^+ + OH^- = H_2O$	13.68	$Cd^{2+} + OH^- = Cd(OH)^+$	4.00
		$Cd^{2+} + 2OH^- = Cd(OH)_2$	7.70
		$Cd^{2+} + 3OH^- = Cd(OH)_3^-$	10.30
		$Cd^{2+} + 4OH^- = Cd(OH)_4^{2-}$	12.00
		$2Cd^{2+} + OH^- = Cd_2(OH)^{3+}$	5.06
		$4Cd^{2+} + 4OH^- = Cd_4(OH)_4^{4+}$	24.90
		$Cd^{2+} + 2OH^- = Cd(OH)_2(s)$	-14.30

(B)

Equilibrium ¹	Model 1	Model 2	Model 3	Model 4
$M + L + 2H \leftrightarrow M(H_2L)$	R	R	26.65 ± 0.008	26.66 ± 0.008
$2M + L + H \leftrightarrow M_2(HL)$	27.83 ± 0.01	27.81 ± 0.01	NI	NI
$M + L + H \leftrightarrow M(HL)$	NI	20.20 ± 0.01	20.26 ± 0.01	NI
$2M + L \leftrightarrow M_2L$	21.18 ± 0.02	R	NI	21.26 ± 0.02
$M + L \leftrightarrow ML$	11.75 ± 0.02	11.63 ± 0.03	12.56 ± 0.03	11.70 ± 0.03
Overall fit (mV)	1.2447	1.0836	1.3724	1.6968

¹Charges are omitted for simplicity; NI- Not included; R- Rejected

The refinement operations started by the model containing $M(H_2L)$, $M_2(HL)$, M_2L and ML . The refinement resulted in the rejection of $M(H_2L)$. When $M(H_2L)$ was replaced by $M(HL)$ and data refined again, the species M_2L was rejected. The species $M(H_2L)$ and $M_2(HL)$, as well as $M(HL)$ and M_2L were predicted to form in solution in the same pH range - see Figure 4.17. It appears that, the refinement procedures favoured species $M_2(HL)$ and $M(HL)$. When the size of the initial model was reduced, the models 3 and 4 were refined without problems with small differences in the overall statistical parameter.

By comparison, the protonated species obtained in Cd(II)–ALN system are similar to those as obtained for Mg(II)–ALN and Ca(II)–ALN ; Cd(II) forms stronger complexes than Mg(II) and Ca(II) with ALN.

vi) Species distribution diagram

The SDD for the model 1 is shown in Figure 4.22. It indicates that species $M_2(HL)$ and M_2L are major in solution and constitute about 95 % and 80 % of solution composition at pH 5.00 and 7.50, respectively; species ML is the minor species in solution below pH 7.5. From SDD it can be see that species $M_2(HL)$ is predominant in pH range where

H_3L is the major form of the ligand and M_2L are formed in pH range where H_2L is predominant form of the ligand. The SDD for the model 2 in Figure 4.23 and model 3 in Figure 4.24 shows $M_2(HL)$ and $M(HL)$, and $M(H_2L)$ and $M(HL)$, respectively. By comparison the SDD of the three models it can be seen that species $M(HL)$ and $M(H_2L)$ replaces M_2L and $M_2(HL)$ in appropriate pH ranges. From Figure 4.25, where all predicted species are present, it can be seen that the species M_2L and $M(HL)$ as well as $M(H_2L)$ and $M_2(HL)$ are formed in the same pH range. This explains the rejection of the species $M(H_2L)$ and M_2L in the refinement operation when these species were incorporated into the model 2.

From above analyses one can say that all species predicted from the modelling seem to be present in solution in smaller or larger fraction and the type of species favoured are $M_2(HL)$ and $M(HL)$ over the species $M(H_2L)$ and M_2L . Thus, the likely model for this system seems to be the model 2, but this does not mean that the other models are not plausible.

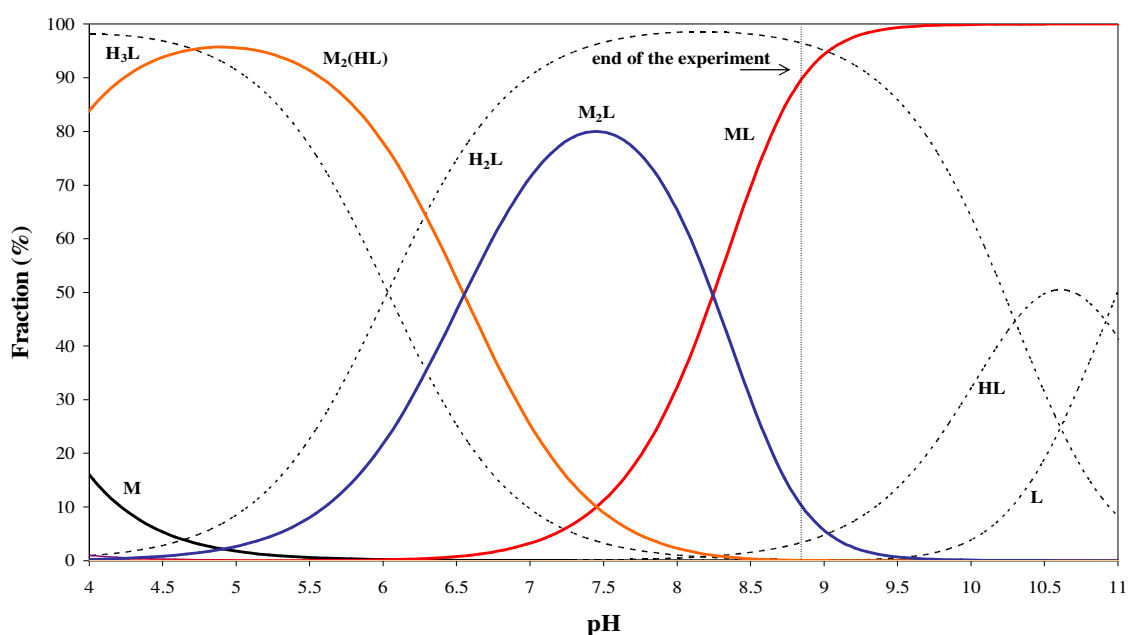


Figure 4.22 Species distribution as a function of pH for the model $M_2(HL)$, M_2L , and ML for $Cd(II)$ -ALN system studied by sampled DC polarography at $L_T : M_T = 266.6$, ionic strength 0.15 M (NaCl), 25 °C, initial $[M_T] = 1.4978 \times 10^{-5}$ M.

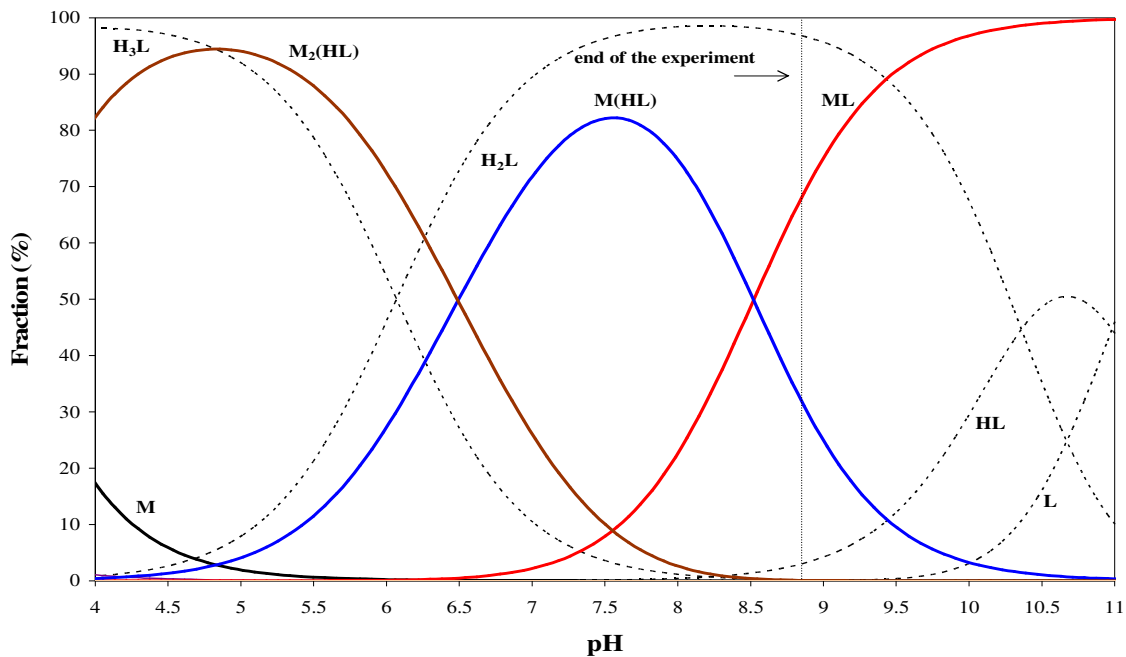


Figure 4.23 Species distribution as a function of pH for the model $M_2(HL)$, $M(HL)$, and ML for Cd(II)–ALN system studied by sampled DC polarography at $L_T : M_T = 266.6$, ionic strength 0.15 M (NaCl), 25 °C, initial $[M_T] = 1.4978 \times 10^{-5}$ M.

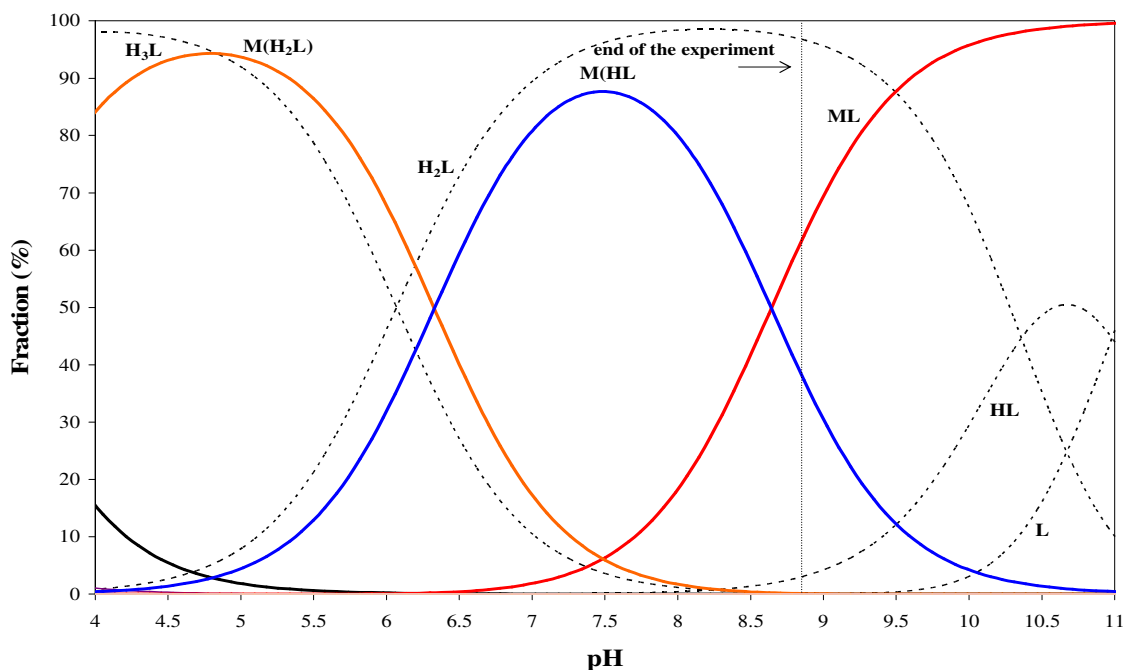


Figure 4.24 Species distribution as a function of pH for the all species predicted $M(H_2L)$, $M(HL)$, and ML for Cd(II)–ALN system studied by sampled DC polarography at $L_T : M_T = 266.6$, ionic strength 0.15 M (NaCl), 25 °C, initial $[M_T] = 1.4978 \times 10^{-5}$ M.

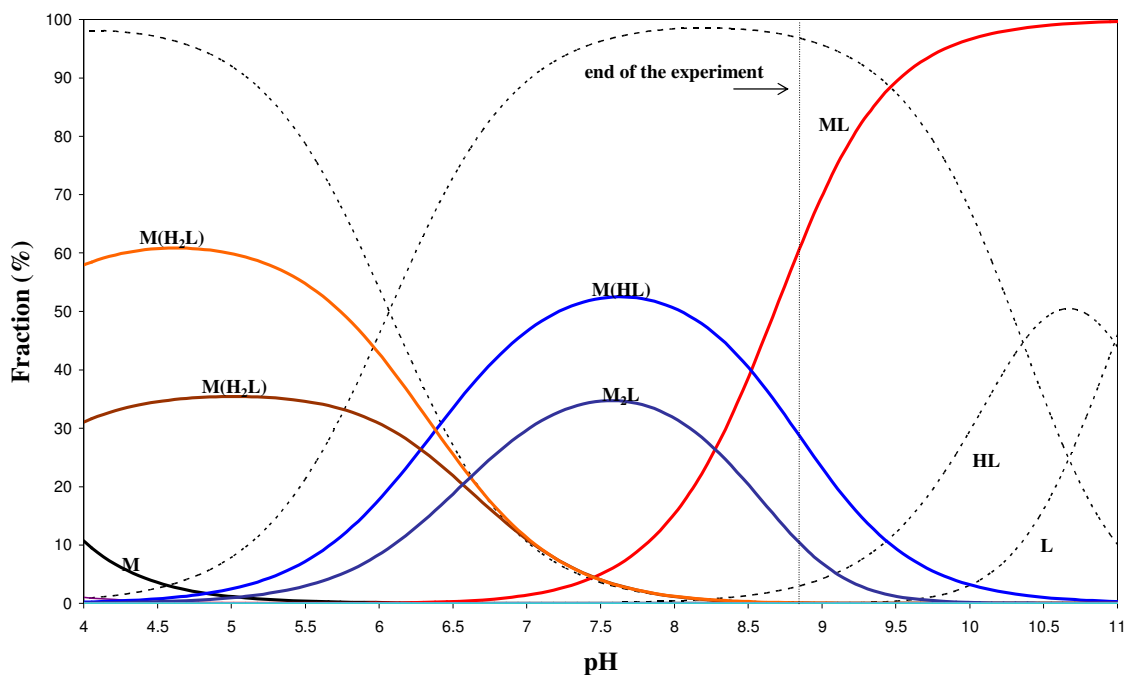


Figure 4.25 Species distribution as a function of pH for the all species predicted $M(H_2L)$, $M_2(HL)$, $M(HL)$, M_2L , and ML for $Cd(II)$ –ALN system studied by sampled DC polarography at $L_T : M_T = 266.6$, ionic strength 0.15 M (NaCl), 25 °C, initial $[M_T] = 1.4978 \times 10^{-5}$ M.

4.2.4 Pb(II)–Alendronate–System

Data fitting

The polarographic study of $Pb(II)$ –ALN was performed by sampled DC polarography at $L_T : M_T$ ratio at 50 and NP polarography at $L_T : M_T$ ratio at 160. The initial curves obtained in sampled DC polarography, between pH 4.34 and 5.44, were well shaped. Above pH 5.44 the shape of the waves started to change, with the second part becoming step. To understand this behaviour, NPP technique was used with shorter time scale of 80 ms. Between pH 4.34–5.44 a single curve was seen. At higher pH the NP curves started to show two overlapping waves due to slow homogeneous kinetics. At highest pH, one and highly irreversible wave was observed – see Figure 4.26.

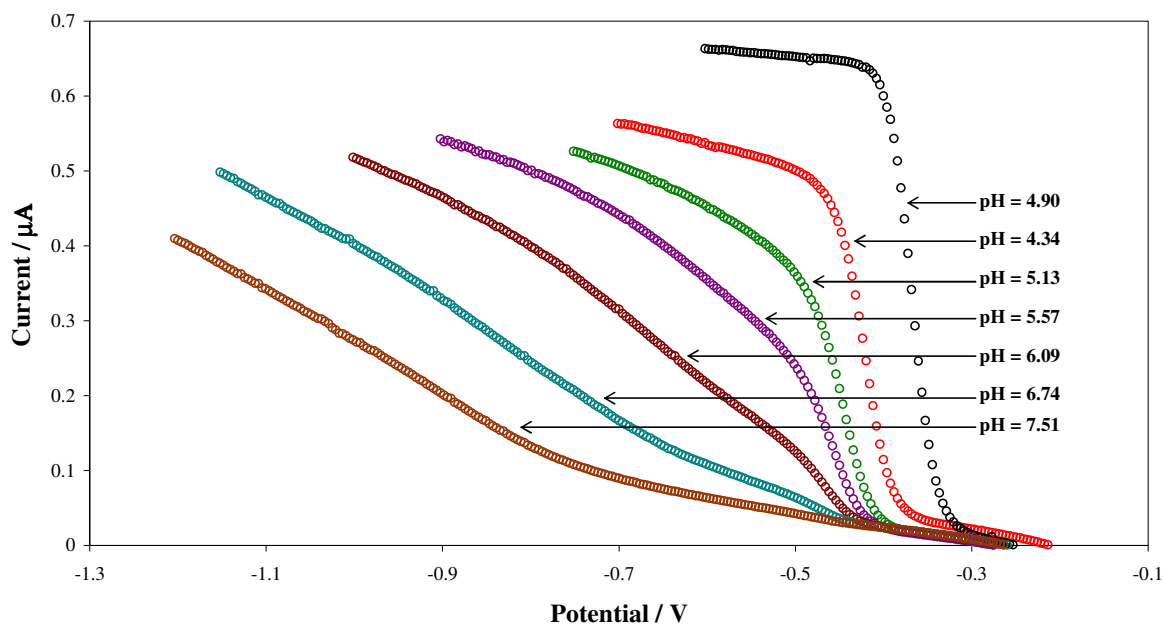


Figure 4.26 Behaviour of some of NP-waves recorded for Pb(II)–ALN system studied by NP polarography at $L_T : M_T = 160$, ionic strength 0.15 M (NaCl), 25 °C, initial $[M_T] = 4.9751 \times 10^{-5}$ M.

Polarograms for this system were analysed using the same procedure as for Cd(II)–ALN system. However, the curves above pH 5.44 with double waves were very difficult to fit; the NPP technique could not sufficiently resolve the curves for accurate analysis in this case. As a result, only experimental curves obtained up to pH of 5.5 were interpreted.

Modelling of experimental data

i) Variation in limiting diffusion current vs pH

From Figure 4.27, a slight change in the normalized current can be seen until pH about 5.44. This is due the formation of a labile complex that could be protonated metal complexes $M_p(H_nL)$.

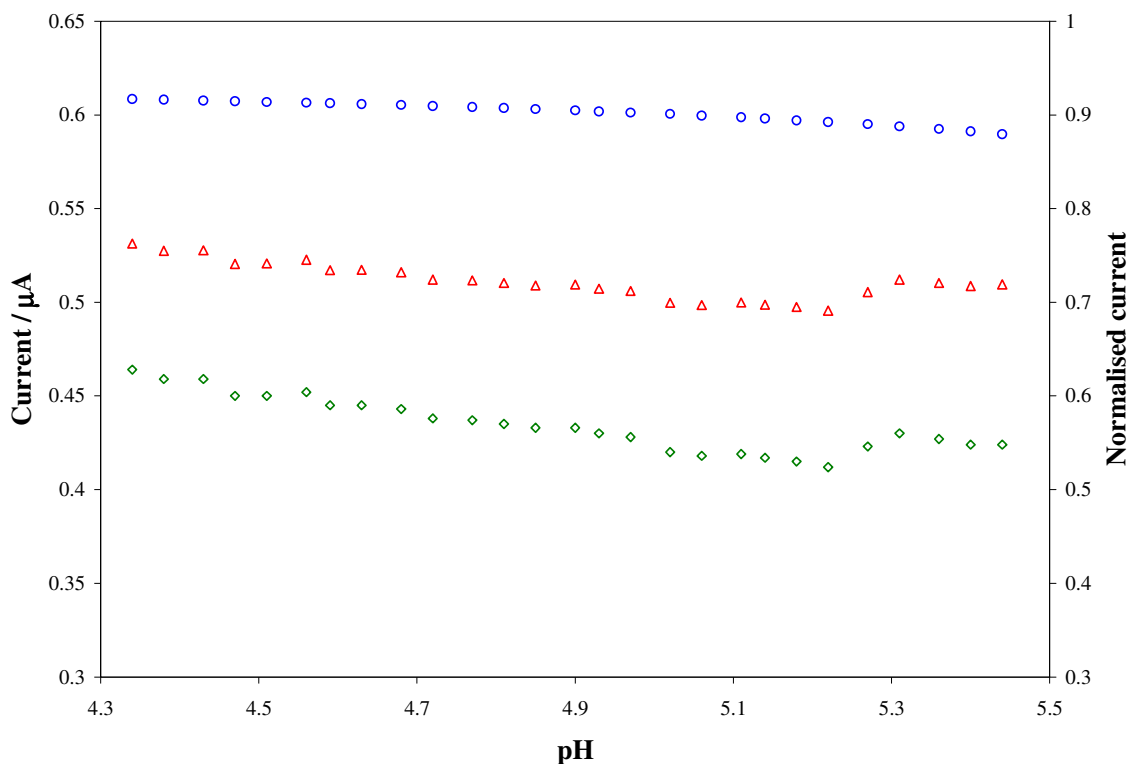


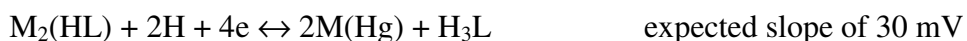
Figure 4.27 Variation in limiting diffusion current for Pb(II)–ALN system studied by NP polarography at $L_T : M_T = 160$, ionic strength 0.15 M (NaCl), 25 °C, initial $[M_T] = 4.9751 \times 10^{-5}$ M. The triangles indicate the normalized limiting diffusion current, diamonds indicate the observed diffusion current and the circles indicate the expected current.

ii) *Variation in virtual half-wave potential vs pH*

The analysis of the plot of $E_{1/2}^T$ (virt) vs. pH is shown in Figure 4.28. A predominant form of the ligand between pH 4.34 and 4.77 is H_3L and a slope of about 31 mV per pH unit is observed which is very close to the theoretical slope of 30 mV per pH unit. This slope indicates the formation of either $M(H_2L)$ or $M_2(HL)$ that requires the involvement of one proton per metal ion according to the following electrochemical reactions (charges was omitted for simplicity):



and/or



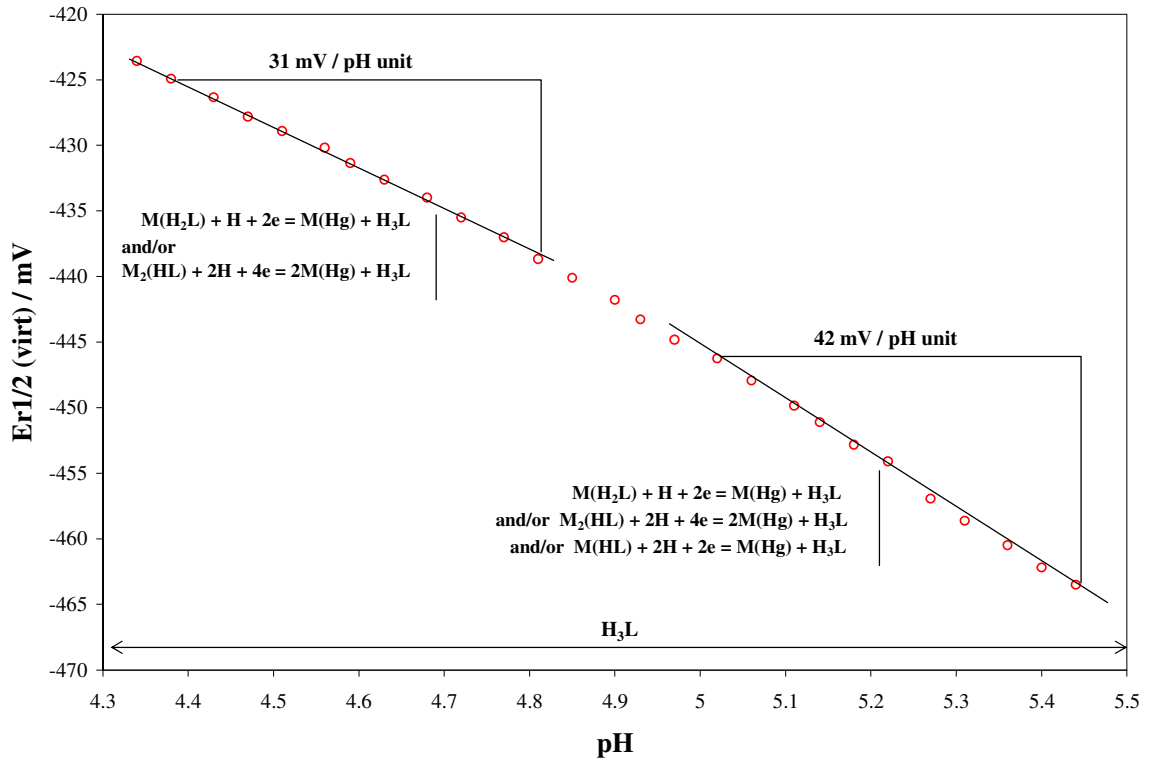
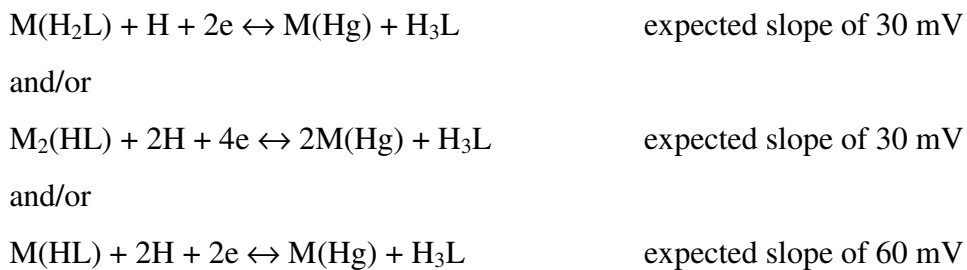


Figure 4.28 Analysis of variation in $E_{1/2}^{virt}$ as a function of pH for Pb(II)–ALN system studied by NP polarography at $L_T : M_T = 160$, ionic strength 0.15 M (NaCl), 25 °C, initial $[M_T] = 4.9751 \times 10^{-5}$ M.

In the pH range between 5.02 and 5.44 the slope of about 42 mV per pH unit is observed. The major form of the ligand is still H_3L . This slope might be a result of the following electrochemical processes:



The reductions of these species require one or two proton per metal ion and hence the expected slope must be 30 or 60 mV per pH unit. Since, the observed slope is close to the 45 mV per pH unit it indicates a mixture of complexes could be present.

(iii) Variation in half-wave potential ($E_{1/2}$) vs. $\log [H_nL]$

The slope of about 32 mV per $\log [H_2L]$ is observed in Figure 4.29 indicating the presence of species $M(H_2L)$ according to the complex formation reaction:



A theoretical slope of about 30 mV per $\log [H_2L]$ unit is expected for $M(H_2L)$. In the same pH range as in Figure 4.28, a slope of about 31 mV per pH unit close to the theoretical slope of about 30, supports the existence of species $M(H_2L)$.

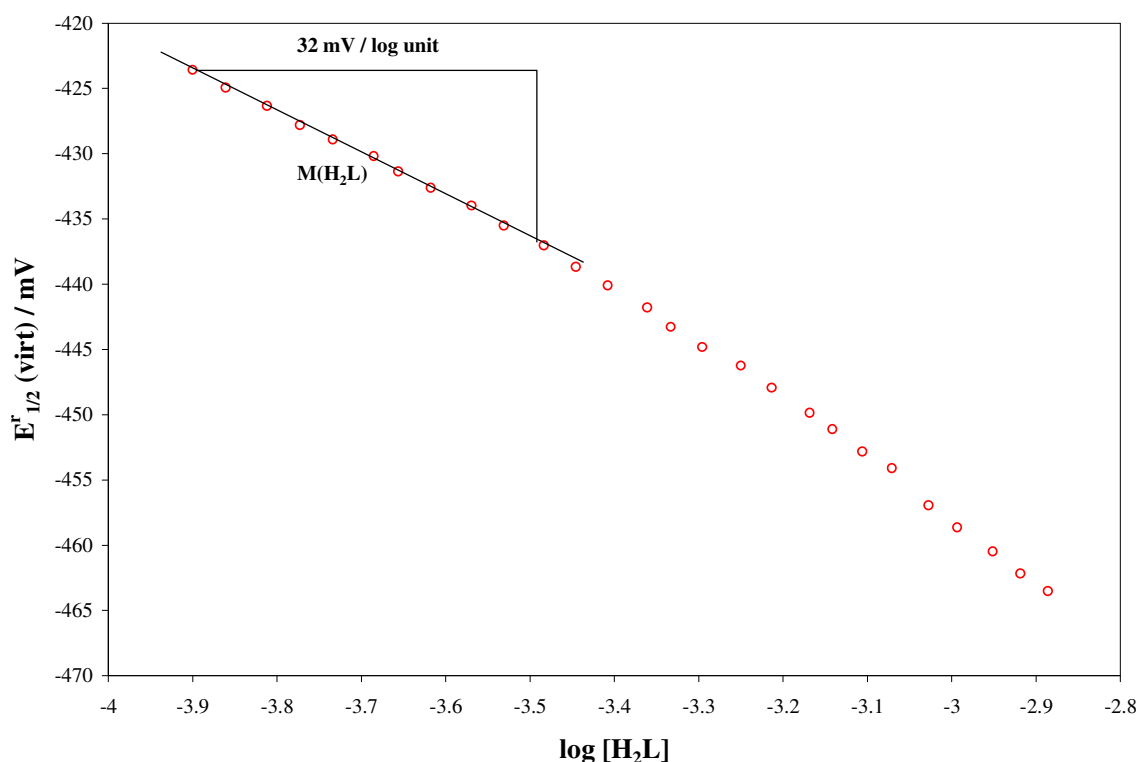


Figure 4.29 Analysis of variation in $E'_{1/2}(\text{virt})$ as a function of $\log [H_2L]$ for Pb(II)–ALN system studied by NP polarography at $L_T : M_T = 160$, ionic strength 0.15 M (NaCl), 25 °C, initial $[M_T] = 4.9751 \times 10^{-5}$ M.

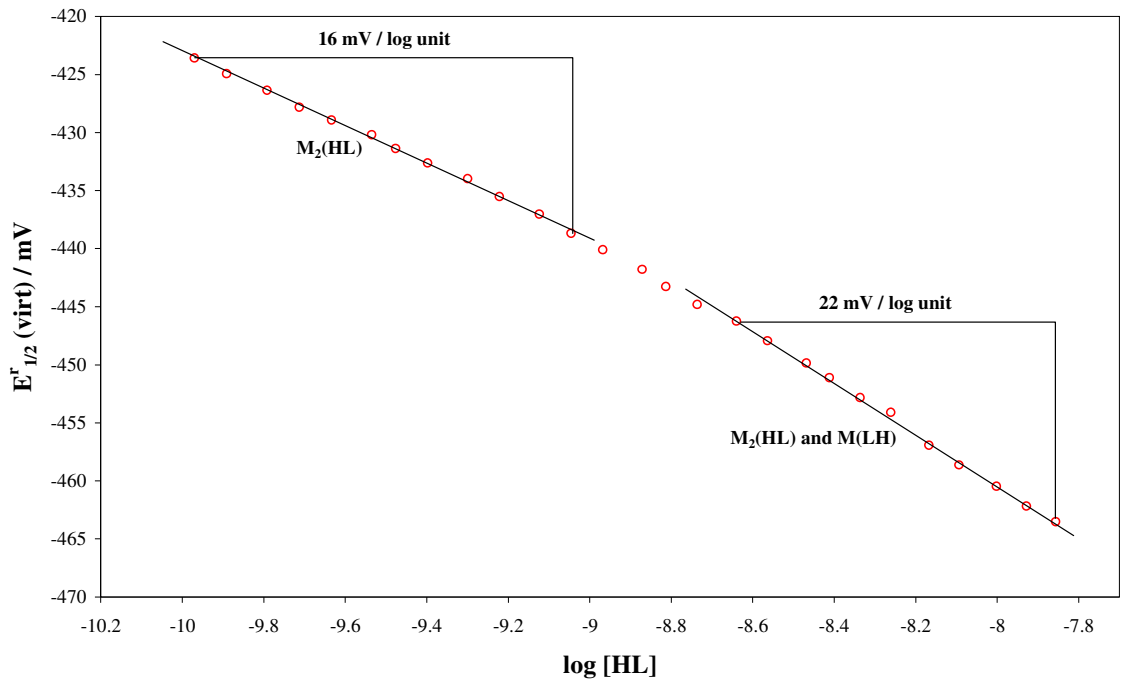


Figure 4.30 Analysis of variation in $E_{1/2}^{virt}$ as a function of $\log [HL]$, respectively, for Pb(II)–ALN system studied by NP polarography at $L_T : M_T = 160$, ionic strength 0.15 M (NaCl), 25 °C, initial $[M_T] = 4.9751 \times 10^{-5}$ M.

On the other hand, in Figure 4.30 a slope of about 16 mV per $\log [HL]$ can be seen which suggests the formation of the species $M_2(HL)$ according to the reaction:



The same metal complex, $M_2(HL)$, was predicted to be formed in solution in the same pH range as shown in Figure 4.28.

A slope of about 22 mV per $\log [HL]$ is also seen in Figure 4.30; clearly a mixture of species with slopes between 15 and 30 mV per $\log [HL]$ should define this slope, they could be $M_2(HL)$ and $M(HL)$ whose resultant slope is about 22.5 mV per $\log [HL]$.



and/or



iv) Variation in half-wave potential ($E_{1/2}$) vs. $\log [L]$

In Figure 4.31 a slope of about 15 mV per $\log [L]$ unit is observed which indicates the presence of M_2L . The reaction involved is:



This observation supports the existence of the species M_2L . However, in the same position in Figure 4.30 formation of $M(HL)$ is predicted.

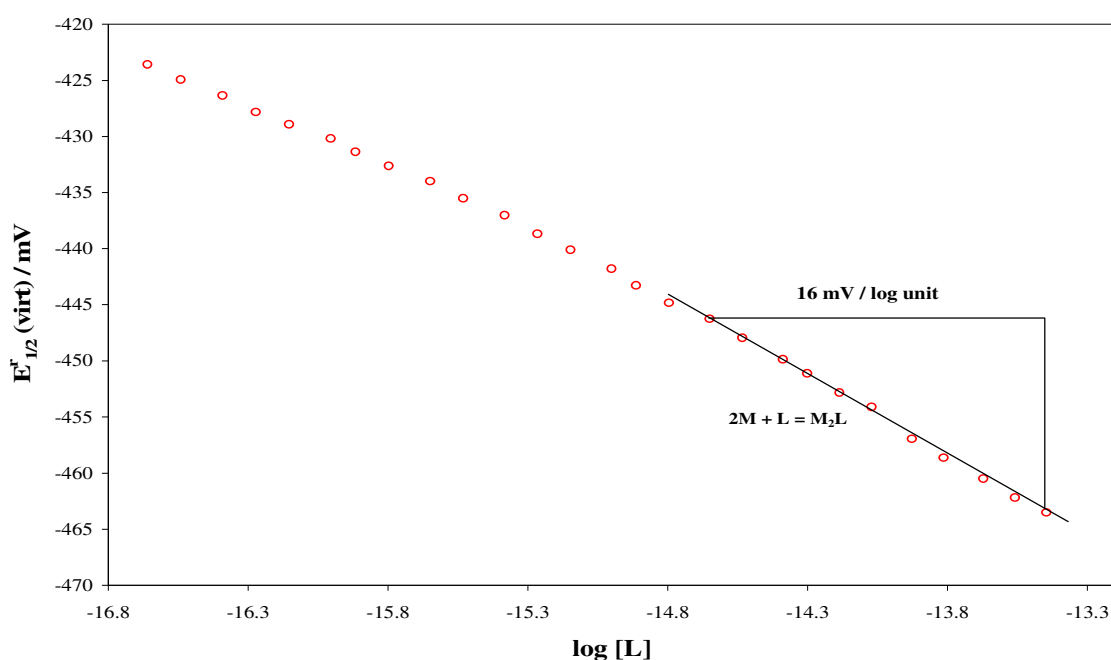


Figure 4.31 Analysis of variation in $E_{1/2}^{virt}$ as a function of $\log [L]$ for Pb(II)–ALN system studied by NP polarography at $L_T : M_T = 160$, ionic strength 0.15 M (NaCl), 25 °C, initial $[M_T] = 4.9751 \times 10^{-5}$ M.

From the above analyses of data (relationships seen in Figures 4.28–4.31) one can suggest two most likely initial metal-ligand model as was observed for Cd(II)–ALN: $M(H_2L)$ and $M(HL)$ or $M_2(HL)$ and M_2L (all labile), plus all known $Pb_x(OH)_y$ species.

v) Optimization of a metal–ligand model and refinement of stability constants

Figure 4.32 displays the complex formation curves for the model 2 seen in Table 4.11.

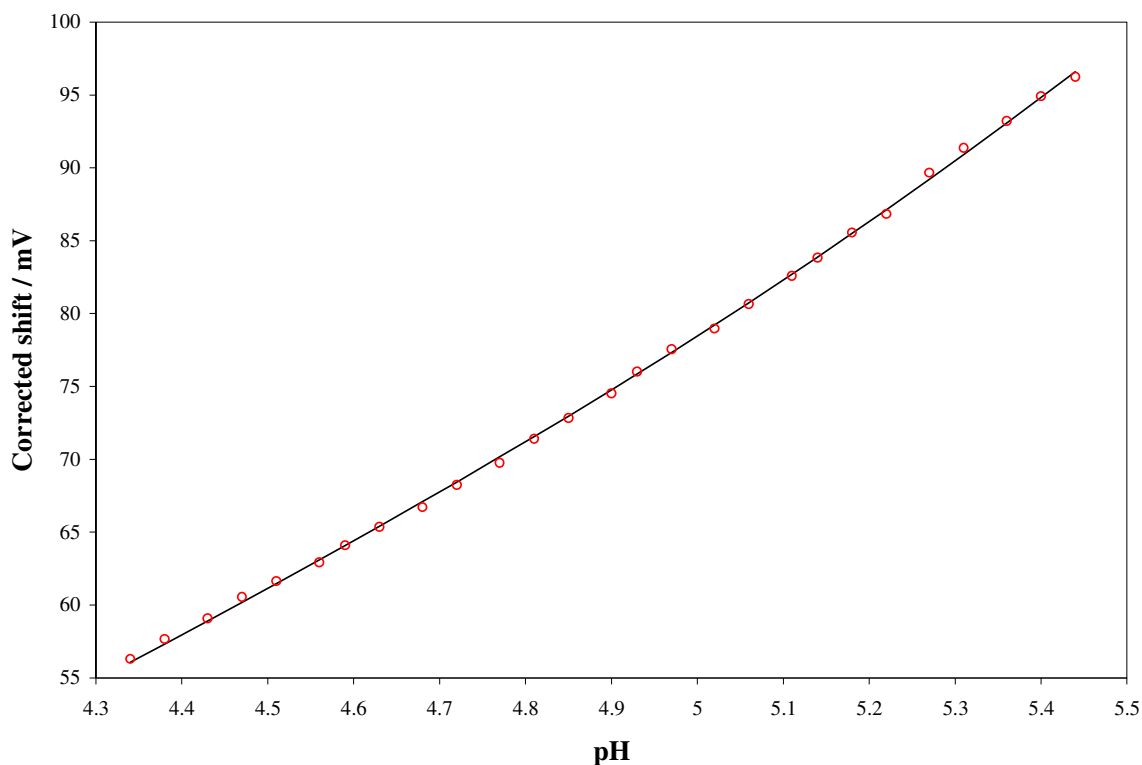


Figure 4.32 Experimental and calculated complex formation curves obtained using reversible half-wave potentials for Pb(II)–ALN system studied by NP polarography at $L_T : M_T = 160$, ionic strength 0.15 M (NaCl), 25 °C, initial $[M_T] = 4.9751 \times 10^{-5}$ M. The circles represents the ECFC and solid line represents the CCFC for the optimized M–L model contained $M_2(\text{HL})$, $M(\text{HL})$.

The strategy used in the refinement process is presented in Table 4.11.(B). The best overall fit of the CCFC to the ECFC was obtained for the refined model with $M_2(\text{HL})$ and $M(\text{HL})$ which could be the likely model for this system. Similar model and refined stability constants were obtained by sampled DC polarography – see Appendix E.

Table 4.11 (A) Dissociation constant for water and overall stability constants for Pb(II) complexes with OH⁻. (B) Overall stability constants for Pb(II)–ALN found in this work by NPP at ionic strength 0.15 M in NaCl and 25 °C, L_T : M_T ratio 160, [M_T] = 4.9751 × 10⁻⁵ M. The proposed final model is indicated in bold.

(A)

Equilibrium	Log β	Equilibrium	Log β
H ⁺ + OH ⁻ = H ₂ O	13.68	Pb ²⁺ + OH ⁻ = Pb(OH) ⁺	6.00
		Pb ²⁺ + 2OH ⁻ = Pb(OH) ₂	10.30
		Pb ²⁺ + 3OH ⁻ = Pb(OH) ₃ ⁻	13.30
		2Pb ²⁺ + OH ⁻ = Pb ₂ (OH) ³⁺	7.60
		3Pb ²⁺ + 4OH ⁻ = Pb ₃ (OH) ₄ ²⁺	31.70
		4Pb ²⁺ + 4OH ⁻ = Pb ₄ (OH) ₄ ⁴⁺	35.20
		6Pb ²⁺ + 8OH ⁻ = Pb ₆ (OH) ₈ ⁴⁺	67.40
		Pb ²⁺ + 2OH ⁻ = Pb(OH) ₂ (s)	15.00

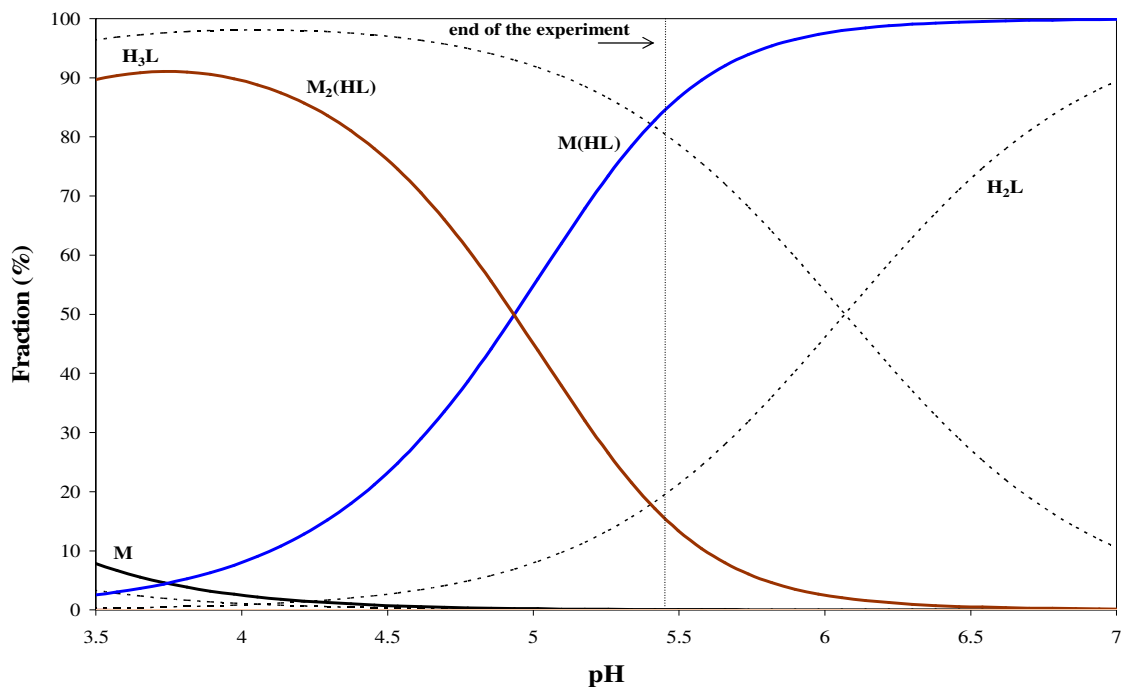
(B)

Equilibrium	Model 1	Model 2	Model 3	Model 4
M + L + 2H = M(H ₂ L)	R	R	27.17 ± 0.02	27.11 ± 0.03
2M + L + H = M ₂ (HL)	28.63 ± 0.04	28.72 ± 0.03	NI	NI
M + L + H = M(HL)	R	22.06 ± 0.03	21.92 ± 0.03	NI
2M + L = M ₂ L	23.84 ± 0.04	R	NI	23.71 ± 0.04
Overall fit (mV)	0.2602	0.0627	0.1120	0.3740

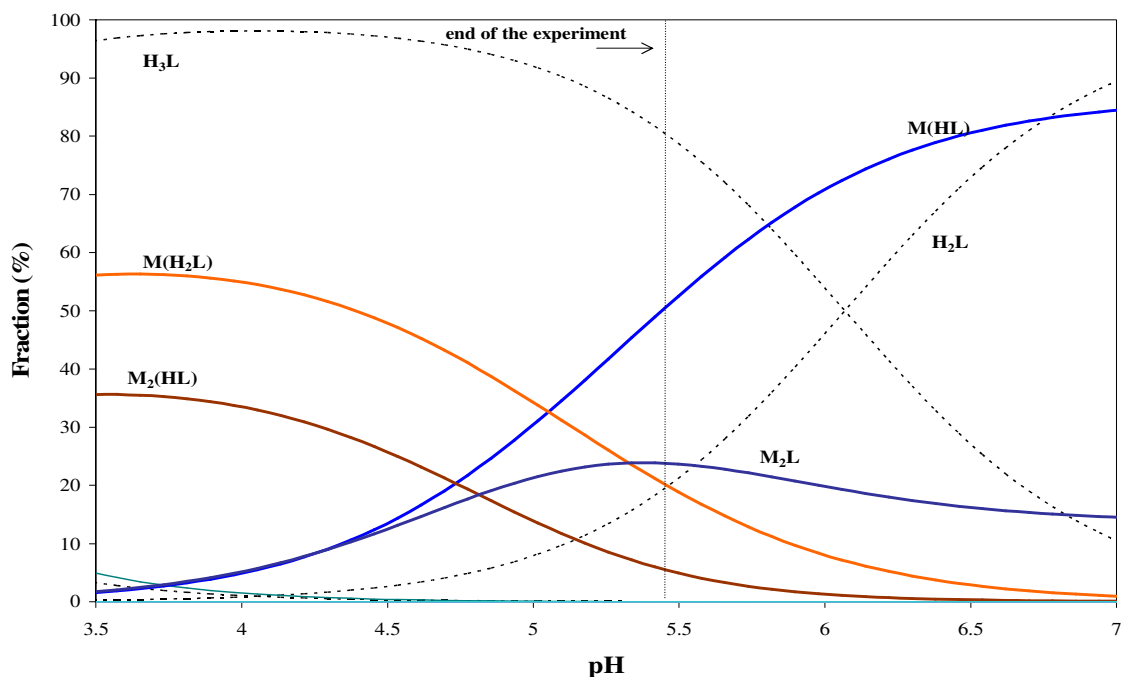
NI- Not included; R- Rejected

vi) *Species distribution diagram*

The species distribution diagrams of the likely model M₂(HL) and M(HL) is seen in Figure 4.33. The species M₂(HL) is predominant below pH of about 4.8 and it is decreasing in solution as pH increases. Above this pH, M(HL) complex becomes predominant species in solution. Considering SDD for the model containing all the species predicted to be formed in solution as shown in Figure 4.34, the species M(H₂L) and M(HL) become major species and seem to be favoured over the species M₂(HL) and M₂L. The species M(H₂L) and M₂(HL) coexist in the same pH range as well as M(HL) and M₂L.



Figures 4.33 Species distribution as a function of pH for the model $M_2(HL)$, $M(HL)$, for Pb(II)–ALN system studied by sampled NP polarography at $L_T : M_T = 160$, ionic strength 0.15 M (NaCl), 25 °C, initial $[M_T] = 4.9751 \times 10^{-5}$ M.



Figures 4.34 Species distribution as a function of pH for the model $M_2(HL)$, $M(HL)$, for Pb(II)–ALN system studied by sampled NP polarography at $L_T : M_T = 160$, ionic strength 0.15 M (NaCl), 25 °C, initial $[M_T] = 4.9751 \times 10^{-5}$ M.

4.2.5 Cd(II)–Neridronate–System

Data fitting

The polarographic study of Cd(II)–NED at $L_T : M_T$ ratio 266.6 was performed by NP and sampled DC polarography. The polarograms were recorded in the pH range 4.63–8.61. Above pH 8.61 the polarographic wave disappeared.

Polarograms for this system were fitted using the same approach and Equations 4.5 and 4.8 as it was done for Cd(II)–ALN. Example of the fitted polarograms for this system is shown in Figure 4.35.

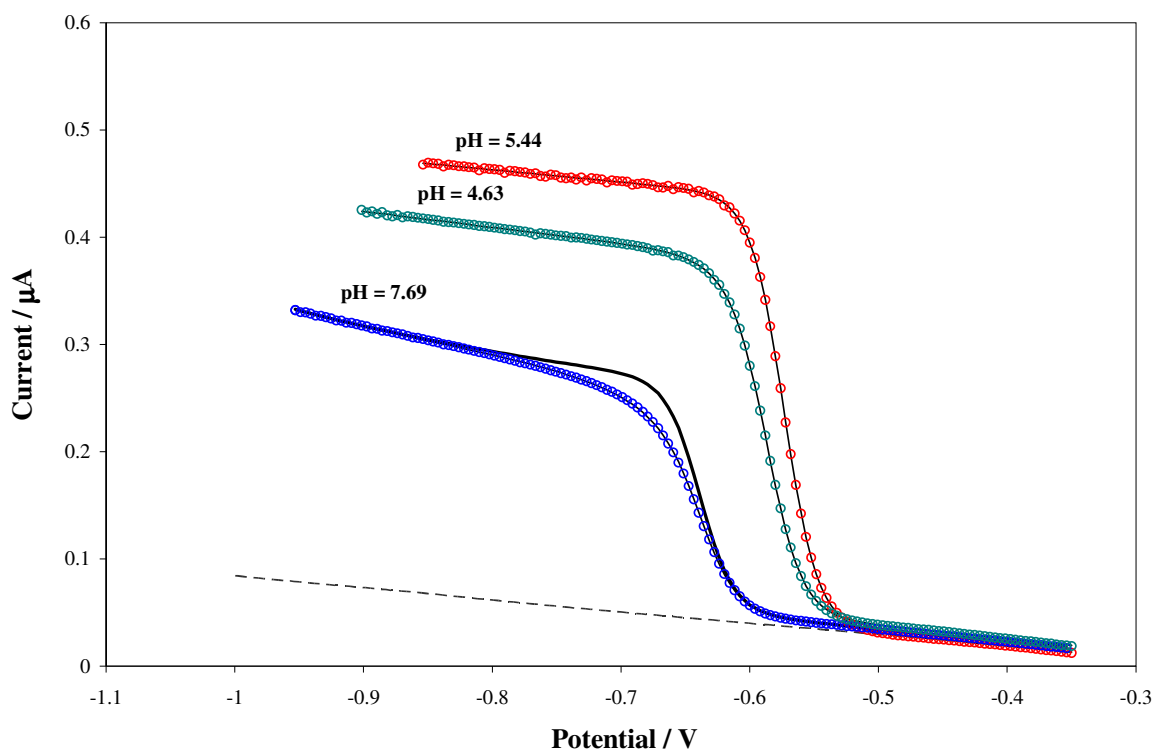


Figure 4.35 Example of fitting from NP polarographic study of Cd(II)–NED system at $L_T : M_T = 266.7$, 25 °C, $[M_T] = 2.9910 \times 10^{-5}$ M. Circles are experimental points representing the recorded current at a particular applied potential; solid lines represent theoretically fitted curves; thick solid line represent computed curves corresponding to fully reversible reduction processes using the I_d and $E_{1/2}^r$ values obtained from curve-fitting based on the Ružić equation; dashed line represent background current.

Modelling of experimental data

i) Variation in limiting diffusion current vs pH

The Cd(II)–NED system can be divided into two parts: (i) first part, between pH 4.63 and 7.33, where the system can be treated as fully labile – see Figure 4.36.

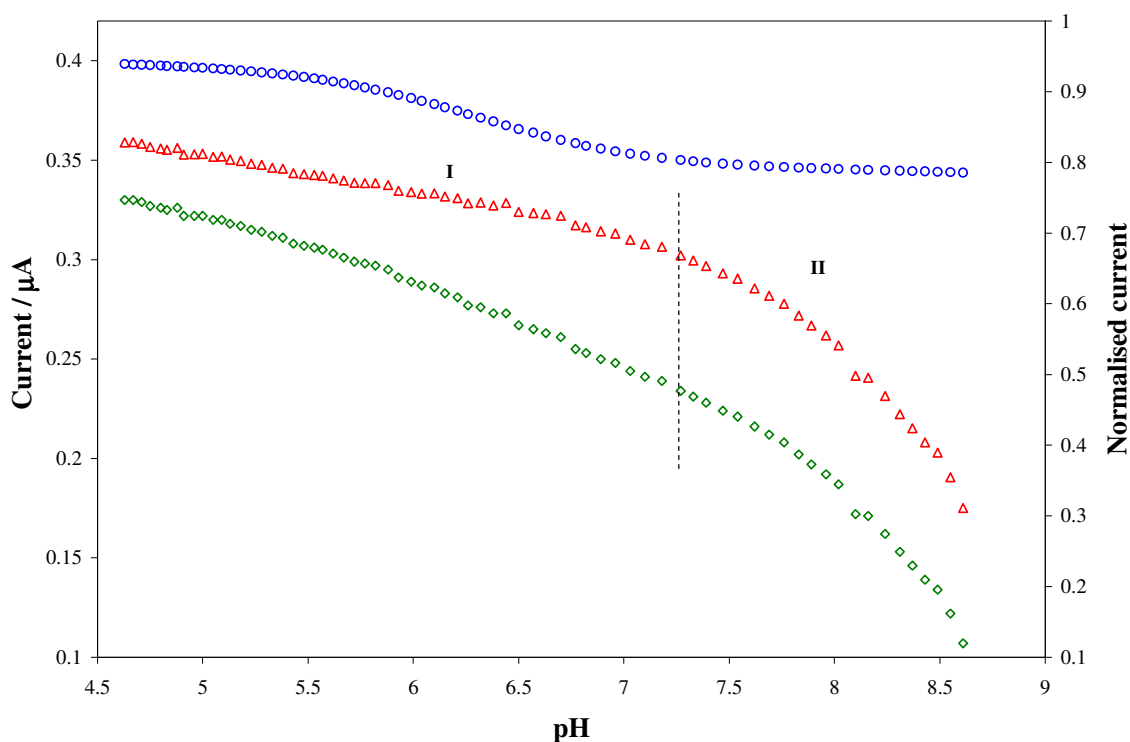


Figure 4.36 Variation in limiting diffusion current for Cd(II)–NED system studied by NP polarography at $L_T : M_T = 266.6$, ionic strength 0.15 M (NaCl), 25 °C, initial $[M_T] = 2.9910 \times 10^{-5}$ M. The triangles indicate the normalized limiting diffusion current, diamonds indicate the observed diffusion current and the circles indicate the expected current.

After addition of the ligand, there is a continuous and small decrease in I_d until pH about 7.33 which might be interpreted as the formation of labile metal species. Above a pH value of about 7.33, continuous and large a decrease in I_d is observed which can be interpreted as the formation of a non-labile metal species. Above pH 8.61 the polarographic wave disappears and the data could not be interpreted.

ii) Variation in virtual half-wave potential vs pH

In Figure 4.37, in the pH range 4.63–5.18, there is no defined shift observed where the predominant ligand is H_3L . This suggests the formation of protonated species in which

no protons are involved according to the following electrochemical process (charges was omitted for simplicity):

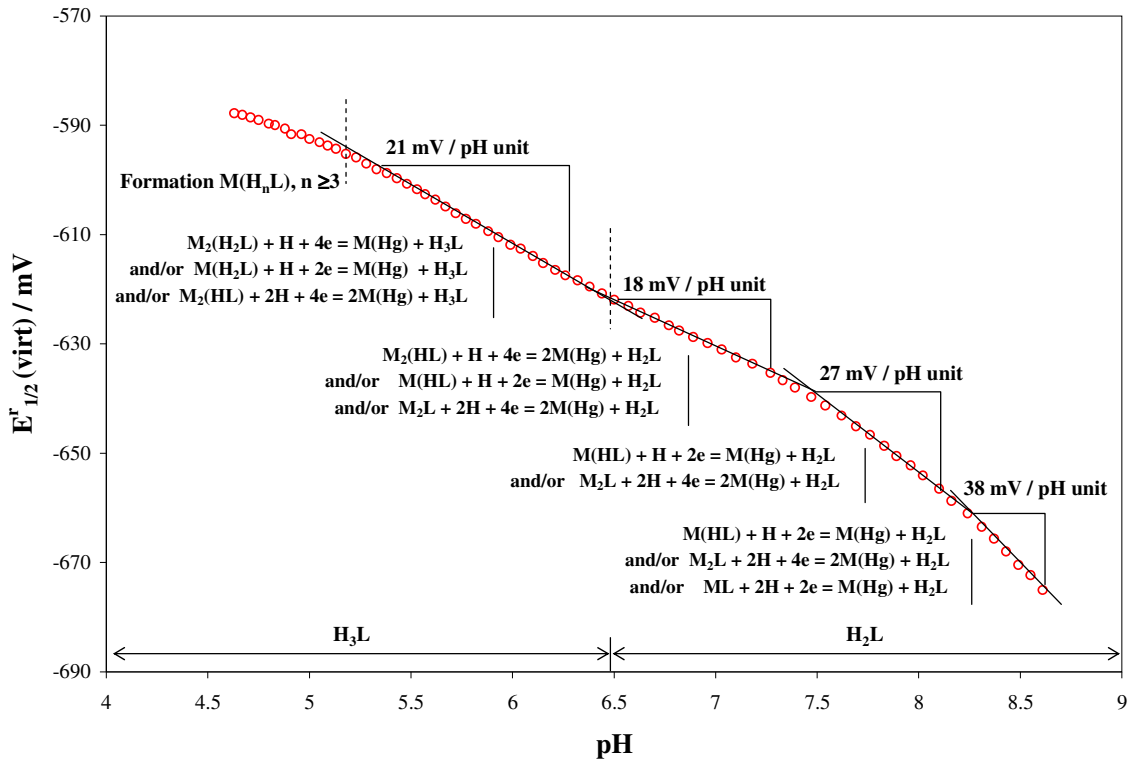
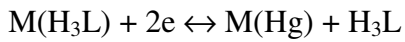


Figure 4.37 Analysis of variation in $E_{1/2}^r$ (virt) as a function of pH for Cd(II)–NED system studied by NP polarography at $L_T : M_T = 266.6$, ionic strength 0.15 M (NaCl), 25 °C, initial $[M_T] = 2.9910 \times 10^{-5}$ M.

The half-wave potential $E_{1/2}$, for Cd(II) was -573.30 mV and the corresponding I_d was 0.39815 μ A (polarogram at pH 5.44, Figure 4.35). After addition of the ligand NED, the half-wave potential $E_{1/2}$, was -585.37 mV and the corresponding I_d was 0.32958 μ A (polarogram at pH 4.63, Figure 4.35). Therefore, after addition the ligand, I_d dropped by 0.06857 μ A and half-wave potential shifted by about 12.07 mV. This shift and the drop in I_d can be attributed to the complexation of the metal ion on addition of the ligand. The AC study showed that no adsorption was observed that means the drop in the limiting diffusion current observed is due to the formation of a complex. The formation of the complex $M(H_3L)$ in solution could be supported by the drop in the limiting diffusion current as well as a shift in potential after addition of the ligand solution – see Figure 4.35.

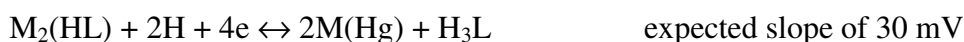
A slope of about 21 mV per pH unit is observed between pH 5.43 and 6.38. A mixture of species is expected in this pH range which involved one proton per metal ion. The reductions of $M_2(H_2L)$, $M(H_2L)$ and $M_2(HL)$ could be considered according to the following reactions:



and/or



and/or



In between pH 6.50 and about 7.47, a slope of about 18 mV per pH unit is observed. The predominant ligand in this pH range is H_2L . The reductions of $M_2(HL)$ and $M(HL)$ or M_2L can be considered here according to the following reactions:



and/or



and/or



A slope of about 27 mV per pH unit is seen in pH range 7.47 and 8.16 which indicates the presence of $M(HL)$ and/or M_2L according to the following electrochemical processes:



and/or



This slope is close to the theoretical slope of 30 mV per pH unit for these complex formation reactions.

Above pH 8.16, where the predominant ligand is still H₂L, a slope of about 38 mV per pH unit is seen. This could be due to ML species whose expected theoretical slope is 60 mV per pH unit but the theoretical slope is higher than observed. A mixture of species should be considered. The reduction of the species M(HL) or M₂L and ML should give the resultant slope expected according the following electrochemical reactions:



and/or



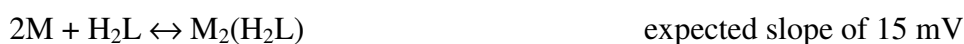
and/or



In this way, M(H₃L), M(H₂L), M₂(HL), M(HL), M₂L and ML were identified as the most likely complexes in solution.

(iii) Variation in half-wave potential ($E_{1/2}$) vs. $\log [H_nL]$

In Figure 4.38 there is no defined slope that confirms the presence of M(H₃L) species in solution. A slope of about 15 mV per $\log [H_2L]$ is seen in Figure 4.39 which indicates the presence of M₂(H₂L) according to the following electrochemical processes:



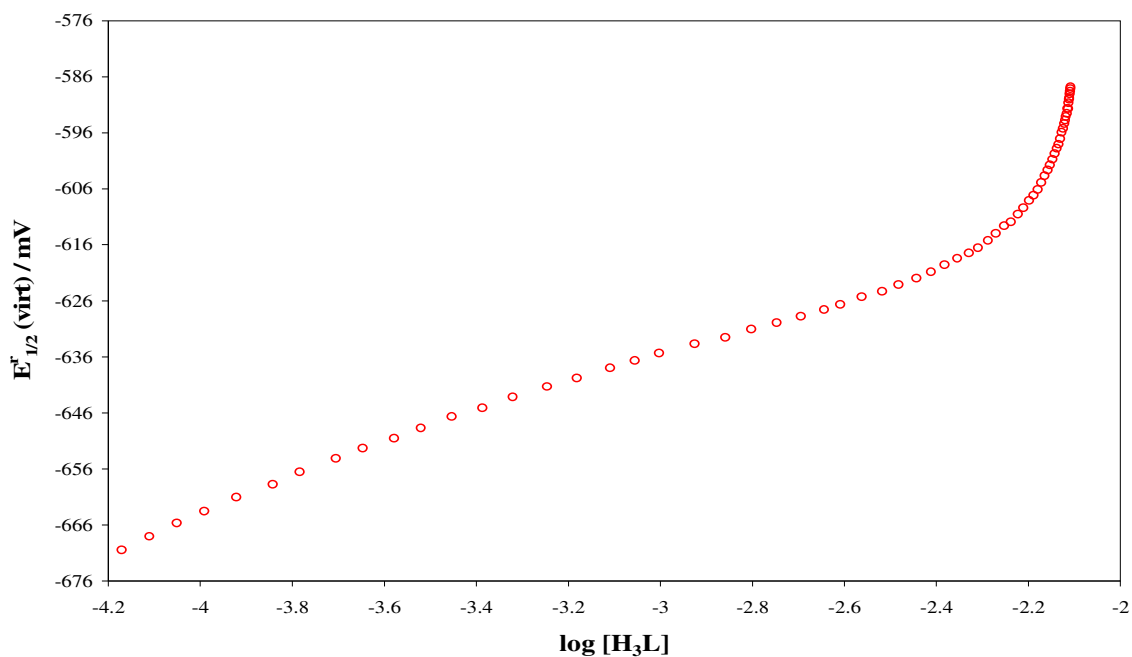


Figure 4.38 Analysis of variation in $E_{1/2}^{virt}$ as a function of $\log [H_3L]$ for Cd(II)–NED system studied by NP polarography at $L_T : M_T = 266.6$, ionic strength 0.15 M (NaCl), 25 °C, initial $[M_T] = 2.9910 \times 10^{-5}$ M.

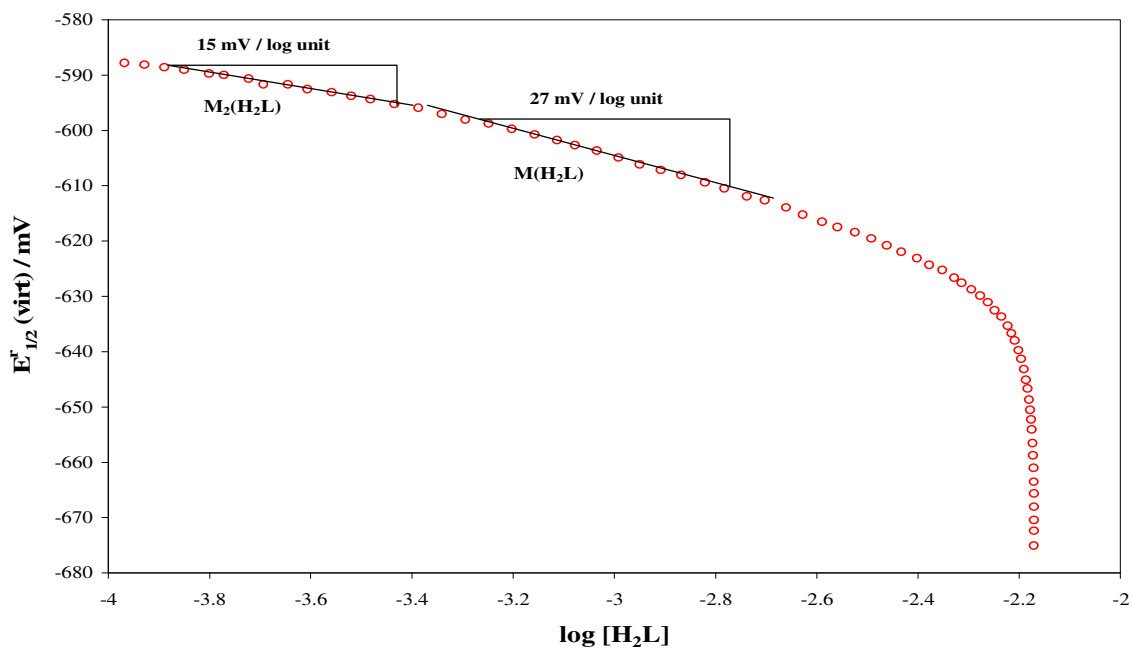


Figure 4.39 Analysis of variation in $E_{1/2}^{virt}$ as a function of $\log [H_2L]$ for Cd(II)–NED system studied by NP polarography at $L_T : M_T = 266.6$, ionic strength 0.15 M (NaCl), 25 °C, initial $[M_T] = 2.9910 \times 10^{-5}$ M.

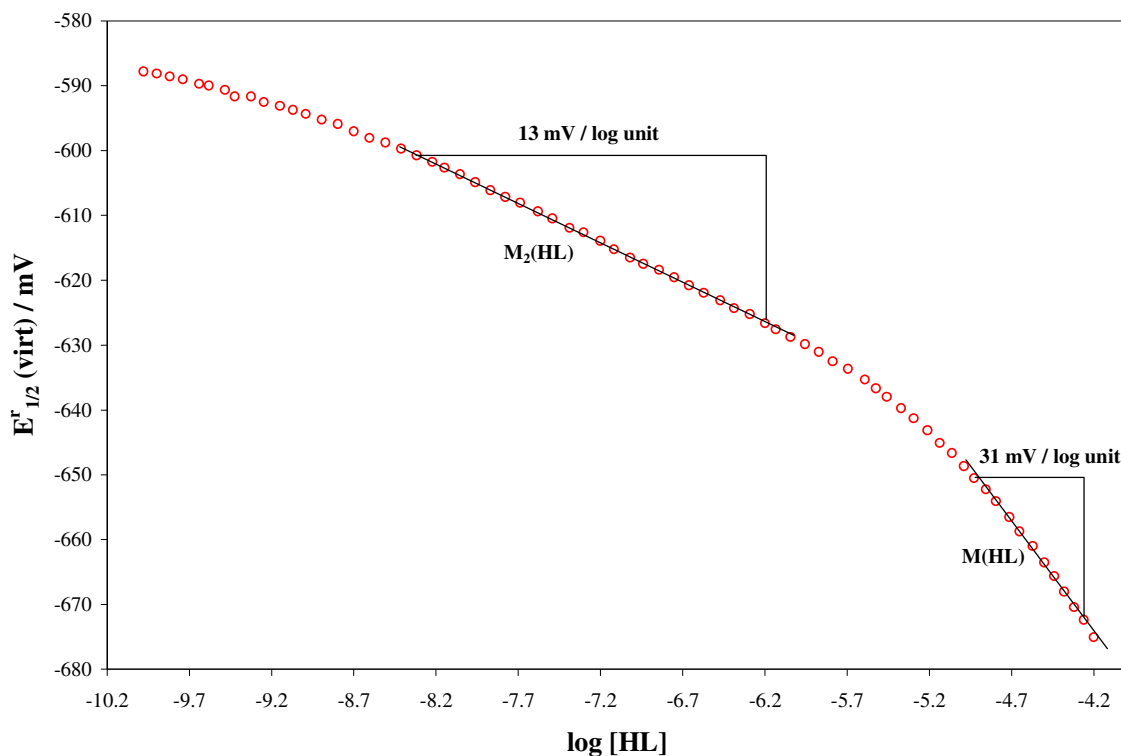


Figure 4.40 Analysis of variation in $E_{1/2}^T(\text{virt})$ as a function of $\log [\text{HL}]$ for Cd(II)–NED system studied by NP polarography at $L_T : M_T = 266.6$, ionic strength 0.15 M (NaCl), 25 °C, initial $[M_T] = 2.9910 \times 10^{-5}$ M.

A slope of 27 mV per $\log [\text{H}_2\text{L}]$ unit is seen in Figure 4.39 which supports the formation of species $\text{M}(\text{H}_2\text{L})$ in solution according to the complex formation reaction:



The same species, $\text{M}(\text{H}_2\text{L})$, was predicted to be formed in solution in the same pH range as shown in Figure 4.37. From Figure 4.40 the slope of about 13 mV per $\log [\text{HL}]$ unit is seen which is close to the theoretical slope 15 mV per $\log [\text{HL}]$. The following electrochemical reaction explains the formation of $\text{M}_2(\text{HL})$:



Figure 4.40 also provides of the $\text{M}(\text{HL})$ species. This species was predicted to be formed in pH range 7.47–8.16 – see Figure 4.37.

iv) Variation in half-wave potential ($E_{1/2}$) vs. $\log [L]$

In Figure 4.41, the slope of about 19 mV per $\log [L]$ unit is observed. This slope could suggest formation of ML but the theoretical slope of about 30 mV per $\log [L]$ is expected here and therefore a mixture of species must form. Another species which could be present is M_2L with theoretical slope of about 15 mV per $\log [L]$ unit.

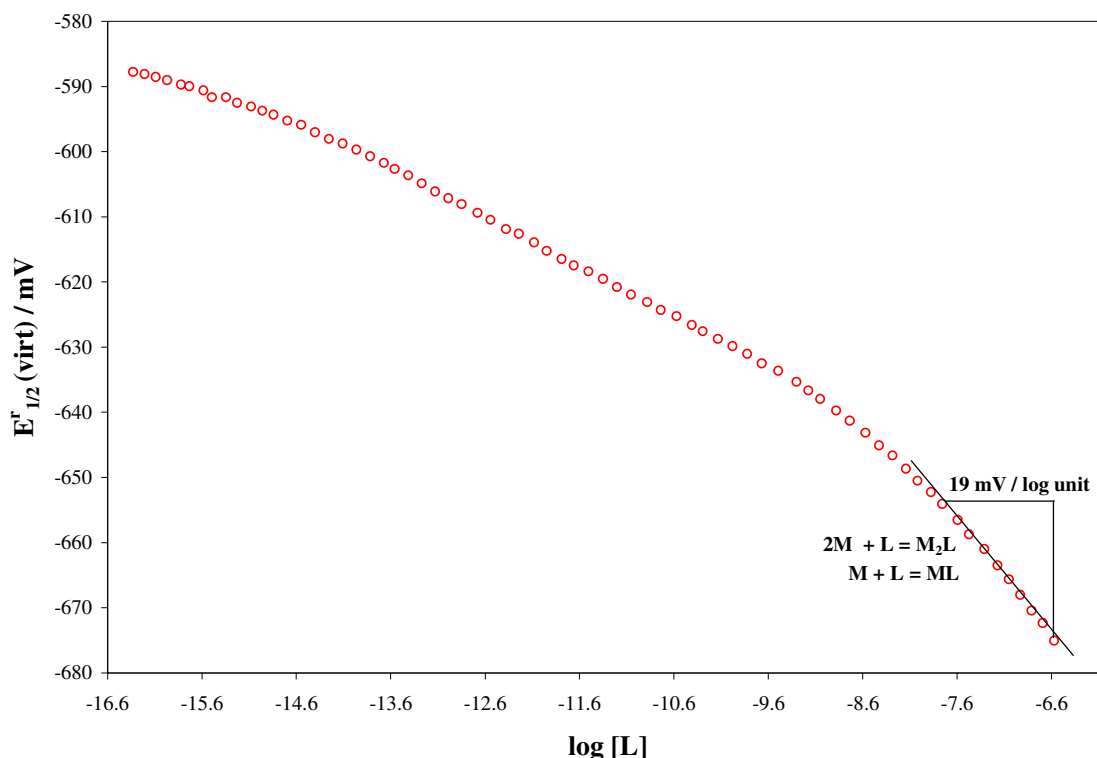


Figure 4.41 Analysis of variation in $E'_{1/2}$ (virt) as a function of $\log [L]$ for Cd(II)–NED system studied by NP polarography at $L_T : M_T = 266.6$, ionic strength 0.15 M (NaCl), 25 °C, initial $[M_T] = 2.9910 \times 10^{-5}$ M.

The average of these slopes is 22.5 mV per $\log [L]$ when formed in equal amounts in solution, which is close to the observed slope. The ML species seems to be non-predominant species and its presence supports the suggestions made in Figure 4.37.

v) Optimization of a metal–ligand model and refinement of stability constants

Different metal–ligand models for this system with refined stability constants are shown in Table 4.12. The complex formation curves for the best values of the refined stability constants are seen in Figure 4.42. The proposed best model for this system is the model 4 with low standard deviations and low overall fit in CCFC into ECFC.

When species M_2L was included into the model 4, it was rejected. However, the model 3 ($M(HL)$ being replaced by M_2L) was fitted without problems with higher overall fit (compared with the model 4) and lower standard deviations of the complexes.

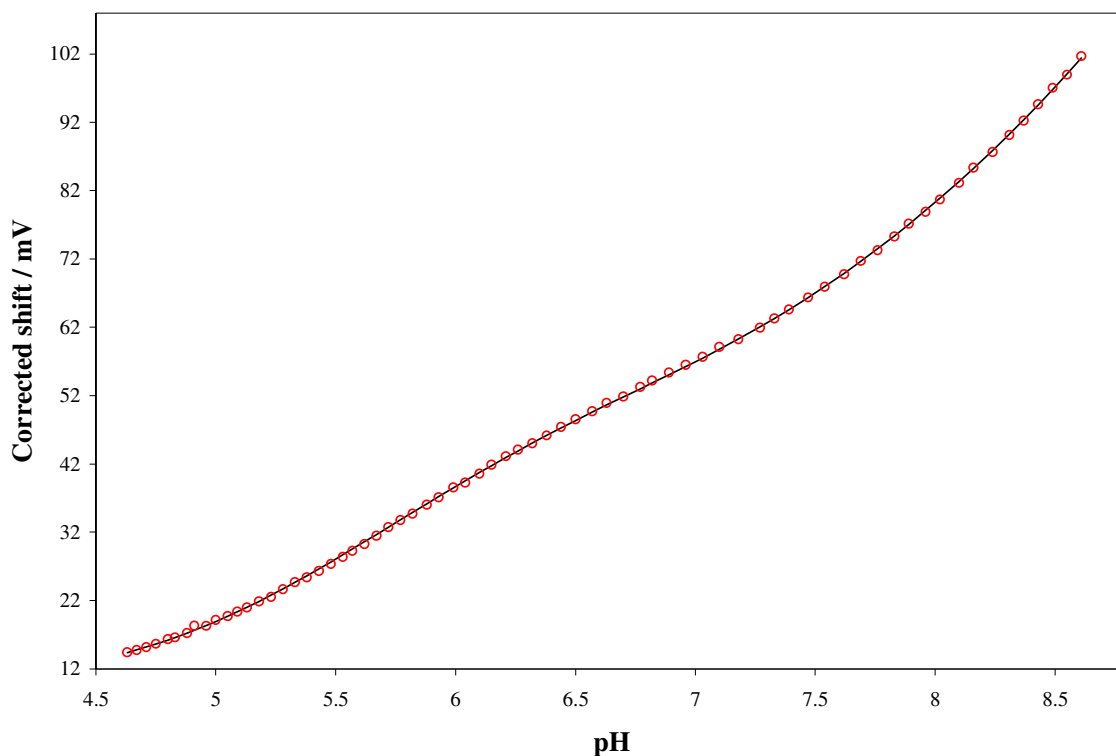


Figure 4.42 Experimental and calculated complex formation curves obtained using reversible half-wave potentials for Cd(II)–NED system studied by NP polarography at $L_T : M_T = 266.6$, ionic strength 0.15 M (NaCl), 25 °C, initial $[M_T] = 2.9910 \times 10^{-5}$ M. The circles represents the ECFC and solid line represents the CCFC for the optimized M–L model contained $M(H_3L)$, $M(H_2L)$, $M(HL)$, and ML .

When the model 5 was fitted the smaller overall fit was obtained and larger standard deviations for the species $M_2(HL)$ was observed. The same situation was observed in the model 6. When the model 2 was fitted without inclusion of $M(H_2L)$ species, small standard deviations was observed for species $M_2(HL)$. From these observations it is clear that species $M(HL)$, M_2L , and $M(H_2L)$, $M_2(HL)$ cannot be incorporated together into the metal-ligand system. These species were predicted to be formed in solution in the same pH range as shown in Figure 4.37. Moreover, higher overall fit and larger standard deviations for the species $M(HL)$ and M_2L in the model 1 and 2, respectively, were observed. When the models 3 and 4 were fitted with exclusion of $M_2(HL)$ much better overall fit and standard deviations for the species were observed. When the model

7 was fitted the lower overall fit of CCFC into the ECFC was obtained with the larger standard deviations for all species.

Table 4.12 Overall stability constants for Cd(II)–NED system determined at 25 C and $\mu = 0.15$ M by NPP for $L_T : M_T$ ratio 266.7, $[M_T] = 2.9910 \times 10^{-5}$ M. The proposed final model is indicated in bold.

Equilibrium	Model 1	Model 2	Model 3	Model 4
$M + L + 3H \leftrightarrow M(H_3L)$	30.58 ± 0.02	30.58 ± 0.02	30.16 ± 0.05	30.24 ± 0.04
$M + L + 2H \leftrightarrow M(H_2L)$	NI	NI	25.63 ± 0.009	25.59 ± 0.009
$2M + L + H \leftrightarrow M_2(HL)$	25.09 ± 0.01	25.09 ± 0.02	NI	NI
$M + L + H \leftrightarrow M(HL)$	NI	17.74 ± 0.15	NI	18.39 ± 0.02
$2M + L \leftrightarrow M_2L$	16.85 ± 0.11	NI	17.42 ± 0.03	R
$M + L \leftrightarrow ML$	9.97 ± 0.04	9.99 ± 0.04	9.61 ± 0.09	9.57 ± 0.07
Overall fit (mV)	0.8361	1.0024	0.2970	0.0383
	Model 5	Model 6	Model 7	Model 8
$M + L + 3H \leftrightarrow M(H_3L)$	30.32 ± 0.05	30.27 ± 0.05	30.28 ± 0.13	-
$2M + L + H \leftrightarrow M_2(H_2L)$	-	-	-	30.18 ± 0.05
$M + L + 2H \leftrightarrow M(H_2L)$	25.48 ± 0.05	25.56 ± 0.04	25.56 ± 0.18	25.56 ± 0.01
$2M + L + H \leftrightarrow M_2(HL)$	24.56 ± 0.12	23.95 ± 0.45	23.97 ± 2.87	NI
$M + L + H \leftrightarrow M(HL)$	NI	18.36 ± 0.04	18.36 ± 1.21	18.41 ± 0.02
$2M + L \leftrightarrow M_2L$	17.27 ± 0.06	NI	15.46 ± 6.37	R
$M + L \leftrightarrow ML$	9.81 ± 0.06	9.63 ± 0.08	9.63 ± 0.52	9.53 ± 0.07
Overall fit (mV)	0.0254	0.0232	0.0232	0.1964

NI- Not included; R- Rejected

Thus, the likely model for this metal-ligand system can be the model 4. The model 3 also seems to be plausible. The same species were obtained by metal-ligand system Cd(II)–ALN in the final model with exception of species $M(H_3L)$. Very much the same models and refined stability constants were obtained by sampled DC polarography – see Appendix E.

vi) Species distribution diagrams

The SDD for the model 4 is shown in Figure 4.43. The experiment started at pH about 4.63 with species $M(H_3L)$ constituting about 30 % of solution composition. The species $M(H_2L)$ and $M(HL)$ are predominant and constitute about 85 % and 75 % of solution composition at pH about 6.0 and 8.0, respectively. The species ML starts to form at pH 7.0 constituting about 40 % of solution composition at pH about 8.6. The SDD for the model 3 shown in Figure 4.44 represent the same feature as of the model 4 simply, $M(HL)$ was replaced by M_2L that is predominant species in the model 3. The SDD for

the model 5 in Figure 4.45 and model 6 in Figure 4.46 shows that $M_2(HL)$ forms about 35 % and 8 % of solution composition, respectively. From Figure 4.45 and 4.46 the species $M(H_2L)$ and $M_2(HL)$ are formed in the same pH range, which explains the larger standard deviations attained for species $M_2(HL)$ in models 5 and 6. When one considers the SDD for the model 7 (Figure 4.47) where all species predicted are present it can be seen that species $M(H_2L)$ and $M(HL)$ are major and constitute about 80 % and 70 % of solution composition, respectively; the species $M_2(HL)$ and M_2L form about 9 % and below 5 % of solution composition, respectively; M_2L is the minor species in the solution. From Figure 4.47 it can be seen that the species $M(H_2L)$ and $M_2(HL)$ as well as $M(HL)$ and M_2L are formed in the same pH range. This explains the larger standard deviations in the stability constants of these species and the rejection of the species M_2L in the model 4. It seems that the species $M(H_2L)$ and $M(HL)$ are favoured over $M_2(HL)$ and M_2L . This makes us suggest that model 4 is favourable model for this system.

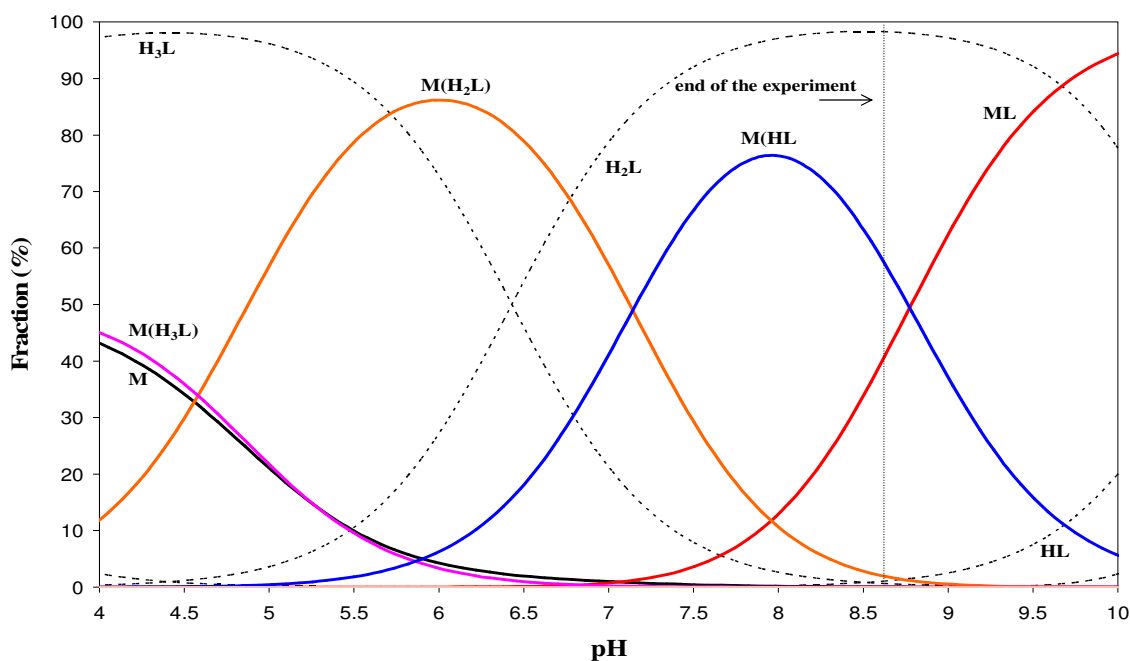


Figure 4.43 Species distribution as a function of pH for the model $M(H_3L)$, $M(H_2L)$, $M(HL)$, and ML for $Cd(II)$ -NED system studied by sampled NP polarography at $L_T : M_T = 266.6$, ionic strength 0.15 M (NaCl), 25 °C, initial $[M_T] = 2.9910 \times 10^{-5}$ M.

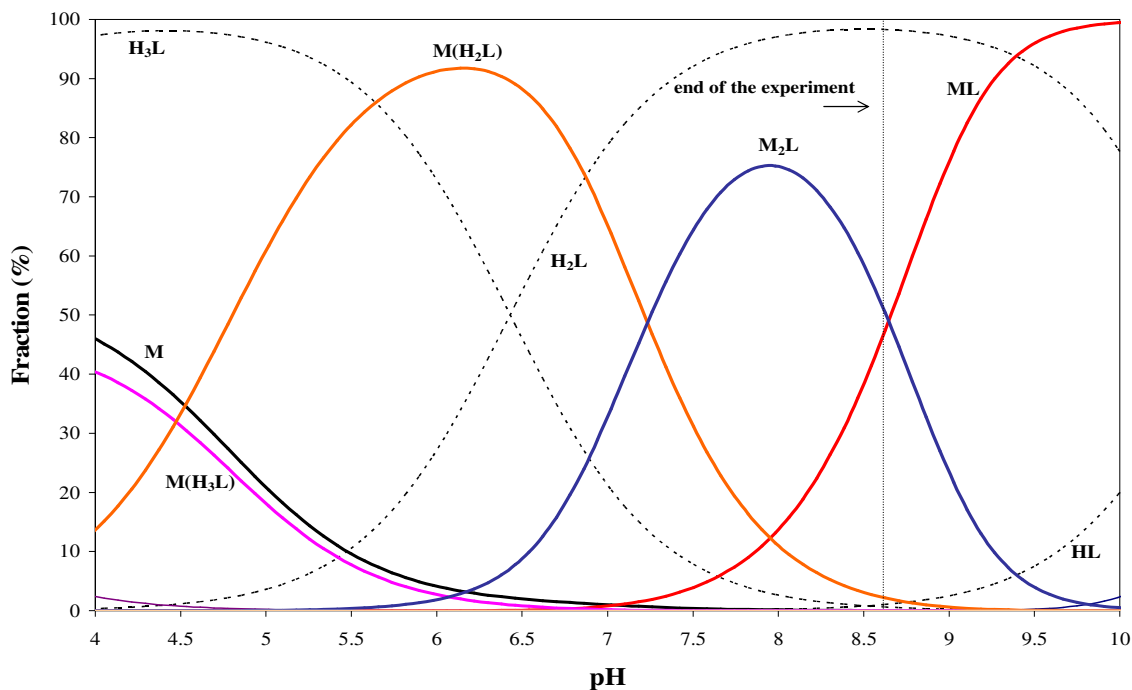


Figure 4.44 Species distribution as a function of pH for the model $M(H_3L)$, $M(H_2L)$, M_2L and ML for Cd(II)–NED system studied by sampled NP polarography at $L_T : M_T = 266.6$, ionic strength 0.15 M (NaCl), 25 °C, initial $[M_T] = 2.9910 \times 10^{-5}$ M.

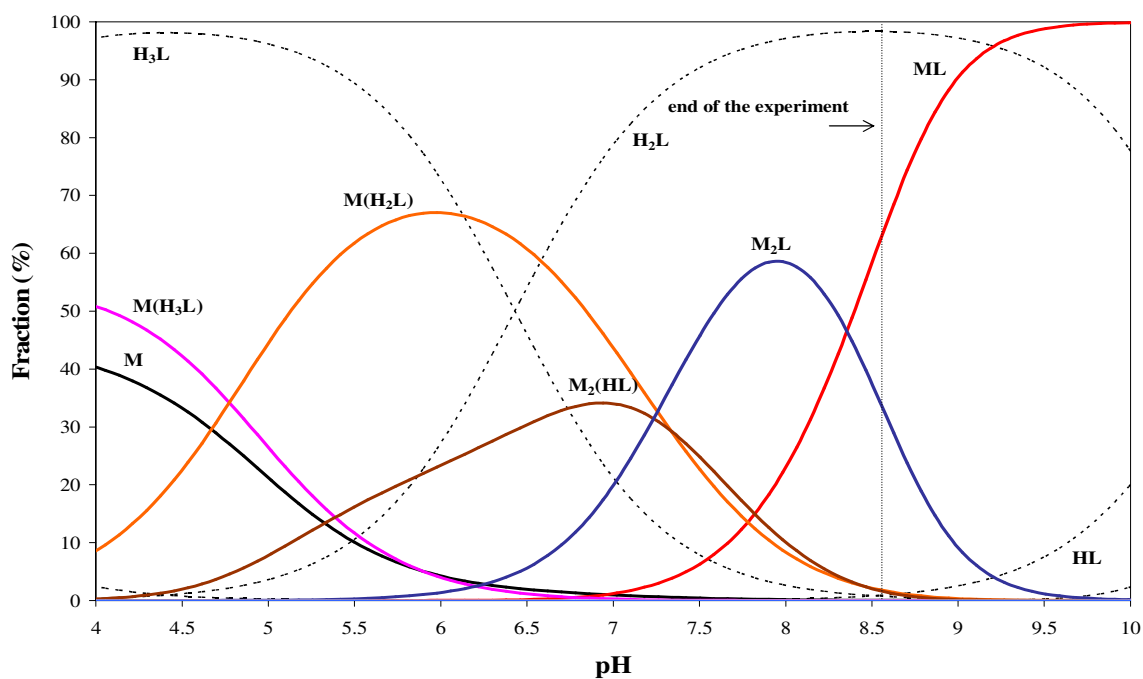


Figure 4.45 Species distribution as a function of pH for the model $M(H_3L)$, $M(H_2L)$, $M_2(HL)$, M_2L and ML for Cd(II)–NED system studied by sampled NP polarography at $L_T : M_T = 266.6$, ionic strength 0.15 M (NaCl), 25 °C, initial $[M_T] = 2.9910 \times 10^{-5}$ M.

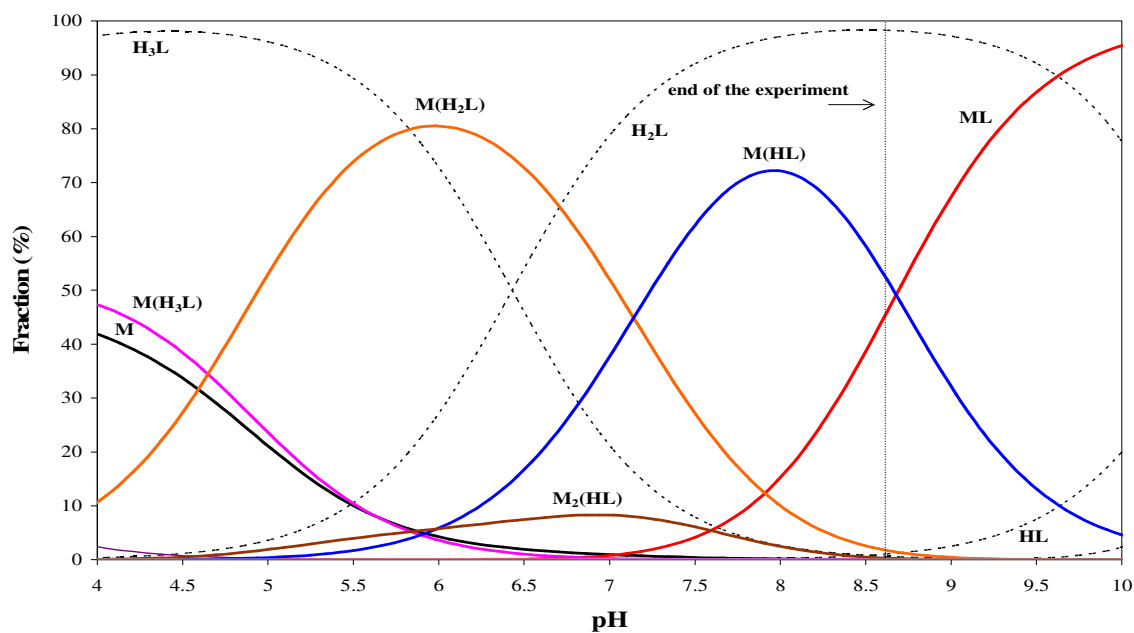


Figure 4.46 Species distribution as a function of pH for the model $M(H_3L)$, $M(H_2L)$, $M_2(HL)$, $M(HL)$, and ML for Cd(II)–NED system studied by sampled NP polarography at $L_T : M_T = 266.6$, ionic strength 0.15 M (NaCl), 25 °C, initial $[M_T] = 2.9910 \times 10^{-5}$ M.

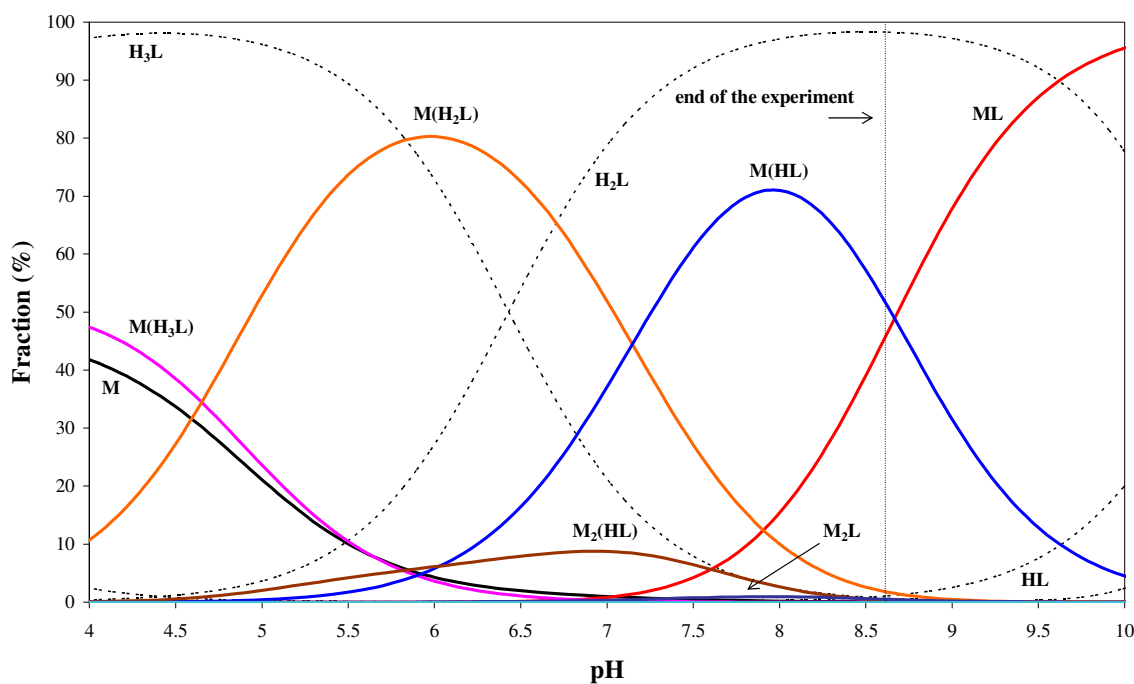


Figure 4.47 Species distribution as a function of pH for the model $M(H_3L)$, $M(H_2L)$, $M_2(HL)$, $M(HL)$, M_2L and ML for Cd(II)–NED system studied by sampled NP polarography at $L_T : M_T = 266.6$, ionic strength 0.15 M (NaCl), 25 °C, initial $[M_T] = 2.9910 \times 10^{-5}$ M.

4.2.6 Pb(II)–Neridronate–System

Data fitting

The study of Pb(II)–NED was performed by sampled DC and NP polarography at $L_T : M_T$ ratio 50. This system has similar characteristics as Pb(II)–ALN studied in section 4.2.3. The curves recorded here showed the same behaviour as those recorded on the Pb(II)–ALN system; above pH 5.66 the polarograms showed two waves. Selected NP–curves recorded at different pH values are presented in Figure 4.48.

Between pH 4.55 and 5.66 the parameter δ varied between 0.89 and 0.95, which indicated a reversible reduction processes. Thus, Equations 4.2–4.3 were used for fitting together with Equation 4.6 to account for a background current. The curves above pH 5.66 with double waves were very difficult to fit.

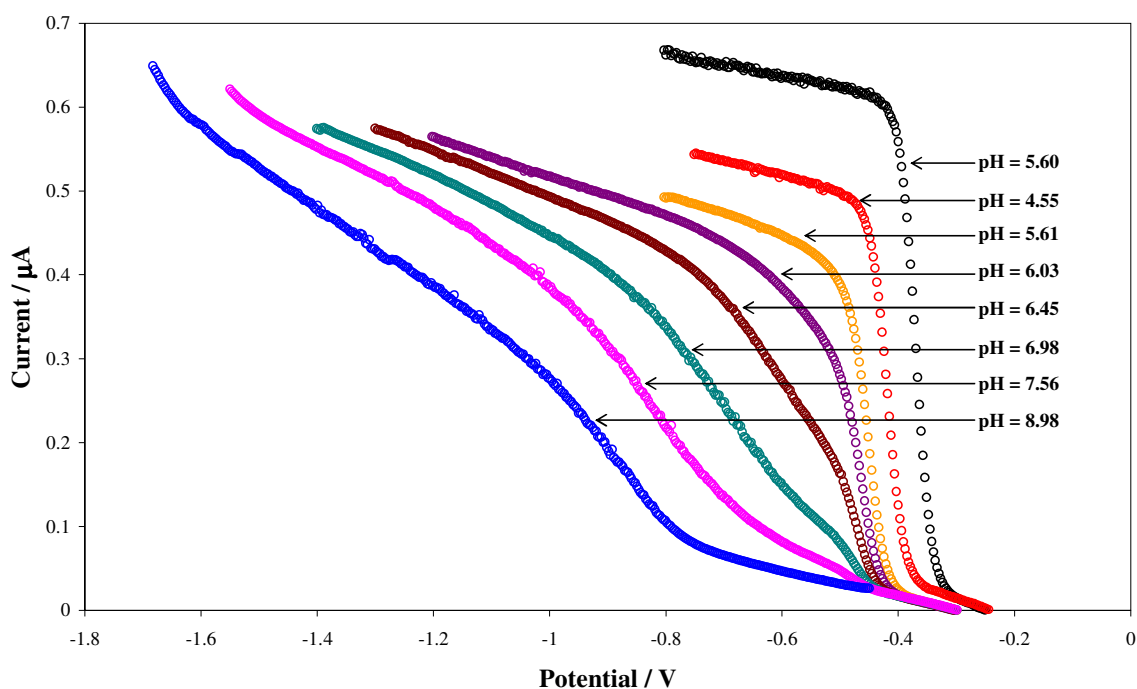


Figure 4.48 Behaviour of some of NP–waves recorded for Pb(II)–NED system studied by NP polarography at $L_T : M_T = 50$, ionic strength 0.15 M (NaCl), 25 °C initial $[M_T] = 7.9365 \times 10^{-5} \text{M}$.

Modelling of experimental data

In case of the Pb(II)–NED system, the same modelling and refinement operation as for Pb(II)–ALN were used – see section 4.2.3.

i) Variation in limiting diffusion current vs pH

From Figure 4.49 it can be observed that there is no change in normalized limiting diffusion current (see triangles in Figure 4.49) between pH 4.55 and 4.83, this suggests the formation of labile metal species in solution on the polarographic time scale used.

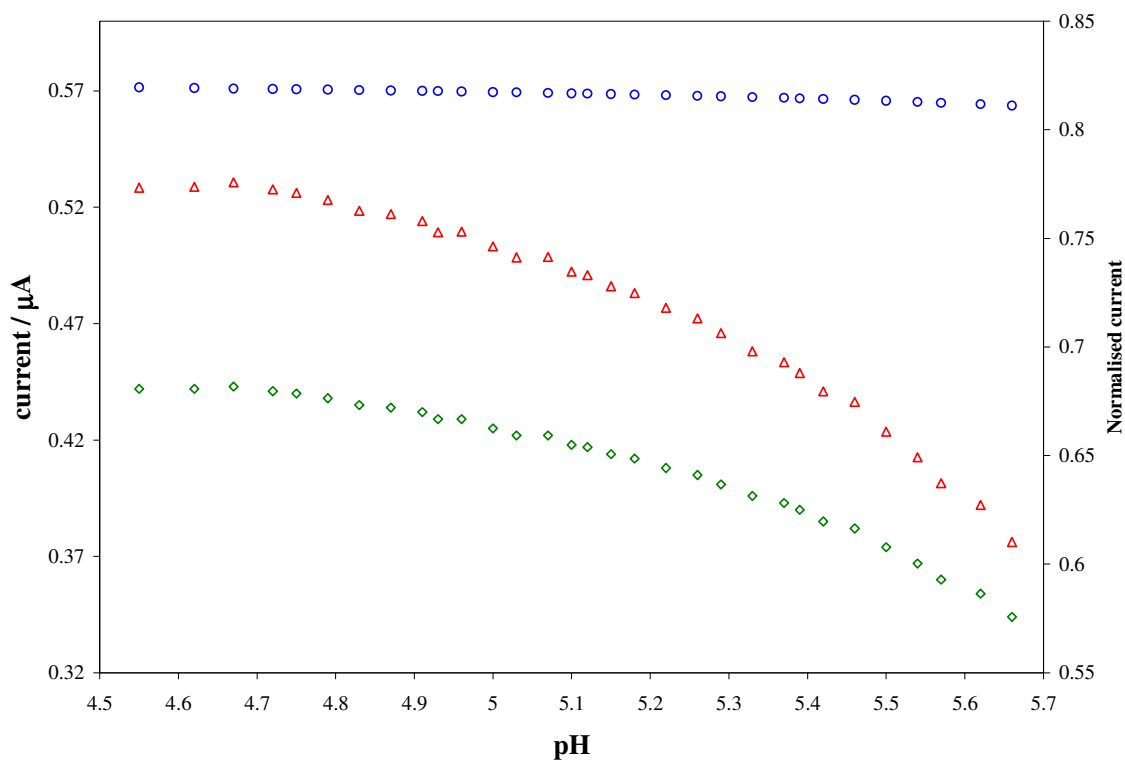


Figure 4.49 Variation in limiting diffusion current for Pb(II)–NED system studied by NP polarography at $L_T : M_T = 50$, ionic strength 0.15 M (NaCl), 25 °C initial $[M_T] = 7.9365 \times 10^{-5} M$. The triangles indicate the normalized limiting diffusion current, diamonds indicate the observed diffusion current and the circles indicate the expected current.

Above pH 4.83 there is a continuous decrease in I_d until pH about 5.66 which can be interpreted as the formation of another labile metal species with lower diffusion coefficient than the previous metal species and above pH 5.66 two waves were seen in the recorded curves or polarograms and could not be fitted for further analysis.

v) Optimization of a metal–ligand model and refinement of stability constants

Figure 4.50 displays the complex formation curves for the model 2.

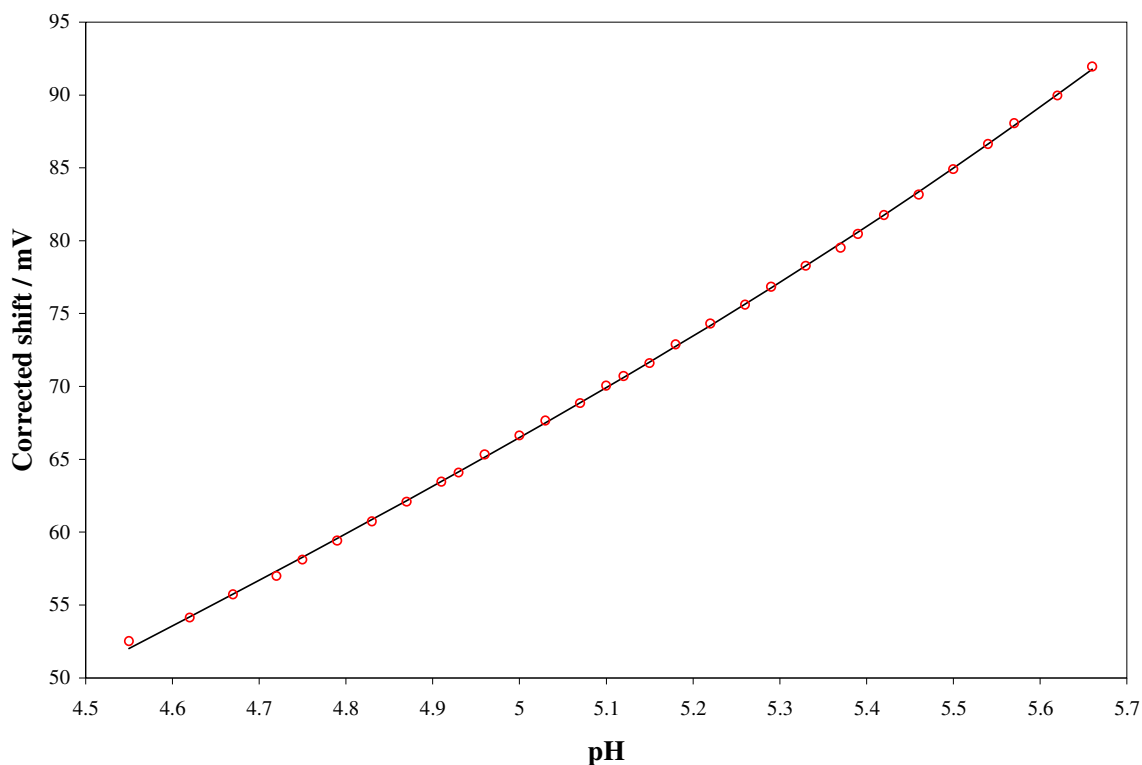


Figure 4.50 Experimental and calculated complex formation curves obtained using reversible half-wave potentials for Pb(II)–NED system studied by NP polarography at $L_T : M_T = 50$, ionic strength 0.15 M (NaCl), 25 °C initial $[M_T] = 7.9365 \times 10^{-5}$ M. The circles represents the ECFC and solid line represents the CCFC for the optimized M–L model contained M(HL), M_2 (HL).

The strategy used in the refinement process was the same as Pb(II)–ALN system and is presented in Table 4.13

Table 4.13 Overall stability constants for Pb(II)–NED system determined at 25 C and $\mu = 0.15$ M by NPP for $L_T : M_T$ ratio 50, $[M_T] = 7.9365 \times 10^{-5}$ M. The proposed final model is indicated in bold.

Equilibrium	Model 1	Model 2	Model 3	Model 4
$M + L + 2H = M(H_2L)$	R	R	27.65 ± 0.02	27.69 ± 0.01
$2M + L + H = M_2(HL)$	28.61 ± 0.04	28.68 ± 0.02	NI	NI
$M + L + H = M(HL)$	R	22.24 ± 0.03	NI	22.09 ± 0.03
$2M + L = M_2L$	23.44 ± 0.04	R	23.29 ± 0.05	NI
Overall fit (mV)	0.1056	0.0276	0.1598	0.0446

NI- Not included; R- Rejected

The model containing $M_2(HL)$ and $M(HL)$ species seems to be likely model for this system since small overall fit and best fit was obtained by this model. This model was suggested as a likely model for $Pb(II)$ –ALN system. Similar model and refined stability constants were obtained by sampled DC polarography – see Appendix E.

(vi) *Species distribution diagram*

The species distribution diagrams of the likely model $M_2(HL)$ and $M(HL)$ is seen in Figure 4.51.

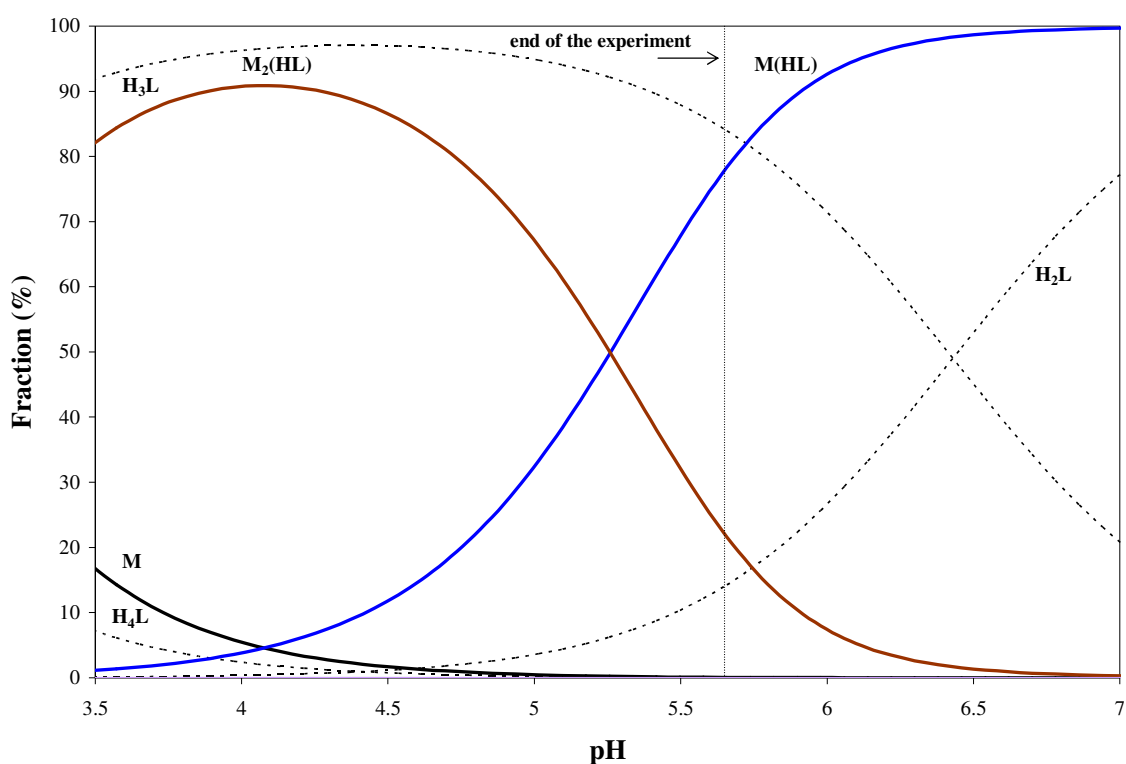


Figure 4.51 Species distribution as a function of pH for the model $M_2(HL)$, $M(HL)$, for $Pb(II)$ –NED system studied by sampled NP polarography at $L_T : M_T = 50$, ionic strength 0.15 M (NaCl), 25 °C initial $[M_T] = 7.9365 \times 10^{-5}M$.

4.3 Linear Free Energy Relationship for Alendronate and Neridronate

Linear free energy relationships (LFER) are common tools utilised in coordination chemistry for analysing metal to ligand bonding. Zeevaart [8,19] used LFER for estimate stability constants of Sm(III) and Ho(III) with HEDP. These two metal ions could not be studied directly hence the need of employing LFER methodology. The LFER technique will provide reasonable prediction for $\log K_1$ of metal concerned when stability constants (for ML) of metal ions in a wide range of stability constants for M(OH) are known [30]. The LFER for the ligands ALN and NED has never been reported; this is because there was not data available in the literature. Thus, in this work selected metal ions were studied with these ligands in order to establish the LFER for ALN and NED.

Table 4.14 shows $\log K_{ML}$ for the ligands ALN and NED and $\log K_{M(OH)}$ for metal ions used in the plot of the LFER to estimate the stability constants of both Sm(III) and Ho(III) with ALN and NED.

Table 4.14 Data for $\log K_{ML}$ for the ligands ALN and NED and $\log K_{M(OH)}$ for several metal ions.

Cation	$\log K_{M(OH)}$	$\log K_{ML}$		Reference
		ALN	NED	
Ca(II)	1.3	7.24	6.89	This Work ¹
Mg(II)	2.5	7.90	7.77	This Work ¹
Cd(II)	4.0	11.63	9.57	This Work ¹
Sm(III)	6.1	14.74	11.58	Predicted
Ho(III)	6.3	15.07	11.78	Predicted

¹From proposed model of system

The LFER for ALN and NED ligands are shown in Figures 4.52–4.53. From these relationships $\log K_{ML}$ values for Sm(III) and Ho(III) were estimated (Table 4.14). These values were estimated from the trend line equation using the $\log K_{M(OH)}$ values for Sm(III) and Ho(III).

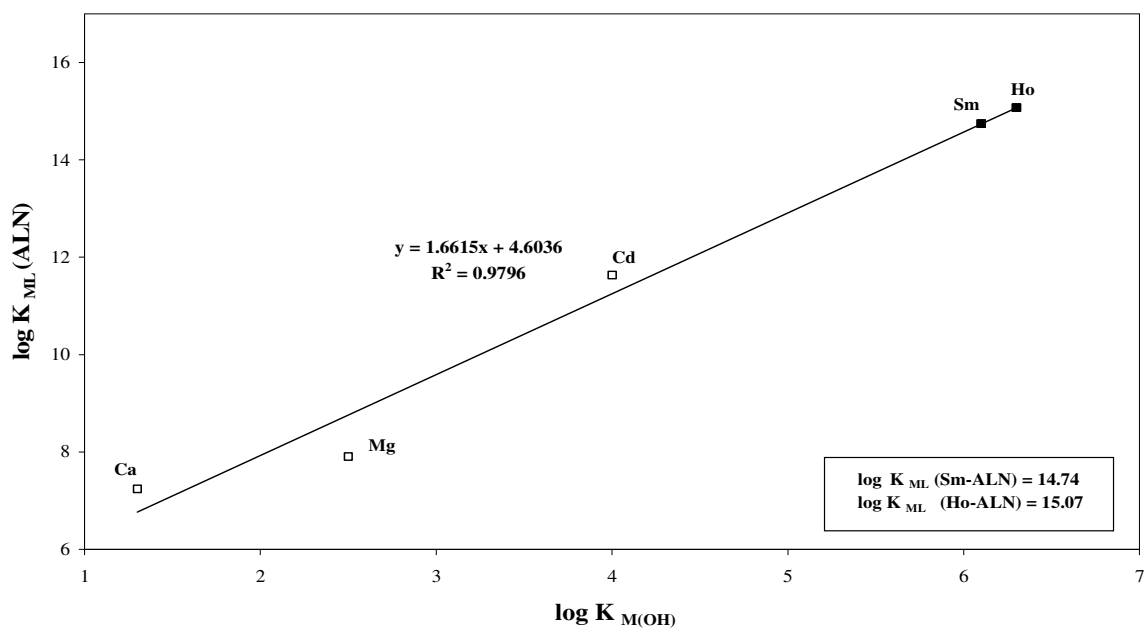


Figure 4.52 Linear free energy relationship of formation constants for metal-ion complexation by ALN and hydroxide.

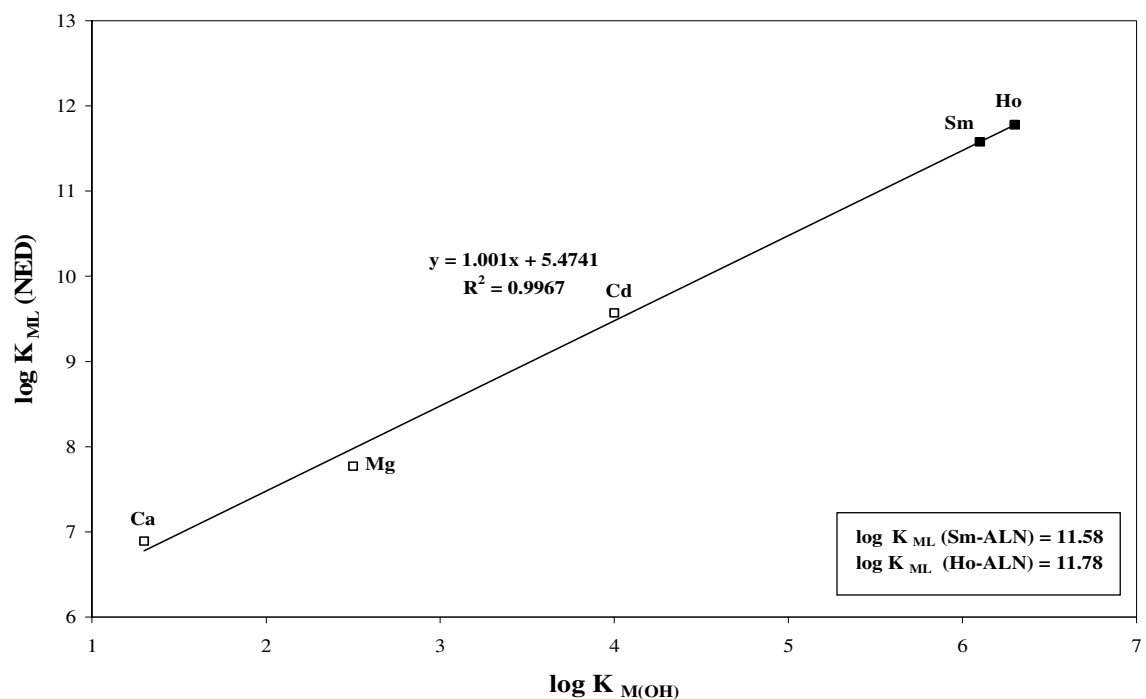


Figure 4.53 Linear free energy relationship of formation constants for metal-ion complexation by NED and hydroxide.

Reasonable correlation was obtained for NED. The estimated stability constants of Sm(III) and Ho(III) obtained are not reliable because only three points (i.e. Ca(II), Mg(II) and Cd(II)) were used in the generation of LFER. Besides, Mg(II) and Ca(II)

have very low first hydrolysis constants and the uncertainty in estimated values for Sm(II) and Ho(II) complexes is expected. It would be useful to have more points in Figures 4.52–4.53. All attempts to establish $\log K_{ML}$ for Pb(II) failed. The NP technique was not useful to resolve double waves which started to appear at pH of about 5.54. Therefore, only protonated metal species were found for Pb(II) ALN and NED systems.

The LFER for stability constants determined for the ML complexes with ALN and NED ligands were used to predict stability constants for radioactive elements, namely Sm(III) and Ho(III). However, ML complexes were not predicted (from the results obtained) to exist at blood plasma pH. Therefore, only blood plasma metal-ions protonated complexes could be present in blood plasma. Thus, two relationships for protonated complexes, such as $M(HL) = ML'$, where $L' = (HL)$ can be drawn.

The stability constants for the ML' complexes as indicated in Table 4.15, were obtained by subtracting $pK_{a(1)}$ (see Table 4.16) value from the $M(HL)$ complex. The values of $\log K_{ML}$ for the ligands MDP [30] and HEDP [19] are indicated in Table 4.15 for comparison reason. The Cd(II)-MDP and Pb(II)-HEDP systems were not reported in literature.

From the Table 4.15, one can note that the values of $\log K_{ML'}$ for Ca(II) and Mg(II) for ALN and NED ligands and Cd(II) for NED are comparable with values of $\log K_{ML}$ for HEDP ligand. This suggests that mode of binding to L' is the same as in HEDP ligand.

Table 4.15 Data for $\log K_{ML}$ for the ligands MDP and HEDP, $\log K_{ML'}$ for the ligands ALN and NED and $\log K_{M(OH)}$ for several metal ions. (Where $L'=HL$)

Cation	$\log K_{M(OH)}$	$\log K_{ML}$		$\log K_{ML'}$	
		MDP	HEDP	ALN ¹	NED ¹
Ca(II)	1.3	4.86	5.34	5.40	5.44
Mg(II)	2.5	5.68	6.03	6.10	5.91
Cd(II)	4.0	-	7.10	9.17	7.41
Pb(II)	6.0	9.42	-	11.03	11.26
Sm(III) ²	6.1	9.55	10.10	11.31	10.83
Ho(III) ²	6.3	9.74	10.40	11.57	11.08

¹This work, ²Predicted

It has been reported in literature that the relative potency of ALN is 700 and NED is ~100 times that of HEDP [33]. On the other hand, the mode of complexation for ALN, NED and HEDP are the same at blood plasma pH. Thus the relative potency of ALN and NED is not related to the nature of ALN or NED metal complexes. The aliphatic carbon chain length appears to be an important factor in potency.

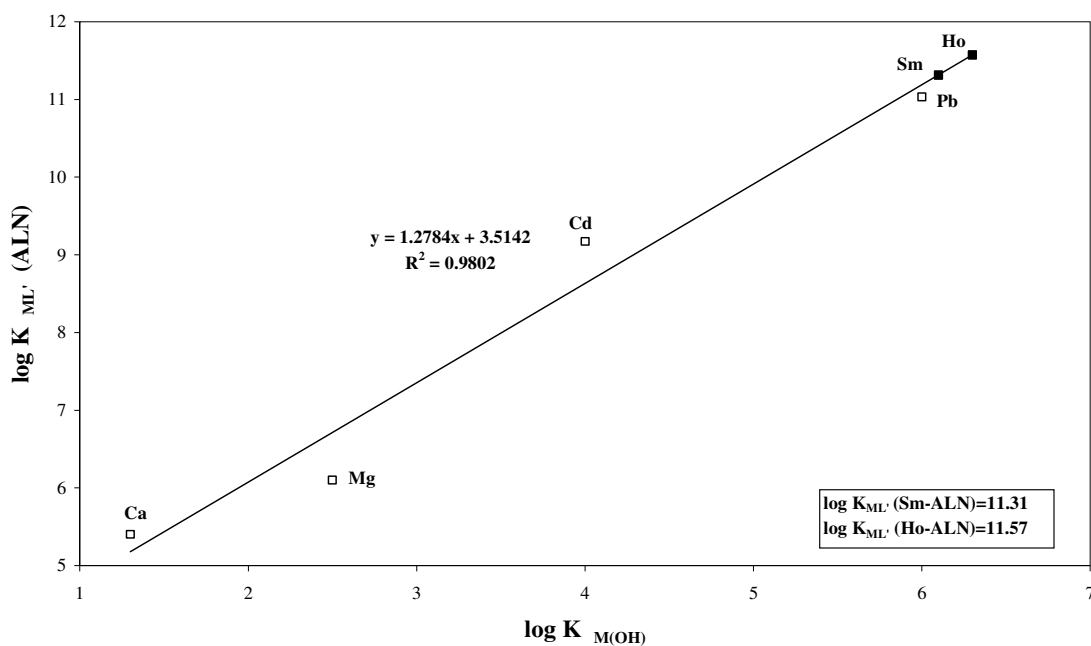


Figure 4.54 Linear free energy relationship between $\log K_{M(OH)}$ and $\log K_{ML'}$ for indicated metal ions (all divalent) and the ligand ALN.

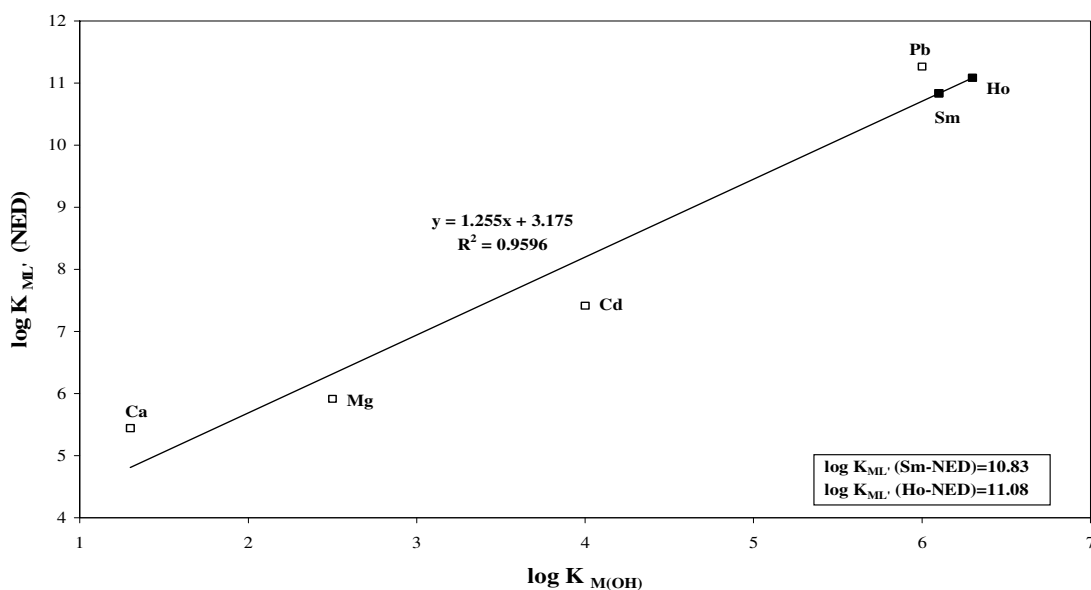


Figure 4.55 Linear free energy relationship between $\log K_{M(OH)}$ and $\log K_{ML'}$ for indicated metal ions (all divalent) and the ligand NED.

The large value of $\log K_{ML}$ for the Cd(II)-L' obtained (see Table 4.15) can be attributed to the extra possible coordination to the hydroxy group-see Figure 4.59. The values of $\log K_{ML}$ for Pb(II)-L' for ALN and NED ligand obtained are similar, but we cannot make comparison with HEDP because the Pb(II)-HEDP system was not reported in literature.

The estimated $\log K_{ML}$ values for Sm(III) and Ho(III) obtained with ALN and NED are somewhat higher than the reported estimated $\log K_{ML}$ values obtained with HEDP [19]. They differ by about 1.2 and 0.7 log unit for ALN and NED, respectively. The few points used to generate the LFER might have contributed for these differences. In order to obtain reliable estimates in stability constants of Sm(III) and Ho(III) more points are needed to generate LFERs.

4.4 Comparison of Formation Constants for Ligands ALN, NED and others Ligands with Metal Ions

For purposes of comparison, Tables 4.16–4.17 contain the reported formation constants of the MDP, HEDP, APD, ALN and NED complexes with the selected metal ions. The ligands APD, ALN and NED have an additional carbon chain with amino group attached to it which is absent in the MDP and HEDP. For MDP and HEDP (Table 4.16), $pK_{a(1)}$ values are similar indicating that the deprotonation occurs at the phosphonate oxygen atoms. These values are also similar to the $pK_{a(2)}$ for APD, ALN and NED, which mean, the deprotonation occurs at the same site. The higher $pK_{a(1)}$ observed in APD, ALN and NED is attributed to the deprotonation of amino proton which is absent in MDP and HEDP.

Table 4.16 Comparison of protonation constants ($\log K$) for MDP, HEDP, APD, ALN and NED.

Ligand	$pK_{a(1)}$	$pK_{a(2)}$	$pK_{a(3)}$	$pK_{a(4)}$	$pK_{a(5)}$	$pK_{a(6)}$	Reference
MDP	9.97	7.00	3.26	2.19	-	-	[19]
HEDP	10.11	6.81	2.97	2.43	-	4.66	[34]
APD	11.95	9.80	6.01	2.56	-	-	[14]
ALN	11.03	10.41	6.13	2.10	1.28	-	This work
NED	10.98	10.64	6.49	2.46	-	-	This work

Table 4.17 Comparison of formation constants ($\log \beta$) for MDP, HEDP, APD, ALN and NED.

Metal ion	Ligand	ML	M ₂ L	M ₂ (HL)	M(HL)	M(H ₂ L)	M(H ₃ L)	Reference
Mg(II)	MDP	5.68	8.36	-	13.24	-	-	[19]
	HEDP	6.03	9.70	-	13.51	-	-	[19]
	APD	7.03	10.85	20.13	16.81	23.67	-	[14]
	ALN	7.90	13.10 ²	20.42	17.13	24.31	-	This work ¹
	NED	7.77	12.53 ²	20.60	16.89	24.70	-	This work ¹
Ca(II)	MDP	4.86	8.39	-	12.69	-	-	[19]
	HEDP	5.34	9.53	-	13.17	-	-	[19]
	APD	6.70	10.79	20.71	17.27	23.58	-	[14]
	ALN	7.24	11.15 ²	20.43	16.43	23.38	-	This work ¹
	NED	6.89	11.57 ²	19.68	16.42	24.25	-	This work ¹
Cd(II)	MDP	-	-	-	-	-	-	-
	HEDP	7.10	12.99	-	-	20.02	-	[35]
	APD	-	18.14	24.15	19.21	-	-	[31]
	ALN	11.63	21.18 ²	27.81	20.20	26.15 ²	-	This work ¹
	NED	9.57	17.42 ²	25.09 ²	18.39	25.59	30.24	This work ¹
Pb(II)	MDP	9.42	15.58	-	-	19.68	-	[35]
	HEDP	-	-	-	-	-	-	-
	APD	-	23.74	28.18	22.19	27.02	30.22	[31]
	ALN	-	23.84	28.72 ²	22.06	26.15 ²	-	This work ¹
	NED	-	23.44 ²	28.68	22.24	27.69 ²	-	This work ¹

¹From proposed model of system; ²Predicted from modelling

From the Table 4.17, in general, differences are found between the stability constants of the Mg(II) and Ca(II) complexes for MDP and HEDP, which can be attributed to the hydroxy group [16]. On the other hand, the stability constants of the Mg(II) and Ca(II) complexes for the ligands APD, ALN and NED are larger than the MDP and HEDP due to the presence of an amino group. The stability constants of the Cd(II) and Pb(II) are larger than those corresponding Mg(II) and Ca(II) complexes for APD, ALN and NED;

Cd(II) and Pb(II) seem to form stronger complexes with APD, ALN and NED than Ca(II) and Mg(II). Most remarkable are the relatively high values for the Cd(II) complexes of the ALN compared with APD and NED which could be attributed to the extra possible coordination to the hydroxy group – see Figure 4.59.

The reported crystal structure of Ca(II) complex with ALN (Catena-(bis(μ_2 -4-Ammonium-1-hydroxybuta-1,1-diylbis(phosphonato))-calcium(II)), [36] is shown below and indicates that amino group is not involved in complex formation; only two phosphonate oxygen atoms form bond with Ca(II).

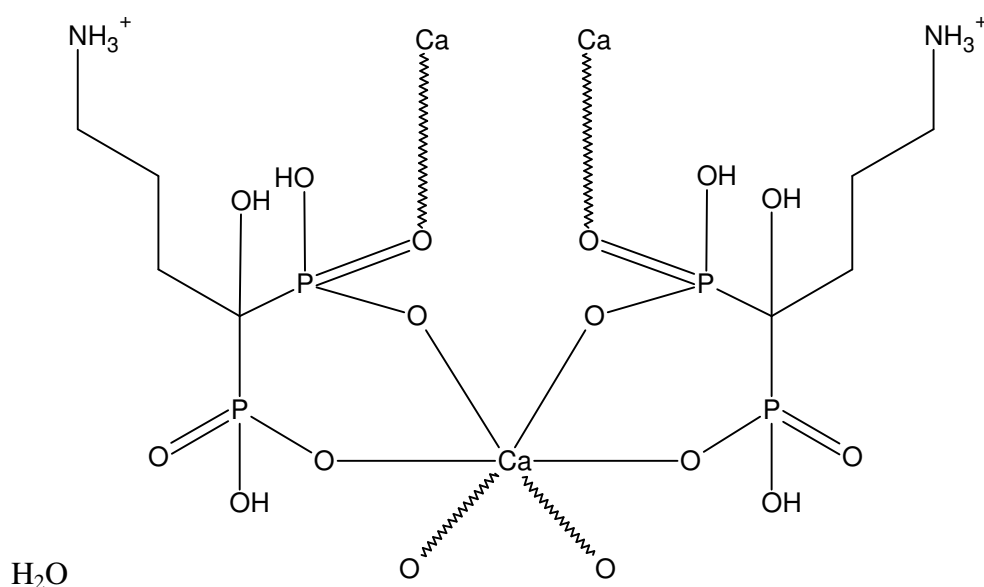


Figure 4.56 Crystallographic structure of Catena-(bis(μ_2 -4-Ammonium-1-hydroxybuta-1,1-diylbis(phosphonato))-calcium(II) [36].

Similar bond formation is observed in Cd(II) complex with NED (Bis(μ_2 -6-amino-1-hydroxyhexylidene-1,1-bisphosphonate)-diaqua-bis(4-amino-1-hydroxyhexylidene-1,1-bisphosphonate)-di-cadmium dehydrate) [15]—see Figure 4.57. All these observations indicate that the mode of complexation of ALN and NED can be seen as similar as that of HEDP.

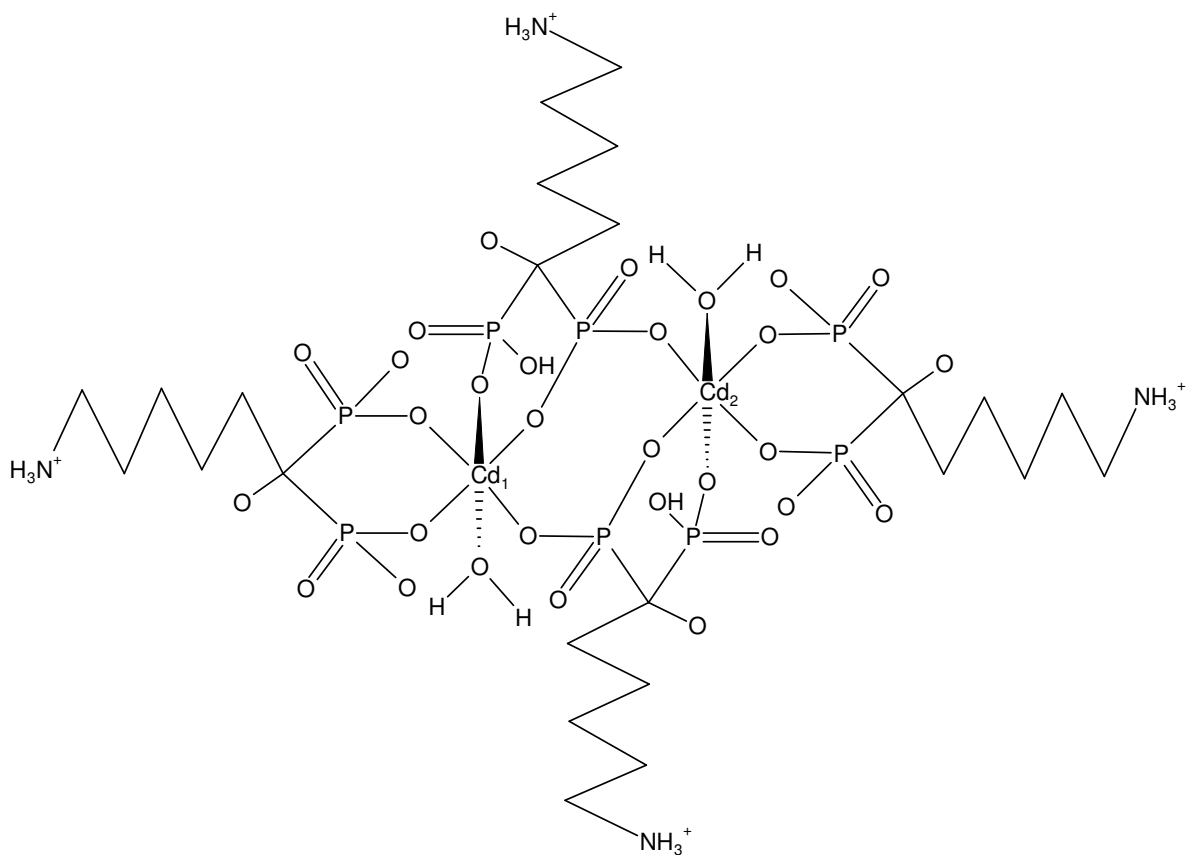
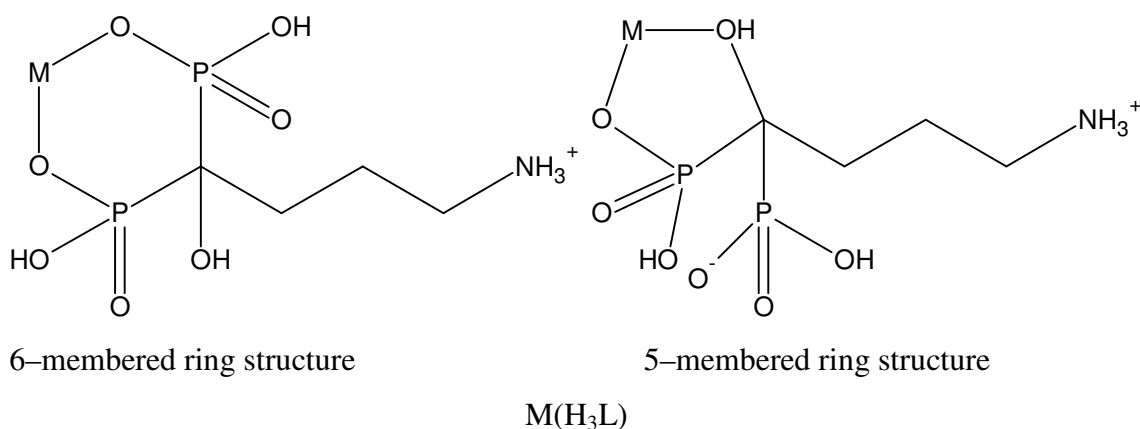


Figure 4.57 Crystallographic structure of Bis(μ_2 -6-amino-1-hydroxyhexylidene-1,1-bisphosphonate)-diaqua-bis(4-amino-1-hydroxyhexylidene-1,1-bisphosphonate)-dicadmium dehydrate [15].

The following proposed structures for $M(H_3L)$, $M(H_2L)$, $M_2(HL)$, and $M(HL)$, can be drawn as follows:



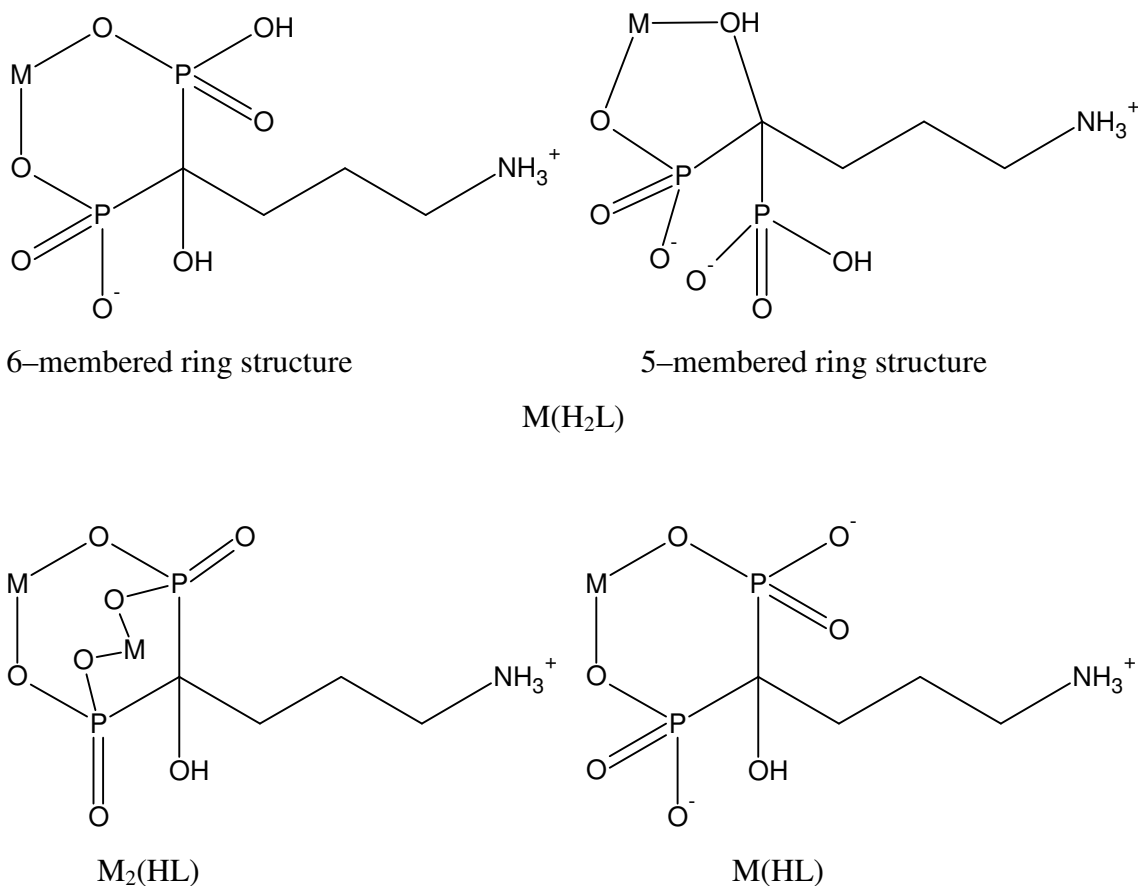


Figure 4.58 Proposed structures for ALN and NED complexation of divalent metal-ions.

From proposed structures above it is seen that the amino group on the ligand is not involved in complex formation as was seen in reported crystal structures and the ligands behave like a bidentate ligands which results in a 6-membered ring with the metal ion. The complex formation with 5-membered ring, bidentate complexation is also possible. There are many other possibilities of how the ligands ALN and NED can form bonds with metal ions. The ligands ALN and NED have hydroxy group and long side chain with amino group attached to it that can take part in complex formation at higher pH and provide a finite set of coordination types. The reported crystal structure of Cd(II) complex with ALN (Catena-(4-Amino-1-hydroxybutylidene)-1,1-bisphosphonite-cadmium monohydrate) [37] shown in Figure 4.59 is an example where hydroxy group takes part in complex formation. This reported crystal structure indicates that ALN is tridentate ligand. Possibility also exists with ligand NED.

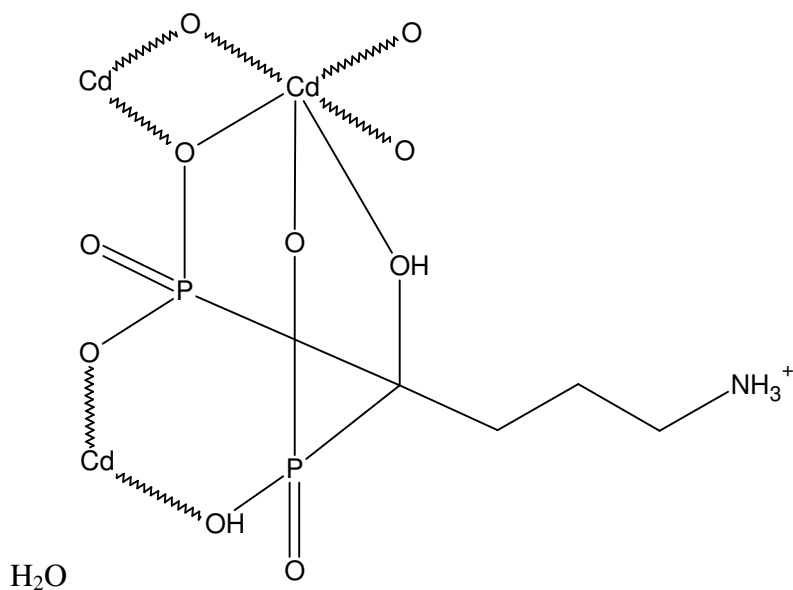


Figure 4.59 Crystallographic structure of Catena-(4-Amino-1-hydroxybutylidene-1,1-bisphosphonite-cadmium monohydrate [37].

The stability constants of M₂L and ML for the metal ions with ALN and NED are larger than HEDP. The only difference between ALN, NED and HEDP is the amino group and hence large first protonation constants. The amino group takes part in complex formation in case of M₂L and ML. From above analysis, structures may be proposed for M₂L and ML species for ALN and NED:

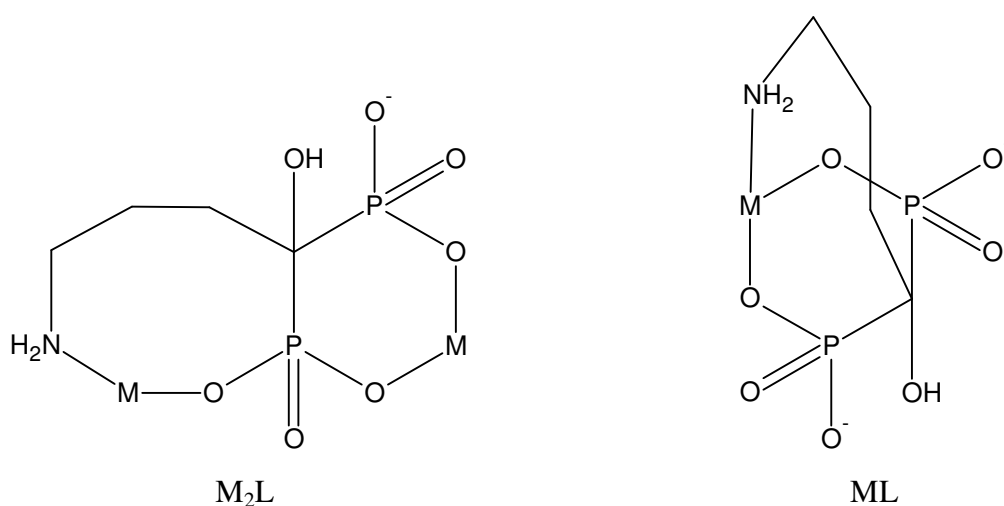


Figure 4.60 Proposed structures for ALN and NED complexation of divalent metal-ions.

4.5 References

- [1] P.M. May, K. Murray and D.R. Williams, *Talanta*, Vol. 32, No. 6, **1985**, p. 483.
- [2] P.M. May, K. Murray and D.R. Williams, *Talanta*, Vol. 35, No. 11, **1988**, p. 825.
- [3] A.E. Martell and R.M. Smith, *Critical Stability Constants*, Vol. 6, Plenum Press, New York, 2nd ed. **1989**.
- [4] NIST Standard Reference Database 46. NIST Critically Selected Stability Constants of Metal Complexes Database. Version 3.0. Data collected and selected by R.M. Smith and A.E. Martell. U.S. Martell. U.S. Department of Commerce, National Institute of Standards and Technology, **1997**.
- [5] F. Marsicano, C. Monberg, B.S. Martincigh, K. Murray, P.M. May and D.R. Williams, *J. Coord. Chem.* Vol. 16, **1988**, p. 321.
- [6] G. Hägele, Z. Szakács, J. Ollig, S. Hermens and C. Pfaff, *Heteroatom Chemistry*, Vol. 11, N° 7, **2000**, p. 562.
- [7] A.P. Katkov, T.A. Matkovskaya, T.M. Balashova, A.S. Monakhov and G.R. Allakhverdov, *Zhurnal Fizicheskoi Khimii*, Vol. 63, No. 6, **1989**, p. 1459.
- [8] J.R. Zeevaart, Complexation of Trivalent Lanthanides by Three Diphosphonate Ligands in Blood Plasma, MSc Thesis, University of Cape Town, South Africa, **1997**.
- [9] P. Dietsche, T. Günther and M. Röhnelt, *Z.Naturforsch*, Vol. 31c, **1976**, p. 661
- [10] K.L. Nash and E.P. Horwitz, *Inorg. Chm. Acta*, Vol. 169, **1990**, p. 245.
- [11] J.G.M. Van der Linden and R.A.M.J. Claessens, *J. Inorg. Biochem.*, Vol. 21, **1984**, p. 73.
- [12] R.J. Grabenstetter, O.T. Quimby and T.J. Flautt, *J. Phys. Chem.*, Vol. 71, **1967**, p. 4195.
- [13] I. Cukrowski, J.R. Zeevaart and N.V. Jarvis, *Anal. Chim. Acta*, Vol. 379, **1999**, p. 217.
- [14] J.R. Zeevaart, N.V. Jarvis, W.K. A. Louw, G.E. Jackson, I. Cukrowski and C.J. Mouton, *Journal of Inorganic Biochemistry*, Vol. 73, **1999**, p. 265.
- [15] S.P. Man, M. Motevalli, S. Gardiner, A. Sullivan, and J. Wilson, *Polyhedron*, Vol. 25, **2006**, p. 1017.
- [16] V.N. Serezhkin, L.B. Serezhkina and V.S. Sergienko, *Russian Journal of Inorganic Chemistry*, Vol. 45, No. 4, **2000**, p. 521.

- [17] C.M.M. Machado, S. Scheerlinck, I. Cukrowski and H.M.V.M. Soares, *Analytica Chimica Acta*, Vol. 518, **2004**, p. 117.
- [18] C.M.M. Machado, I. Cukrowski, P. Gameiro and H.M.V.M. Soares, *Analytica Chimica Acta*, Vol. 493, **2003**, p. 105.
- [19] J.R. Zeevaart, N.V. Jarvis, I. Cukrowski and G.E. Jackson, *S. Afr. J. Chem.*, Vol. 50, **1997**, p. 189.
- [20] I. Cukrowski, *J. Electroanal. Chem.*, Vol. 460, **1999**, p. 197.
- [21] D.R. Crow, *Polarography of Metal Complexes*, New York: Academic Press, **1969**.
- [22] G.H. Nancollas and M. B. Tomson, *Pure and Applied Chemistry*, Vol. 54, **1982**, p. 2676.
- [23] I. Cukrowski, *Analytica Chimica Acta*, Vol. 336, **1996**, p. 23.
- [24] I. Cukrowski and M. Adsetts, *J. Electroanal. Chem.* Vol. 429, **1997**, p.129.
- [25] I. Cukrowski, *Electroanalysis*, Vol. 9, No. 9, **1997**, p.699.
- [26] I. Cukrowski, J.M. Zhang and A. Van Aswegen, *Helv. Chim. Acta*, Vol. 87, **2004**, p. 2135.
- [27] I. Cukrowski and J.M. Zhang, *Electroanalysis*, Vol. 16, No. 8, **2004**, p. 612.
- [28] I. Cukrowski, P. Magampa and T.S. Mkwizu, *Helv. Chim. Acta*, Vol. 89, **2006**, p. 2934.
- [29] I. Ružić, A. Baric and M. Branica, *journal of Electroanalytical Chemistry*, Vol. 29, **1971**, p. 411.
- [30] I. Cukrowski, D.M. Mogano and J.R. Zeevaart, *Journal of Inorganic Biochemistry*, Vol. 99, **2005**, p. 2308.
- [31] P.P. Magampa, Electrochemical studies of the ligand 1- hydroxyl-3-aminopropylidenediphosphonic acid (APD) towards bone cancer therapy, MSc Thesis, University of Pretoria, South Africa, **2006**.
- [32] I. Cukrowski and P. Franklyn, 3D Complex Formation Curves Package, Windows version 1.2.1, **2003**.
- [33] J.H. Lin, *Bone*, Vol. 18, No. 2, **1996**, p. 75.
- [34] J.R. Zeevaart, Metal Ion Speciation in Blood Plasma as a Tool in Predicting the In vivo Behaviour of Potential Bone-seeking Radiopharmaceuticals, Ph.D. Thesis, Delft University Press, The Netherlands, **2001**.
- [35] D.M. Mogano, Electrochemical studies of metal-ligand complexation of HEDP

and MDP ligands for bone cancer therapy, MSc Thesis, University of the Witwatersrand, Johannesburg, South Africa, **2004**.

- [36] D. Fernandez, D. Vega and A. Goeta, *Acta Crystallogr., Sect. C: Cryst. Struct. Commun.*, Vol. 59, **2003**, p. m543.
- [37] C. Dufau, M. Benramdane, Y. Leroux, D. El Manouni, A. Neuman, T. Prange, J.P. Silvestre and H. Gillier, *Phosphorus, Sulfur, Silicon, Relat. Elem.*, Vol. 107, **1995**, p. 145.

CHAPTER 5

Conclusions

5.1 Conclusions and Future work

The main aim of this work was to estimate $\log K_{ML}$ of Sm(III) and Ho(III) using LFER involving two N-containing bisphosphonate ligands viz. ALN and NED. To achieve this one needed to know the formation constants for the complexation of metal ions with the ligands ALN and NED. Glass electrode potentiometry was used in the determination of protonation and stability constants for the complexation of Mg(II) and Ca(II) while polarography was used in the study of Cd(II) and Pb(II) with ALN and NED. Glass electrode potentiometry could not be used for Cd(II) and Pb(II) because precipitation of complexes occurs during titration, and Mg(II) and Ca(II) are polarographically inactive and could not be determined by polarography.

The ligands ALN and NED have very much the same protonation constants, since they are structurally similar. Few data are available in literature regarding to the protonation constants of these ligands. However, the protonation constants for the ligand ALN are comparable to those reported by Hägele *et al* [1]. The small differences observed were attributed to the different medium and ionic strengths. The larger difference in protonation constants were observed in the 3rd protonation constants of the ligand ALN, and 2nd and 3rd of the NED, when compared with data reported by Katkov *et al* [2]. The differences could not be attributed to ionic strength and medium. The result reported by Katkov *et al* appears to be suspect.

The refinement of stability constants was performed by ESTA and 3D-CFC programs which were able to refine several models. The use of statistics did not provide enough information on rejection or acceptance of a particular model. Moreover, the use of one technique, was too difficult to provide the final model and reliable stability constants.

The results obtained have evidenced the same type of metal-complex for ALN and NED.

The ligands ALN and NED coordinate metal ions via the phosphonate functions or hydroxy group with N-atom remaining protonated in the pH range 4.5–8.0. This mode of complexation that is similar as that HEDP is supported by reported crystal structures of the ligands ALN and NED regarding the protonated species. The N-atom becomes important in complexation above pH about 7.5-8.0 for species such as M_2L and ML . Therefore, only blood plasma metal-ions protonated complexes could be present in blood plasma, hence N-atom is not involved in complexation. From this follows that higher activity of N-containing BPs in bone cancer are not directly related to complexation because the N-atom is not involved in complex formation reaction with the central metal ion at blood plasma pH.

The LFER for the ligands ALN and NED was employed to estimate $\log K_{ML}$ and $\log K_{ML'}$ (where $L' = HL$) of Sm(III) and Ho(III) complexes using data attained in this work from the study of the ligands ALN and NED with metal ions Mg(II), Ca(II) and Cd(II). Because of complications of homogeneous kinetics in the DC/NP polarography in the study of complexation of the Pb(II) with ligands ALN and NED only a partial model could be refined from polarographic data. The complex ML was not found in this case, only protonated metal species were found. Therefore, the estimates of $\log K_{ML}$ and $\log K_{ML'}$ values for Sm(II) and Ho(III) with ALN and NED were not reliable because few points were used for estimate $\log K_{ML}$ and $\log K_{ML'}$. To increase certainty in estimated values for Sm(III) and Ho(III) further, the $\log K_{ML}$ and $\log K_{ML'}$ values for Pb(II) and others metal ion, such as, Zn(II) and Sn(II) would be necessary.

The precipitate of the Cd(II) and Pb(II) species at typical potentiometric conditions, the polarographic inactivity of Mg(II) and Ca(II) and the difficulty in determination of stability constant of complex ML of the Pb(II) with ALN and NED by polarography showed the need of another analytical technique such as spectrophotometry, nuclear magnetic resonance or others to determine, confirm and help in arriving to most likely final metal-ligand model.

To understand more how the ligands ALN and NED form complexes at different pH values and to confirm the proposed models of metal-ligand systems, the precipitate that forms during titrations of Ca(II), Cd(II) and Pb(II) may be isolated, analysed and crystallised.

5.2 References

- [1] G. Hägele, Z. Szakács, J. Ollig, S. Hermens and C. Pfaff, *Heteroatom Chemistry*, Vol. 11, N° 7, **2000**, p. 562.
- [2] A.P. Katkov, T.A. Matkovskaya, T.M. Balashova, A.S. Monakhov and G.R. Allakhverdov, *Zhumal Fizicheskoi Khimii*, Vol. 63, No. 6, **1989**, p. 1459.

APPENDICES

APPENDIX A

Additional GEP results

APPENDIX B

Experimental data from GEP studies of the protonation equilibria of the ligands ALN and NED

APPENDIX C

Experimental data from GEP, DCP and NPP studies of complexation of Mg(II), Ca(II), Cd(II) and Pb(II) with ligand ALN

APPENDIX D

Experimental data from GEP, DCP and NPP studies of complexation of Mg(II), Ca(II), Cd(II) and Pb(II) with ligand NED

APPENDIX E

Additional sampled DCP results

APPENDIX A

Additional GEP results

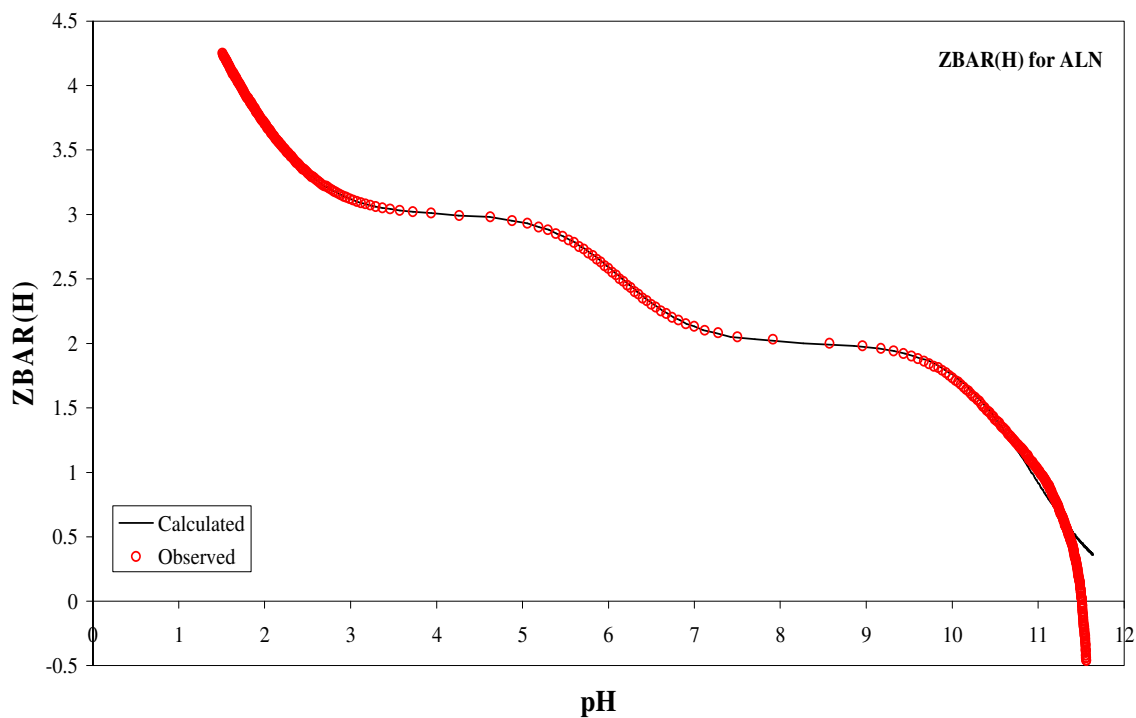


Figure A.1 Experimental (circles) and theoretical (solid line) protonation curves for ALN at ionic strength 0.15 M in NaCl and 25° C, $[L_T] = 1.0000 \times 10^{-2}$ M. At high pH the theoretical and experimental curves diverged.

Table A.1 Protonation constants (as log K) for ALN at 25 °C and ionic strength of 0.15 M in NaCl obtained by GEP.

	HL	H ₂ L	H ₃ L	H ₄ L	H ₅ L	Refinement		% change	R-factor	Refined Initial parameter
						Before (M)	After (M)			
Titration 1	11.48 ±0.02	10.50 ±0.01	6.16 ±0.01	2.11 ±0.01	1.32 ±0.03	-	-	-	0.00598	Nothing
	11.53 ±0.009	10.45 ±0.007	6.11 ±0.007	2.05 ±0.009	1.40 ±0.01	0.043473	0.043371	-0.25 %	0.00305	Acid
	11.519 ± 0.004	10.433 ± 0.003	6.127 ±0.004	2.116 ± 0.004	1.332 ± 0.006	0.010000	0.009867	-1.33 %	0.00142	Ligand
	11.525 ±0.007	10.448 ±0.006	6.114 ±0.006	2.055 ±0.008	1.398 ±0.01	0.050200	0.050307	+0.21 %	0.00258	Base
Titration 2	11.61 ±0.02	10.49 ±0.02	6.15 ±0.02	2.07 ±0.02	1.18 ±0.03	-	-	-	0.00468	Nothing
	11.66 ±0.01	10.44 ±0.01	6.12 ±0.01	2.01 ±0.01	1.26 ±0.02	0.0434942	0.043420	-0.17 %	0.00251	Acid
	11.654 ± 0.006	10.424 ± 0.005	6.126 ±0.005	2.073 ± 0.005	1.194 ± 0.002	0.0080000	0.007907	-1.16 %	0.00127	Ligand
	11.660 ±0.008	10.438 ±0.007	6.114 ±0.007	2.02 ±0.01	1.27 ±0.01	0.0503700	0.050449	+0.16 %	0.00220	Base
Titration 1 and 2	11.53 ±0.01	10.50 ±0.01	6.16 ±0.01	2.09 ±0.01	1.26 ±0.02	-	-	-	0.00557	Nothing
	11.576 ±0.008	10.450 ±0.007	6.114 ±0.007	2.032 ±0.008	1.345 ±0.01	0.043473 0.043494	0.043368 0.043423	-0.24 % -0.29 %	0.00313	Acid
	11.567 ± 0.005	10.430 ± 0.004	6.126 ±0.004	2.0992 ± 0.005	1.279 ± 0.007	0.010000 0.008000	0.009870 0.007905	-1.30 % -1.19 %	0.00199	Ligand,1
	11.573 ±0.007	10.444 ±0.006	6.114 ±0.006	2.040 ±0.007	1.347 ±0.01	0.050200 0.050370	0.050308 0.050447	+0.22 % +0.15 %	0.00280	Base
Martell & Smith (25°C) μ=0.1M	(11.6)	10.5	8.73	2.72	-	-	-	-	-	-

Table A.2 Protonation constants (as log K) for NED at 25 °C and ionic strength of 0.15 M in NaCl obtained by GEP.

	HL	H ₂ L	H ₃ L	H ₄ L	Refinement		% change	R-factor	Refined Initial parameter
					Before (M)	After (M)			
Titration 1	11.06 ±0.03	10.94 ±0.02	6.58 ±0.02	2.42 ±0.02	-	-	-	0.02080	Nothing
	11.19 ±0.02	10.81 ±0.01	6.46 ±0.01	2.32 ±0.02	0.012106	0.011864	-2.00 %	0.01196	Acid
	11.207 ± 0.006	10.724 ± 0.004	6.489 ± 0.005	2.447 ± 0.005	0.009979	0.009623	-0.96 %	0.00453	Ligand
	11.198 ±0.009	10.750 ±0.006	6.458 ±0.007	2.358 ±0.008	0.050620	0.051382	+1.51 %	0.00642	Base
Titration 2	11.24 ±0.05	10.75 ±0.04	6.57 ±0.04	2.46 ±0.04	-	-	-	0.02055	Nothing
	11.38 ±0.03	10.61 ±0.02	6.45 ±0.02	2.33 ±0.02	0.014547	0.014315	-1.59 %	0.00998	Acid
	11.38 ±0.03	10.55 ±0.02	6.48 ±0.02	2.49 ±0.02	0.008000	0.007692	-3.85 %	0.01022	Ligand
	11.39 ±0.02	10.57 ±0.01	6.44 ±0.02	2.37 ±0.02	0.049840	0.050502	+1.33 %	0.00719	Base
Titration 1 and 2	11.11 ±0.03	10.89 ±0.02	6.57 ±0.02	2.43 ±0.02	-	-	-	0.02118	Nothing
	11.24 ±0.02	10.75 ±0.01	6.46 ±0.01	2.32 ±0.01	0.012106 0.014547	0.011852 0.014347	-2.10 % -1.37 %	0.01228	Acid
	11.251 ± 0.009	10.675 ± 0.007	6.488 ± 0.007	2.457 ± 0.008	0.009979 0.008000	0.009602 0.007750	-3.79 % -3.13 %	0.00790	Ligand
	11.248 ±0.009	10.698 ±0.007	6.454 ±0.007	2.361 ±0.008	0.050620 0.049840	0.051426 0.050399	+1.59 % +1.12 %	0.00787	Base
Martell & Smith (25°C) μ=0.1M	(10.9)	8.63	5.49	2.90	-	-	-	-	-

APPENDIX B

Experimental data from GEP studies of the protonation equilibria of the ligands
ALN and NED

GEP data for protonation constants of the ligand ALN from combined refinement

TASK	ZBAR	H	TITRATION		ALN:Prot.		const.								
MODL	ALNO	1	1	1	1	1	1	1							
CPLX	0	0	-13.68	H	ALNO(H	+1(-1)							
CPLX	1	0	11.03	ALNO(1)	H	+1(1)							
CPLX	1	0	21.44	ALNO(1)	H	+1(2)							
CPLX	0	0	27.57	ALNO(1)	H	+1(3)							
CPLX	1	0	29.67	ALNO(1)	H	+1(4)							
CPLX	1	0	30.95	ALNO(1)	H	+1(5)							
CONC															
VESL	IVOL	20	0	0											
VESL	H	1	0.043473	0	0										
VESL	ALNO	3	0.0098714	1											
BUR1	H	1	-0.0502	0											
ELEC															
ZERO	H	1	413.81	0											
GRAD	H	1	61.2	0											
DATA															
EMF	PH	ZBAR(H)	POINT	PA	RESID	OBS	ZBAR(M)	POINT							
OBS	OBS	CALC	RESID	OBS	CALC	RESID	OBS	CALC	RESID	OBS	CALC	RESID			
321.5	1.508	1.499	0.01	4.26	4.19	0.071	0.071	0	0	0	0	0			
321.2	1.513	1.504	0.01	4.26	4.19	0.07	0.07	0	0	0	0	0			
320.9	1.518	1.509	0.01	4.25	4.18	0.069	0.069	0	0	0	0	0			
320.6	1.523	1.514	0.009	4.24	4.18	0.068	0.069	0	0	0	0	0			
319.8	1.528	1.519	0.009	4.24	4.17	0.067	0.066	0	0	0	0	0			
320	1.533	1.524	0.009	4.23	4.17	0.066	0.067	0	0	0	0	0			
319.7	1.538	1.529	0.009	4.23	4.16	0.065	0.066	0	0	0	0	0			
319.4	1.543	1.534	0.009	4.22	4.16	0.064	0.065	0	0	0	0	0			
319.1	1.548	1.539	0.009	4.21	4.15	0.063	0.063	0	0	0	0	0			
318.8	1.552	1.544	0.009	4.21	4.15	0.062	0.062	0	0	0	0	0			
318.5	1.557	1.549	0.009	4.2	4.14	0.06	0.061	0	0	0	0	0			
318.2	1.562	1.554	0.009	4.2	4.14	0.059	0.06	0	0	0	0	0			
317.9	1.567	1.559	0.009	4.19	4.13	0.058	0.059	0	0	0	0	0			
317.6	1.572	1.564	0.008	4.18	4.13	0.057	0.057	0	0	0	0	0			
317.3	1.577	1.569	0.008	4.18	4.12	0.055	0.056	0	0	0	0	0			
317	1.582	1.574	0.008	4.17	4.12	0.054	0.054	0	0	0	0	0			
316.7	1.587	1.579	0.008	4.16	4.11	0.052	0.053	0	0	0	0	0			
316.4	1.592	1.584	0.008	4.16	4.11	0.051	0.051	0	0	0	0	0			
316.1	1.597	1.589	0.008	4.15	4.1	0.049	0.05	0	0	0	0	0			
315.8	1.601	1.594	0.007	4.14	4.1	0.048	0.048	0	0	0	0	0			
315.5	1.606	1.599	0.007	4.14	4.09	0.046	0.046	0	0	0	0	0			
315.2	1.611	1.604	0.007	4.13	4.09	0.044	0.045	0	0	0	0	0			
314.9	1.615	1.609	0.007	4.12	4.08	0.042	0.043	0	0	0	0	0			
314.6	1.621	1.615	0.006	4.12	4.08	0.04	0.041	0	0	0	0	0			
314.3	1.626	1.62	0.006	4.11	4.07	0.039	0.039	0	0	0	0	0			
313.9	1.633	1.625	0.008	4.11	4.07	0.047	0.047	0	0	0	0	0			
313.6	1.637	1.63	0.007	4.1	4.06	0.045	0.045	0	0	0	0	0			
313.3	1.642	1.635	0.007	4.1	4.06	0.042	0.043	0	0	0	0	0			
313	1.647	1.641	0.007	4.09	4.05	0.04	0.041	0	0	0	0	0			
312.7	1.652	1.646	0.006	4.08	4.04	0.038	0.039	0	0	0	0	0			
312.4	1.657	1.651	0.006	4.07	4.04	0.036	0.036	0	0	0	0	0			
312	1.664	1.656	0.007	4.06	4.03	0.043	0.043	0	0	0	0	0			
311.7	1.668	1.662	0.007	4.07	4.03	0.04	0.041	0	0	0	0	0			
311.4	1.673	1.667	0.007	4.06	4.02	0.038	0.038	0	0	0	0	0			
311.1	1.678	1.672	0.006	4.05	4.02	0.035	0.036	0	0	0	0	0			
310.8	1.683	1.677	0.006	4.05	4.01	0.033	0.033	0	0	0	0	0			
310.4	1.689	1.683	0.007	4.05	4.01	0.039	0.04	0	0	0	0	0			
310.1	1.695	1.688	0.006	4.04	4	0.036	0.037	0	0	0	0	0			
309.8	1.7	1.694	0.006	4.03	4	0.033	0.034	0	0	0	0	0			
309.5	1.704	1.699	0.005	4.02	3.99	0.03	0.031	0	0	0	0	0			
309.1	1.711	1.704	0.007	4.02	3.99	0.036	0.037	0	0	0	0	0			
308.8	1.716	1.71	0.006	4.01	3.98	0.033	0.034	0	0	0	0	0			
308.5	1.721	1.715	0.006	4	3.97	0.03	0.03	0	0	0	0	0			
308.1	1.727	1.721	0.007	4	3.97	0.035	0.036	0	0	0	0	0			
307.8	1.732	1.726	0.006	4	3.96	0.032	0.032	0	0	0	0	0			
307.5	1.737	1.732	0.005	3.99	3.96	0.028	0.029	0	0	0	0	0			
307.1	1.744	1.737	0.006	3.99	3.95	0.033	0.034	0	0	0	0	0			
306.8	1.749	1.743	0.006	3.98	3.95	0.03	0.03	0	0	0	0	0			
306.5	1.753	1.748	0.005	3.97	3.94	0.026	0.026	0	0	0	0	0			
306.2	1.758	1.754	0.004	3.96	3.94	0.022	0.023	0	0	0	0	0			
305.8	1.765	1.76	0.005	3.96	3.93	0.027	0.027	0	0	0	0	0			
305.5	1.77	1.765	0.005	3.95	3.92	0.023	0.023	0	0	0	0	0			
305.1	1.776	1.771	0.005	3.95	3.92	0.027	0.027	0	0	0	0	0			
304.8	1.781	1.777	0.005	3.94	3.91	0.023	0.023	0	0	0	0	0			
304.5	1.786	1.782	0.004	3.93	3.91	0.018	0.019	0	0	0	0	0			
304.1	1.793	1.788	0.005	3.92	3.9	0.022	0.022	0	0	0	0	0			
303.8	1.798	1.794	0.004	3.91	3.9	0.018	0.018	0	0	0	0	0			
303.4	1.804	1.8	0.004	3.91	3.89	0.021	0.021	0	0	0	0	0			
303	1.811	1.805	0.005	3.91	3.88	0.024	0.025	0	0	0	0	0			
302.7	1.816	1.811	0.004	3.9	3.88	0.019	0.02	0	0	0	0	0			
302.3	1.822	1.817	0.005	3.89	3.87	0.022	0.023	0	0	0	0	0			
302	1.827	1.823	0.004	3.88	3.87	0.017	0.018	0	0	0	0	0			
301.6	1.833	1.829	0.004	3.88	3.86	0.02	0.02	0	0	0	0	0			
301.2	1.84	1.835	0.005	3.88	3.85	0.022	0.023	0	0	0	0	0			
300.9	1.845	1.841	0.004	3.87	3.85	0.017	0.017	0	0	0	0	0			
300.5	1.851	1.847	0.004	3.86	3.84	0.019	0.019	0	0	0	0	0			
300.1	1.858	1.853	0.005	3.86	3.84	0.021	0.021	0	0	0	0	0			
299.8	1.863	1.859	0.004	3.85	3.83	0.015	0.016	0	0	0	0	0			
299.4	1.869	1.865	0.004	3.84	3.82	0.017	0.017	0	0	0	0	0			
299	1.876	1.872	0.004	3.84	3.82	0.018	0.019	0	0	0	0	0			
298.6	1.883	1.878	0.005	3.83	3.81	0.019	0.02	0	0	0	0	0			
298.2	1.889	1.884	0.005	3.83	3.81	0.02	0.021	0	0	0	0	0			
297.9	1.894	1.89	0.003	3.81	3.8	0.014	0.015	0	0	0	0	0			
297.5	1.9	1.897	0.004	3.81	3.79	0.015	0.015	0	0	0	0	0			
297.1	1.907	1.903	0.004	3.8	3.79	0.015	0.016	0	0	0	0	0			
296.7	1.914	1.91	0.004	3.8	3.78	0.016	0.016	0	0	0	0	0			
296.3	1.92	1.916	0.004	3.79	3.78	0.016	0.016	0	0	0	0	0			
295.9	1.927	1.923	0.004	3.78	3.77	0.016	0.016	0	0	0	0	0			
295.5	1.933	1.929	0.004	3.78	3.76	0.015	0.016	0	0	0	0	0			
295.1	1.94	1.936	0.004	3.77	3.76	0.015	0.016	0	0	0	0	0			
294.7	1.946	1.942	0.004	3.76	3.75	0.015	0.015	0	0	0	0	0			
294.3	1.953	1.949	0.004	3.76	3.74	0.014	0.014	0	0	0	0	0			
293.9	1.959	1.956	0.004	3.75	3.74	0.013	0.013	0	0	0	0	0			
293.5	1.966	1.963	0.003	3.74	3.73	0.012	0.012	0	0	0	0	0			
293.1	1.972	1.969	0.003	3.74	3.72	0.011	0.011	0	0	0	0	0			
292.6	1.981	1.976	0.004	3.73	3.72	0.015	0.016	0	0	0	0	0			
292.2	1.987	1.983	0.004	3.72	3.71	0.013	0.014	0	0	0	0	0			
291.8	1.994	1.99	0.003	3.72	3.7	0.012	0.012	0	0	0	0	0			
291.4	2	1.997	0.003	3.71	3.7	0.01	0.01	0	0	0	0	0			
290.9	2.008	2.004	0.004	3.7	3.69	0.013	0.014	0	0	0	0	0			
290.5	2.015	2.012	0.003	3.7	3.69	0.011	0.011	0	0	0	0	0			
290	2.023	2.019	0.004	3.69	3.68	0.014	0.015	0	0	0	0	0			
289.6	2.03	2.026	0.004	3.68	3.67	0.011	0.012	0	0	0	0	0			
289.1	2.038	2.033	0.004	3.68	3.66	0.014	0.014	0	0	0	0	0			
288.7	2.044	2.041	0.003	3.67	3.66	0.011	0.011	0	0	0	0	0			
288.2	2.052	2.048	0.004	3.66	3.65	0.013	0.013	0	0	0	0	0			
287.7	2.061	2.056	0.005	3.66	3.64	0.014	0.015	0	0	0	0	0			
287.3	2.067	2.063	0												

279.6	2.193	2.188	0.005	3.54	3.53	0.012	0.013	0	0	0	0	0	0	0
279.1	2.201	2.197	0.004	3.53	3.52	0.009	0.01	0	0	0	0	0	0	0
278.5	2.211	2.206	0.005	3.53	3.52	0.011	0.011	0	0	0	0	0	0	0
277.9	2.216	2.212	0.005	3.52	3.51	0.012	0.012	0	0	0	0	0	0	0
277.3	2.221	2.225	0.005	3.51	3.5	0.012	0.013	0	0	0	0	0	0	0
276.7	2.24	2.235	0.006	3.51	3.49	0.012	0.013	0	0	0	0	0	0	0
276.1	2.25	2.244	0.006	3.5	3.49	0.012	0.013	0	0	0	0	0	0	0
275.5	2.26	2.254	0.006	3.49	3.48	0.012	0.013	0	0	0	0	0	0	0
274.9	2.27	2.264	0.005	3.48	3.47	0.011	0.012	0	0	0	0	0	0	0
274.3	2.28	2.275	0.005	3.47	3.46	0.01	0.011	0	0	0	0	0	0	0
273.6	2.291	2.285	0.006	3.47	3.46	0.012	0.013	0	0	0	0	0	0	0
273	2.301	2.295	0.005	3.46	3.45	0.01	0.012	0	0	0	0	0	0	0
272.3	2.312	2.306	0.006	3.45	3.44	0.012	0.013	0	0	0	0	0	0	0
271.7	2.322	2.317	0.005	3.44	3.43	0.009	0.011	0	0	0	0	0	0	0
271	2.333	2.328	0.006	3.43	3.42	0.01	0.011	0	0	0	0	0	0	0
270.3	2.345	2.339	0.006	3.43	3.42	0.01	0.012	0	0	0	0	0	0	0
269.6	2.356	2.351	0.006	3.42	3.41	0.01	0.011	0	0	0	0	0	0	0
268.9	2.368	2.362	0.006	3.41	3.4	0.009	0.011	0	0	0	0	0	0	0
268.2	2.379	2.374	0.005	3.4	3.39	0.008	0.01	0	0	0	0	0	0	0
267.4	2.392	2.386	0.006	3.39	3.38	0.01	0.011	0	0	0	0	0	0	0
266.7	2.404	2.399	0.005	3.38	3.38	0.008	0.01	0	0	0	0	0	0	0
265.9	2.417	2.411	0.006	3.38	3.37	0.009	0.01	0	0	0	0	0	0	0
265.1	2.43	2.424	0.006	3.37	3.36	0.009	0.01	0	0	0	0	0	0	0
264.3	2.443	2.437	0.006	3.36	3.35	0.008	0.01	0	0	0	0	0	0	0
263.5	2.456	2.451	0.005	3.35	3.34	0.008	0.009	0	0	0	0	0	0	0
262.6	2.471	2.464	0.006	3.34	3.33	0.009	0.011	0	0	0	0	0	0	0
261.7	2.485	2.479	0.007	3.34	3.33	0.009	0.012	0	0	0	0	0	0	0
260.9	2.499	2.493	0.006	3.32	3.32	0.007	0.009	0	0	0	0	0	0	0
259.9	2.515	2.508	0.007	3.32	3.31	0.009	0.011	0	0	0	0	0	0	0
259	2.53	2.523	0.007	3.31	3.3	0.008	0.01	0	0	0	0	0	0	0
258.1	2.544	2.538	0.006	3.3	3.29	0.007	0.009	0	0	0	0	0	0	0
257.1	2.561	2.555	0.006	3.29	3.28	0.007	0.009	0	0	0	0	0	0	0
256	2.579	2.571	0.008	3.28	3.27	0.008	0.011	0	0	0	0	0	0	0
255	2.595	2.588	0.007	3.27	3.27	0.007	0.01	0	0	0	0	0	0	0
254.9	2.613	2.606	0.007	3.26	3.26	0.007	0.01	0	0	0	0	0	0	0
254.2	2.631	2.624	0.007	3.25	3.25	0.007	0.01	0	0	0	0	0	0	0
251.6	2.65	2.643	0.008	3.25	3.24	0.007	0.011	0	0	0	0	0	0	0
250.5	2.668	2.662	0.006	3.24	3.23	0.005	0.008	0	0	0	0	0	0	0
249.2	2.69	2.682	0.007	3.23	3.22	0.006	0.009	0	0	0	0	0	0	0
247.9	2.711	2.703	0.007	3.22	3.21	0.006	0.01	0	0	0	0	0	0	0
246.6	2.732	2.725	0.007	3.21	3.2	0.005	0.009	0	0	0	0	0	0	0
245.2	2.755	2.748	0.007	3.2	3.19	0.005	0.008	0	0	0	0	0	0	0
243.7	2.78	2.772	0.007	3.19	3.19	0.005	0.009	0	0	0	0	0	0	0
242.2	2.804	2.797	0.007	3.18	3.18	0.004	0.008	0	0	0	0	0	0	0
240.6	2.824	2.816	0.006	3.17	3.17	0.004	0.008	0	0	0	0	0	0	0
238.9	2.858	2.852	0.006	3.16	3.16	0.004	0.007	0	0	0	0	0	0	0
237.1	2.887	2.881	0.006	3.15	3.15	0.003	0.007	0	0	0	0	0	0	0
235.1	2.92	2.913	0.008	3.14	3.14	0.004	0.008	0	0	0	0	0	0	0
233.1	2.953	2.946	0.007	3.13	3.13	0.003	0.007	0	0	0	0	0	0	0
230.9	2.989	2.982	0.007	3.12	3.12	0.003	0.007	0	0	0	0	0	0	0
228.5	3.028	3.021	0.007	3.11	3.11	0.003	0.008	0	0	0	0	0	0	0
225.9	3.07	3.063	0.007	3.1	3.1	0.003	0.008	0	0	0	0	0	0	0
223	3.118	3.11	0.008	3.09	3.09	0.003	0.009	0	0	0	0	0	0	0
218.8	3.17	3.161	0.009	3.08	3.08	0.003	0.009	0	0	0	0	0	0	0
216.3	3.227	3.219	0.008	3.07	3.07	0.002	0.009	0	0	0	0	0	0	0
212.4	3.291	3.285	0.006	3.06	3.06	0.001	0.007	0	0	0	0	0	0	0
207.7	3.368	3.361	0.006	3.05	3.05	0.001	0.007	0	0	0	0	0	0	0
202.1	3.459	3.453	0.006	3.04	3.04	0.001	0.006	0	0	0	0	0	0	0
195.2	3.572	3.567	0.005	3.03	3.03	0.001	0.005	0	0	0	0	0	0	0
186	3.722	3.717	0.005	3.02	3.02	0	0.005	0	0	0	0	0	0	0
172.8	3.938	3.93	0.008	3.01	3.01	0	0.008	0	0	0	0	0	0	0
152.9	4.263	4.244	0.019	2.99	2.99	0	0.019	0	0	0	0	0	0	0
130.9	4.623	4.595	0.028	2.98	2.97	0	0.028	0	0	0	0	0	0	0
115.2	4.879	4.853	0.026	2.95	2.95	0	0.026	0	0	0	0	0	0	0
104.4	5.056	5.033	0.022	2.93	2.93	0	0.022	0	0	0	0	0	0	0
96.3	5.188	5.17	0.018	2.9	2.9	0	0.018	0	0	0	0	0	0	0
89.8	5.294	5.28	0.014	2.88	2.88	0	0.014	0	0	0	0	0	0	0
84.2	5.386	5.373	0.013	2.85	2.85	0	0.013	0	0	0	0	0	0	0
79.4	5.464	5.454	0.011	2.83	2.83	0	0.011	0	0	0	0	0	0	0
75.1	5.534	5.526	0.008	2.8	2.8	0	0.008	0	0	0	0	0	0	0
71.2	5.598	5.592	0.006	2.78	2.78	0	0.006	0	0	0	0	0	0	0
67.6	5.657	5.653	0.004	2.75	2.75	0	0.004	0	0	0	0	0	0	0
64.2	5.713	5.709	0.003	2.72	2.72	0	0.003	0	0	0	0	0	0	0
61	5.765	5.763	0.002	2.7	2.7	0	0.002	0	0	0	0	0	0	0
57.9	5.816	5.814	0.001	2.67	2.67	0	0.001	0	0	0	0	0	0	0
55	5.863	5.864	-0.001	2.65	2.65	0	0.001	0	0	0	0	0	0	0
52.1	5.911	5.911	-0.001	2.62	2.62	0	0.001	0	0	0	0	0	0	0
49.4	5.954	5.958	-0.003	2.6	2.6	0	0.003	0	0	0	0	0	0	0
46.7	5.999	6.003	-0.005	2.57	2.57	0	0.005	0	0	0	0	0	0	0
44	6.043	6.048	-0.005	2.55	2.55	0	0.005	0	0	0	0	0	0	0
41.3	6.087	6.092	-0.005	2.52	2.52	0	0.005	0	0	0	0	0	0	0
38.7	6.129	6.136	-0.007	2.5	2.5	0	0.007	0	0	0	0	0	0	0
36	6.173	6.181	-0.007	2.47	2.47	0	0.007	0	0	0	0	0	0	0
33.4	6.216	6.225	-0.009	2.45	2.45	0	0.009	0	0	0	0	0	0	0
30.7	6.26	6.27	-0.01	2.42	2.42	0	0.01	0	0	0	0	0	0	0
28	6.304	6.316	-0.012	2.39	2.39	0	0.012	0	0	0	0	0	0	0
25.2	6.35	6.362	-0.012	2.37	2.37	0	0.012	0	0	0	0	0	0	0
22.3	6.397	6.41	-0.013	2.34	2.34	0	0.013	0	0	0	0	0	0	0
19.3	6.446	6.46	-0.014	2.32	2.32	0	0.014	0	0	0	0	0	0	0
16.1	6.499	6.512	-0.014	2.29	2.29	0	0.014	0	0	0	0	0	0	0
12.9	6.551	6.567	-0.016	2.27	2.27	0	0.016	0	0	0	0	0	0	0
9.3	6.61	6.625	-0.015	2.24	2.24	0	0.015	0	0	0	0	0	0	0
5.5	6.672	6.687	-0.016	2.22	2.22	0	0.016	0	0	0	0	0	0	0
1.4	6.739	6.755	-0.017	2.19	2.19	0	0.017	0	0	0	0	0	0	0
-3.2	6.814	6.83	-0.018	2.17	2.17	0	0.018	0	0	0	0	0	0	0
-8.4	6.899	6.915	-0.016	2.14	2.14	0	0.016	0	0	0	0	0	0	0
-14.4	6.997	7.014	-0.017	2.12	2.12	0	0.017	0	0	0	0	0	0	0
-21.8	7.118	7.133	-0.016	2.09	2.09	0	0.016	0	0	0	0	0	0	0
-31.4	7.275	7.287	-0.013	2.06	2.06	0	0.013	0	0	0	0	0	0	0
-45.3	7.502	7.508	-0.006	2.04	2.04	0	0.006	0	0	0	0	0	0	0

293.3	1.943	1.952	-0.009	3.7	3.74	-0.041	0.042	0	0	0	0	0	0	0	0
292.9	1.95	1.959	-0.009	3.69	3.73	-0.042	0.043	0	0	0	0	0	0	0	0
292.5	1.956	1.966	-0.01	3.68	3.73	-0.044	0.045	0	0	0	0	0	0	0	0
292.1	1.963	1.973	-0.01	3.67	3.72	-0.046	0.047	0	0	0	0	0	0	0	0
291.6	1.971	1.98	-0.009	3.67	3.71	-0.041	0.042	0	0	0	0	0	0	0	0
291.2	1.978	1.987	-0.01	3.66	3.71	-0.043	0.044	0	0	0	0	0	0	0	0
290.8	1.984	1.995	-0.01	3.66	3.7	-0.046	0.047	0	0	0	0	0	0	0	0
290.3	1.992	2.002	-0.01	3.65	3.69	-0.041	0.042	0	0	0	0	0	0	0	0
289.9	1.999	2.009	-0.01	3.64	3.69	-0.044	0.046	0	0	0	0	0	0	0	0
289.4	2.007	2.017	-0.01	3.64	3.68	-0.041	0.042	0	0	0	0	0	0	0	0
288.9	2.015	2.024	-0.009	3.64	3.67	-0.037	0.038	0	0	0	0	0	0	0	0
288.5	2.022	2.032	-0.01	3.63	3.67	-0.041	0.042	0	0	0	0	0	0	0	0
288	2.04	2.04	-0.01	3.62	3.64	-0.039	0.04	0	0	0	0	0	0	0	0
287.5	2.038	2.048	-0.009	3.62	3.65	-0.036	0.037	0	0	0	0	0	0	0	0
287.1	2.045	2.055	-0.01	3.6	3.65	-0.041	0.042	0	0	0	0	0	0	0	0
286.6	2.053	2.063	-0.01	3.6	3.64	-0.039	0.04	0	0	0	0	0	0	0	0
286.1	2.061	2.071	-0.01	3.59	3.63	-0.038	0.039	0	0	0	0	0	0	0	0
285.6	2.07	2.079	-0.01	3.59	3.62	-0.037	0.038	0	0	0	0	0	0	0	0
285.1	2.078	2.088	-0.01	3.58	3.62	-0.036	0.038	0	0	0	0	0	0	0	0
284.6	2.086	2.096	-0.01	3.57	3.61	-0.036	0.037	0	0	0	0	0	0	0	0
284	2.096	2.104	-0.009	3.57	3.6	-0.03	0.031	0	0	0	0	0	0	0	0
283.5	2.104	2.113	-0.009	3.56	3.59	-0.031	0.032	0	0	0	0	0	0	0	0
283	2.112	2.121	-0.009	3.56	3.59	-0.031	0.033	0	0	0	0	0	0	0	0
282.5	2.12	2.13	-0.01	3.55	3.58	-0.032	0.034	0	0	0	0	0	0	0	0
281.9	2.13	2.139	-0.009	3.54	3.57	-0.028	0.03	0	0	0	0	0	0	0	0
281.4	2.138	2.148	-0.009	3.53	3.56	-0.03	0.031	0	0	0	0	0	0	0	0
280.8	2.148	2.157	-0.008	3.53	3.56	-0.027	0.028	0	0	0	0	0	0	0	0
280.3	2.156	2.166	-0.009	3.52	3.55	-0.029	0.031	0	0	0	0	0	0	0	0
279.7	2.166	2.175	-0.009	3.51	3.54	-0.027	0.028	0	0	0	0	0	0	0	0
279.1	2.176	2.184	-0.008	3.51	3.53	-0.025	0.026	0	0	0	0	0	0	0	0
278.6	2.184	2.194	-0.009	3.5	3.53	-0.028	0.03	0	0	0	0	0	0	0	0
278	2.194	2.203	-0.009	3.49	3.52	-0.027	0.029	0	0	0	0	0	0	0	0
277.4	2.204	2.213	-0.009	3.48	3.51	-0.026	0.028	0	0	0	0	0	0	0	0
276.8	2.214	2.223	-0.009	3.48	3.5	-0.026	0.028	0	0	0	0	0	0	0	0
276.2	2.224	2.233	-0.009	3.47	3.49	-0.026	0.028	0	0	0	0	0	0	0	0
275.6	2.233	2.243	-0.01	3.46	3.49	-0.027	0.028	0	0	0	0	0	0	0	0
274.9	2.245	2.254	-0.009	3.46	3.48	-0.023	0.025	0	0	0	0	0	0	0	0
274.3	2.255	2.264	-0.009	3.45	3.47	-0.024	0.026	0	0	0	0	0	0	0	0
273.6	2.266	2.275	-0.009	3.44	3.46	-0.022	0.024	0	0	0	0	0	0	0	0
273	2.276	2.286	-0.01	3.43	3.45	-0.024	0.026	0	0	0	0	0	0	0	0
272.3	2.288	2.297	-0.009	3.42	3.45	-0.023	0.025	0	0	0	0	0	0	0	0
271.6	2.299	2.308	-0.009	3.42	3.44	-0.022	0.024	0	0	0	0	0	0	0	0
270.9	2.31	2.32	-0.009	3.41	3.43	-0.021	0.023	0	0	0	0	0	0	0	0
270.2	2.322	2.331	-0.009	3.4	3.42	-0.021	0.023	0	0	0	0	0	0	0	0
269.4	2.335	2.343	-0.008	3.39	3.41	-0.018	0.02	0	0	0	0	0	0	0	0
268.7	2.347	2.356	-0.009	3.39	3.4	-0.019	0.021	0	0	0	0	0	0	0	0
267.9	2.36	2.368	-0.008	3.38	3.4	-0.017	0.019	0	0	0	0	0	0	0	0
267.2	2.371	2.381	-0.01	3.37	3.39	-0.019	0.022	0	0	0	0	0	0	0	0
266.4	2.384	2.394	-0.009	3.36	3.38	-0.019	0.021	0	0	0	0	0	0	0	0
265.5	2.399	2.407	-0.008	3.36	3.37	-0.015	0.017	0	0	0	0	0	0	0	0
264.7	2.412	2.42	-0.008	3.35	3.36	-0.016	0.018	0	0	0	0	0	0	0	0
263.9	2.425	2.434	-0.009	3.34	3.35	-0.017	0.019	0	0	0	0	0	0	0	0
263	2.44	2.449	-0.009	3.33	3.34	-0.015	0.017	0	0	0	0	0	0	0	0
262.1	2.455	2.463	-0.008	3.32	3.34	-0.014	0.017	0	0	0	0	0	0	0	0
261.2	2.47	2.478	-0.009	3.31	3.33	-0.014	0.017	0	0	0	0	0	0	0	0
260.3	2.484	2.494	-0.009	3.3	3.32	-0.015	0.018	0	0	0	0	0	0	0	0
259.3	2.501	2.509	-0.009	3.29	3.31	-0.014	0.016	0	0	0	0	0	0	0	0
258.3	2.517	2.526	-0.009	3.29	3.3	-0.013	0.015	0	0	0	0	0	0	0	0
257.3	2.533	2.542	-0.009	3.28	3.29	-0.013	0.016	0	0	0	0	0	0	0	0
256.2	2.551	2.56	-0.008	3.27	3.28	-0.011	0.014	0	0	0	0	0	0	0	0
255.1	2.57	2.578	-0.008	3.26	3.27	-0.011	0.013	0	0	0	0	0	0	0	0
254	2.588	2.596	-0.008	3.25	3.26	-0.011	0.014	0	0	0	0	0	0	0	0
252.8	2.607	2.615	-0.008	3.24	3.25	-0.01	0.013	0	0	0	0	0	0	0	0
251.6	2.627	2.635	-0.008	3.23	3.24	-0.01	0.013	0	0	0	0	0	0	0	0
250.4	2.647	2.656	-0.009	3.22	3.23	-0.01	0.014	0	0	0	0	0	0	0	0
249.1	2.668	2.677	-0.009	3.21	3.22	-0.01	0.013	0	0	0	0	0	0	0	0
247.7	2.691	2.699	-0.009	3.21	3.21	-0.009	0.012	0	0	0	0	0	0	0	0
246.3	2.714	2.723	-0.009	3.2	3.2	-0.009	0.013	0	0	0	0	0	0	0	0
244.8	2.738	2.747	-0.009	3.19	3.19	-0.008	0.012	0	0	0	0	0	0	0	0
243.2	2.765	2.773	-0.008	3.18	3.18	-0.007	0.011	0	0	0	0	0	0	0	0
241.6	2.791	2.8	-0.009	3.17	3.18	-0.008	0.012	0	0	0	0	0	0	0	0
239.9	2.819	2.829	-0.01	3.16	3.17	-0.008	0.013	0	0	0	0	0	0	0	0
238	2.85	2.859	-0.009	3.15	3.15	-0.007	0.012	0	0	0	0	0	0	0	0
236	2.883	2.892	-0.009	3.14	3.14	-0.006	0.011	0	0	0	0	0	0	0	0
233.9	2.917	2.926	-0.009	3.13	3.13	-0.006	0.011	0	0	0	0	0	0	0	0
231.6	2.955	2.964	-0.009	3.12	3.12	-0.005	0.01	0	0	0	0	0	0	0	0
229.2	2.994	3.004	-0.01	3.11	3.11	-0.005	0.012	0	0	0	0	0	0	0	0
226.5	3.038	3.049	-0.01	3.1	3.1	-0.005	0.011	0	0	0	0	0	0	0	0
223.4	3.089	3.098	-0.008	3.09	3.09	-0.004	0.009	0	0	0	0	0	0	0	0
220.1	3.143	3.152	-0.009	3.08	3.08	-0.003	0.009	0	0	0	0	0	0	0	0
216.3	3.206	3.214	-0.008	3.07	3.07	-0.003	0.009	0	0	0	0	0	0	0	0
212	3.276	3.285	-0.009	3.06	3.06	-0.003	0.009	0	0	0	0	0	0	0	0
206.9	3.36	3.369	-0.009	3.05	3.05	-0.002	0.01	0	0	0	0	0	0	0	0
200.6	3.463	3.472	-0.009	3.04	3.04	-0.002	0.009	0	0	0	0	0	0	0	0
192.5	3.596	3.604	-0.008	3.03	3.03	-0.001	0.008	0	0	0	0	0	0	0	0
181.3	3.779	3.787	-0.007	3.02	3.02	-0.001	0.007	0	0	0	0	0	0	0	0
163.7	4.068	4.067	0	3	3	0	0	0	0	0	0	0	0	0	0
137.8	4.492	4.475	0.017	2.98	2.98	0	0.017	0	0	0	0	0	0	0	0
116.5	4.842	4.822	0.02	2.96	2.96	0	0.02	0	0	0	0	0	0	0	0
103	5.063	5.048	0.015	2.92	2.92	0	0.015	0	0	0	0	0	0	0	0
83.3	5.21	5.222	0.012	2.89	2.89	0	0.012	0	0	0	0	0	0	0	0
85.8	5.345	5.336	0.009	2.86	2.86	0	0.009	0	0	0	0	0	0	0	0
79.5	5.448	5.441	0.007	2.83	2.83	0	0.007	0	0	0	0	0	0	0	0
74.1	5.537	5.532	0.005	2.8	2.8	0	0.005	0	0	0	0	0	0	0	0
69.3	5.615	5.613	0.002	2.7											

52.8	5.963	5.963	0	2.77	2.77	0	0	0	0	0	0	0	0	0
50.9	5.994	5.994	0	2.76	2.76	0	0	0	0	0	0	0	0	0
49.1	6.024	6.025	-0.001	2.75	2.75	0	0.001	0	0	0	0	0	0	0
47.4	6.052	6.054	-0.002	2.73	2.73	0	0	0	0	0	0	0	0	0
45.7	6.079	6.083	-0.004	2.72	2.72	0	0.004	0	0	0	0	0	0	0
44.1	6.106	6.111	-0.005	2.71	2.71	0	0.005	0	0	0	0	0	0	0
42.5	6.132	6.138	-0.006	2.69	2.69	0	0.006	0	0	0	0	0	0	0
40.9	6.158	6.165	-0.006	2.68	2.68	0	0.006	0	0	0	0	0	0	0
39.4	6.183	6.191	-0.008	2.67	2.67	0	0.008	0	0	0	0	0	0	0
37.9	6.207	6.216	-0.009	2.65	2.65	0	0.009	0	0	0	0	0	0	0
36.4	6.232	6.241	-0.009	2.64	2.64	0	0.009	0	0	0	0	0	0	0
34.9	6.256	6.266	-0.009	2.63	2.63	0	0.009	0	0	0	0	0	0	0
33.5	6.279	6.29	-0.011	2.61	2.61	0	0.011	0	0	0	0	0	0	0
32.1	6.302	6.314	-0.011	2.6	2.6	0	0.011	0	0	0	0	0	0	0
30.7	6.325	6.337	-0.012	2.59	2.59	0	0.012	0	0	0	0	0	0	0
29.3	6.348	6.361	-0.013	2.57	2.57	0	0.013	0	0	0	0	0	0	0
27.9	6.371	6.384	-0.013	2.56	2.56	0	0.013	0	0	0	0	0	0	0
26.5	6.394	6.407	-0.013	2.55	2.55	0	0.013	0	0	0	0	0	0	0
25.2	6.415	6.43	-0.015	2.53	2.53	0	0.015	0	0	0	0	0	0	0
23.8	6.438	6.453	-0.015	2.52	2.52	0	0.015	0	0	0	0	0	0	0
22.4	6.461	6.476	-0.015	2.51	2.51	0	0.015	0	0	0	0	0	0	0
21	6.484	6.499	-0.015	2.49	2.49	0	0.015	0	0	0	0	0	0	0
19.7	6.506	6.522	-0.016	2.48	2.48	0	0.016	0	0	0	0	0	0	0
18.3	6.529	6.545	-0.016	2.47	2.47	0	0.016	0	0	0	0	0	0	0
16.9	6.552	6.568	-0.016	2.46	2.46	0	0.016	0	0	0	0	0	0	0
15.6	6.573	6.591	-0.018	2.44	2.44	0	0.018	0	0	0	0	0	0	0
14.2	6.596	6.614	-0.019	2.43	2.43	0	0.019	0	0	0	0	0	0	0
12.8	6.619	6.638	-0.019	2.42	2.42	0	0.019	0	0	0	0	0	0	0
11.4	6.642	6.661	-0.02	2.4	2.4	0	0.02	0	0	0	0	0	0	0
9.9	6.666	6.685	-0.019	2.39	2.39	0	0.019	0	0	0	0	0	0	0
8.5	6.689	6.71	-0.02	2.38	2.38	0	0.02	0	0	0	0	0	0	0
7	6.714	6.734	-0.02	2.36	2.36	0	0.02	0	0	0	0	0	0	0
5.5	6.738	6.759	-0.021	2.35	2.35	0	0.021	0	0	0	0	0	0	0
4	6.763	6.784	-0.021	2.34	2.34	0	0.021	0	0	0	0	0	0	0
2.4	6.789	6.81	-0.021	2.32	2.32	0	0.021	0	0	0	0	0	0	0
0.8	6.815	6.837	-0.021	2.31	2.31	0	0.021	0	0	0	0	0	0	0
-0.8	6.842	6.864	-0.022	2.3	2.3	0	0.022	0	0	0	0	0	0	0
-2.4	6.868	6.891	-0.023	2.28	2.28	0	0.023	0	0	0	0	0	0	0
-4.1	6.896	6.92	-0.024	2.27	2.27	0	0.024	0	0	0	0	0	0	0
-5.9	6.925	6.949	-0.024	2.26	2.26	0	0.024	0	0	0	0	0	0	0
-7.7	6.955	6.98	-0.025	2.24	2.24	0	0.025	0	0	0	0	0	0	0
-9.6	6.986	7.011	-0.025	2.23	2.23	0	0.025	0	0	0	0	0	0	0
-11.6	7.019	7.044	-0.025	2.22	2.22	0	0.025	0	0	0	0	0	0	0
-13.7	7.053	7.078	-0.025	2.2	2.2	0	0.025	0	0	0	0	0	0	0
-15.9	7.089	7.114	-0.025	2.19	2.19	0	0.025	0	0	0	0	0	0	0
-18.2	7.127	7.152	-0.025	2.18	2.18	0	0.025	0	0	0	0	0	0	0
-20.6	7.166	7.192	-0.026	2.17	2.17	0	0.026	0	0	0	0	0	0	0
-23.2	7.209	7.235	-0.026	2.15	2.15	0	0.026	0	0	0	0	0	0	0
-26	7.255	7.28	-0.025	2.14	2.14	0	0.025	0	0	0	0	0	0	0
-29	7.304	7.33	-0.026	2.13	2.13	0	0.026	0	0	0	0	0	0	0
-32.3	7.358	7.384	-0.026	2.11	2.11	0	0.026	0	0	0	0	0	0	0
-36	7.419	7.443	-0.025	2.1	2.1	0	0.025	0	0	0	0	0	0	0
-40.1	7.486	7.51	-0.024	2.09	2.09	0	0.024	0	0	0	0	0	0	0
-44.9	7.565	7.587	-0.022	2.07	2.07	0	0.022	0	0	0	0	0	0	0
-50.5	7.656	7.676	-0.02	2.06	2.06	0	0.02	0	0	0	0	0	0	0
-57.2	7.766	7.784	-0.018	2.05	2.05	0	0.018	0	0	0	0	0	0	0
-65.9	7.909	7.921	-0.012	2.03	2.03	0	0.012	0	0	0	0	0	0	0
-77.5	8.099	8.105	-0.005	2.02	2.02	0	0.005	0	0	0	0	0	0	0
-93.7	8.365	8.363	0.002	2.01	2.01	0	0.002	0	0	0	0	0	0	0
-112.5	8.673	8.678	-0.005	2	2	0	0.005	0	0	0	0	0	0	0
-127.8	8.924	8.94	-0.017	1.98	1.98	0	0.017	0	0	0	0	0	0	0
-138.9	9.106	9.125	-0.019	1.97	1.97	0	0.019	0	0	0	0	0	0	0
-147.3	9.243	9.263	-0.016	1.96	1.96	0	0.016	0	0	0	0	0	0	0
-153.9	9.352	9.365	-0.013	1.95	1.95	0	0.013	0	0	0	0	0	0	0
-159.4	9.442	9.45	-0.008	1.94	1.94	0	0.008	0	0	0	0	0	0	0
-164.1	9.519	9.522	-0.003	1.93	1.93	0	0.003	0	0	0	0	0	0	0
-168.2	9.586	9.584	0.002	1.91	1.91	0	0.002	0	0	0	0	0	0	0
-171.8	9.645	9.638	0.007	1.9	1.9	0	0.007	0	0	0	0	0	0	0
-175.1	9.699	9.687	0.012	1.89	1.89	0	0.012	0	0	0	0	0	0	0
-177.9	9.745	9.731	0.014	1.88	1.88	0.001	0.014	0	0	0	0	0	0	0
-180.4	9.786	9.771	0.015	1.87	1.87	0.001	0.015	0	0	0	0	0	0	0
-182.7	9.824	9.807	0.016	1.86	1.86	0.001	0.016	0	0	0	0	0	0	0
-184.9	9.86	9.841	0.018	1.85	1.84	0.001	0.018	0	0	0	0	0	0	0
-186.9	9.893	9.873	0.019	1.83	1.83	0.001	0.019	0	0	0	0	0	0	0
-188.8	9.924	9.903	0.021	1.82	1.82	0.001	0.021	0	0	0	0	0	0	0
-190.6	9.953	9.931	0.022	1.81	1.81	0.001	0.022	0	0	0	0	0	0	0
-192.3	9.981	9.957	0.024	1.8	1.8	0.002	0.024	0	0	0	0	0	0	0
-193.9	10.007	9.982	0.025	1.79	1.79	0.002	0.025	0	0	0	0	0	0	0
-195.4	10.032	10.006	0.026	1.78	1.78	0.002	0.026	0	0	0	0	0	0	0
-196.8	10.055	10.029	0.026	1.77	1.76	0.002	0.026	0	0	0	0	0	0	0
-198.2	10.078	10.05	0.028	1.76	1.75	0.002	0.028	0	0	0	0	0	0	0
-199.5	10.099	10.071	0.028	1.74	1.74	0.003	0.028	0	0	0	0	0	0	0
-200.7	10.119	10.091	0.028	1.73	1.73	0.003	0.028	0	0	0	0	0	0	0
-201.9	10.138	10.11	0.029	1.72	1.72	0.003	0.029	0	0	0	0	0	0	0
-203.1	10.158	10.128	0.03	1.71	1.71	0.003	0.03	0	0	0	0	0	0	0
-204.2	10.176	10.146	0.03	1.7	1.7	0.003	0.03	0	0	0	0	0	0	0
-205.3	10.194	10.163	0.031	1.69	1.69	0.003	0.031	0	0	0	0	0	0	0
-206.3	10.211	10.18	0.031	1.68	1.67	0.004	0.031	0	0	0	0	0	0	0
-207.3	10.227	10.196	0.031	1.67	1.66	0.004	0.031	0	0	0	0	0	0	0
-208.3	10.243	10.212	0.032	1.66	1.65	0.004	0.032	0	0	0	0	0	0	0
-209.3	10.26	10.227	0.033	1.64	1.64	0.004	0.033	0	0	0	0	0	0	0
-210.2	10.275	10.242	0.033	1.63	1.63	0.005	0.033	0	0	0	0	0	0	0
-211.1	10.289	10.256	0.033	1.62	1.62	0.005	0.034	0	0	0	0	0	0	0
-212	10.304	10.27	0.034	1.61	1.61	0.005	0.034	0	0	0	0	0	0	0
-212.8	10.317	10.284	0.033	1.6	1.6	0.005	0.034	0	0	0	0	0	0	0
-213.6	10.33	10.297	0.033	1.59	1.59	0.005	0.034	0	0	0	0	0	0	0
-214.4	10.343	10.31	0.033	1.58	1.57	0.005	0.034	0	0	0	0	0	0	0
-215.2	10.356	10.323	0.034	1.57	1.56	0.006	0.034	0	0	0	0	0	0	0
-216	10.37	10.335	0.034	1.56	1.55	0.006	0.035	0	0	0	0	0	0	0
-216.8	10.383	10.348	0.035	1.55	1.54	0.006	0.036	0	0	0	0	0	0	0
-217.5	10.394	10.36	0.035	1.54	1.53	0.006	0.036	0	0	0	0	0		

APPENDIX C

Experimental data from GEP, DCP and NPP studies of complexation of Mg(II), Ca(II), Cd(II) and Pb(II) with ligand ALN

-53.8	7.608	7.661	-0.053	1.73	1.73	0	0.053	9.03	8.922	0.107	0.3	0.3	0.003	0.108
-56.8	7.657	7.706	-0.048	1.72	1.72	0	0.048	8.933	8.834	0.099	0.31	0.31	0.003	0.099
-60	7.71	7.751	-0.041	1.7	1.7	0	0.041	8.829	8.745	0.084	0.32	0.32	0.002	0.084
-63.2	7.797	7.837	-0.04	1.69	1.69	0	0.04	8.726	8.656	0.07	0.32	0.32	0.002	0.071
-66.5	7.816	7.843	-0.027	1.68	1.68	0	0.027	8.62	8.566	0.054	0.34	0.34	0.001	0.054
-69.8	7.87	7.889	-0.019	1.67	1.67	0	0.019	8.514	8.476	0.038	0.35	0.35	0.001	0.038
-73.2	7.926	7.935	-0.009	1.65	1.65	0	0.009	8.404	8.386	0.019	0.36	0.36	0	0.019
-76.6	7.981	7.981	0	1.64	1.64	0	0	8.295	8.296	-0.001	0.37	0.37	0	0.001
-80	8.037	8.027	0.01	1.63	1.63	0	0.01	8.187	8.207	-0.021	0.38	0.38	0	0.021
-83.3	8.091	8.072	0.019	1.62	1.62	0	0.019	8.081	8.119	-0.038	0.39	0.39	-0.001	0.038
-86.5	8.143	8.117	0.026	1.6	1.6	0	0.026	7.979	8.032	-0.053	0.4	0.4	-0.001	0.053
-89.6	8.194	8.162	0.032	1.59	1.59	0	0.032	7.881	7.946	-0.065	0.41	0.41	-0.001	0.065
-92.6	8.243	8.205	0.038	1.58	1.58	0	0.038	7.786	7.862	-0.076	0.42	0.42	-0.001	0.076
-95.4	8.289	8.248	0.041	1.57	1.57	0	0.041	7.697	7.779	-0.082	0.43	0.43	-0.001	0.082
-98.1	8.333	8.29	0.043	1.56	1.56	0	0.043	7.612	7.699	-0.087	0.44	0.44	-0.001	0.087
-100.6	8.374	8.331	0.043	1.54	1.54	0	0.043	7.534	7.621	-0.087	0.45	0.45	-0.001	0.087
-103	8.413	8.37	0.043	1.53	1.53	0	0.043	7.459	7.545	-0.086	0.46	0.46	-0.001	0.086
-105.3	8.451	8.409	0.042	1.52	1.52	0	0.042	7.387	7.471	-0.084	0.48	0.48	-0.001	0.084
-107.5	8.487	8.446	0.041	1.51	1.51	0	0.041	7.318	7.4	-0.081	0.49	0.49	-0.001	0.081
-109.6	8.521	8.483	0.039	1.5	1.5	0	0.039	7.253	7.331	-0.078	0.5	0.5	-0.001	0.078
-111.6	8.554	8.518	0.036	1.48	1.48	0	0.036	7.192	7.265	-0.073	0.51	0.51	-0.001	0.073
-113.5	8.585	8.552	0.034	1.47	1.47	0	0.034	7.133	7.201	-0.067	0.52	0.52	-0.001	0.067
-115.3	8.615	8.584	0.03	1.46	1.46	0	0.03	7.078	7.139	-0.061	0.53	0.53	0.001	0.061
-117	8.643	8.616	0.026	1.45	1.45	0	0.026	7.026	7.079	-0.053	0.54	0.54	-0.001	0.053
-118.7	8.67	8.647	0.024	1.44	1.44	0	0.024	6.975	7.022	-0.047	0.55	0.55	-0.001	0.047
-120.3	8.697	8.676	0.02	1.42	1.42	0	0.02	6.926	6.967	-0.04	0.57	0.57	-0.001	0.04
-121.8	8.721	8.705	0.016	1.41	1.41	0	0.016	6.881	6.913	-0.032	0.58	0.58	-0.001	0.032
-123.3	8.746	8.733	0.013	1.4	1.4	0	0.013	6.836	6.862	-0.026	0.59	0.59	-0.001	0.026
-124.8	8.77	8.76	0.01	1.39	1.39	0	0.01	6.791	6.812	-0.021	0.6	0.6	-0.001	0.021
-126.2	8.793	8.786	0.007	1.38	1.38	0	0.007	6.75	6.764	-0.015	0.61	0.61	0	0.015
-127.6	8.816	8.811	0.005	1.36	1.36	0	0.005	6.708	6.718	-0.01	0.62	0.62	0	0.01
-128.9	8.837	8.838	0.002	1.35	1.35	0	0.002	6.67	6.673	-0.003	0.63	0.63	0	0.003
-130.2	8.859	8.86	-0.001	1.34	1.34	0	0.001	6.631	6.629	0.002	0.64	0.64	0	0.002
-131.5	8.88	8.883	-0.003	1.33	1.33	0	0.003	6.593	6.587	0.006	0.66	0.66	0	0.006
-132.7	8.9	8.906	-0.006	1.32	1.32	0	0.006	6.558	6.546	0.012	0.67	0.67	0	0.012
-134	8.921	8.928	-0.007	1.3	1.3	0	0.007	6.52	6.507	0.014	0.68	0.68	0.001	0.014
-135.2	8.94	8.949	-0.009	1.29	1.29	0	0.009	6.485	6.468	0.017	0.69	0.69	0.001	0.017
-136.4	8.96	8.97	-0.01	1.28	1.28	0	0.01	6.451	6.43	0.02	0.7	0.7	0.001	0.02
-137.6	8.98	8.991	-0.011	1.27	1.27	0	0.011	6.416	6.394	0.022	0.71	0.71	0.001	0.022
-138.8	8.999	9.011	-0.011	1.26	1.26	0	0.011	6.381	6.358	0.023	0.72	0.72	0.001	0.023
-139.9	9.017	9.031	-0.013	1.24	1.24	0	0.013	6.35	6.324	0.026	0.73	0.73	0.001	0.026
-141	9.035	9.05	-0.014	1.23	1.23	0	0.014	6.318	6.29	0.029	0.74	0.74	0.001	0.029
-142.1	9.053	9.069	-0.015	1.22	1.22	0	0.015	6.287	6.257	0.031	0.75	0.75	0.001	0.031
-143.2	9.071	9.087	-0.016	1.21	1.21	0	0.016	6.256	6.224	0.032	0.77	0.77	0.002	0.032
-144.3	9.089	9.106	-0.016	1.2	1.2	-0.001	0.016	6.225	6.193	0.032	0.78	0.77	0.002	0.032
-145.4	9.107	9.123	-0.016	1.19	1.19	-0.001	0.016	6.194	6.162	0.032	0.79	0.79	0.002	0.032
-146.4	9.124	9.141	-0.017	1.17	1.17	-0.001	0.017	6.166	6.132	0.034	0.8	0.8	0.002	0.034
-147.5	9.142	9.158	-0.017	1.16	1.16	-0.001	0.017	6.135	6.102	0.033	0.81	0.81	0.002	0.033
-148.5	9.158	9.176	-0.017	1.15	1.15	-0.001	0.017	6.107	6.073	0.034	0.82	0.82	0.002	0.034
-149.5	9.175	9.192	-0.018	1.14	1.14	-0.001	0.018	6.081	6.044	0.035	0.83	0.83	0.002	0.035
-150.5	9.191	9.209	-0.018	1.13	1.13	-0.001	0.018	6.052	6.016	0.036	0.84	0.84	0.002	0.036
-151.5	9.207	9.225	-0.018	1.11	1.12	-0.001	0.018	6.024	5.989	0.036	0.85	0.85	0.002	0.036
-152.5	9.224	9.241	-0.018	1.1	1.1	-0.001	0.018	5.997	5.962	0.035	0.86	0.86	0.002	0.035
-153.5	9.24	9.257	-0.017	1.09	1.09	-0.001	0.017	5.969	5.935	0.034	0.87	0.87	0.002	0.034
-154.5	9.256	9.273	-0.017	1.08	1.08	-0.001	0.017	5.942	5.909	0.033	0.88	0.88	0.002	0.033
-155.5	9.273	9.289	-0.016	1.07	1.07	-0.001	0.016	5.915	5.883	0.032	0.89	0.89	0.002	0.032
-156.5	9.289	9.304	-0.015	1.06	1.06	-0.001	0.015	5.888	5.858	0.03	0.91	0.9	0.002	0.03
-157.4	9.304	9.319	-0.016	1.05	1.05	-0.001	0.016	5.864	5.833	0.031	0.92	0.91	0.002	0.031
-158.4	9.32	9.335	-0.014	1.03	1.03	-0.001	0.014	5.838	5.808	0.03	0.93	0.93	0.002	0.03
-159.3	9.335	9.349	-0.014	1.02	1.02	-0.001	0.015	5.813	5.784	0.029	0.94	0.93	0.002	0.029
-160.3	9.351	9.364	-0.013	1.01	1.01	-0.001	0.013	5.786	5.76	0.026	0.95	0.94	0.002	0.026
-161.2	9.366	9.379	-0.013	1	1	-0.001	0.013	5.762	5.736	0.025	0.96	0.96	0.002	0.025
-162.1	9.381	9.393	-0.013	0.99	0.99	-0.001	0.013	5.738	5.713	0.025	0.97	0.97	0.002	0.025
-163	9.396	9.408	-0.012	0.98	0.98	-0.001	0.012	5.715	5.69	0.024	0.98	0.98	0.002	0.024
-163.9	9.41	9.422	-0.012	0.96	0.97	-0.001	0.012	5.691	5.668	0.023	0.99	0.99	0.002	0.023
-164.8	9.425	9.436	-0.011	0.95	0.95	-0.001	0.011	5.668	5.646	0.022	1	1	0.002	0.022
-165.7	9.44	9.45	-0.01	0.94	0.94	-0.001	0.011	5.644	5.624	0.021	1.01	1.01	0.002	0.021
-166.6	9.454	9.464	-0.01	0.93	0.93	-0.001	0.011	5.621	5.602	0.019	1.02	1.02	0.002	0.019
-167.5	9.469	9.478	-0.009	0.92	0.92	-0.001	0.009	5.598	5.581	0.017	1.03	1.03	0.002	0.017
-168.3	9.482	9.491	-0.009	0.91	0.91	-0.001	0.009	5.578	5.56	0.018	1.04	1.04	0.002	0.018
-169.1	9.495	9.505	-0.01	0.9	0.9	-0.001	0.01	5.558	5.539	0.019	1.05	1.05	0.002	0.019
-169.9	9.509	9.518	-0.01	0.89	0.89	-0.001	0.01	5.538	5.519	0.019	1.06	1.06	0.002	0.019
-170.7	9.522	9.532	-0.01	0.87	0.88	-0.001	0.01	5.519	5.499	0.02	1.07	1.07	0.002	0.02
-171.5	9.535	9.545	-0.01	0.86	0.86	-0.001	0.01	5.499	5.48	0.02	1.08	1.08	0.002	0.02
-172.3	9.548	9.558	-0.01	0.85	0.85	-0.001	0.01	5.48	5.46	0.019	1.09	1.09	0.002	0.02
-173.1	9.561	9.57	-0.01	0.84	0.84	-0.001	0.01	5.46	5.441	0.019	1.1	1.1	0.002	0.019
-173.9	9.574	9.583	-0.009	0.83	0.83	-0.001	0.009	5.441	5.423	0.018	1.11	1.11	0.002	0.018
-174.7	9.587	9.596	-0.009	0.82	0.82	-0.001	0.009	5.422	5.405	0.017	1.12	1.12	0.002	0.017
-175.5	9.6	9.608	-0.008	0.81	0.81	-0.001	0.008	5.402	5.387	0.016	1.13	1.13	0.002	0.016
-176.3	9.613	9.62	-0.007	0.8	0.8	-0.001	0.007	5.383	5.369	0.014	1.14	1.14	0.002	0.014
-177.1	9.626	9.632	-0.006	0.79	0.79	-0.001	0.006	5.364	5.352	0.012	1.15	1.15	0.002	0.012
-177.9	9.639	9.644	-0.005	0.78	0.78	-0.001	0.005	5.345	5.336	0.01	1.16	1.16	0.001	0.01
-178.7	9.653	9.656	-0.004	0.76	0.77	0	0.004	5.326	5.319	0.007	1.17	1.17	0.001	0.007
-179.5	9.666	9.668	-0.002	0.75	0.75	0								

-204.3	10.072	10.072	-0.001	0.21	0.21	0	0.001	5.116	5.115	0.001	1.75	1.75	0	0.001
-204.5	10.075	10.078	-0.003	0.2	0.2	-0.001	0.003	5.134	5.127	0.007	1.76	1.76	0.001	0.007
-204.8	10.08	10.083	-0.004	0.19	0.19	-0.001	0.004	5.15	5.141	0.009	1.77	1.77	0.002	0.01
-205	10.083	10.089	-0.006	0.18	0.18	-0.002	0.006	5.171	5.156	0.016	1.79	1.78	0.003	0.016
-205.3	10.088	10.095	-0.007	0.16	0.17	-0.002	0.007	5.19	5.172	0.018	1.8	1.8	0.003	0.018
-205.6	10.093	10.1	-0.007	0.15	0.16	-0.002	0.008	5.21	5.19	0.02	1.81	1.81	0.004	0.02
-205.9	10.098	10.106	-0.008	0.14	0.15	-0.003	0.008	5.233	5.21	0.022	1.82	1.82	0.004	0.023
-206.1	10.101	10.111	-0.01	0.13	0.14	-0.003	0.011	5.262	5.233	0.03	1.84	1.83	0.005	0.03
-206.4	10.106	10.117	-0.011	0.12	0.13	-0.004	0.011	5.29	5.258	0.032	1.85	1.85	0.005	0.033
-206.7	10.111	10.122	-0.011	0.11	0.11	-0.004	0.012	5.321	5.286	0.035	1.86	1.86	0.006	0.036
-207	10.116	10.128	-0.012	0.1	0.1	-0.004	0.012	5.356	5.317	0.039	1.88	1.87	0.006	0.039
-207.3	10.121	10.133	-0.012	0.09	0.09	-0.004	0.013	5.396	5.353	0.043	1.89	1.88	0.006	0.043
-207.6	10.126	10.138	-0.013	0.08	0.08	-0.005	0.014	5.441	5.394	0.047	1.9	1.9	0.006	0.046
-207.9	10.131	10.144	-0.013	0.07	0.07	-0.005	0.014	5.494	5.441	0.053	1.92	1.91	0.007	0.054
-208.2	10.135	10.149	-0.014	0.06	0.06	-0.005	0.014	5.558	5.497	0.061	1.93	1.92	0.007	0.061
-208.5	10.14	10.154	-0.014	0.05	0.05	-0.005	0.015	5.635	5.564	0.071	1.94	1.94	0.007	0.071
-208.8	10.145	10.16	-0.014	0.04	0.04	-0.006	0.015	5.733	5.648	0.086	1.96	1.95	0.007	0.086
-209.1	10.15	10.165	-0.015	0.03	0.03	-0.006	0.016	5.867	5.756	0.11	1.97	1.96	0.008	0.111
-209.4	10.155	10.17	-0.015	0.02	0.02	-0.006	0.016	6.07	5.909	0.161	1.98	1.97	0.008	0.161
-209.7	10.16	10.176	-0.016	0.01	0.01	-0.006	0.017	6.49	6.16	0.329	2	1.99	0.008	0.329
-210	10.165	10.181	-0.016	0	0	-0.006	0.017	0	6.895	0	0	2	0	0
-210.3	10.17	10.186	-0.016	-0.01	-0.01	-0.007	0.018	0	0	0	0	0	0	0
-210.6	10.175	10.191	-0.017	-0.02	-0.02	-0.007	0.018	0	0	0	0	0	0	0
-210.9	10.18	10.197	-0.017	-0.04	-0.03	-0.007	0.018	0	0	0	0	0	0	0
-211.2	10.185	10.202	-0.017	-0.05	-0.04	-0.007	0.019	0	0	0	0	0	0	0
-211.6	10.191	10.207	-0.016	-0.05	-0.05	-0.007	0.017	0	0	0	0	0	0	0
-211.9	10.196	10.212	-0.016	-0.07	-0.06	-0.007	0.018	0	0	0	0	0	0	0
-212.2	10.201	10.217	-0.017	-0.08	-0.07	-0.007	0.018	0	0	0	0	0	0	0
-212.5	10.206	10.223	-0.017	-0.09	-0.08	-0.008	0.018	0	0	0	0	0	0	0
-212.8	10.211	10.228	-0.017	-0.1	-0.09	-0.008	0.019	0	0	0	0	0	0	0
-213.1	10.216	10.233	-0.017	-0.11	-0.1	-0.008	0.019	0	0	0	0	0	0	0
-213.4	10.221	10.238	-0.018	-0.12	-0.11	-0.008	0.02	0	0	0	0	0	0	0
-213.7	10.225	10.244	-0.018	-0.13	-0.12	-0.008	0.02	0	0	0	0	0	0	0
-214	10.23	10.249	-0.018	-0.14	-0.13	-0.009	0.02	0	0	0	0	0	0	0
-214.4	10.237	10.254	-0.017	-0.14	-0.14	-0.008	0.019	0	0	0	0	0	0	0
-214.7	10.242	10.259	-0.017	-0.15	-0.15	-0.008	0.019	0	0	0	0	0	0	0
-215	10.247	10.264	-0.018	-0.16	-0.16	-0.009	0.02	0	0	0	0	0	0	0
-215.3	10.252	10.27	-0.018	-0.17	-0.17	-0.009	0.02	0	0	0	0	0	0	0
-215.6	10.257	10.275	-0.018	-0.18	-0.18	-0.009	0.021	0	0	0	0	0	0	0
-216	10.263	10.28	-0.017	-0.19	-0.18	-0.009	0.019	0	0	0	0	0	0	0
-216.3	10.268	10.285	-0.017	-0.2	-0.19	-0.009	0.02	0	0	0	0	0	0	0
-216.8	10.276	10.291	-0.014	-0.21	-0.2	-0.008	0.016	0	0	0	0	0	0	0
-218.1	10.298	10.296	0.002	-0.21	-0.21	0.001	0.002	0	0	0	0	0	0	0
-219.9	10.327	10.301	0.026	-0.21	-0.22	0.015	0.03	0	0	0	0	0	0	0
-220.6	10.342	10.307	0.035	-0.21	-0.23	0.02	0.041	0	0	0	0	0	0	0
-221.2	10.348	10.312	0.036	-0.22	-0.24	0.021	0.042	0	0	0	0	0	0	0
-221.2	10.348	10.317	0.031	-0.23	-0.25	0.018	0.036	0	0	0	0	0	0	0
-221.4	10.352	10.322	0.029	-0.24	-0.26	0.017	0.034	0	0	0	0	0	0	0
-221.7	10.356	10.328	0.029	-0.25	-0.27	0.017	0.033	0	0	0	0	0	0	0
-221.9	10.36	10.333	0.027	-0.26	-0.28	0.016	0.031	0	0	0	0	0	0	0
-222.2	10.365	10.339	0.026	-0.27	-0.29	0.016	0.031	0	0	0	0	0	0	0
-222.5	10.37	10.344	0.026	-0.28	-0.3	0.016	0.03	0	0	0	0	0	0	0
-222.8	10.374	10.349	0.025	-0.29	-0.3	0.016	0.03	0	0	0	0	0	0	0
-223.1	10.379	10.355	0.025	-0.3	-0.31	0.016	0.029	0	0	0	0	0	0	0
-223.3	10.383	10.36	0.023	-0.31	-0.32	0.015	0.027	0	0	0	0	0	0	0
-223.6	10.388	10.366	0.022	-0.32	-0.33	0.014	0.026	0	0	0	0	0	0	0
-223.9	10.392	10.371	0.022	-0.33	-0.34	0.014	0.026	0	0	0	0	0	0	0
-224.1	10.396	10.376	0.019	-0.34	-0.35	0.013	0.023	0	0	0	0	0	0	0
-224.4	10.401	10.382	0.019	-0.34	-0.36	0.013	0.023	0	0	0	0	0	0	0
-224.6	10.404	10.387	0.017	-0.35	-0.37	0.011	0.02	0	0	0	0	0	0	0
-224.9	10.409	10.393	0.016	-0.36	-0.37	0.011	0.019	0	0	0	0	0	0	0
-225.2	10.414	10.398	0.015	-0.37	-0.38	0.011	0.019	0	0	0	0	0	0	0
-225.4	10.417	10.404	0.013	-0.38	-0.39	0.009	0.016	0	0	0	0	0	0	0
-225.7	10.422	10.409	0.013	-0.39	-0.4	0.009	0.015	0	0	0	0	0	0	0
-225.9	10.425	10.415	0.01	-0.4	-0.41	0.007	0.013	0	0	0	0	0	0	0
-226.2	10.43	10.421	0.01	-0.41	-0.42	0.007	0.012	0	0	0	0	0	0	0
-226.5	10.435	10.426	0.009	-0.42	-0.42	0.007	0.011	0	0	0	0	0	0	0
-226.7	10.438	10.432	0.007	-0.43	-0.43	0.005	0.008	0	0	0	0	0	0	0
-227	10.443	10.437	0.006	-0.44	-0.44	0.005	0.007	0	0	0	0	0	0	0
-227.2	10.446	10.443	0.004	-0.45	-0.45	0.003	0.004	0	0	0	0	0	0	0
-227.5	10.451	10.449	0.003	-0.45	-0.46	0.002	0.004	0	0	0	0	0	0	0
-227.7	10.455	10.454	0	-0.46	-0.46	0	0.001	0	0	0	0	0	0	0
-228	10.46	10.46	0	-0.47	-0.47	0	0	0	0	0	0	0	0	0
-228.2	10.463	10.466	-0.003	-0.48	-0.48	-0.002	0.003	0	0	0	0	0	0	0
-228.4	10.466	10.471	-0.005	-0.49	-0.49	-0.004	0.007	0	0	0	0	0	0	0
-228.6	10.469	10.477	-0.008	-0.5	-0.49	-0.006	0.01	0	0	0	0	0	0	0
-228.9	10.474	10.483	-0.008	-0.51	-0.5	-0.007	0.011	0	0	0	0	0	0	0
-229.1	10.478	10.488	-0.011	-0.52	-0.51	-0.009	0.014	0	0	0	0	0	0	0
-229.3	10.481	10.494	-0.013	-0.53	-0.52	-0.011	0.018	0	0	0	0	0	0	0
-229.5	10.484	10.5	-0.016	-0.54	-0.52	-0.014	0.021	0	0	0	0	0	0	0
-229.7	10.487	10.506	-0.018	-0.55	-0.53	-0.016	0.024	0	0	0	0	0	0	0
-229.9	10.491	10.511	-0.021	-0.56	-0.54	-0.018	0.028	0	0	0	0	0	0	0
-230.1	10.494	10.517	-0.023	-0.57	-0.54	-0.021	0.031	0	0	0	0	0	0	0
-230.3	10.497	10.523	-0.026	-0.57	-0.55	-0.023	0.035	0	0	0	0	0	0	0
-230.5	10.5	10.529	-0.028	-0.58	-0.56	-0.026	0.038	0	0	0	0	0	0	0
-230.7	10.504	10.535	-0.031	-0.59	-0.56	-0.028	0.042	0	0	0	0	0	0	0
-230.9	10.507	10.54	-0.033	-0.6	-0.57	-0.031	0.046	0	0	0	0	0	0	0
-231.3	10.514	10.546	-0.033	-0.61	-0.58	-0.031	0.045	0	0	0	0	0	0	0
-231.7	10.52	10.552	-0.032	-0.61	-0.58	-0.031	0.044	0	0	0	0	0	0	0
-231.9	10.523	10.558	-0.034	-0.62	-0.59	-0.033	0.048	0	0	0	0	0	0	0
-232.1	10.527	10.564	-0.037	-0.63	-0.6	-0.036	0.052	0	0	0	0	0	0	0
-232.4	10.532	10.57	-0.038	-0.64	-0.6	-0.038	0.054	0	0	0	0	0	0	0
-232.5	10.533	10.575	-0.042	-0.65	-0.61	-0.042	0.06	0	0	0	0	0	0	0
-232.8														

GEP data for Ca(II)-ALN system

TASK	ZBAR	1	TITRATION of	Ca-ALNR2
MODL	Ca+2	ALNO	H 1	
CPLX	0	-13.68	H	+1(-1)
CPLX	0	11.03	ALNO(1)	H +1(1)
CPLX	0	21.44	ALNO(2)	H +1(2)
CPLX	0	27.57	ALNO(3)	H +1(3)
CPLX	0	29.67	ALNO(4)	H +1(4)
CPLX	0	30.95	ALNO(5)	H +1(5)
CPLX	0	-12.12	Ca+2(1)	H +1(-1)
CPLX	1	23.38	Ca+2(2)	ALNO(1) H +1(2)
CPLX	1	20.43	Ca+2(2)	ALNO(1) H +1(1)
CPLX	1	16.43	Ca+2(1)	ALNO(1) H +1(1)
CPLX	1	7.243	Ca+2(1)	ALNO(1) H +1(1)
CPLX	1	-4.069	Ca+2(1)	ALNO(1) H +1(-1)
CPLX	1	-13.41	Ca+2(1)	ALNO(1) H +1(-2)
COND				
VEVL	IVOL	20	0	0
VEVL	H	1	0	0
VEVL	ALNO	0.002	3	0
VEVL	Ca+2	0.0009985	0	0
BURR	H	1	-0.04961	0
ELEC	H	1	415.51	0
ZERO	H	1	61.364	0
GRAD	H	1		
DATA				
EMF	PH		ZBAR(H)	POINT
OBS	OBS	RESID	OBS	RESID
	CALC	RESID	CALC	RESID
135.7	4.58	4.449	0.111	2.99
129.8	4.656	4.57	0.086	2.98
124.1	4.749	4.684	0.065	2.97
119	4.832	4.786	0.046	2.96
114.4	4.907	4.877	0.03	2.94
110.4	4.972	4.956	0.016	2.93
106.7	5.032	5.026	0.006	2.92
103.4	5.086	5.089	-0.003	2.91
100.3	5.137	5.146	-0.009	2.9
97.3	5.186	5.198	-0.012	2.89
94.5	5.245	5.221	-0.014	2.87
92	5.272	5.289	-0.017	2.86
89.7	5.309	5.33	-0.02	2.85
87.5	5.345	5.368	-0.023	2.84
85.4	5.386	5.404	-0.024	2.82
83.4	5.412	5.438	-0.026	2.81
81.4	5.445	5.47	-0.026	2.8
79.5	5.476	5.501	-0.025	2.79
77.6	5.507	5.531	-0.024	2.78
75.5	5.534	5.559	-0.025	2.76
74.2	5.562	5.586	-0.024	2.75
72.5	5.59	5.612	-0.023	2.74
70.9	5.616	5.638	-0.022	2.73
69.4	5.64	5.663	-0.022	2.71
67.9	5.665	5.687	-0.022	2.7
66.4	5.689	5.71	-0.021	2.69
64.9	5.714	5.733	-0.019	2.68
63.5	5.736	5.755	-0.018	2.66
62.1	5.759	5.777	-0.017	2.65
60.7	5.782	5.798	-0.016	2.64
59.4	5.803	5.819	-0.016	2.63
58	5.826	5.839	-0.013	2.61
56.6	5.849	5.86	-0.011	2.6
55.3	5.87	5.88	-0.01	2.59
54	5.891	5.899	-0.008	2.58
52.7	5.912	5.919	-0.006	2.57
51.4	5.934	5.938	-0.004	2.55
50.1	5.955	5.957	-0.002	2.54
48.8	5.976	5.976	0	2.53
47.4	5.999	5.994	0.005	2.52
46.2	6.018	6.013	0.006	2.5
44.9	6.04	6.031	0.008	2.49
43.1	6.059	6.049	0.01	2.48
42.5	6.079	6.068	0.011	2.47
41.3	6.098	6.086	0.012	2.45
40.1	6.118	6.104	0.014	2.44
38.9	6.137	6.122	0.015	2.43
37.7	6.157	6.14	0.017	2.42
36.5	6.176	6.158	0.018	2.4
35.3	6.196	6.176	0.02	2.39
34.1	6.215	6.194	0.021	2.38
33	6.233	6.212	0.021	2.37
31.8	6.253	6.231	0.022	2.35
30.7	6.271	6.249	0.022	2.34
29.5	6.29	6.267	0.023	2.33
28.4	6.308	6.286	0.023	2.32
27.3	6.326	6.304	0.022	2.31
26.2	6.344	6.323	0.021	2.29
25.1	6.362	6.342	0.02	2.28
24	6.38	6.361	0.019	2.27
22.9	6.398	6.38	0.018	2.26
21.7	6.418	6.4	0.018	2.24
20.6	6.436	6.42	0.016	2.23
19.5	6.453	6.44	0.014	2.22
18.3	6.473	6.46	0.013	2.21
17.1	6.493	6.481	0.012	2.19
15.9	6.512	6.502	0.011	2.18
14.7	6.532	6.523	0.009	2.17
13.5	6.551	6.545	0.007	2.16
12.2	6.572	6.567	0.006	2.14
10.9	6.594	6.589	0.004	2.13
9.6	6.615	6.612	0.003	2.12
8.3	6.636	6.636	0	2.11
6.9	6.659	6.66	-0.001	2.09
5.5	6.682	6.685	-0.003	2.08
4	6.706	6.71	-0.004	2.07
2.5	6.737	6.737	-0.006	2.06
0.9	6.767	6.764	-0.007	2.04
-0.7	6.793	6.792	-0.009	2.03
-2.4	6.81	6.82	-0.01	2.02
-4.1	6.838	6.85	-0.012	2.01
-5.9	6.867	6.881	-0.014	2
-7.8	6.898	6.914	-0.015	1.98
-9.8	6.931	6.947	-0.017	1.97
-11.9	6.965	6.982	-0.017	1.96
-14.1	7.001	7.019	-0.018	1.95
-16.5	7.04	7.057	-0.017	1.93
-18.9	7.079	7.097	-0.019	1.92
-21.6	7.123	7.14	-0.017	1.91
-24.3	7.167	7.185	-0.017	1.9
-27.3	7.216	7.232	-0.016	1.88
-30.4	7.267	7.282	-0.015	1.87
-33.8	7.32	7.335	-0.013	1.86
-37.4	7.381	7.391	-0.01	1.85
-41.3	7.444	7.45	-0.006	1.83
-45.4	7.511	7.513	-0.002	1.82
-49.7	7.581	7.579	0.002	1.81
-54.3	7.656	7.648	0.008	1.8
-59	7.733	7.72	0.013	1.79
-63.8	7.811	7.793	0.018	1.77
-68.6	7.889	7.868	0.021	1.76
-73.3	7.966	7.943	0.023	1.75
-77.9	8.041	8.017	0.024	1.74
-82.2	8.111	8.089	0.022	1.72

-86.3	8.178	8.157	0.02	1.71	1.71	0	0.02	7.88	7.921	-0.041	0.29	0.29	-0.001	0.041
-90.1	8.24	8.222	0.017	1.7	1.7	0	0.017	7.759	7.794	-0.034	0.3	0.3	-0.001	0.034
-93.7	8.298	8.284	0.014	1.69	1.69	0	0.014	7.645	7.674	-0.029	0.31	0.31	0	0.029
-97	8.352	8.341	0.011	1.68	1.68	0	0.011	7.564	7.592	-0.028	0.32	0.32	0	0.028
-100.1	8.402	8.395	0.007	1.66	1.66	0	0.007	7.442	7.457	-0.015	0.33	0.33	0	0.015
-102.9	8.448	8.445	0.003	1.65	1.65	0	0.003	7.354	7.36	-0.006	0.34	0.34	0	0.006
-105.6	8.492	8.492	0	1.64	1.64	0	0	7.27	7.269	0	0.36	0.36	0	0
-108.1	8.533	8.536	-0.003	1.63	1.63	0	0.003	7.192	7.185	0.007	0.37	0.37	0	0.007
-110.5	8.572	8.578	-0.006	1.62	1.62	0	0.006	7.117	7.106	0.011	0.38	0.38	0	0.011
-112.8	8.609	8.616	-0.007	1.6	1.6	0	0.007	7.046	7.032	0.014	0.39	0.39	0	0.014
-114.9	8.644	8.653	-0.009	1.59	1.59	0	0.009	6.981	6.962	0.019	0.4	0.4	0	0.019
-117	8.678	8.688	-0.01	1.58	1.58	0	0.01	6.916	6.896	0.019	0.41	0.41	0.001	0.02
-118.9	8.709	8.721	-0.012	1.57	1.57	0	0.012	6.858	6.834	0.023	0.42	0.42	0.001	0.023
-120.8	8.74	8.752	-0.012	1.55	1.56	0	0.012	6.8	6.775	0.024	0.43	0.43	0.001	0.024
-122.6	8.769	8.782	-0.013	1.54	1.54	0	0.013	6.745	6.719	0.025	0.44	0.44	0.001	0.025
-124.3	8.797	8.811	-0.014	1.53	1.53	0	0.014	6.693	6.666	0.027	0.45	0.45	0.001	0.027
-126	8.825	8.838	-0.013	1.52	1.52	0	0.013	6.642	6.615	0.027	0.46	0.46	0.001	0.027
-127.6	8.851	8.864	-0.014	1.51	1.51	0	0.014	6.593	6.566	0.028	0.47	0.47	0.001	0.028
-129.2	8.877	8.89	-0.013	1.5	1.5	0	0.013	6.545	6.518	0.027	0.48	0.48	0.001	0.027
-130.7	8.901	8.915	-0.014	1.48	1.48	0	0.014	6.5	6.473	0.027	0.5	0.49	0.001	0.027
-132.2	8.926	8.939	-0.013	1.47	1.47	0	0.013	6.455	6.429	0.026	0.51	0.51	0.001	0.026
-133.7	8.95	8.962	-0.012	1.46	1.46	0	0.012	6.41	6.387	0.024	0.52	0.52	0.001	0.024
-135.1	8.973	8.985	-0.012	1.45	1.45	0	0.012	6.369	6.346	0.023	0.53	0.53	0.001	0.023
-136.5	8.996	9.007	-0.011	1.44	1.44	0	0.011	6.327	6.306	0.022	0.54	0.54	0.001	0.022
-137.9	9.018	9.028	-0.01	1.42	1.42	0	0.01	6.286	6.267	0.019	0.55	0.55	0.001	0.019
-139.2	9.04	9.049	-0.01	1.41	1.41	0	0.01	6.248	6.229	0.019	0.56	0.56	0.001	0.019
-140.5	9.061	9.07	-0.009	1.4	1.4	0	0.009	6.21	6.192	0.018	0.57	0.57	0.001	0.018
-141.8	9.082	9.09	-0.008	1.39	1.39	0	0.008	6.172	6.156	0.016	0.58	0.58	0.001	0.016
-143.1	9.103	9.11	-0.007	1.38	1.38	0	0.007	6.134	6.12	0.013	0.59	0.59	0.001	0.013
-144.4	9.124	9.13	-0.005	1.37	1.37	0	0.005	6.096	6.085	0.01	0.6	0.6	0.001	0.01
-145.7	9.146	9.149	-0.003	1.35	1.35	0	0.003	6.058	6.051	0.007	0.61	0.61	0	0.007
-146.8	9.165	9.168	-0.003	1.34	1.34	0	0.003	6.023	6.018	0.006	0.62	0.62	0	0.006
-148.1	9.185	9.187	-0.002	1.33	1.33	0	0.002	5.989	5.984	0.004	0.63	0.63	0	0.004
-149.3	9.204	9.205	-0.001	1.32	1.32	0	0.001	5.954	5.952	0.002	0.64	0.64	0	0.002
-150.5	9.224	9.224	0	1.31	1.31	0	0	5.919	5.919	0	0.65	0.65	0	0
-151.7	9.243	9.242	0.001	1.3	1.3	0	0.001	5.885	5.888	-0.003	0.66	0.66	0	0.003
-152.9	9.263	9.26	0.003	1.28	1.28	0	0.003	5.851	5.856	-0.005	0.67	0.67	0	0.005
-154.1	9.282	9.278	0.004	1.27	1.27	0	0.004	5.816	5.825	-0.009	0.68	0.68	-0.001	0.009
-155.3	9.302	9.296	0.006	1.26	1.26	0	0.006	5.782	5.794	-0.012	0.69	0.69	-0.001	0.012
-156.5	9.322	9.314	0.008	1.25	1.25	0	0.008	5.748	5.763	-0.015	0.7	0.7	-0.001	0.015
-157.7	9.341	9.331	0.01	1.24	1.24	0.001	0.01	5.714	5.733	-0.019	0.71	0.71	-0.001	0.019
-158.8	9.359	9.349	0.01	1.23	1.23	0.001	0.01	5.683	5.702	-0.02	0.72	0.72	-0.002	0.02
-159.9	9.377	9.367	0.01	1.22	1.22	0.001	0.01	5.652	5.672	-0.021	0.73	0.73	-0.002	0.021
-161	9.395	9.384	0.011	1.2	1.2	0.001	0.011	5.621	5.642	-0.022	0.74	0.74	-0.002	0.022
-162.1	9.413	9.401	0.011	1.19	1.19	0.001	0.011	5.591	5.613	-0.023	0.75	0.75	-0.002	0.023
-163.2	9.431	9.419	0.012	1.18	1.18	0.001	0.012	5.559	5.583	-0.024	0.76	0.76	-0.003	0.024
-164.3	9.449	9.436	0.013	1.17	1.17	0.001	0.013	5.529	5.554	-0.025	0.77	0.77	-0.003	0.025
-165.4	9.467	9.453	0.013	1.16	1.16	0.001	0.013	5.498	5.525	-0.027	0.78	0.78	-0.003	0.027
-166.5	9.485	9.47	0.014	1.15	1.15	0.001	0.014	5.468	5.496	-0.028	0.79	0.79	-0.003	0.028
-167.5	9.501	9.487	0.014	1.14	1.14	0.001	0.014	5.437	5.467	-0.027	0.79	0.79	-0.003	0.027
-168.5	9.517	9.504	0.013	1.13	1.13	0.001	0.013	5.413	5.439	-0.026	0.8	0.81	-0.003	0.026
-169.5	9.533	9.521	0.012	1.12	1.12	0.001	0.012	5.386	5.411	-0.025	0.81	0.81	-0.003	0.025
-170.5	9.55	9.538	0.012	1.11	1.11	0.001	0.012	5.359	5.383	-0.024	0.82	0.82	-0.003	0.024
-171.5	9.566	9.554	0.012	1.09	1.09	0.001	0.012	5.332	5.355	-0.023	0.83	0.83	-0.003	0.023
-172.5	9.582	9.571	0.012	1.08	1.08	0.001	0.012	5.305	5.328	-0.023	0.84	0.84	-0.003	0.023
-173.5	9.599	9.587	0.012	1.07	1.07	0.001	0.012	5.278	5.301	-0.023	0.85	0.85	-0.003	0.023
-174.4	9.613	9.603	0.01	1.06	1.06	0.001	0.01	5.254	5.275	-0.02	0.86	0.86	-0.003	0.02
-175.3	9.628	9.619	0.009	1.05	1.05	0.001	0.009	5.231	5.249	-0.018	0.86	0.87	-0.003	0.018
-176.2	9.643	9.635	0.008	1.04	1.04	0.001	0.008	5.209	5.223	-0.016	0.87	0.88	-0.003	0.016
-177.1	9.657	9.65	0.007	1.03	1.03	0.001	0.007	5.184	5.198	-0.014	0.88	0.88	-0.002	0.014
-178	9.672	9.665	0.007	1.02	1.02	0.001	0.007	5.16	5.173	-0.013	0.89	0.89	-0.002	0.013
-178.8	9.685	9.68	0.005	1.01	1.01	0.001	0.005	5.14	5.149	-0.009	0.9	0.9	-0.002	0.009
-179.6	9.698	9.695	0.003	1	1	0.001	0.003	5.12	5.125	-0.001	0.91	0.91	-0.001	0.003
-180.4	9.711	9.71	0.001	0.99	0.99	0	0.001	5.1	5.102	-0.002	0.92	0.92	0	0.002
-181.2	9.724	9.724	0	0.98	0.98	0	0	5.08	5.08	0	0.92	0.92	0	0
-182	9.737	9.738	-0.001	0.97	0.97	0	0.001	5.06	5.058	0.002	0.93	0.93	0	0.002
-182.8	9.75	9.752	-0.002	0.96	0.96	0	0.002	5.04	5.037	0.003	0.94	0.94	0.001	0.003
-183.6	9.763	9.765	-0.002	0.94	0.94	0	0.002	5.02	5.016	0.004	0.95	0.95	0.001	0.004
-184.4	9.776	9.779	-0.002	0.93	0.93	0	0.002	5.001	4.996	0.005	0.96	0.96	0.001	0.005
-185.1	9.788	9.792	-0.004	0.92	0.92	-0.001	0.004	4.984	4.976	0.008	0.97	0.97	0.002	0.008
-185.8	9.799	9.804	-0.005	0.91	0.91	-0.001	0.005	4.968	4.957	0.01	0.98	0.97	0.002	0.01
-186.5	9.81	9.817	-0.006	0.9	0.9	-0.001	0.006	4.951	4.939	0.012	0.99	0.98	0.003	0.012
-187.2	9.822	9.829	-0.007	0.89	0.89	-0.001	0.007	4.935	4.921	0.014	0.99	0.99	0.003	0.014
-187.9	9.833	9.841	-0.008	0.88	0.88	-0.001	0.008	4.919	4.904	0.015	1	1	0.004	0.015
-188.6	9.845	9.853	-0.008	0.87	0.87	-0.001	0.008	4.903	4.887	0.016	1.01	1.01	0.004	0.016
-189.3	9.856	9.864	-0.008	0.86	0.86	-0.002	0.008	4.887	4.871	0.016	1.02	1.02	0.004	0.016
-189.9	9.866	9.875	-0.009	0.85	0.85	-0.002	0.009	4.874	4.855	0.017	1.03	1.03	0.005	0.017
-190.6	9.877	9.886	-0.009	0.84	0.84	-0.002	0.009	4.858	4.84	0.018	1.04	1.03	0.005	0.018
-191.2	9.887	9.897	-0.01	0.83	0.83	-0.002	0.01	4.845	4.825	0.02	1.05	1.04	0.005	0.02
-191.8	9.897	9.908	-0.011	0.82	0.82	-0.002	0.011	4.832	4.811	0.021	1.06	1.05	0.006	0.021
-192.4	9.907	9.918	-0.011	0.81	0.81	-0.002	0.011	4.82	4.798	0.022	1.07	1.06	0.006	0.022
-193	9.916	9.928	-0.012	0.8	0.8	-0.003	0.012	4.807	4.784	0.023	1.07	1.07	0.007	0.023
-193.6	9.926	9.938	-0.012	0.79	0.79	-0.003	0.012	4.795	4.772	0.023	1.08	1.08	0.007	0.023
-194.2	9.936	9.948	-0.012	0.78	0.78	-0.003	0.012	4.783	4.759	0.023	1			

NPP data for Pb(II)-ALN system

27 Experimental points																				
5	No. of protonation constants																			
Alendronate Level	[L]([M]) ² 159.9397																			
3	2006 Date when experiment was performed																			
Colin Files recorded during the experiment																				
DPP	DCT ISE																			
0	0 indicators for mode of experiment																			
DCT	EXPERIMENT																			
OH-titrant	M-titrant																			
1	0																			
indicators for mode of titration																				
Titration	with																			
No.:	protons																			
1	NaOH(mV)																			
2	L-sol/ml																			
3	M-sol/ml																			
4	b(eps)																			
5	lp(eps)																			
6	lp(corr)																			
7	Log[M]																			
8	Log[L]																			
9	Ep(eps)/mV																			
10	ini Ep/mV																			
11	Shift/mV																			
12	ECFC/mV																			
13	CCFC/mV																			
14	[L]																			
15	[M]																			
16	Virtual E																			
17	LOG[H]																			
18	LOG[H2]																			
19	LOG[H3]																			
1	4.34	0	0	0.464	0.69842	0.702831	-6.19843	-16.8952	-450.09	387.27	52.82001	56.20113	56.96033	0.007957	4.96E-05	-463.5711	-9.87024	-3.902025	-2.110265	
2	4.38	0.015	0	0	0.459	0.69827	0.754863	-8.24122	-16.541	-421.32	387.27	54.05002	57.66265	57.31849	7.95E-03	4.97E-05	-454.9326	-9.86596	-3.860963	-2.110983
3	4.43	0.031	0	0	0.459	0.67071	0.755344	-6.25513	-16.3919	-422.74	387.27	55.47	59.07446	58.30462	7.95E-03	4.97E-05	-426.3443	-9.79154	-3.811941	-2.111854
4	4.47	0.046	0	0	0.45	0.607308	0.742975	-6.33861	-16.2729	-423.96	387.27	56.69	60.5412	60.18341	7.94E-03	4.97E-05	-427.8112	-9.71286	-3.772862	-2.112862
5	4.51	0.064	0	0	0.45	0.606974	0.741505	-6.38244	-16.1539	-425.07	387.27	57.80002	61.64203	61.47064	7.94E-03	4.96E-05	-428.912	-9.63393	-3.739393	-2.113932
6	4.56	0.081	0	0	0.452	0.609465	0.742903	-6.43775	-16.0203	-426.41	387.27	59.14001	62.91628	63.02864	7.93E-03	4.96E-05	-430.1864	-9.55531	-3.683393	-2.115393
7	4.59	0.095	0	0	0.445	0.608128	0.734168	-6.47125	-15.9163	-427.39	387.27	60.12003	64.08978	64.08193	7.93E-03	4.96E-05	-431.3598	-9.47628	-3.656284	-2.116284
8	4.63	0.113	0	0	0.445	0.609586	0.734892	-6.5163	-15.7977	-428.66	387.27	61.29001	65.35059	65.40539	7.93E-03	4.96E-05	-432.5206	-9.39767	-3.617671	-2.117671
9	4.68	0.131	0	0	0.443	0.605264	0.731912	-6.57328	-15.6495	-429.97	387.27	62.70001	66.7093	67.08167	7.92E-03	4.95E-05	-433.9793	-9.2995	-3.569393	-2.119393
10	4.72	0.153	0	0	0.438	0.604728	0.724281	-6.61945	-15.5312	-431.37	387.27	64.10001	68.24393	68.43616	7.91E-03	4.94E-05	-435.5129	-9.22124	-3.531243	-2.121243
11	4.77	0.176	0	0	0.437	0.604188	0.722395	-6.67796	-15.3836	-432.96	387.27	65.59	69.75199	70.1501	7.90E-03	4.94E-05	-437.0216	-9.12355	-3.483547	-2.123547
12	4.81	0.198	0	0	0.435	0.603963	0.720201	-6.72545	-15.2656	-434.46	387.27	67.19	71.39927	71.54864	7.89E-03	4.94E-05	-438.6984	-9.04563	-3.445263	-2.125263
13	4.85	0.224	0	0	0.433	0.603044	0.718024	-6.77599	-15.1479	-436.84	387.27	68.57001	72.82528	72.99962	7.88E-03	4.93E-05	-440.5954	-8.96795	-3.407945	-2.127945
14	4.9	0.25	0	0	0.433	0.603426	0.718761	-6.83477	-15.001	-437.54	387.27	70.27002	74.51223	74.75604	7.88E-03	4.93E-05	-441.7822	-8.87099	-3.369897	-2.130897
15	4.93	0.274	0	0	0.43	0.601857	0.714656	-6.87204	-14.9131	-438.95	387.27	71.69002	75.9994	75.84627	7.87E-03	4.92E-05	-443.2694	-8.81311	-3.331303	-2.133103
16	4.97	0.301	0	0	0.429	0.601217	0.711889	-6.90245	-14.796	-440.45	387.27	73.18002	77.54958	77.329	7.86E-03	4.92E-05	-444.8156	-8.73603	-3.293031	-2.135031
17	5.02	0.333	0	0	0.42	0.600462	0.699462	-6.98568	-14.65	-441.65	387.27	74.38	78.97186	79.20451	7.85E-03	4.91E-05	-446.2419	-8.63998	-3.249977	-2.139977
18	5.06	0.368	0	0	0.418	0.599637	0.697986	-7.05989	-14.5338	-443.29	387.27	75.02002	80.85558	80.73417	7.84E-03	4.92E-05	-447.5205	-8.56358	-3.21358	-2.143759
19	5.11	0.405	0	0	0.419	0.598768	0.69977	-7.10556	-14.3883	-445.27	387.27	76	82.5862	82.68774	7.83E-03	4.90E-05	-449.8562	-8.46835	-3.168346	-2.148346
20	5.14	0.434	0	0	0.417	0.598089	0.699721	-7.14627	-14.3015	-446.47	387.27	76.20001	83.83399	83.87733	7.83E-03	4.88E-05	-451.1031	-8.41154	-3.141541	-2.151541
21	5.18	0.476	0	0	0.415	0.597188	0.699517	-7.20139	-14.1861	-448.15	387.27	80.89	85.5376	85.48668	7.81E-03	4.86E-05	-452.8237	-8.33613	-3.109134	-2.156134
22	5.22	0.518	0	0	0.412	0.59613	0.699125	-7.25747	-14.0711	-449.35	387.27	82.08002	86.82591	87.12461	7.80E-03	4.87E-05	-454.0959	-8.26106	-3.071061	-2.161061
23	5.27	0.565	0	0	0.423	0.595028	0.710878	-7.32894	-13.9279	-452.55	387.27	85.28	89.88388	89.21494	7.79E-03	4.87E-05	-456.3338	-8.16764	-3.027637	-2.167637
24	5.31	0.618	0	0	0.43	0.593914	0.724133	-7.38717	-13.8136	-454.48	387.27	87.21002	91.35658	90.91091	7.77E-03	4.86E-05	-458.6266	-8.056	-2.983598	-2.173597
25	5.36	0.677	0	0	0.427	0.593456	0.720729	-7.46123	-13.6715	-456.27	387.27	89	93.20709	93.07219	7.75E-03	4.84E-05	-460.4771	-8.00352	-2.951519	-2.181519
26	5.4	0.733	0	0	0.424	0.591173	0.717218	-7.52143	-13.5565	-457.91	387.27	90.64001	94.80983	94.80514	7.73E-03	4.83E-05	-462.1795	-7.93951	-2.918513	-2.189513
27	5.44	0.796	0	0	0.424	0.589736	0.718966	-7.58241	-13.4461	-459.27	387.27	92	96.23856	96.59766	7.71E-03	4.82E-05	-463.5085	-7.85611	-2.88611	-2.19611

6.27E-02 Overall fit of CCFC in ECFC/mV	
ini-VT/mV	ini-LTM
25.125	0.007957
ini-Ep/mV	ini-Ip
-367.3	0.60842

5 No. of protonation constants	
LogKa:	
11.53	
10.41	
6.13	
2.1	
1.28	

2 No. of ML and MHL complexes	
Log(Beta)	M L H
22.05852	1 1 1
2.52E-02	Stand. deviation in Log(beta)
6.36E-04	COVAR for this log
0.0255688	2 1 1
6.54E-04	COVAR for this log

7 No. of MOH and MLOH complexes	
Log(Beta)	M L OH
6	1 0 0
10.3	1 0 2
13.3	1 0 3
7.6	2 0 1
31.7	3 0 4
35.2	4 0 4
67.4	6 0 8
Temp.	I-strength pKw SLOPE n-ELECTRONS
25	0.15 13.68 29.57885 2

AMAX APOS ANEG	
6	2 6

Software indicators	
1	1 1 1 1 1 1

APPENDIX D

Experimental data from GEP, DCP and NPP studies of complexation of Mg(II), Ca(II), Cd(II) and Pb(II) with ligand NED



-86.3	8.137	8.147	-0.01	1.72	1.72	0	0.01	8.149	8.128	0.021	0.3	0.3	0.001	0.021
-88.7	8.176	8.188	-0.012	1.7	1.7	0	0.012	8.073	8.049	0.024	0.31	0.31	0.001	0.024
-91.1	8.215	8.228	-0.012	1.69	1.69	0	0.012	7.996	7.971	0.025	0.32	0.32	0.001	0.025
-93.5	8.255	8.267	-0.012	1.68	1.68	0	0.012	7.926	7.902	0.024	0.33	0.33	0.001	0.024
-95.8	8.292	8.304	-0.012	1.67	1.67	0	0.012	7.847	7.823	0.024	0.34	0.34	0.001	0.024
-98	8.328	8.341	-0.013	1.66	1.66	0	0.013	7.778	7.753	0.025	0.35	0.35	0.001	0.025
-100.2	8.364	8.376	-0.012	1.64	1.64	0	0.012	7.709	7.684	0.024	0.36	0.36	0	0.024
-102.4	8.4	8.411	-0.01	1.63	1.63	0	0.01	7.64	7.619	0.021	0.37	0.37	0	0.021
-104.4	8.433	8.444	-0.011	1.62	1.62	0	0.011	7.577	7.555	0.022	0.38	0.38	0	0.022
-106.5	8.467	8.476	-0.009	1.61	1.61	0	0.009	7.511	7.494	0.018	0.4	0.4	0	0.018
-108.4	8.499	8.507	-0.009	1.59	1.59	0	0.009	7.452	7.435	0.018	0.41	0.41	0	0.018
-110.3	8.53	8.537	-0.008	1.58	1.58	0	0.008	7.393	7.377	0.016	0.42	0.42	0	0.016
-112.2	8.561	8.567	-0.006	1.57	1.57	0	0.006	7.334	7.322	0.012	0.43	0.43	0	0.012
-114	8.59	8.595	-0.005	1.56	1.56	0	0.005	7.279	7.269	0.011	0.44	0.44	0	0.011
-115.7	8.618	8.623	-0.005	1.55	1.55	0	0.005	7.226	7.217	0.009	0.45	0.45	0	0.009
-117.4	8.646	8.649	-0.003	1.53	1.53	0	0.003	7.174	7.167	0.007	0.46	0.46	0	0.007
-119.1	8.674	8.675	-0.002	1.52	1.52	0	0.002	7.122	7.119	0.003	0.48	0.48	0	0.003
-120.7	8.7	8.701	-0.001	1.51	1.51	0	0.001	7.073	7.072	0.001	0.49	0.49	0	0.001
-122.3	8.726	8.725	0.001	1.5	1.5	0	0.001	7.024	7.026	-0.002	0.5	0.5	0	0.002
-123.8	8.751	8.749	0.001	1.49	1.49	0	0.001	6.979	6.982	-0.003	0.51	0.51	0	0.003
-125.3	8.775	8.773	0.002	1.47	1.47	0	0.002	6.934	6.938	-0.005	0.52	0.52	0	0.005
-126.8	8.8	8.796	0.004	1.46	1.46	0	0.004	6.888	6.896	-0.008	0.53	0.53	0	0.008
-128.2	8.823	8.818	0.004	1.45	1.45	0	0.004	6.846	6.855	-0.009	0.54	0.54	0	0.009
-129.6	8.846	8.841	0.005	1.44	1.44	0	0.005	6.804	6.814	-0.01	0.55	0.55	0	0.01
-131	8.868	8.862	0.006	1.43	1.43	0	0.006	6.762	6.775	-0.012	0.57	0.57	0	0.012
-132.3	8.89	8.884	0.006	1.41	1.41	0	0.006	6.724	6.736	-0.012	0.58	0.58	0	0.012
-133.6	8.911	8.905	0.006	1.4	1.4	0	0.006	6.685	6.698	-0.013	0.59	0.59	0	0.013
-134.9	8.932	8.925	0.007	1.39	1.39	0	0.007	6.646	6.66	-0.014	0.6	0.6	0	0.014
-136.2	8.954	8.946	0.008	1.38	1.38	0	0.008	6.608	6.623	-0.015	0.61	0.61	0	0.015
-137.5	8.975	8.966	0.009	1.37	1.37	0	0.009	6.569	6.587	-0.018	0.62	0.62	-0.001	0.018
-138.8	8.996	8.986	0.01	1.35	1.35	0	0.01	6.531	6.551	-0.02	0.63	0.63	-0.001	0.02
-140	9.016	9.006	0.01	1.34	1.34	0	0.01	6.496	6.516	-0.022	0.64	0.64	0	0.022
-141.2	9.035	9.025	0.01	1.33	1.33	0	0.01	6.461	6.481	-0.02	0.66	0.66	-0.001	0.02
-142.4	9.055	9.045	0.01	1.32	1.32	0	0.01	6.426	6.446	-0.02	0.67	0.67	-0.001	0.02
-143.6	9.075	9.064	0.01	1.31	1.31	0	0.01	6.391	6.412	-0.021	0.68	0.68	-0.001	0.021
-144.8	9.094	9.083	0.011	1.3	1.3	0	0.011	6.356	6.377	-0.022	0.69	0.69	-0.001	0.022
-146	9.114	9.103	0.011	1.28	1.28	0	0.011	6.321	6.344	-0.023	0.7	0.7	-0.001	0.023
-147.2	9.134	9.122	0.012	1.27	1.27	0	0.012	6.286	6.31	-0.024	0.71	0.71	-0.001	0.024
-148.4	9.153	9.14	0.013	1.26	1.26	0	0.013	6.251	6.277	-0.026	0.72	0.72	-0.001	0.026
-149.6	9.173	9.159	0.014	1.25	1.25	0.001	0.014	6.216	6.243	-0.027	0.73	0.73	-0.001	0.027
-150.7	9.191	9.178	0.014	1.24	1.24	0.001	0.014	6.181	6.208	-0.028	0.74	0.74	-0.001	0.028
-151.9	9.211	9.197	0.014	1.23	1.23	0.001	0.014	6.15	6.177	-0.027	0.75	0.75	-0.001	0.027
-153	9.229	9.216	0.013	1.21	1.21	0.001	0.013	6.119	6.144	-0.026	0.76	0.76	-0.001	0.026
-154.1	9.247	9.234	0.012	1.2	1.2	0.001	0.012	6.087	6.111	-0.024	0.77	0.77	-0.001	0.024
-155.2	9.265	9.253	0.011	1.19	1.19	0.001	0.011	6.056	6.079	-0.023	0.79	0.79	-0.001	0.023
-156.3	9.283	9.272	0.011	1.18	1.18	0.001	0.011	6.025	6.046	-0.021	0.8	0.8	-0.001	0.021
-157.4	9.301	9.291	0.01	1.17	1.17	0.001	0.01	5.993	6.013	-0.02	0.81	0.81	-0.001	0.02
-158.5	9.319	9.309	0.009	1.16	1.16	0	0.009	5.962	5.982	-0.019	0.82	0.82	-0.001	0.019
-159.6	9.337	9.328	0.009	1.15	1.15	0	0.009	5.931	5.948	-0.017	0.83	0.83	-0.001	0.017
-160.7	9.355	9.347	0.008	1.13	1.13	0	0.008	5.9	5.916	-0.016	0.84	0.84	-0.001	0.016
-161.7	9.371	9.365	0.006	1.12	1.12	0	0.006	5.872	5.884	-0.011	0.85	0.85	-0.001	0.011
-162.8	9.389	9.384	0.005	1.11	1.11	0	0.005	5.841	5.851	-0.01	0.86	0.86	-0.001	0.01
-163.8	9.405	9.402	0.003	1.1	1.1	0	0.003	5.814	5.819	-0.006	0.87	0.87	0	0.006
-164.9	9.421	9.421	0.001	1.09	1.09	0	0.001	5.786	5.787	-0.001	0.88	0.88	0	0.001
-165.8	9.438	9.44	-0.002	1.08	1.08	0	0.002	5.758	5.755	0.003	0.89	0.89	0	0.003
-166.9	9.456	9.458	-0.002	1.07	1.07	0	0.002	5.728	5.724	0.004	0.9	0.9	0	0.004
-167.9	9.472	9.477	-0.004	1.06	1.06	0	0.004	5.7	5.692	0.008	0.91	0.91	0.001	0.008
-168.9	9.489	9.495	-0.006	1.04	1.05	0	0.006	5.673	5.661	0.012	0.92	0.92	0.001	0.012
-169.9	9.505	9.503	-0.002	1.03	1.03	-0.001	0.008	5.645	5.628	0.015	0.93	0.93	0.001	0.015
-170.9	9.522	9.531	-0.01	1.02	1.02	-0.001	0.01	5.618	5.598	0.019	0.94	0.94	0.002	0.019
-171.9	9.538	9.549	-0.011	1.01	1.01	-0.001	0.011	5.591	5.568	0.023	0.95	0.95	0.002	0.023
-172.9	9.554	9.567	-0.013	1	1	-0.001	0.013	5.563	5.537	0.026	0.96	0.96	0.003	0.026
-173.9	9.571	9.585	-0.014	0.99	0.99	-0.001	0.014	5.536	5.507	0.029	0.97	0.97	0.003	0.029
-174.9	9.587	9.603	-0.016	0.98	0.98	-0.002	0.016	5.509	5.477	0.032	0.98	0.97	0.003	0.032
-175.8	9.602	9.62	-0.019	0.97	0.97	-0.002	0.019	5.485	5.448	0.037	0.99	0.98	0.004	0.037
-176.8	9.618	9.638	-0.02	0.96	0.96	-0.002	0.02	5.458	5.419	0.039	1	0.99	0.005	0.039
-177.8	9.634	9.655	-0.02	0.95	0.95	-0.002	0.021	5.431	5.39	0.041	1.01	1	0.005	0.041
-178.7	9.649	9.672	-0.023	0.94	0.94	-0.003	0.023	5.407	5.362	0.045	1.02	1.01	0.006	0.045
-179.7	9.666	9.689	-0.023	0.93	0.93	-0.003	0.023	5.381	5.334	0.046	1.02	1.02	0.006	0.046
-180.6	9.68	9.705	-0.025	0.92	0.92	-0.003	0.025	5.357	5.307	0.05	1.03	1.03	0.007	0.05
-181.6	9.697	9.722	-0.025	0.91	0.91	-0.003	0.025	5.33	5.28	0.05	1.04	1.04	0.007	0.051
-182.6	9.713	9.738	-0.025	0.9	0.9	-0.003	0.025	5.303	5.254	0.05	1.05	1.04	0.007	0.05
-183.5	9.728	9.754	-0.026	0.89	0.89	-0.004	0.026	5.278	5.228	0.052	1.06	1.05	0.008	0.052
-184.5	9.744	9.769	-0.025	0.88	0.88	-0.004	0.025	5.253	5.203	0.051	1.07	1.06	0.008	0.051
-185.5	9.761	9.785	-0.024	0.87	0.87	-0.004	0.025	5.227	5.178	0.049	1.08	1.07	0.008	0.049
-186.5	9.777	9.8	-0.023	0.86	0.86	-0.004	0.023	5.2	5.154	0.046	1.08	1.08	0.008	0.046
-187.4	9.792	9.815	-0.022	0.85	0.85	-0.004	0.024	5.177	5.127	0.047	1.09	1.09	0.008	0.047
-188.4	9.808	9.83	-0.022	0.84	0.84	-0.004	0.022	5.151	5.107	0.044	1.1	1.09	0.008	0.044
-189.3	9.823	9.844	-0.021	0.83	0.83	-0.004	0.022	5.127	5.084	0.043	1.11	1.1	0.008	0.043
-190.3	9.839	9.858	-0.019	0.82	0.82	-0.004	0.019	5.101	5.063	0.038	1.12	1.11	0.007	0.038
-191.2	9.854	9.872	-0.018	0.81	0.81	-0.003	0.018	5.078	5.041	0.037	1.12	1.12	0.007	0.037
-192.1	9.869	9.886	-0.017	0.8	0.8	-0.003	0.017	5.055	5.02	0.035	1.13	1.13	0.007	0.035
-193	9.883	9.899	-0.016	0.79	0.79	-0.003	0.016	5.032	5	0.032	1.14	1.13	0.006	0.032
-193.9	9.898	9.912	-0.014	0.78	0.78	-0.003	0.014	5.009	4.981	0.029	1.15	1.1		

-221.4	10.348	10.329	0.019	0.32	0.31	0.011	0.022	4.568	4.618	-0.05	1.59	1.61	-0.019	0.053
-221.8	10.355	10.334	0.02	0.31	0.3	0.012	0.024	4.568	4.621	-0.054	1.6	1.62	-0.02	0.057
-222.1	10.36	10.34	0.02	0.3	0.29	0.012	0.023	4.572	4.625	-0.053	1.61	1.63	-0.02	0.057
-222.4	10.365	10.345	0.02	0.29	0.28	0.012	0.023	4.577	4.63	-0.053	1.62	1.64	-0.02	0.057
-222.8	10.371	10.35	0.021	0.28	0.27	0.013	0.025	4.578	4.635	-0.058	1.63	1.65	-0.022	0.062
-223.1	10.376	10.355	0.021	0.27	0.26	0.013	0.024	4.583	4.641	-0.058	1.64	1.66	-0.021	0.062
-223.4	10.381	10.36	0.02	0.27	0.25	0.013	0.024	4.589	4.647	-0.058	1.65	1.67	-0.021	0.062
-223.8	10.387	10.366	0.022	0.26	0.24	0.014	0.026	4.591	4.654	-0.063	1.66	1.68	-0.023	0.067
-224.1	10.392	10.371	0.022	0.25	0.23	0.014	0.026	4.598	4.662	-0.064	1.67	1.69	-0.023	0.068
-224.4	10.397	10.376	0.022	0.24	0.23	0.014	0.026	4.605	4.67	-0.065	1.68	1.7	-0.023	0.069
-224.7	10.402	10.381	0.022	0.23	0.22	0.014	0.026	4.613	4.679	-0.066	1.69	1.72	-0.023	0.07
-225	10.407	10.386	0.022	0.22	0.21	0.014	0.026	4.621	4.689	-0.068	1.7	1.73	-0.023	0.072
-225.3	10.412	10.39	0.022	0.21	0.2	0.015	0.026	4.627	4.7	-0.069	1.71	1.74	-0.024	0.073
-225.6	10.417	10.395	0.022	0.2	0.19	0.015	0.026	4.634	4.711	-0.071	1.73	1.75	-0.024	0.075
-225.9	10.422	10.4	0.022	0.2	0.18	0.015	0.026	4.651	4.724	-0.073	1.74	1.76	-0.024	0.077
-226.2	10.427	10.405	0.022	0.19	0.17	0.015	0.027	4.662	4.737	-0.076	1.75	1.77	-0.024	0.079
-226.5	10.432	10.41	0.022	0.18	0.16	0.016	0.027	4.674	4.752	-0.078	1.76	1.78	-0.025	0.082
-226.8	10.437	10.415	0.022	0.17	0.15	0.016	0.027	4.687	4.768	-0.082	1.77	1.79	-0.025	0.085
-227.1	10.441	10.419	0.022	0.16	0.15	0.016	0.028	4.701	4.786	-0.085	1.78	1.81	-0.026	0.089
-227.3	10.445	10.424	0.021	0.15	0.14	0.015	0.026	4.722	4.805	-0.083	1.79	1.82	-0.024	0.086
-227.6	10.45	10.429	0.021	0.14	0.13	0.016	0.026	4.739	4.826	-0.087	1.8	1.83	-0.024	0.091
-227.9	10.455	10.433	0.021	0.13	0.12	0.016	0.027	4.757	4.849	-0.093	1.81	1.84	-0.025	0.096
-228.2	10.459	10.438	0.025	0.12	0.11	0.016	0.027	4.778	4.875	-0.098	1.83	1.85	-0.025	0.102
-228.4	10.463	10.443	0.02	0.12	0.1	0.016	0.026	4.805	4.903	-0.098	1.84	1.86	-0.024	0.101
-228.7	10.468	10.447	0.021	0.11	0.09	0.016	0.026	4.829	4.934	-0.105	1.85	1.87	-0.025	0.108
-229	10.473	10.452	0.021	0.1	0.08	0.016	0.027	4.855	4.969	-0.115	1.86	1.89	-0.025	0.117
-229.2	10.476	10.455	0.02	0.09	0.08	0.016	0.025	4.893	5.009	-0.117	1.87	1.9	-0.024	0.119
-229.5	10.481	10.461	0.02	0.08	0.07	0.016	0.026	4.925	5.055	-0.129	1.89	1.91	-0.024	0.132
-229.7	10.484	10.465	0.019	0.07	0.06	0.015	0.024	4.973	5.108	-0.135	1.9	1.92	-0.023	0.137
-230	10.489	10.47	0.019	0.06	0.05	0.016	0.025	5.016	5.17	-0.155	1.91	1.93	-0.024	0.156
-230.2	10.492	10.474	0.018	0.06	0.04	0.015	0.023	5.078	5.246	-0.168	1.92	1.95	-0.022	0.169
-230.5	10.497	10.479	0.018	0.05	0.04	0.015	0.023	5.138	5.342	-0.204	1.93	1.96	-0.023	0.205
-230.7	10.5	10.483	0.017	0.04	0.02	0.015	0.023	5.228	5.469	-0.241	1.95	1.97	-0.022	0.242
-231	10.505	10.488	0.018	0.03	0.01	0.015	0.023	5.321	5.658	-0.336	1.96	1.98	-0.022	0.337
-231.2	10.509	10.492	0.017	0.02	0.01	0.014	0.022	5.476	6.015	-0.539	1.97	1.99	-0.021	0.539
-231.4	10.512	10.496	0.016	0.01	0	0.014	0.021	5.728	0	0	1.99	0	0	0
-231.7	10.517	10.501	0.016	0	-0.01	0.014	0.021	6.21	0	0	2	0	0	0
-231.9	10.52	10.505	0.015	-0.01	-0.02	0.013	0.02	0	0	0	0	0	0	0
-232.1	10.523	10.509	0.014	-0.01	-0.03	0.012	0.019	0	0	0	0	0	0	0
-232.4	10.528	10.514	0.014	-0.02	-0.04	0.013	0.019	0	0	0	0	0	0	0
-232.6	10.531	10.518	0.013	-0.03	-0.04	0.012	0.018	0	0	0	0	0	0	0
-232.8	10.535	10.522	0.012	-0.04	-0.05	0.011	0.017	0	0	0	0	0	0	0
-233	10.538	10.527	0.011	-0.05	-0.06	0.011	0.015	0	0	0	0	0	0	0
-233.3	10.543	10.531	0.012	-0.06	-0.07	0.011	0.016	0	0	0	0	0	0	0
-233.5	10.546	10.535	0.011	-0.07	-0.08	0.011	0.015	0	0	0	0	0	0	0
-233.7	10.549	10.54	0.01	-0.08	-0.08	0.009	0.014	0	0	0	0	0	0	0
-233.9	10.553	10.544	0.009	-0.08	-0.09	0.009	0.012	0	0	0	0	0	0	0
-234.1	10.556	10.548	0.008	-0.09	-0.1	0.008	0.011	0	0	0	0	0	0	0
-234.3	10.559	10.553	0.007	-0.1	-0.11	0.007	0.01	0	0	0	0	0	0	0
-234.5	10.563	10.557	0.006	-0.11	-0.12	0.006	0.008	0	0	0	0	0	0	0
-234.8	10.567	10.561	0.006	-0.12	-0.12	0.007	0.009	0	0	0	0	0	0	0
-235	10.571	10.565	0.005	-0.13	-0.13	0.006	0.008	0	0	0	0	0	0	0
-235.2	10.574	10.57	0.005	-0.14	-0.14	0.005	0.006	0	0	0	0	0	0	0
-235.4	10.577	10.574	0.004	-0.14	-0.15	0.004	0.005	0	0	0	0	0	0	0
-235.6	10.581	10.578	0.003	-0.15	-0.16	0.003	0.004	0	0	0	0	0	0	0
-235.8	10.584	10.582	0.002	-0.16	-0.16	0.002	0.002	0	0	0	0	0	0	0
-236	10.587	10.586	0.001	-0.17	-0.17	0.001	0.001	0	0	0	0	0	0	0
-236.2	10.59	10.591	0	-0.18	-0.18	0	0	0	0	0	0	0	0	0
-236.4	10.594	10.595	-0.001	-0.19	-0.19	-0.001	-0.002	0	0	0	0	0	0	0
-236.6	10.597	10.599	-0.002	-0.2	-0.19	-0.002	0.003	0	0	0	0	0	0	0
-236.8	10.6	10.603	-0.003	-0.21	-0.2	-0.003	0.004	0	0	0	0	0	0	0
-237	10.603	10.607	-0.004	-0.21	-0.21	-0.004	0.006	0	0	0	0	0	0	0
-237.2	10.607	10.612	-0.005	-0.22	-0.22	-0.005	0.007	0	0	0	0	0	0	0
-237.4	10.61	10.616	-0.006	-0.23	-0.22	-0.007	0.009	0	0	0	0	0	0	0
-237.6	10.613	10.62	-0.007	-0.24	-0.23	-0.008	0.01	0	0	0	0	0	0	0
-237.8	10.617	10.624	-0.008	-0.25	-0.24	-0.009	0.012	0	0	0	0	0	0	0
-238	10.62	10.628	-0.008	-0.26	-0.25	-0.01	0.013	0	0	0	0	0	0	0
-238.2	10.623	10.632	-0.009	-0.26	-0.25	-0.011	0.014	0	0	0	0	0	0	0
-238.4	10.626	10.637	-0.01	-0.27	-0.26	-0.012	0.016	0	0	0	0	0	0	0
-238.6	10.63	10.641	-0.011	-0.28	-0.27	-0.013	0.017	0	0	0	0	0	0	0
-238.7	10.631	10.645	-0.014	-0.29	-0.27	-0.016	0.021	0	0	0	0	0	0	0
-238.9	10.635	10.649	-0.015	-0.3	-0.28	-0.018	0.023	0	0	0	0	0	0	0
-239.1	10.638	10.653	-0.015	-0.31	-0.29	-0.019	0.024	0	0	0	0	0	0	0
-239.3	10.641	10.657	-0.016	-0.32	-0.3	-0.02	0.026	0	0	0	0	0	0	0
-239.5	10.644	10.662	-0.017	-0.32	-0.3	-0.021	0.027	0	0	0	0	0	0	0
-239.7	10.648	10.666	-0.018	-0.33	-0.31	-0.023	0.029	0	0	0	0	0	0	0
-239.8	10.649	10.67	-0.021	-0.34	-0.32	-0.026	0.033	0	0	0	0	0	0	0
-240	10.653	10.674	-0.021	-0.35	-0.32	-0.027	0.035	0	0	0	0	0	0	0
-240.2	10.656	10.678	-0.022	-0.36	-0.33	-0.029	0.036	0	0	0	0	0	0	0
-240.4	10.659	10.682	-0.023	-0.37	-0.34	-0.03	0.038	0	0	0	0	0	0	0
-240.5	10.661	10.686	-0.026	-0.38	-0.34	-0.034	0.04	0	0	0	0	0	0	0
-240.7	10.664	10.69	-0.026	-0.38	-0.35	-0.035	0.044	0	0	0	0	0	0	0
-240.9	10.667	10.695	-0.027	-0.39	-0.36	-0.036	0.046	0	0	0	0	0	0	0
-241	10.669	10.699	-0.03	-0.4	-0.36	-0.04	0.05	0	0	0	0	0	0	0
-241.2	10.672	10.703	-0.031	-0.41	-0.37	-0.042	0.052	0	0	0	0	0	0	0
-241.4	10.676	10.707	-0.031	-0.42	-0.37	-0.043	0.053	0	0	0	0	0	0	0
-241.5	10.677	10.711	-0.034	-0.43	-0.38	-0.047	0.058	0	0	0	0	0	0	0
-241.7	10.68	10.715	-0.035	-0.44	-0.39	-0.048	0.06	0	0	0	0	0	0	0
-241.9	10.684	10.719	-0.035	-0.44	-0.39	-0.05	0.061	0	0	0	0	0	0	0
-242	10.685	10.723	-0.038	-0.45	-0.4	-0.054	0.066	0	0	0	0	0		

NNP data for Pb(II)-NED system

31		Experimental points		4		No. of protonation constants		Nerdronate Pb(II)		[LT][MT] = 49.9937		22		3		2006		Wednesday Date when experiment was performed			
pH		Files recorded during the experiment		DPP		DCT		ISE		0		1		0		indicators for mode of experiment		DCT			
EXPERIMENT		L-titrant		M-titrant		0		0		0		0		0		indicators for mode of titration		0			
Titration No.		with protons		L-sol/ml		M-sol/ml		I _p (obs)		I _p (exp)		I _p (corr)		Log[M/F]		Log[L/F]		E _p (obs)/mV		Init Ep/mV	
pH		NaOH/ml																			
1	4.55	0	0	0	0.442	0.57157	0.773309	-5.85842	-16.8747	-419.21	-370	49.20999	52.5125	52.00374	0.003968	7.94E-05	-422.5125	-10.44465	-4.354653	-2.414654	-4.50465
2	4.62	0.013	0	0	0.442	0.571275	0.773708	-5.95222	-16.8653	-420.84	-370	50.84	54.15888	54.18004	3.97E-03	7.93E-05	-424.1359	-10.30531	-4.26531	-2.41531	-4.57531
3	4.67	0.024	0	0	0.443	0.571028	0.773796	-6.0654	-16.516	-422.46	-370	52.45999	55.72124	55.74741	3.96E-03	7.93E-05	-425.7213	-10.22995	-4.23951	-2.415952	-4.62955
4	4.72	0.032	0	0	0.441	0.570845	0.772539	-6.039	-16.3667	-423.68	-370	53.67999	56.98529	57.32884	3.96E-03	7.93E-05	-426.9853	-10.10667	-4.18667	-2.41667	-4.67667
5	4.75	0.038	0	0	0.44	0.570709	0.77097	-6.07139	-16.2772	-424.76	-370	54.76001	58.10142	58.28378	3.96E-03	7.93E-05	-428.1014	-10.04718	-4.157184	-2.417184	-4.70718
6	4.79	0.046	0	0	0.438	0.570529	0.767709	-6.11485	-16.1579	-425.02	-370	56.01999	59.41586	59.58537	3.96E-03	7.92E-05	-429.4159	-9.987944	-4.117944	-2.417944	-4.74794
7	4.83	0.054	0	0	0.435	0.570348	0.762693	-6.15866	-16.0388	-427.26	-370	57.26001	60.74009	60.85709	3.96E-03	7.92E-05	-430.7401	-9.88796	-4.078795	-2.418796	-4.788
8	4.87	0.062	0	0	0.434	0.570167	0.76118	-6.20284	-15.9198	-428.58	-370	58.57999	62.08557	62.16003	3.96E-03	7.92E-05	-432.0856	-9.809749	-4.039748	-2.419748	-4.82975
9	4.91	0.07	0	0	0.432	0.569987	0.757913	-6.24743	-15.8008	-429.9	-370	59.89999	63.46085	63.47485	3.96E-03	7.92E-05	-433.4608	-9.730803	-4.000802	-2.420802	-4.8708
10	4.93	0.074	0	0	0.429	0.569897	0.752768	-6.29589	-15.7414	-430.44	-370	60.44	64.08834	64.13715	3.96E-03	7.91E-05	-434.0883	-9.69137	-3.981369	-2.42137	-4.89137
11	4.96	0.082	0	0	0.429	0.569716	0.753007	-6.30379	-15.6523	-431.68	-370	61.67999	65.32426	65.13591	3.96E-03	7.91E-05	-435.3243	-9.63231	-3.95231	-2.42231	-4.92231
12	5	0.091	0	0	0.425	0.569513	0.746291	-6.34942	-15.5336	-432.87	-370	62.87	66.63004	66.48098	3.95E-03	7.91E-05	-436.6301	-9.553941	-3.913941	-2.423941	-4.96394
13	5.03	0.098	0	0	0.422	0.569356	0.741189	-6.38398	-15.4447	-433.8	-370	63.79999	67.64748	67.49776	3.95E-03	7.91E-05	-437.6475	-9.494722	-3.884722	-2.424722	-4.99472
14	5.07	0.107	0	0	0.422	0.569153	0.741452	-6.43055	-15.3283	-435.01	-370	65.01001	68.85293	68.87275	3.95E-03	7.90E-05	-438.8529	-9.416283	-3.846282	-2.426282	-5.03628
15	5.1	0.116	0	0	0.418	0.568951	0.734685	-6.46586	-15.2376	-436.09	-370	66.09	70.0507	69.91273	3.95E-03	7.90E-05	-440.0507	-9.357586	-3.817585	-2.427586	-5.06759
16	5.12	0.121	0	0	0.417	0.568839	0.732073	-6.48396	-15.1785	-436.71	-370	66.70999	70.88993	70.91227	3.95E-03	7.90E-05	-440.8899	-9.318482	-3.798482	-2.428482	-5.08848
17	5.15	0.128	0	0	0.414	0.568681	0.728	-6.52551	-15.0899	-437.51	-370	67.51001	71.58814	71.67102	3.95E-03	7.90E-05	-441.5881	-9.259895	-3.769895	-2.429895	-5.1199
18	5.18	0.139	0	0	0.412	0.568435	0.724798	-6.56181	-15.0015	-438.75	-370	68.75	72.88477	72.73907	3.95E-03	7.89E-05	-442.8848	-9.201471	-3.741471	-2.431471	-5.15147
19	5.22	0.151	0	0	0.408	0.568156	0.718101	-6.61083	-14.8837	-440.06	-370	70.06	74.31402	74.18318	3.94E-03	7.89E-05	-444.314	-9.12389	-3.70389	-2.43389	-5.18389
20	5.26	0.162	0	0	0.405	0.567919	0.71313	-6.66082	-14.7661	-441.27	-370	71.28999	75.61324	75.65033	3.94E-03	7.89E-05	-445.6133	-9.046035	-3.666035	-2.436035	-5.23606
21	5.29	0.173	0	0	0.401	0.567673	0.706393	-6.69849	-14.678	-442.38	-370	72.38	76.85419	76.76499	3.94E-03	7.88E-05	-446.8542	-8.98802	-3.63802	-2.43802	-5.26802
22	5.33	0.183	0	0	0.396	0.56736	0.69737	-6.74972	-14.5608	-443.65	-370	73.64999	78.26929	78.27328	3.94E-03	7.88E-05	-448.2693	-8.910613	-3.600613	-2.440613	-5.31061
23	5.37	0.2	0	0	0.393	0.567069	0.690337	-6.80183	-14.4438	-444.8	-370	74.79999	79.51039	79.69912	3.94E-03	7.87E-05	-449.5104	-8.833821	-3.563821	-2.443821	-5.35382
24	5.39	0.21	0	0	0.39	0.566846	0.683017	-6.82823	-14.3855	-445.65	-370	75.64999	80.45378	80.58391	3.94E-03	7.87E-05	-450.4538	-8.795475	-3.545475	-2.445475	-5.37547
25	5.42	0.224	0	0	0.385	0.566534	0.675971	-6.86827	-14.2981	-446.79	-370	76.79001	81.75248	81.76124	3.93E-03	7.87E-05	-451.7525	-8.739002	-3.519002	-2.448002	-5.40906
26	5.46	0.24	0	0	0.382	0.566178	0.6747	-6.9225	-14.1817	-448.11	-370	78.10999	83.16487	83.35707	3.93E-03	7.86E-05	-453.1649	-8.661703	-3.481703	-2.451703	-5.4517
27	5.5	0.26	0	0	0.374	0.565733	0.661089	-6.9777	-14.0657	-449.59	-370	79.59	84.90668	84.97984	3.93E-03	7.85E-05	-454.9067	-8.585702	-3.445702	-2.455702	-5.4957
28	5.54	0.28	0	0	0.367	0.565289	0.648226	-7.03389	-13.95	-451.09	-370	81.09	86.63931	86.6319	3.92E-03	7.85E-05	-456.6393	-8.510012	-3.410011	-2.460011	-5.54001
29	5.57	0.298	0	0	0.36	0.56489	0.637292	-7.07669	-13.8635	-452.27	-370	82.26999	88.05762	87.89874	3.92E-03	7.84E-05	-458.0576	-8.43351	-3.38351	-2.463511	-5.57351
30	5.62	0.323	0	0	0.354	0.564537	0.627895	-7.14824	-13.7197	-453.95	-370	83.95999	89.95964	90.02219	3.92E-03	7.84E-05	-459.9591	-8.35971	-3.359709	-2.469709	-5.62971
31	5.66	0.35	0	0	0.344	0.56374	0.61621	-7.20835	-13.6052	-455.6	-370	85.60001	91.9455	91.75723	3.91E-03	7.83E-05	-461.9455	-8.285213	-3.305212	-2.475212	-5.67521

2.78E-02		Overall fit of CFCF in ECF/mV	
ini-VT/ml	ini-LTM	ini-MTM	ini-Ep/mV
25.2	0.003968	7.94E-05	-370
0.57157			

4		No. of protonation constants	
Log(Ka)	10.98		
10.64	6.49		
2.46			

2		No. of ML and M(HL) complexes	
Log(Beta)	M	L	H
28.6789	2	1	1
2.39E-02	Stand. deviation in Log(beta)		
5.79E-04	COVAR for this log		
22.23966	1	1	1
0.0299225	Stand. deviation in Log(beta)		
8.95E-04	COVAR for this log		

7		No. of MOH and ML(OH) complexes	
Log(Beta)	M	L	OH
6	1	0	1
10.3	1	0	2
13.3	1	0	3
7.6	2	0	1
31.7	3	0	4
35.2	4	0	4
67.4	6	0	6
Temp.	H-strength	pKw	SLOPE
25	0.15	13.68	29.57985
AMAX	APOS	ANEG	
6	2	6	

Software		Indicators	
1	1	1	1

APPENDIX E

Additional sampled DCP results

Table E.1 Overall stability constants found in this work by DCP at ionic strength 0.15 M in NaCl and 25 °C.

a) Stability constants for Pb(II)–ALN system $L_T : M_T$ ratio 50, $[M_T] = 7.9365 \times 10^{-5}$ M.

Equilibrium	Model 1	Model 2	Model 3	Model 4
$M + L + 2H = M(H_2L)$	R	R	27.18 ± 0.02	26.94 ± 0.08
$2M + L + H = M_2(HL)$	27.96 ± 0.10	28.26 ± 0.03	NI	NI
$M + L + H = M(HL)$	R	22.18 ± 0.02	22.08 ± 0.03	NI
$2M + L = M_2L$	23.60 ± 0.03	R	NI	23.53 ± 0.04
Overall fit (mV)	0.1855	0.2086	0.0850	0.2696

NI- Not included; R- Rejected

b) Stability constants for Cd(II)–NED system $L_T : M_T$ ratio 266.6, $[M_T] = 1.4978 \times 10^{-5}$ M.

Equilibrium	Model 1	Model 2	Model 3	Model 4
$M + L + 3H \leftrightarrow M(H_3L)$	30.68 ± 0.02	30.69 ± 0.02	30.21 ± 0.06	30.31 ± 0.05
$M + L + 2H \leftrightarrow M(H_2L)$	NI	NI	25.51 ± 0.01	25.47 ± 0.01
$2M + L + H \leftrightarrow M_2(HL)$	24.84 ± 0.02	24.82 ± 0.02	NI	NI
$M + L + H \leftrightarrow M(HL)$	NI	17.89 ± 0.08	NI	18.28 ± 0.02
$2M + L \leftrightarrow M_2L$	16.79 ± 0.08	NI	17.19 ± 0.03	R
$M + L \leftrightarrow ML$	9.80 ± 0.03	9.78 ± 0.03	9.66 ± 0.04	9.55 ± 0.04
Overall fit (mV)	1.0762	1.3248	0.3528	0.1169
	Model 5	Model 6	Model 7	-
$M + L + 3H \leftrightarrow M(H_3L)$	30.39 ± 0.06	30.35 ± 0.06	-	-
$2M + L + H \leftrightarrow M_2(H_2L)$	-	-	30.21 ± 0.06	-
$M + L + 2H \leftrightarrow M(H_2L)$	25.39 ± 0.05	25.44 ± 0.04	25.43 ± 0.02	-
$2M + L + H \leftrightarrow M_2(HL)$	24.27 ± 0.13	23.64 ± 0.50	NI	-
$M + L + H \leftrightarrow M(HL)$	NI	18.25 ± 0.03	18.30 ± 0.02	-
$2M + L \leftrightarrow M_2L$	17.07 ± 0.05	NI	R	-
$M + L \leftrightarrow ML$	9.72 ± 0.03	9.58 ± 0.08	9.53 ± 0.04	-
	0.1140	0.1041	0.2815	-

NI- Not included; R- Rejected

c) Stability constants for Pb(II)–NED system $L_T : M_T$ ratio 50, $[M_T] = 7.9365 \times 10^{-5}$ M.

Equilibrium	Model 1	Model 2	Model 3	Model 4
$M + L + 2H = M(H_2L)$	R	R	27.61 ± 0.02	27.62 ± 0.02
$2M + L + H = M_2(HL)$	28.52 ± 0.04	28.53 ± 0.03	NI	NI
$M + L + H = M(HL)$	R	21.83 ± 0.07	NI	21.68 ± 0.07
$2M + L = M_2L$	22.86 ± 0.08	R	22.70 ± 0.08	NI
Overall fit (mV)	0.0414	0.0639	0.0344	0.0544

NI- Not included; R- Rejected